Salinity detection and control of sodium transport in *Arabidopsis thaliana*

Sandra Manuela Schmöckel

B.Sc., M.Sc.

A thesis submitted for the degree of

Doctor of Philosophy

School for Agriculture, Food and Wine

Faculty of Sciences

The University of Adelaide

THE UNIVERSITY of ADELAIDE

December 2013

Table of contents

List of Figures

List of Tables

List of Abbreviations

3′	three prime, of nucleic acid sequence
5′	five prime, of nucleic acid sequence number
%	percent
~	approximately
×	times
°C	degrees Celsius
aa	amino acid
ACPFG	Australian Centre for Plant Functional Genomics
AGRF	Australian Genome Research Facility
ANOVA	analysis of variance
Arabidopsis	*Arabidopsis thaliana*
At	*Arabidopsis thaliana*
AtHKT1;1-C24	*AtHKT1;1* allele from C24
AtHKT1;1-Col-0	*AtHKT1;1* allele from Col-0
AtHKT1;1-C24	AtHKT1;1 protein form C24
AtHKT1;1-Col-0	AtHKT1;1 protein from Col-0
AVP	Arabidopsis vacuolar pyrophosphatase
BAC	bacterial artificial chromosome
BLAST	basic local alignment search tool
bp	base pairs, of nucleic acid
BSA	bovine serum albumin
C24	Arabidopsis ecotype C24
Ca^{2+}	calcium ion
$[Ca^{2+}]_{cyt}$	cytosolic free calcium concentration
$CaCl_2$	calcium chloride
CaMV	cauliflower mosaic virus
Cat. #	catalogue number
CBL	calcineurin like-B protein
cDNA	complimentary deoxyribonucleic acid
Cl^-	chloride ion
CIPK	calcineurin like-B interacting protein kinase
cm	centimetre(s)
Col-0	Arabidopsis ecotype Columbia-0

Col-0×C24	mapping population with Col-0 and C24 as parents
cRNA	complimentary ribonucleic acid
d	day(s)
dATP	deoxyadenosine triphosphate
dCTP	deoxycytidine triphosphate
dGTP	deoxyguanosine triphosphate
dH_20	deionised water
DNA	deoxyribonucleic acid
dNTP	deoxynucleotide triphosphate
dS	deciSiemens
DTT	dithiothreitol
dTTP	deoxythymidine triphosphate
ECe	electrical conductivity
EDTA	ethylenediaminetetraacetic acid
E_{rev}	reversal potential
FAO	Food and Agricultural Organization of the United Nations
g	gram(s)
G	conductance
g	gravity
gDNA	genomic deoxyribonucleic acid
GFP	green fluorescent protein
GUS	β -glucuronidase protein
H^+	hydrogen ion
H_20	water
HCl	hydrochloric acid
HKT	high affinity potassium transport
hr	hour(s)
I	current
IDSE	intron dependent spatial expression
IME	intron mediated enhancement
K^+	potassium ion
kb	kilo base pairs, of nucleic acid
KCl	potassium chloride
kg	kilogram(s)
KOH	potassium hydroxide

L	litre(s)
L*er*	Arabidopsis ecotype Landsberg *erecta*
LB	left border, of T-DNA sequence
LB	media luria betani media
M	molar
mg	milligram(s)
Mg^{2+}	magnesium ion
$MgCl_2$	magnesium chloride
min	minute(s)
mRNA	messenger ribonucleic acid
miRNA	micro ribonucleic acid
mL	millilitre(s)
mm	millimetre(s)
mM	millimolar
mol	mole
mOsm	milliosmole
MS-media	media, Murashige and Skoog media
mV	millivolt
n	sample size
N/A	not applicable
N_2	nitrogen
mA	milliampere
Na^+	sodium ion
NaCl	sodium chloride
NaOH	sodium hydroxide
NCBI	National Center for Biotechnology Information
ng	nanogram(s)
NHX	Na+/H+ exchanger
nm	nanometre(s)
nM	nanomolar
nosT	bacterial nopaline synthase terminator sequence
NPK	ratio of nitrogen, phosphate and potassium in fertilizer
o/n	overnight
OD_{600}	optical density measured at 600 nm
pC24	2.7 kb promoter region upstream of *AtHKT1;1* from C24

pCol-0	2.7 kb promoter region upstream of *AtHKT1;1* from Col-0
PCR	polymerase chain reaction
pCR8	entry vector pCR™8/GW/TOPO Gateway®
PI	propidium iodide
qRT-PCR	quantitative reverse transcription polymerase chain reaction
QTL	quantitative trait loci
RB	right border, of T-DNA sequence
RdDM	RNA mediated DNA methylation
RIL	recombinant inbred line
RNA	ribonucleic acid
RO	reverse osmosis
rpm	rounds per minute
RT	room temperature
RT-PCR	reverse transcription polymerase chain reaction
s	second(s)
Salty	Salt water crocodile, mascot
Sc	Saccharomyces cerevisiae
SDS	sodium dodecyl sulfate
Semi-qPCR	semi-quantitative polymerase chain reaction
siRNA	short interfering ribonucleic acid
SNP	single nucleotide polymorphism(s)
SOS	salt overly sensitive
T1	primary Arabidopsis transformant containing T-DNA
T2	progeny of T1 plant
TAE	tris-acetate-EDTA
T-DNA	transfer deoxyribonucleic acid TE transposable element
TE	transposable element
TF	transcription factor
T_m	melting temperature, of primers
U	units
UAS	upstream activation sequence
uidA	β -glucuronidase gene
UTR	untranslated region
UV	ultraviolet
V	voltage

v/v	volume per volume
wk	week(s)
w/v	weight per volume
Xenopus	*Xenopus laevis*
µg	microgram(s)
µL	microlitre(s)
µm	micrometre(s)
µM	micromolar
µmol	micromole(s)

Abstract of thesis

Soil salinity is a major abiotic stress, reducing crop yields and endangering global food security. With salt affected areas increasing, understanding the molecular mechanisms of salinity stress is of great importance. Plant salinity stress can be categorised into two phases, the initial shoot ion independent osmotic stress and the later ionic stress. Osmotic stress occurs as soon as the plant encounters salt in the soil and results in an immediate reduction in the shoot growth rate. Ionic stress is caused by the accumulation of ions such as Na^+ and Cl^- in the cytosol of cells in the shoot and results in the inhibition of cellular processes and induces premature leaf senescence.

The two *Arabidopsis thaliana* ecotypes Col-0 and C24 have previously been identified as interesting candidates to study plant salinity tolerance. The Col-0 ecotype is less salt tolerant than the C24 ecotype, based on its reduction in dry weight under stressed conditions. This is despite C24 accumulating significantly more Na^+ in the shoot than Col-0. Interestingly, C24 also appeared to be less responsive to salt stress, as transcript levels of several key salt responsive genes are not substantially altered in response to salt stress. The *AtHKT1;1* gene is one key gene found to be not up-regulated in C24 during salt stress. *AtHKT1;1* encodes a protein likely to be involved in the retrieval of Na^+ from the xylem thereby reducing the amount of Na^+ translocating to the shoot. In this thesis the C24 and Col-0 *HKTs* are compared at the protein and transcriptional levels. Electrophysiological analysis in Xenopus oocytes and a functional assay in yeast confirm Na^+ transport properties of both AtHKT1;1 proteins and, interestingly, indicated AtHKT1;1 from both ecotypes had the ability to transport K^+. To determine the difference in expression profile between the two ecotypes, a series of *AtHKT1;1promoter::GFP* and *AtHKT1;1promoter::AtHKT1;1cDNA* constructs were tested in Arabidopsis. Results suggest that both the Col-0 and C24 *AtHKT1;1* promoters are able to drive expression of the downstream genes, suggesting that differences in the promoter region are not responsible for the lack of *AtHKT1;1* expression in C24. A transposable element identified in the second intron of the C24 *AtHKT1;1* genomic sequence may be important in causing the lack of *AtHKT1;1* expression in roots.

Furthermore, the reduced responsiveness of C24 to salt stress is investigated in relation to how salt is initially perceived by the plant. An assay using aequorin bioluminescence was used to compare the responses in the salt stress inducible Ca^{2+}-signatures of Col-0 and C24 seedlings. Excitingly, C24 appears to be missing part of the Ca^{2+} signature observed in the salt responsive plant Col-0, suggesting that C24 may not detect the ion component of salt stress. This potentially provides a suitable screening methodology for the identification of as yet unknown components in the early stages of the salt signalling pathway. An attempt is made to develop a screening assay suitable for performing QTL analysis on an available Col-0 $\times$ C24 mapping population, based on measuring changes in transcript levels of salt responsive genes.

Declaration

This work contains no material which has been accepted for the award of any other degree or diploma in any university or other tertiary institution to Sandra Manuela Schmöckel and, to the best of my knowledge and belief, contains no material previously published or written by another person, except where due reference has been made in the text.

I give consent to this copy of my thesis, when deposited in the University Library, being made available for loan and photocopying, subject to the provisions of the Copyright Act 1968.

I also give permission for the digital version of my thesis to be made available on the web, *via* the University's digital research repository, the Library catalogue, the Australasian Digital Theses Program (ADTP) and also through web search engines, unless permission has been granted by the University to restrict access for a period of time.

……

Sandra M. Schmöckel

……

Date

Acknowledgements

Firstly I would like to thank my supervisors Dr. Stuart Roy, Dr. Bettina Berger and Prof. Mark Tester who were a fantastic combination of supervisors. Thank you for all your support, guidance, encouragement, inspiration and care, in particular during challenging times. I would also like to thank my external advisor Dr. Andrew Jacobs and my mentor Dr. Darren Plett for their guidance.

I gratefully acknowledge the financial support I have received during my candidature from The Australian Centre for Plant Functional Genomics (ACPFG). In particular I would like to thank Prof. Peter Langridge and Dr. Monica Ogierman for all their support and effort to facilitate my scholarship. I am very grateful for all the financial support I was provided to fund attendance at interstate and overseas conferences, laboratory visits and facilitating my research in Dr. Alex Webb's laboratory. For financial travel support I would like to thank the ACPFG, the University of Adelaide, the Waite Research Institute, the Australian Federation of University Women, the Australian Society of Plant Scientists and the Grain Research and Development Corporation.

I would like to thank Dr. Alex Webb from The University of Cambridge for welcoming me in his laboratory and allowing me to undertake part of my research project there. I would also like to thank all members of the Webb and Davies lab for their technical help and entertainment during my time in Cambridge. Cambridge has indeed been a great experience. From the University of Adelaide I would like to thank the Tyerman lab and Gilliham lab for their help with electrophysiology. I also would like to thank Dr. Neil Shirley and Mrs. Yuan Li who performed the qRT-PCR analysis, Ms. Margaret Pallotta and Ms. Alison Hay for their help with Northern Blot analysis. And in particular I would like to thank Dr. Joanna Sundstrom, for letting me take over some of her babies (plants).

A great thanks goes to all present and past members of the ACPFG Salt Focus Group and the whole ACPFG, especially the Admin team, for all their support and for being such an amazing group. In particular I would like to thank Melissa Pickering, Monique Shearer and Gordon Wellman for a daily dose of laughs and for teaching me 'Aussie'. Thank you Rhiannon, Jess, Li, Nawar, Damien, Aris, Yuri and, not to forget, Salty Croc for general support and entertainment, thank you all!

I would also like to thank my 'old' friends in Germany and my 'new' friends here in Australia, in particular Ms. Amanda Rad and Corinne and James Preuss, for their support and caring.

Allergrößter Dank gilt natürlich meiner Familie, vor allem meiner Mutter und meinem Vater, die mich in Allem unterstützt haben, auch wenn das bedeutete mich an das andere Ende der Welt gehen zu lassen. Diese Arbeit ist ihnen und meiner Großmutter (Katzenoma) gewidmet.

Chapter 1 **Review of literature and research aims**

1.1 Soil salinity is negatively impacting crop yields

Australia has 5.7 million hectares of land area which is either already affected by dryland salinity or is at high risk of being affected (http://lwa.gov.au/). It is estimated that by 2050 this area could increase to 17 million hectares. Worldwide, approximately 77 million hectares of agricultural land is salt affected, of which approximately 45 million hectares are under irrigated agriculture - irrigated agriculture produces three times more yield than dryland agriculture (FAO 2002, FAO 2008, Roy *et al.* 2013). This equates to nearly 20 % of irrigated farmland that is salt affected (Koohafkan and Stewart 2008). Maintaining high crop yields under saline conditions will be essential to ensure a stable economy and future food security. One approach to achieve this is to increase our understanding on how a plant responds to and manages salt stress.

1.2 The plants' response to salt stress

In general, stress can be defined as the change of an environmental factor to the extent where it inhibits the normal function and well-being of an organism (Jones and Jones 1989). Plants have developed different response mechanisms to tolerate stress, to prevent damage or to change to a different developmental state.

Soil salinity is predominantly caused by sodium chloride (salt) and plants respond to salt stress in two overlapping phases (Munns and Tester 2008). Initially, the plant is affected by the shoot ion independent osmotic stress which occurs immediately after the plant encounters salt stress. Osmotic stress results in an immediate decrease in cell expansion, leaf elongation, tillering and/or branching (Greenway and Munns 1983, Munns and Passioura 1984, Munns and Tester 2008). The shoot ionic stress occurs later during salt stress when sodium (Na^+) and/or chloride (Cl^-) accumulate to toxic levels in the cytoplasm of plant cells in the shoot. While a few species, like grapevine, are sensitive to high levels of Cl^- (Bernstein *et al.* 1956, Ehlig 1960), the majority of plant species, particularly cereal crops, are more sensitive to Na^+ (Shah *et al.* 1987, Yeo 1992), hence Na^+ toxicity will be the primary focus of this thesis. The accumulation of Na^+ to toxic concentrations in leaves causes the inhibition of photosynthesis and increases premature leaf senescence (Seemann and Critchley 1985, Tsugane *et al.* 1999). For certain proteins, including numerous enzymes and transcription factors, the essential potassium ion (K^+) is displaced by Na^+, which interferes with the ribosome complex and the produced protein's function and results in a disruption of metabolic processes (Murguía *et al.* 1995, Tester and Davenport 2003, Wu *et al.* 1996). Tolerance mechanisms can be found at both the plant and cellular level and have been described across a diverse range of plant species, including

crops such as wheat, barley and rice (Forster 2001, Garthwaite *et al.* 2005, Gorham 1990, Munns and James 2003, Poustini and Siosemardeh 2004, Ren *et al.* 2005, Schachtman and Munns 1992, Wei *et al.* 2003, Zhu *et al.* 2001).

Plants have evolved three major mechanisms to tolerate salt stress: The first mechanism is osmotic tolerance, which is the ability to maintain growth during the initial stages of salinity stress through mechanisms which are as yet, primarily, unknown (Munns and Tester 2008, Rajendran *et al.* 2009, Roy and Tester 2012, Roy *et al.* 2012). The second and third mechanisms, Na^+ exclusion and Na^+ tissue tolerance, aim to reduce the concentration of Na^+ in the cytosol, especially in photosynthetically active leaves. In *Arabidopsis thaliana* (Arabidopsis, thale cress), Na^+ exclusion can be mediated by transporters such as AtSOS1 and AtHKT1;1, which are involved in reducing the amount of Na^+ being translocated from the root to the shoot, thereby excluding it from the photosynthetic active tissues (Apse and Blumwald 2007, Horie and Schroeder 2004, Mäser *et al.* 2002, Shi *et al.* 2000, Uozumi *et al.* 2000, Wu *et al.* 1996). AtHKT1;1, for instance, is proposed to be localised in the root stele, with a role in retention of Na^+ in the root, thus preventing Na^+ from reaching the shoot *via* the transpiration stream (Møller and Tester 2007, Munns and Tester 2008, Tester and Davenport 2003). Tissue tolerance refers to the mechanism of compartmentalising Na^+ into vacuoles, thereby removing it from the plant cell cytoplasm. It is proposed that sodium/proton (Na^+/H^+) antiporters are involved in the transport of Na^+ across the tonoplast (Apse *et al.* 1999, Munns and Tester 2008, Pardo *et al.* 2006). While the Na^+/H^+ antiporter activity was initially attributed to NHX1 (Apse *et al.* 2003), recent research indicates that NHX1 may be a K^+/H^+ antiporter (Bassil *et al.* 2011).

1.3 Natural variation in salinity tolerance

Salinity tolerance can be described as the ability of a plant to maintain biomass and/or yield under salt stress conditions. Salinity tolerance is often determined by comparing the biomass, germination rate, survival rate or plant tissue Na^+ content under salt and control conditions. The levels of salt tolerance can vary greatly between species (Figure 1.1). Salt sensitive species include rice and Arabidopsis, which are severely affected by 100 mM NaCl. Salt tolerant species such as tall wheatgrass and saltbush are only slightly affected by 100 mM NaCl and can maintain growth in NaCl concentrations as strong as seawater (approximately 600 mM); saltbush even shows improved growth in low levels (100 mM NaCl) of salt. Salinity tolerance can also vary greatly within one species. Ecotypes of Arabidopsis (the model species used in this study), for example, show a great variation under salt stress for germination rate (DeRose-Wilson and Gaut 2011), shoot Na^+ accumulation (Baxter *et al.* 2010) and salinity tolerance (Jha *et al.* 2010, Katori *et al.* 2010).

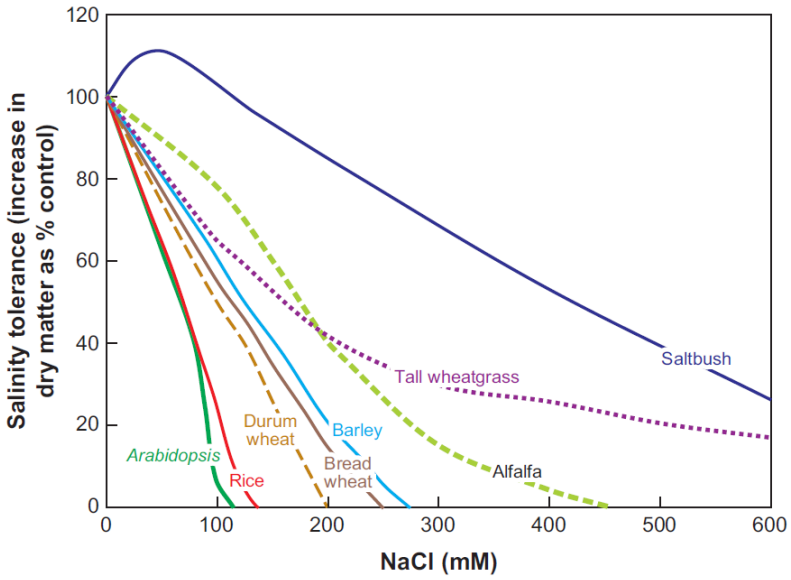

Figure 1.1: Variation in salinity tolerance of various species (Munns and Tester 2008).

Salinity tolerance is presented as the relative dry matter biomass of plants grown under the indicated levels of salt stress relative to plants grown under control conditions. The salinity tolerance of several key species (Arabidopsis, rice, durum wheat, bread wheat, barley, alfalfa, tall wheatgrass and saltbush) are shown.

The variation in salt tolerance traits in Arabidopsis ecotypes can be exploited to increase our understanding of salt tolerance in plants, in general, and to direct research into crop improvement. Although Arabidopsis is evolutionarily distant to cereal crop plants and the direct application of knowledge gained from Arabidopsis into cereals is often not straightforward, the general principles and pathways (such as the movement of Na^+ from the root to the shoot) are often similar and therefore knowledge is potentially transferable (Jha *et al.* 2010, Møller and Tester 2007). Arabidopsis has been used for many salt stress studies because of its fully sequenced genome (The Arabidopsis Genome Initiative 2000), well established transformation methods (Zhang *et al.* 2006b), libraries of mutant populations (Somerville and Koornneef 2002) and other key features that make it a suitable model organism. Indeed, by using the model plant Arabidopsis, many genes have been identified as being important in plant salt tolerance, for example *AtCIPK16* (Roy *et al.* 2013), *AtCPK6* (Xu *et al.* 2010), *AtABCG36* (Kim *et al.* 2010), *AtSOS1* (Wu *et al.* 1996) *AtAVP1* (Gaxiola *et al.* 2001) and *AtNHX1* (Apse *et al.* 1999, Gaxiola *et al.* 1999) to name just a few.

Two Arabidopsis accessions in particular attracted attention: Colombia-0 (Col-0) and C24. Under salt stress, it was found that C24 accumulated 2.5 times more Na^+ in the shoot compared to Col-0 but had similar levels of salt tolerance, based on whole plant dry weight (Jha *et al.* 2010). Additionally, the analysis of salt responsive genes showed that in C24 roots, expression of genes encoding

important proteins in Na^+ transport pathways (*AtSOS1*, *AtAVP1*, *AtNHX1* and *AtHKT1;1*) were not substantially increased 5 days after salt application, while they were substantially increased in Col-0, Wassilewskija (Ws) and Landsberg *erecta* (L*er*) (with the exception of *AtHKT1;1* in L*er*). In a separate study, the significant difference in shoot Na^+ content between Col-0 and C24 had been used to perform quantitative trait loci (QTL) analysis on a Col-0 $\times$ C24 mapping population. A significant QTL was identified on chromosome 4 spanning a region containing the *AtHKT1;1* gene (Roy, unpublished). Differences in *AtHKT1;1* expression in Col-0 and C24 roots were observed and, as AtHKT1;1 is strongly linked to shoot Na^+ accumulation (Møller and Tester 2007, Munns and Tester 2008, Tester and Davenport 2003), this makes it a likely candidate gene for the QTL (Sundstrom 2011). *AtHKT1;1* will be further described in the following section.

1.4 High-affinity Potassium Transporters (HKTs) are involved in Na^+ exclusion

HKTs are a family of ion transport proteins found in a number of plant species (Hauser and Horie 2010, Horie *et al.* 2009, Platten *et al.* 2006). The family of HKT transporters is only found in plants, but are functionally and structurally similar to the Trk/Ktr family from bacteria and fungi (Corratgé-Faillie *et al.* 2010). This HKT/Trk/Ktr family is thought to have evolved from a bacterial K^+ channel (Durell *et al.* 1999).

The family of HKT transporters in plants can be divided into two classes based and their amino acid sequence similarities (Platten *et al.* 2006). AtHKT1;1 belongs to class 1, indicated by the first digit after the protein's name, and is the only HKT member identified in Arabidopsis. In other species a number of HKTs have been identified. The majority of class 1 transporters appear to play a role in Na^+ transport and can often be related to salinity tolerance. In class 2 transporters, K^+ and Na^+ transport characteristics have been described and their role *in planta* is largely inconclusive. The Arabidopsis HKT has been widely studied and will be introduced first.

1.4.1 AtHKT1;1 mediates Na^+ exclusion from the shoot

AtHKT1;1 is the only member of the HKT family in Arabidopsis and has been shown to be involved in Na^+ transport when analysed using heterologous expression systems, such as yeast and *Xenopus laevis* (Xenopus) oocytes (Uozumi *et al.* 2000), and *in planta* (Xue *et al.* 2011).

The physiological role of AtHKT1;1 was initially evaluated in the *sos3-1* knock out mutant background. SOS3, a calcineurin like-B Ca^{2+} sensing protein, together with the protein kinase SOS2, has been found to activate the plasma membrane localised Na^+/H^+ antiporter SOS1 upon salt stress, thereby aiding to maintain ion homeostasis in the cytosol (reviewed by Mahajan *et al.* (2008)). The

sos3 single knock-out mutant has been described to have an increased sensitivity to salt due to the lack of SOS1 activity and therefore has insufficient removal of Na^+ from the cytosol *via* the plasma membrane (Liu and Zhu 1997a). It was observed that young seedlings of the double knock-out mutants *sos3-1 hkt1-1* and *sos3-1 hkt1-2* harboured decreased Na^+ levels compared to the single *sos3-1* mutant and were able to maintain root growth under salt stress conditions (Rus *et al.* 2001). Initially, these findings led to the hypothesis that AtHKT1;1 acts as the long sought after Na^+ influx system responsible for bringing Na^+ from the soil into the root (Rus *et al.* 2001). However, the results also support an alternative hypothesis that AtHKT1;1 is involved in the retrieval of Na^+ from the root xylem, therefore reducing the translocation of Na^+ to the shoot. In the *hkt1-1* knock out mutant, Na^+ is not retained in the root but instead accumulates in the shoot, resulting in reduced root Na^+ content, allowing root growth of young seedlings comparable to wild type. Also, longer term studies of the double knock-out mutant and analysis of the *hkt1-3* single knock out mutant showed increased Na^+ accumulation in the shoot and severe premature shoot senescence in the knockout plants, which indicates that Na^+ enters the plant and is translocated to the shoot (Mäser *et al.* 2002). Additionally, AtHKT1;1 was also found to be predominantly expressed in the root stele and leaf vasculature, further supporting the hypothesis that AtHKT1;1 is involved in Na^+ root to shoot translocation (Berthomieu *et al.* 2003, Mäser *et al.* 2002, Sunarpi *et al.* 2005).

Subsequently accumulated evidence further supports the involvement of AtHKT1;1 in the reduction of shoot Na^+, mediated by retrieval of Na^+ from the xylem and transport into the xylem parenchyma cells. In this way, Na^+ accumulation is reduced in the root xylem sap and consequently long distance Na^+ transport from the root to shoot is decreased (Berthomieu *et al.* 2003, Davenport *et al.* 2007, Horie *et al.* 2006, Møller *et al.* 2009, Plett *et al.* 2010, Sunarpi *et al.* 2005, Xue *et al.* 2011). While constitutive overexpression of *AtHKT1;1* results in increased shoot Na^+ and reduced salinity tolerance as determined by dry mass under saline conditions, tissue specific overexpression of *AtHKT1;1* in the root stele of Arabidopsis using an enhancer trap system leads to increased salinity tolerance by reducing the root to shoot translocation of Na^+ and greater retention of Na^+ in root cortical cells (Møller *et al.* 2009). Interestingly, tissue specific expression of *AtHKT1;1* in root cortical cells also results in reduced shoot Na^+ accumulation, potentially due to pleotropic effects resulting in an upregulation of native *AtHKT1;1* expression in the stele (Plett *et al.* 2010). Recently, AtHKT1;1 activity has been characterised *in planta* using electrophysiological analysis of protoplasts obtained specifically from root stelar cells that had been GFP-labelled using an enhancer trap system (Xue *et al.* 2011). Na^+ dependent influx currents could be observed in protoplasts of wild-type plants, but were substantially reduced in protoplasts of *AtHKT1;1* knock-out plants (Xue *et al.* 2011). A difference in current densities was not found for K^+ (Xue *et al.* 2011). This confirms results from the

Xenopus oocytes and yeast heterologous expression systems (Uozumi *et al*. 2000). For Na^+, Nernstian reversal potential changes were observed, suggesting AtHKT1;1 acts as a channel, therefore passively translocating Na^+ (Xue *et al.* 2011). This electrophysiological characterisation of *AtHKT1;1* expressing protoplasts provides further evidence for a role of AtHKT1;1 in the retrieval of Na^+ from the root xylem.

While AtHKT1;1*;* expression can be observed in the shoots of Arabidopsis (Berthomieu *et al.* 2003, Sunarpi *et al.* 2005) the role of HKT in the shoot is not fully understood. The hypothesis that AtHKT1;1 is mediating the recirculation of Na^+ in the phloem sap (Berthomieu *et al.* 2003) has not been confirmed yet and experiments with radioactive tracers do not link AtHKT1;1 as being involved in shoot to root transport of Na^+ (Davenport *et al.* 2007).

Several regulatory elements for controlling *AtHKT1;1* expression have been proposed. Expression of the genomic *AtHKT1;1* sequence driven by 2 kb of the *AtHKT1;1* promoter, 5′ of the coding sequence, leads to increased transcript levels of *AtHKT1;1* and reduced root growth in transgenic plants, compared to the Col-0 *gl1* background (Rus *et al.* 2004). The *gl1* mutation affects formation of trichomes (Xia *et al.* 2010) and therefore should not have an effect on analysing AtHKT1;1 function. A tandem repeat region between 5.3 to 3.9 kb upstream of the *AtHKT1;1* start codon was proposed as an enhancer element for *AtHKT1;1* expression; with plants containing the tandem repeat having higher *AtHKT1;1* expression and lower shoot Na^+ accumulation, than those plants without (Baek *et al.* 2011, Rus *et al.* 2006). Additionally, a methylated RNA binding site 2.6 kb upstream of the ATG start codon has been identified which, when non-methylated, reduces *AtHKT1;1* expression in the shoot of Col-0 plants (Baek *et al.* 2011). Another regulatory factor controlling *AtHKT1;1* gene expression is the protein ABI4 (Shkolnik-Inbar *et al.* 2013). ABI4 has been shown to bind to the promoter of *AtHKT1;1*, thereby reducing expression (Shkolnik-Inbar *et al.* 2013). Also, cytokinin application results in a Type-B response that mediates an upregulation of *AtHKT1;1* expression in the root *via* the transcription factors ARR1 and ARR12 (Mason *et al.* 2010). Glycosylation of the AtHKT1;1 protein has been identified in L*er*, but does not appear to be essential for protein function (Kato *et al.* 2001).

A genome-wide association study based on a SNP-tilling array of 349 Arabidopsis accessions, identified *AtHKT1;1* as an important locus for determining Na^+ content in the shoot of all accessions (Baxter *et al.* 2010). However, in Arabidopsis a reduced shoot Na^+ content (i.e. by high AtHKT1;1 activity) does not necessarily improve the salinity tolerance of natural accessions. Indeed, Arabidopsis may rely on a tissue tolerance strategy. The accessions Ts-1 and Tsu-1 are more salinity tolerant than the ecotype Col-0, however, they have lower *AtHTK1;1* expression in the root and have higher shoot Na^+ accumulation (Rus *et al.* 2006). Interestingly, several Arabidopsis

accessions found on very saline soils have been shown to have reduced expression of *AtHKT1;1* and accumulate more shoot Na^+ (Baxter *et al.* 2010).

While these lines of investigation in Arabidopsis suggest that reducing the level of *HKT* expression in plants, and thereby increasing shoot Na^+ accumulation, can lead to improved salt tolerance, in rice and wheat improved salinity tolerance is conferred by *HKT* alleles that mediate reduced shoot Na^+ content. This is likely due to these cultivars relying more on Na^+ exclusion than Na^+ tissue tolerance mechanisms. QTL mapping in both rice and wheat has identified HKTs of Class 1 to be strongly linked to reduced shoot Na^+ content as well as increased salinity tolerance (Byrt *et al.* 2007, Huang *et al.* 2006, Lindsay *et al.* 2004, Munns *et al.* 2012, Ren *et al.* 2005).

1.4.2 HKTs that increase salinity tolerance in crops

1.4.2.1 HKTs in wheat

QTL mapping in durum wheat identified two loci, *Nax1* (chromosome 2A) and *Nax2* (chromosome 5A), which have been shown to be associated with a 2- to 4-fold reduction in the leaf Na^+ concentration (Munns *et al.* 2003). The likely candidate genes underlying the two loci, *Nax1* and *Nax2*, are HKTs belonging to class 1, *TmHKT1;4-A2* and *TmHKT1;5-A*, respectively (Byrt *et al.* 2007, Huang *et al.* 2006, Lindsay *et al.* 2004, Munns *et al.* 2012). The naming indicates that the genes originate from the wild wheat relative *Triticum monococcum L.* after a durum wheat line was crossed with *T. monococcum* as part of a breeding program to introduce novel traits for a variety of stresses (Huang *et al.* 2008). It has been shown that the *TmHKT14-A2* and *TmHKT1;5-A* gene products are involved in the increased removal of Na^+ from the xylem, resulting in reduced Na^+ content in the leaves (James *et al.* 2006). While *Nax1* expression can be found in the roots, the lower part of the leaf blades and the leaf sheaths, suggesting a role for the corresponding protein in Na^+ retention in the sheath and root, *Nax2* expression is primarily detected in the roots (James *et al.* 2006). Another locus for Na^+ exclusion, *Kna1*, identified in bread wheat, *T. aestivum*, has been shown to be homeologous to *Nax2* and the putative underlying gene is *TaHKT1;5-D* (Byrt *et al.* 2007).

When *Nax1*, *Nax2* or both *Nax1* and *Nax2* are introduced into commercial bread wheat varieties, a substantial reduction in Na^+ content in the leaf blade can be observed under salt stress in hydroponic growth conditions, with 50%, 30% and 60% reductions in leaf blade Na^+, respectively (James *et al.* 2011). In particular, *Nax1* expressing lines showed a high ratio for Na^+ in the leaf sheath to Na^+ in the leaf blade, with these lines also showing improved growth when exposed to both waterlogging and salinity stress conditions (James *et al.* 2011). Taken together, *Nax1* and *Nax2* mediate

increased salinity tolerance in commercially relevant bread wheat lines under greenhouse conditions, i.e. in supported hydroponics (James *et al.* 2011).

The functional analysis of the *Nax2* candidate, *TmHKT1;5,* in yeast and Xenopus shows that under physiologically relevant conditions, TmHKT1;5 exclusively transports Na^+ with high affinity (Munns *et al.* 2012). *In situ* PCR shows expression of *TmHKT1;5* in the root xylem parenchyma and pericycle cells adjacent to the xylem. These findings are consistent with the hypothesis that TmHKT1;5 is involved in retrieving Na^+ from the xylem, thereby reducing translocation of Na^+ to the shoot and consequently mediating salinity tolerance. Recently, the native *TdHKT1;4* from durum wheat was functionally characterised in the Xenopus expression system, with the encoded protein showing low affinity but high selectivity for Na^+ transport (Ben Amar *et al.* 2013).

The introgression of *Nax2* into the commercial durum wheat line Tamaroi revealed that under field conditions, a yield increase of 24% is observed under high saline conditions, accompanied with a reduction of Na^+ in the flag leaf of 5-10%, while producing similar yields under low saline field conditions relative to wild type controls (Munns *et al.* 2012). The Na^+ content is reduced an additional 100-fold in the flag leaf of Tamaroi wheat introgressed with the *Nax1* locus, compared to corresponding *Nax2* introgression lines (James *et al.* 2012). Surprisingly, under low and high saline conditions, *Nax1* lines yield 5-10% less than the Tamaroi parents (James *et al.* 2012). This may be the result of too much Na^+ being excluded from the shoot (thereby the plant cannot use the Na^+ as a "cheap" osmoticum to generate turgor) or it is possible that this result is due to linkage drag as the DNA region introgressed from *T. monococcum* is large.

1.4.2.2 HKTs in rice

In rice, QTL analysis of the salt tolerant Indica variety Nona Bokra and salt sensitive Japonica variety, Koshihikari, linked shoot K^+ content to the *SKC1* locus, which contains the candidate gene *OsHKT1;5* (Ren *et al.* 2005). The expression of *OsHKT1;5* is increased in the root during salt stress and a *GUS* reporter gene assay suggested that the gene is mainly expressed in the parenchyma cells adjacent to the xylem of the root and shoot (Ren *et al.* 2005). Electrophysiological studies in Xenopus oocytes confirm that the *SKC1* gene product resembles a transporter with exclusive selectivity for Na^+ (Ren *et al.* 2005). An increased K^+ and reduced Na^+ content in the shoot and xylem sap after salt stress leads to the hypothesis that OsHKT1;5 is involved in the removal of Na^+ from the xylem in the roots, reducing Na^+ translocation to the shoot (Ren *et al.* 2005). The removal of Na^+ from the xylem could influence the membrane potential and thereby indirectly enhance K^+ loading into the xylem (Ren *et al.* 2005, Sunarpi *et al.* 2005, Xue *et al.* 2011), thus maintaining a favourable low Na^+ to K^+ ratio within the photosynthetic active tissues (Ren *et al.* 2005). Sequencing

of the *OsHKT1;5* gene from Nona Bokra and Koshihikari identified four amino acid changes between the two alleles. While both *OsHKT1;5* alleles have identical expression levels and localisation of the gene product, electrophysiological analysis revealed altered ion transport activity as a result of four amino acid changes, enabling Nona Bokra to retain a higher Na^+/K^+ ratio compared to Koshihikari in the root (Ren *et al.* 2005). Very recently, this hypothesis was supported by molecular modelling of OsHKT1;5, comparing the protein structure from the Pokkali allele (identical amino acid sequence to Nona Bokra) with the Nipponbare allele (identical amino acid sequence to Koshihikari) (Cotsaftis *et al.* 2012). Based on the molecular model, the amino acid change V395L could lead to a sterical rearrangement of the transporter pore region, resulting in slower transport rates of Na^+ in the Nipponbare/Koshihikari varieties (Cotsaftis *et al.* 2012).

Another HKT belonging to class 1 of the HKT family is *OsHKT1;4*. *OsHKT1;4* is mainly expressed in the shoot and appears to be involved in sheath to blade transfer of Na^+. Identification of three splice forms of *OsHKT1;4* (two of them likely to be non-functional), together with expression data, suggest that the salt tolerant variety Pokkali is able to retain more Na^+ in the leaf sheath, while in the salt susceptible variety Nipponbare, more Na^+ reaches the photosynthetic active tissue (Cotsaftis *et al.* 2012).

Recently, 392 rice lines were genotyped by EcoTILLING, identifying 15 new *OsHKT1;5* alleles (Negrão *et al.* 2013). This broad approach of allele analysis offers a source of natural variation for *HKT*s that can be used to identify superior alleles for future improvement of crop salinity tolerance.

In a transgenic approach, the specific overexpression of *AtHKT1;1* in the root cortex of rice, using an enhancer trap system, leads to increased salinity tolerance by reducing the root to shoot translocation of Na^+ (Plett *et al.* 2010). This was accompanied by an increase in native *OsHKT1;5* expression leading to further retrieval of Na^+ from the xylem and increased *OsOVP* expression in the roots indirectly enhancing the sequestration of Na^+ into the vacuoles (Plett *et al.* 2010).

Other *HKTs* belonging to class 1 have been characterized in other species such as *TsAtHKT1;1* and *TsHKT1;2* from *Thellungiella salsuginea* (Ali *et al.* 2012)., *McAtHKT1;1* from *Mesembryanthemum crystallinum,* ice plant (Su *et al.* 2003), *SsAtHKT1;1* found in *Suaeda salsa* (Shao *et al.* 2008) and *EcAtHKT1;1* and *EcHKT1;2* from *Eucalyptus camaldulensis* (Liu *et al.* 2001). For further *HKT*s belonging to class 1 refer to the recent review by Hauser and Horie (2010).

1.4.1 Class 2 HKT transporters

Being the most abundant cation in plants, potassium has crucial physiological functions in the cytosol such as balancing the charge across membranes, facilitating the movement of solutes across membranes, activating enzymatic reactions and mediating osmoregulation (Kochian and Lucas 1989, Maathuis and Amtmann 1999, Maathuis and Sanders 1996, Wakeel et al. 2011). As such, the characterisation of K^+ uptake systems was a key target in the 1990's. Trk and Ktr transporter families are found in bacteria and fungi and are involved in the uptake of K^+, with some members of the family also co-transporting Na^+ or H^+. The search for genes involved in the high affinity potassium uptake in plants led to the discovery of the first HKT in bread wheat, *HKT1* (now termed *TaHKT2;1*) (Schachtman and Schroeder 1994). *TaHKT2;1* was identified from a wheat cDNA library complementation screen that allowed a yeast mutant defective for K^+ transport to grow on media containing low K^+ (Schachtman and Schroeder 1994). Because of their importance within the HKT family, class 2 HKTs will be briefly introduced in a table (Table 1.1).

Table 1.1 Summary of characterised class 2 HKTs

Gene name	Transport properties	Expression pattern	Potential role *in planta*	References
TaHKT2;1	· Na^+ coupled K^+ transport with low $[K^+]_{ext}$ or equal $[K^+]_{ext}$ and $[Na^+]_{ext}$ · Na^+ when low $[K^+]_{ext}$ and high $[Na^+]_{ext}$ · no transport when low $[Na^+]_{ext}$	Upregulated gene expression when K^+ starved	Maintaining plant growth under K^+ starvation	(Wang *et al.* 1998)
HvHKT2;1	· Na^+ and K^+ transport across great range of $[K^+]_{ext}$ and $[Na^+]_{ext}$ · No transport when high $[K^+]_{ext}$	Upregulated gene expression when K^+ starved	Increasing salinity tolerance	(Mian *et al.* 2011, Wang *et al.* 1998)
OsHKT2;1	· Na^+ when low $[K^+]_{ext}$ and high $[Na^+]_{ext}$ · No transport when high $[K^+]_{ext}$ and/or $[Na^+]_{ext}$ · Na^+ and K^+ transport when low $[K^+]_{ext}$ and $[Na^+]_{ext}$	Upregulated gene expression K^+ starved, under salt stress first decrease, then increase; Expressed in root cortex and epidermis, in shoot around phloem and mesophyll	Maintaining plant growth under K^+ starvation	(Garciadeblás *et al.* 2003, Horie *et al.* 2007, Horie *et al.* 2001, Yao *et al.* 2010)
OsHKT2;2	Na^+ and K^+ transport across great range of $[K^+]_{ext}$ and $[Na^+]_{ext}$	Upregulated gene expression K^+ starved; Expressed in root cortex, epidermis and around xylem, in shoot around phloem and mesophyll	Maintaining plant growth under K^+ starvation	(Yao *et al.* 2010)
OsHKT2;2/1	Na^+ and K^+ transport across great range of $[K^+]_{ext}$ and $[Na^+]_{ext}$	Down regulation when NaCl treated, only expressed in roots	Maintaining plant growth under K^+ starvation	(Oomen *et al.* 2012)
OsHKT2;3	N/A	N/A	N/A	(Garciadeblás *et al.* 2003, Horie *et al.* 2011)
OsHKT2;4	Mainly transporting K^+	Leaf sheath and root	K^+ uptake and long distance K^+ transport	(Horie *et al.* 2011, Lan *et al.* 2010, Sassi *et al.* 2012)
PaHKT2;1	Na^+ and K^+ transport	Upregulated gene expression when K^+ starved	Maintaining K^+ levels when under salt stress	(Takahashi *et al.* 2007)
PtHKT2;1	K^+ transport with low $[K^+]_{ext}$ and high $[Na^+]_{ext}$	Upregulated gene expression K^+ starved or high salt stress	Maintaining K^+ levels when under K^+ starvation and salt stress	(Ardie *et al.* 2009)

N/A: no transport activity could be detected in the yeast and Xenopus oocyte expression systems

1.5 Salt "perception" and stress signalling in plants

The expression levels of *HKT* genes change when a plant experiences salt stress, indicating that these genes are involved in the salt response. These alterations in gene expression in response to salt occur for both class 1 and class 2 *HKT* genes and across a range of species, as described above. For the response to take place, a signalling pathway must exist that is induced by salt

perception and through signalling mechanisms this pathway leads to alterations in gene expression, to increase tolerance to the salt stress. However, a change in gene expression was not observed for *AtHKT1;1* in the ecotype C24 (section 1.3) (Jha *et al.* 2010). It is possible that the lack in responsiveness in C24 is caused by a dysfunctional signalling pathway. Components of the salt signalling pathway characterised to date will be discussed in the following sections.

1.5.1 Salt signalling in Arabidopsis

1.5.1.1 Network of signalling molecules that is activated by Ca^{2+}

It is not yet known how salt stress is perceived by plants, however immediately after application of salt stress, alterations in cytosolic calcium $[Ca^{2+}]_{cyt}$ can be observed (Knight *et al.* 1997). These alterations in $[Ca^{2+}]_{cyt}$ are believed to encode for the stress specific signals and transmit the information to effector proteins. Calcium signalling pathways are very complex and a number of recent reviews cover this topic in detail (Batistič and Kudla 2012, Dodd *et al.* 2010, Kudla *et al.* 2010). Ca^{2+} is sensed and decoded by Ca^{2+}-binding proteins. There are three major groups of EF-hand proteins which bind Ca^{2+}, the calmodulins (CaMs) and CaM-like proteins (CMLs); Ca^{2+}-dependent protein kinases (CDPKs); and calcineurin B-like proteins (CBLs) (Batistič and Kudla 2012, DeFalco *et al.* 2010). CaMs were identified in plants in 1980 using a bioluminescence assay with purified calmodulin from plants where the calmodulin's ability to activate a phosphodiesterase and a NAD kinase was determined (Anderson *et al.* 1980). The first CDPK was identified in 1982 by isolating the total shoot membrane of pea and measuring the kinase activity after the addition of Ca^{2+} (Hetherington and Trewavas 1982). The first plant CBL was identified in Arabidopsis using homology-based cloning in order to discover the corresponding protein to the animal and yeast calcineurin protein (Kudla *et al.* 1999). The EF-hand motif is a common motif shared by many Ca^{2+}-binding proteins and its helix-loop-helix structure facilitates binding of calcium ions (Gifford *et al.* 2007, Ikura and Ames 2006, Kawasaki *et al.* 1998). Ca^{2+} is one of the major second messengers in a plant, and although calcium binding proteins were identified 20 years ago, their complex network of interactions with target proteins and involvement in signalling processes is still not fully understood and is therefore a focus of intense research (Batistič and Kudla 2012). A variety of Ca^{2+} binding proteins exist that allow the specific interaction and activation of target proteins, for instance, by phosphorylating target proteins, as is the case for CDPKs, or by participating in protein-protein-interactions, which then mediate downstream cellular processes (Batistič and Kudla 2012).

This network of interactions, starting with alterations in $[Ca^{2+}]_{cyt}$ that are stress specific, followed by detection and transmission of these signals to specific targets, allow the plant to respond to different

stresses and to activate different tolerance mechanisms. One example of a salt specific signalling pathway is the salt overly sensitive (SOS)-pathway, which ultimately leads to the activation of a Na^+/H^+ antiporter, which reduces the cytoplasmic Na^+ content.

1.5.1.2 Salt stress signalling mediated by the SOS-pathway

Parts of the SOS-pathway were initially identified by generating ethylmethane sulfonate (EMS) mutants of Arabidopsis, which were then screened for hypersensitivity to NaCl (Wu *et al.* 1996). The proteins, which were found in this approach, are termed SOS1 (Wu *et al.* 1996), SOS2 (Zhu *et al.* 1998), SOS3 (Liu and Zhu 1998), SOS4 and SOS5 (Liu and Zhu 1997b) and were shown to be important for salt tolerance. Recently, a sixth member was defined, SOS6 (Zhu *et al.* 2010).

After identifying the genes and proteins responsible for the salt sensitivity in mutated plants, many studies have been undertaken to characterise them further, investigating which proteins interact and their relationship to each other within the pathway. It should be noted that the gene names do not describe the function of the gene they encode, but rather the phenotype of the plant observed when the gene is knocked out. The three proteins SOS1 (a plasma membrane bound Na^+/H^+ antiporter), SOS2 (a calcineurin like-B interacting protein kinase (CIPK)) and SOS3 (a calcium binding calcineurin like-B protein (CBL)) were found to be involved in a signalling pathway that is activated under salt stress. Salt stress causes alterations in $[Ca^{2+}]_{cyt}$. The Ca^{2+} binds to the Ca^{2+}-binding protein SOS3, which in turn recruits SOS2 to the plasma membrane (Halfter *et al.* 2000). SOS2, a protein kinase (Liu *et al.* 2000), is then able to activate SOS1 by phosphorylation. SOS1, a Na^+/H^+ antiporter in the plasma membrane (Shi *et al.* 2000), then expels Na^+ from the cell, thus maintaining low Na^+ levels in the cytoplasm, leading to salinity tolerance (Figure 1.2).

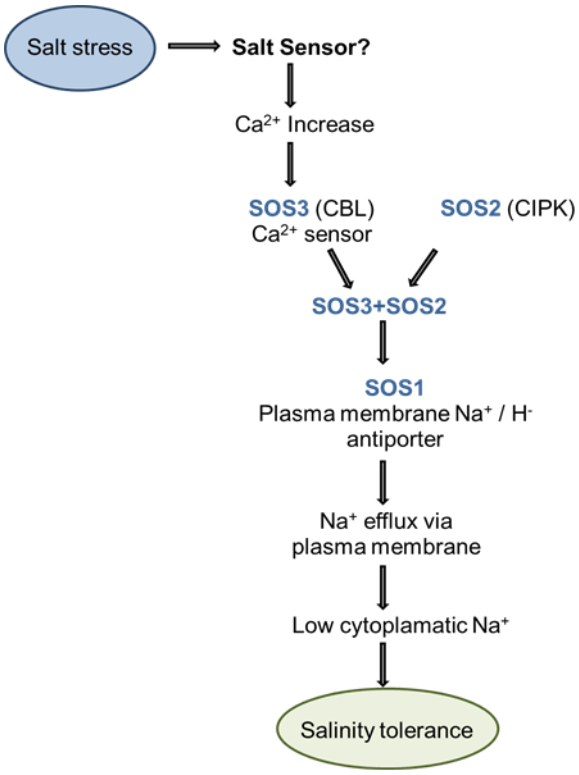

Figure 1.2: Schematic of the SOS signalling pathway (modified from Mahajan and Tuteja 2005).

During salt stress, excess Na^+ is recognised by an unknown sensor, resulting in increases in cytosolic calcium concentrations. The calcium binding protein SOS3 changes its conformation and interacts with SOS2, leading to the activation of SOS2's kinase function. The phosphorylation and therefore activation of the transporter SOS1 leads to a decrease in cytoplasmic Na^+ by facilitating the Na^+ efflux *via* the plasma membrane.

It is notable, that the first important step in this cascade, the salt sensor, has yet to be discovered. To date, nothing is known about the initial sensing of the salt and how this leads to an increased $[Ca^{2+}]_{cyt}$. No information is available about a potential protein(s), which could be involved in the initial sensing, and there is no information on whether the receptor is membrane bound or cytosolic. With this being the case, a forward genetic approach is required, in which a salt unresponsive phenotype is utilised to identify the gene(s) responsible for the receptor. It is this difference in responsiveness to salt between C24 and Col-0, indicated by differences in gene expression that could be used as a phenotype for QTL analysis.

1.5.2 Known ion sensors

To be able to evaluate the probability that a gene is responsible for a QTL and, in this case to find the gene responsible for the initial step of sensing Na^+, it is advantageous to know features of other ion sensors which are already identified. During evolution, events like gene duplications in the

genome can result in the change of function or specificity of proteins, which explains, for example, the existence of different types of haemoglobin in the mammalian system (Huxley 1942) and the HKT transporters in plants with different ion selectivity (Corratgé-Faillie *et al.* 2010, Waters *et al.* 2013). It is possible, that the Na^+ sensor evolved from another ion sensor, which was duplicated and then evolved its specificity to Na^+. Three other ion sensors or sensor-families have been identified so far in plants. CHL-1 (also known as NRT1.1), a nitrate transporter and sensor (Ho *et al.* 2009), SKOR, a voltage dependent potassium transporter and potassium sensor (Johansson *et al.* 2006) and proteins with an EF-hand motif, which are involved in sensing calcium ions (summerised by DeFalco *et al.* 2010).

1.5.2.1 CHL1- a nitrate transporter and sensor

Three identified nitrate transporter gene families in Arabidopsis are *AtNRT1, AtNRT2* and *AtCLC.* Based on structural predictions utilising their amino acid sequences, these transporters have between 9 and 12 trans-membrane spanning domains (Okamoto *et al.* 2003) and they differ in their affinity for transporting nitrate. For CHL1 it is known that the phosphorylation status determines whether it acts as a low or high affinity nitrate transporter (Liu and Tsay 2003).

The function of CHL1 as a sensor was discovered indirectly using qPCR. After treating plants with nitrate, gene expression of nitrate assimilatory enzymes and nitrate transporters was shown to increase (Wang *et al.* 2003). This so called primary response was eliminated in *chl1* knockdown mutants, showing that CHL1 is not only a nitrate transporter but also has a role as a nitrate sensor (Ho *et al.* 2009).

1.5.2.2 SKOR- a voltage dependent potassium transporter and sensor

SKOR (stelar K^+ outward rectifier) is a voltage dependent transporter that also detects extracellular K^+. This was determined by heterologous expression of site-mutated *SKOR* genes in Xenopus oocytes and analysing the properties of the resulting proteins using electrophysiology (Johansson *et al.* 2006). It was discovered that the sensor region lies close to the pore region of the sixth transmembrane domain. Due to the protein's homology with the *Drosophila ssp.* Shaker K^+ channel, SKOR's structure is predicted to be similar. The Drosophila channel consists of 6 trans-membrane domains (S1-S6) with the pore region between S5 and S6 (Long *et al.* 2005).

1.5.2.3 Calcium sensing proteins

As discussed in the previous section (1.5.1.1), a common feature of many Ca^{2+}-binding proteins is the EF-hand motif. If a similar Na^+ binding motif could be identified, it would enable the homology based search for Na^+ binding proteins and therefore possibly limit the number of candidate genes.

1.5.3 Possible candidates for the sodium sensor

As described in paragraph 1.5.2, ion sensors can be membrane bound, as in the case of CHL1 and SKOR, or they can be cytosolic as is the case for many calcium ion sensing proteins. Importantly, K^+ and NO_3^- ions are nutritional, so it is important that they are sensed at an early stage to ensure their efficient uptake from the soil. Na^+ is often not essential for plant nutrition and mostly toxic in higher concentrations, but can be beneficial for plant growth in low concentrations (Marschner 1995). The immediate response to salt stress (Tracy *et al.* 2008) implies an early sensing of salt, which leads to the notion that the sensing occurs at the root plasma membrane. A possible candidate is the sodium-proton-exchanger SOS1, which on detecting Na^+ could induce calcium release, thus mediating its own activation to expel Na^+ back into the soil. Simultaneously, the increase in cytosolic Ca^{2+} could activate other signalling mechanisms. Zhu (2003) proposed AtSOS1 as a Na^+ sensor, because it has an extended cytoplasmic domain which could facilitate Na^+ sensing just after it enters the cell, however, no experimental evidence supporting this hypothesis has been presented.

Other Na^+ transporters in the plasma membrane in the roots include members of the HKT1 family, voltage insensitive channels, non-selective channels and low-affinity cation transporters (Serrano and Rodríguez-Navarro 2001). Besides facilitating transport, they could also operate as Na^+ sensors.

1.6 Arabidopsis accessions Col-0 and C24 as genetic resources to analyse salinity tolerance

As described above, the two ecotypes Col-0 and C24 are of particular interest in relation to salinity tolerance. While the expression patterns of salt responsive genes were substantially altered in the shoot and root tissue when Col-0, L*er* or Ws were salt stressed, only minor changes in the expression of these genes could be observed in C24. C24 plants also appear healthier under salt stress when compared to those with a Col-0 background, although they accumulate more shoot Na^+ than Col-0 – however, both Col-0 and C24 are less salt tolerant than either Ws or L*er* (Jha *et al.* 2010, Munns and Tester 2008). This thesis investigates the variation in the salinity response of Col-0 and C24, where the tolerant variety, C24, appears to be less responsive to salt. Previous research by Sundstrom (2011) found that C24 lacks *AtHKT1;1* expression in the root, which is likely to be the cause for the increased shoot Na^+ accumulation. Sundstrom (2011) subsequently investigated the control of *AtHKT1;1* and was able to resolve the nucleotide sequence of both the *AtHKT1;1* promoter and gene (Figure 1.3). The promoter sequences showed two major polymorphisms between the ecotypes, one being a 700 bp sequence located approximately 5.4 kb upstream of the start codon, which is repeated twice in Col-0 and present once in C24. The other polymorphic region in the promoter is located within 240 bp upstream of the start codon and contains a number of nucleotides that are altered between Col-0 and C24. The genomic *AtHKT1;1* region has one major difference between Col-0 and C24, with the C24 *AtHKT1;1* having a 1.6 kb insertion in the second intron. Additionally, the coding sequence between Col-0 and C24 varies in 22 nucleotides, leading to 9 predicted amino acid changes. An attempt was made by Sundstrom (2011) to determine the regulation of *AtHKT1;1* gene expression by using transgenic lines. It was hypothesised that the promoter region caused the lack of *AtHKT1;1* expression in the roots of C24 plants. A series of transgenic lines were generated that contained Col-0 and C24 *AtHKT1;1promoter::GFP* and *AtHKT1;1promoter*::*AtHKT1;1cDNA* constructs. Preliminary results from analysing the T_1 generation of *AtHKT1;1promoter*::*GFP* lines suggested that both the Col-0 and C24 promoter may activate *GFP* expression. However, subsequent experiments with the T_2 generation did not yield any GFP fluorescence (Sundstrom 2011). The experiments were performed on MS plates under non-transpiring conditions, which may have led to very low *GFP* expression, resulting in undetectable fluorescence. It has previously been shown that *AtHKT1;1* expression is low under non-transpiring conditions (Sundstrom 2011). As *GFP* is being driven by part of the *AtHKT1;1* promoter, it is likely that *GFP* expression is also low under non-transpiring conditions. Sundstrom (2011) confirmed that the transgene is expressed in *AtHKT1;1promoter::AtHKT1;1cDNA* lines, however functionality of HKT was not tested. The transgenic lines that were generated by Sundstrom (2011), containing the

AtHKT1;1promoter::*GFP* and *AtHKT1;1promoter*::*AtHKT1;1cDNA* constructs, were obtained for this study for further analysis of *GFP* expression and to test for functionality of the *HKT* transgene.

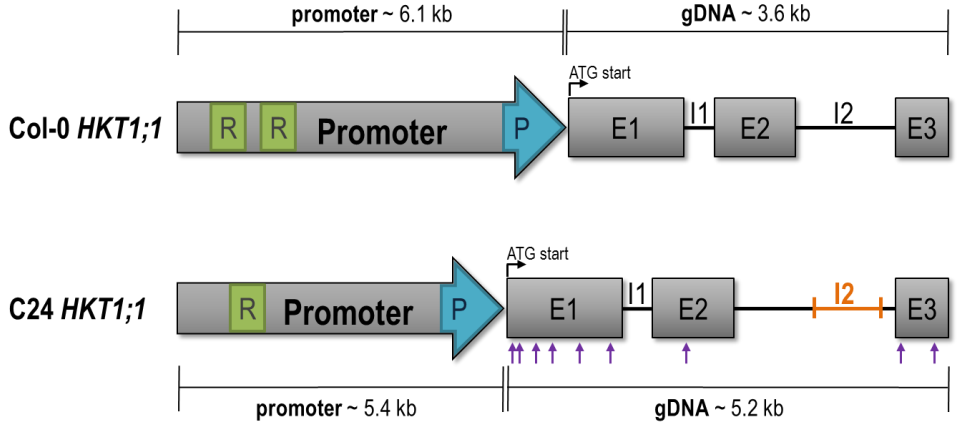

Comparison of the *AtHKT1;1* gene between the ecotypes Col-0 and C24

R Repeat sequence in Col-0 promoter only present once in C24 promoter

P Polymorphic region comparing Col-0 and C24 sequences just 5' of *AtHKT1;1*

↑ 9 amino acid changes in exons due to single nucleotide polymorphisms (SNPs)

I2 1.6 kb insertion in intron 2 in C24 compared to Col-0

Figure 1.3: Comparison of the *AtHKT1;1* promoter and genomic DNA sequence between Arabidopsis ecotype Col-0 and C24.

The approximately 6.1 kb long promoter sequence of Col-0 contains two 700 bp repeat sequences (in green), while the approximately 5.4 kb of C24 promoter sequence contains only one of these repeats (in green). A 240 bp region just 5′ of the ATG start codon (in blue) is highly polymorphic and contains a number of insertions/deletions and SNPs comparing Col-0 and C24. The coding sequence of the Col-0 and C24 *HKT* contains 22 SNPs, resulting in 9 amino acid changes (position indicated with purple arrows). The second intron in C24 contains a 1.6 kb additional sequence, which is not present in Col-0 (indicated in orange).

1.7 Research aims

The Arabidopsis ecotype C24 has been shown to not substantially change the expression pattern of salt responsive genes, unlike other ecotypes such as Col-0 and C24 also accumulates significantly more Na^+ in the shoot than Col-0, while being more salt tolerant (Jha *et al.* 2010). One gene that has been identified to be involved in accumulation of shoot Na^+ is *AtHKT1;1*. It has been hypothesised by Sundstrom (2011) that the control of *AtHKT1;1* expression in Col-0 and C24, leading to differences in shoot Na^+ accumulation, is caused by variations found in the *AtHKT1;1*promoter regions. Preliminary experiments suggested that this is not the case. The aim of this project is to confirm that the Col-0 and C24 promoters are able to drive gene expression, and are therefore not the main determent for the lack of *AtHKT1;1* expression in C24 roots. Furthermore, the project also aims to analyse

transport properties of both HKT proteins, to determine if the 9 amino acid changes result in altered transport properties, aims to test if the insertion in the second intron found in the C24 *AtHKT1;1* gene, results in a lack of *AtHKT1;1* expression in C24 roots. This PhD project will also compare the salt responsiveness of Col-0 and C24 using different salt stress treatments to investigate the potential cause for the difference in gene expression in response to salt stress. The prospects are to set up a screening assay for QTL analysis to identify novel genes involved in the salt signalling pathway.

In order to meet these aims, the following objectives were set:

1. Examine Na^+ and K^+ transport properties of the Col-0 and C24 HKT proteins using the Xenopus oocyte and yeast heterologous expression systems.
2. Analyse *AtHKT1;1promoter::GFP* and *AtHKT1;1promoter::AtHKT1;1cDNA* transgenic lines to evaluate if the Col-0 and C24 *AtHKT1;1* promoter are able to drive target gene expression *in planta*.
3. Investigate the role of the 1.6 kb insertion in the second intron of the C24 *AtHKT1;1* gene by bioinformatics analysis and generating transgenic lines that express variations of the genomic *AtHKT1;1* DNA *in planta*.
4. Develop assays for measuring the Na^+ responsiveness of Arabidopsis seedling to early stages of salinity stress.
5. Expose Col-0 and C24 plants to different salt stress treatments to assess the lack of responsiveness to salt in C24 plants.
6. Evaluate which salt stress treatment in Objective 4, if any, is suitable to be used as a screening assay to perform a QTL mapping.

Chapter 2 **General materials and methods**

2.1 Molecular cloning of expression vectors

2.1.1 Amplification of DNA using polymerase chain reaction (PCR)

DNA fragments of genes, introns and promoters, were amplified using polymerase chain reaction (PCR) (Mullis and Faloona 1987) following the polymerase manufacturer's protocols.

Depending on the final downstream application of the DNA fragment to be amplified, different polymerases were used throughout this study. The standard reaction components and cycling conditions specific for the various polymerases are listed in Table 2.1. Elongase® (Life Technologies™, Mulgrave, Australia), a proof reading enzyme designed to amplify large DNA fragments, was used to amplify DNA to generate entry vector plasmids containing the DNA fragment of interest; QIAGEN *Taq* DNA polymerase (QIAGEN, Chadstone Centre, Australia) was used to verify the presence of plasmid DNA in bacterial clones; and Platinum® *Taq* DNA polymerase (Life Technologies™, Mulgrave, Australia) was chosen for all other PCRs that did not require high-fidelity. All primers were designed using primer3 (Rozen and Skaletsky 2000) and synthesised by Geneworks Pty. Ltd. (Thebarton, South Australia, Australia).

DNA fragments were visualised using agarose gel electrophoresis (section 2.1.2).

Table 2.1: Overview of polymerase chain reaction components and cycling conditions used for cloning and analysis

Component	Elongase®	QIAGEN DNA polymerase	Platinum® *Taq* DNA polymerase
PCR buffer	1x Buffer B	1x Coral loading buffer	1x PCR buffer
$MgCl_2$	2 mM[1]	1.5 mM	1.5 mM
Solution to aid difficult PCRs	-	1x Q-solution	-
Forward primer	200 nM	200 nM	200 nM
Reverse primer	200 nM	200 nM	200 nM
dNTPs	200 µM	200 µM	200 µM
Polymerase	1 U	1 U	0.6 U
Template DNA (ng)	100 to 200 ng	100 to 200 ng	10 to 200 ng
Cycling conditions:			
Denaturation	3 min at 95 °C	4 min at 95 °C	4 min at 95 °C
Denaturation	30 s at 95 °C	45 s at 95 °C	45 s at 95 °C
Annealing	30 s at 55 °C[2]	45 s at 55 °C[2]	45 s at 55 °C[2]
Polymerisation	1 min/kb at 68 °C	1 min/kb at 72 °C	40 s/kb at 72 °C
Repeat step 2 to 4; 25-35 ×			
Final elongation	10 min at 68 °C	10 min at 72 °C	10 min at 72 °C

[1] Mg^{2+} is already contained in Elongase buffer B. [2] The annealing temperature is dependent on primer sequence, enzyme, buffer components and template characteristics. The standard temperature was 55 °C and was adjusted if necessary.

2.1.2 Electrophoretic separation of nucleic acid

Agarose gel electrophoresis was used for the preparative isolation and analysis of DNA-fragments, which had been generated either by PCR or restriction digest, as well as for the analysis of plasmid DNA. The separation of small fragments (size < 200 bp) was performed using 2 % (w/v) agarose gels, whereas bigger fragments (size > 200 bp) were separated in 1 % (w/v) agarose gels. The desired amount of agarose powder was mixed with TAE buffer (40 mM Tris-acetate, 1 mM EDTA, pH 8) and dissolved by heating gently in a microwave. SYBR® Safe (Life Technologies™, Mulgrave, Australia) was added to a final concentration of 0.006 % (v/v) to visualise DNA in the gel.

DNA samples (~300 ng) were supplemented with 6 × DNA loading buffer (15 % Ficoll, 0.2 % Orange G) and loaded into the wells of the solidified agarose gel. A voltage of 120 V was applied for 30 to 50 min until the DNA bands were sufficiently separated. DNA fragment sizes and concentrations were estimated using 5 µL of HyperLadder™ I (Bioline, Alexandria, Australia) as a reference. The DNA in the agarose gel was visualised using a UV transilluminator (Gelflash, Syngene, Cambridge, United Kingdom).

2.1.3 DNA extraction from agarose gels

To isolate desired DNA fragments from agarose gels, fragments were excised from a gel using low UV light and a scalpel before DNA was extracted with an Isolate PCR and Gel Kit (Bioline, Alexandria, Australia) following manufacturer's instructions. In brief, the slice of agarose containing the DNA was dissolved in binding buffer (200 µL per 100 mg agarose). The binding buffer contains chaotropic salts that facilitate dissolving of the agarose and brings the pH to 5.0 - 6.0. The solution was then transferred onto spin columns, supplied in the kit. Due to the slightly acidic pH of the solution, DNA is bound to the column's silica membrane while salts and small fragments of nucleic acid (nucleotides and primers) were removed by washing the membrane twice with washing buffer. The silica membrane was dried by centrifugation and DNA eluted with 20 µL of sterile water (pH 8.5).

2.1.4 Cloning PCR products into pCR™8/GW/TOPO TA Gateway® entry vectors

Purified PCR fragments were ligated into the entry vector pCR™8/GW/TOPO Gateway® (pCR8 for short) (Life Technologies™, Mulgrave, Australia) by TA-cloning. To obtain an adenosine overhang which facilitates TA-cloning, purified PCR fragments were mixed with 0.5 U Platinum® Taq polymerase in 1 × PCR buffer, 2.5 mM dATP and 1.5 mM $MgCl_2$ and incubated for 15 min at 72 °C. DNA fragments were then cloned into a pCR8 following the manufacturer's instructions. Briefly, 1 µL

of the desired DNA fragment was incubated for 5 min at RT with 1 µL salt solution, 1 µL pCR8 and ddH_2O to bring the mixture up to a volume of 6 µL. The incubation time was prolonged to o/n for difficult fragments or fragments larger than 2 kb. An aliquot of 2 µL of the mixture was transformed into TOP10 cells (section 2.1.6) and resulting bacterial colonies were subject to plasmid DNA extraction (section 2.1.7). Plasmid DNA was first analysed using restriction digest (section 2.1.8) and the sequence of positive plasmid DNA was determined by BigDye® reaction and capillary separation (section 2.1.11) to ensure the plasmid contained the correct nucleotide sequence. The pCR8 vector allowed the cloning into destination vectors using a Gateway® recombination reaction (section 2.1.10).

2.1.5 Making chemically competent cells

The transformation of plasmid DNA into *Escherichia coli* (*E.coli)* requires competent cells of a strain that is amenable to transformation. The standard strain used for most entry vectors was TOP10 (Life Technologies™, Mulgrave, Australia). The strain DB3.1 can tolerate plasmids containing the lethal *ccdB* gene and was therefore used for the amplification of empty Gateway® enabled destination vectors which had yet to have a DNA fragment of interest inserted into the Gateway® site. Chemically competent *E.coli* cells were prepared as described by Hanahan (1985). Briefly, a single colony of the required *E.coli* strain was inoculated into 2.5 mL LB medium (10 g/L tryptone, 5 g/L yeast extract, 5 g/L NaCl, pH 7.5) and grown o/n at 37 °C with constant shaking (225 rpm). The o/n culture was subcultured by inoculating 2.5 mL of culture in 250 mL of LB supplemented with 20 mM $MgSO_4$ in a 1 L flask. Cells were grown at 37 °C with constant shaking (225 rpm) until the optical density at 600 nm (OD_{600}) reached 0.4 - 0.6 absorbance units. Cultures were centrifuged to a pellet at 5,500 *g* for 5 min at 4 °C and subsequently kept at 4 °C at all times. The cell pellet was gently resuspended in 100 mL of ice-cold TFB1 (30 mM potassium acetate, 10 mM $CaCl_2$, 50 mM $MnCl_2$, 100 mM $RbCl_2$, 15% (v/v) glycerol, pH 5.8 with acetic acid, sterile filtrated) and incubated for 5 min at 4 °C. The cells were centrifuged at 4,500 *g* for 5 min at 4 °C to obtain a cell pellet that was resuspended in 10 mL of ice-cold TFB2 (100 mM 3-(N-moprpholino) propanesulfonic acid (MOPS), 75 mM $CaCl_2$, 10 mM $RbCl_2$, 15 % glycerol, pH 6.5 with KOH, sterile filtrated). Cells were incubated a further 60 min at 4 °C and dispensed in 50 µL aliquots, snap frozen in liquid nitrogen and stored at - 80 °C until used for transformation.

2.1.6 Transformation of plasmid DNA into *E.coli*

Chemically competent *E.coli* was transformed using the heat shock method. For this, a 50 µL aliquot of competent cells (section 2.1.5) was thawed on ice for 10 min, then 10 pg to 200 ng of plasmid

DNA was added to the culture and the cells and DNA incubated together for 30 min on ice. The plasmid-containing cell suspension was heat shocked at 42 °C for 30 s to allow the plasmid DNA to enter the cells and the suspension was immediately transferred to ice for 5 min. The suspension was supplemented with 500 µL of LB and incubated at 37 °C for 1 h with shaking at 225 rpm. A 200 µL aliquot of cells was spread on LB agar plates containing the correct antibiotic(s) for selection of transformed cells and incubated o/n at 37 °C. The antibiotic used for selection depended on the antibiotic resistance gene in the entry and destination vectors. The entry vector used in this study was pCR8, which mediates spectinomycin resistance, and all destination vectors (pMDC107, pMDC100noT and pMDC162) mediate kanamycin resistance in bacteria. The bacterial colonies were subject to plasmid DNA extraction for further analysis (section 2.1.7).

2.1.7 Isolation of plasmid DNA

Plasmid DNA was isolated for either restriction analysis, verification of the insert by sequencing, or for transformation into bacteria. Depending on the downstream application of plasmid DNA, two methods of plasmid isolation were used as outlined below:

2.1.7.1 Mini-preparation of plasmid DNA with standard purity

Isolation of plasmid DNA according to Birnboim and Doly (1979) delivers standard quality plasmid DNA, which is sufficient for restriction analysis. Briefly, the cell pellet from a 2 mL o/n bacterial culture was resuspended in 100 µL of solution I (50 mM glucose, 25 mM Tris-HCL, pH 8.0 and 10 mM EDTA). Plasmid DNA was lysed from the cells by the addition of 200 µL of solution II (0.2 M NaOH and 1% SDS) and cell debris was precipitated by addition of 150 µL of solution III (3 M potassium acetate, pH 4.8 with acetic acid). After centrifugation at 16,000 *g* for 15 min, nucleic acids in the remaining supernatant were precipitated by the addition of 750 µL of isopropanol (100% v/v) and incubating for 15 min at RT. A pellet of nucleic acid was formed by centrifugation for 15 min at 16,000 *g* in a bench top centrifuge, was washed with 70% (v/v) ethanol and air dried. The plasmid DNA was then resuspended in 30 µL of MQ-water containing 50 µg/mL of RNase (Thermo Fisher Scientific Australia Pty Ltd., Scoresby, Australia) for removal of contaminating RNA. The plasmid DNA was used for further analysis such as restriction digests (section 2.1.8).

2.1.7.2 Mini-preparation of plasmid DNA with high purity

High purity plasmid DNA, required for cloning and sequencing purposes, was obtained using the ISOLATE Plasmid Mini Kit (Bioline, Alexandria, Australia), following manufacturer's instructions. Briefly, after alkaline lysis of the bacterial cells using the solutions contained in the kit and removal of

cell debris, the supernatant containing plasmid DNA was transferred onto spin columns provided in the kit. Due to its pH, plasmid DNA bound to the column's silica membrane while salts and other contaminations were removed by washing the membrane twice with washing buffer. The silica membrane was dried by centrifugation and plasmid DNA eluted with 20 µL of sterile water (pH 8.5).

2.1.8 Analysis of plasmid DNA using restriction digest

Restriction analysis was performed to verify the presence and orientation of a specific DNA insert within a vector. Restriction enzymes, which cut open the plasmid DNA, were used to cleave the plasmid DNA into characteristic fragments, which were then analysed on an agarose gel (section 2.1.2). The chosen restriction enzymes cut in the vector backbone and in the inserted fragment of DNA. Ideally, the cut occurs towards either the 5' or 3' end of the inserted fragment, thereby giving different size bands on an agarose gel depending on whether the fragment had been inserted in the correct orientation or not. The size of DNA fragments observed as bands in the agarose gel was compared to the predicted size of the fragments resulting from the *in silico* digest using the sequence analysis program Vector NTI Advance™ 11.0 (Life Technologies™, Mulgrave, Australia).

A typical digest had the following composition: 2 µL of standard purity plasmid DNA (~ 500 ng), 1 µL of 10 × restriction buffer appropriate for the enzyme, 1 µL of 10 × BSA (if required for the restriction enzyme), 1 U of restriction enzyme and sterile water to bring the mixture to a final volume of 10 µL. The reaction was incubated for 1 h at the temperature optimal for the given restriction enzyme and the size of DNA fragments visualised using agarose gel electrophoresis (section 2.1.2). If the fragments of the restriction digest were to be used for a ligation reaction (section 2.1.9), the total reaction volume was increased to 50 µL, the incubation time prolonged to 4 h and 10 U of the appropriate enzyme were used.

2.1.9 Ligation of DNA fragments

A ligation reaction was used to covalently connect two fragments of double stranded DNA with overlapping, complementary ends that were generated through restriction digest (section 2.1.8).

For efficient ligation of vector and insert fragment, approximately three-times more insert fragments were used than vector fragments. The desired amount of insert fragments per 100 ng vector DNA was therefore determined using the following equation: ng of insert DNA = (size of insert DNA/size of vector DNA) · 3 · 100ng of vector DNA.

A standard reaction mix of T4 DNA Ligase (Life Technologies™, Mulgrave, Australia) consisted of 100 ng vector, the appropriate amount of insert, 4 µL of 5 × ligase buffer, 1 µL of T4 DNA Ligase (1 U/ µL) and water to bring the mixture to a final volume of 20 µL. After incubation at 15 °C o/n, the mixture was transformed into chemically competent *E.coli* TOP10 cells (section 2.1.5) and the resulting bacterial colonies were subject to plasmid DNA extraction for further analysis (section 2.1.7).

2.1.10 Gateway® cloning into destination vectors (LR reactions)

The amplified DNA fragment of interest was transferred from the pCR8 entry vector into the destination vector by recombination. The respective vectors are detailed in subsequent chapters. In most cases this is a binary vector facilitating the expression of the gene of interest *in planta*. Recombination was carried out using LR Clonase™ II (Life Technologies™, Mulgrave, Australia) following the manufacturer's instructions. Briefly, 100 ng of the entry clone and 100 ng of the destination vector in a total volume of 4 µL are supplemented with 2 µL of LR Clonase™ and incubated for 1 h at RT. The incubation time was prolonged to o/n for vectors over 10 kb. An aliquot of 2 µL of the mixture was transformed into TOP10 cells (section 2.1.6) and resulting bacterial colonies were used for plasmid DNA extraction (section 2.1.7). Plasmid DNA was first analysed using restriction digest (section 2.1.8) and the sequence of positive plasmid DNA was determined by BigDye® reaction and capillary separation (section 2.1.11) to ensure the plasmid contained the correct nucleotide sequence and confirm insert orientation. The two most commonly used primers for the sequencing reaction were GWI and GWII. GWI is the forward primer, annealing upstream of the inserted DNA fragment and GWII is the reverse primer, annealing downstream of the inserted DNA fragment (Table 2.2).

Table 2.2: Sequences of primers used for sequencing reactions

Primer name	Sequence (5'-3')	Annealing location
GWI	GTTGCAACAAATTGATGAGCAATGC	upstream of inserted DNA fragment
GWII	GTTGCAACAAATTGATGAGCAATTA	downstream of inserted DNA fragment

2.1.11 Sequencing of plasmid DNA

The BigDye® Terminator V3.1 Cycle Sequencing Kit (Life Technologies™, Mulgrave, Australia) was used to determine the nucleotide sequence of vectors by Sanger sequencing. The reaction was done

in a 10 µL volume using 100 ng of plasmid DNA, 3.5 µL of BigDye® buffer, 1 µL of BigDye® Enzyme mix (which contains the desired mix of dNTPs and ddNTPs), 3.2 pmol of one primer and sterile water to bring the mixture to a final volume of 10 µL. The reaction was completed in a thermo cycler under the following conditions: 96 °C for 1 min, then 29 cycles of: 96 °C for 10 s, 50 °C for 5 s and 60 °C for 4 min. The product was cleaned by precipitation of labelled DNA using 75 µL of 0.2 mM $MgSO_4$ in 70% (v/v) ethanol for 15 min at RT, followed by centrifugation for 15 min at 16,000 *g* in a bench top centrifuge. The pellet was washed with 70% (v/v) ethanol and air dried before samples were submitted to the Australian Genome Research Facility Ltd. (AGRF, Urrbrae, Australia) for capillary separation and sequence determination. The obtained sequences were analysed using the program Vector NTI Advance™ 11.0 (Life Technologies™, Mulgrave, Australia).

2.2 Growth of *Arabidopsis thaliana*

2.2.1 Growth facilities

Five different facilities were used for the growth of Arabidopsis. While the Long Day Arabidopsis growth facility and WI4 were mainly used for increasing seed numbers of desired plant lines or to raise plants suitable for transformation, the Short Day Arabidopsis growth room and The Plant Accelerator® growth room WI3 were used to carry out salt stress experiments using plate and hydroponically grown plants. Calcium measurements (Chapter 6) were performed in the laboratory of Dr. Alex Webb (Dept. Plant Sciences, The University of Cambridge, Cambridge, UK) and their facilities were used for plant growth in growth chambers.

Table 2.3: Overview of plant growth facilities and growth conditions used in this study

Growth Facility	Light/dark photoperiod (h)	Temperature day/night (°C)	Light intensity (µmol m-2 s-1)	Humidity (%)
Long Day Arabidopsis (Undercroft)	16/8	23/21	100	60-75
Short Day Arabidopsis (Undercroft)	10/14	23/23	100	60-75
WI4 long day in The Plant Accelerator®	14/10	23/20	120	60-75
WI3 short day in The Plant Accelerator®	10/14	23/20	100	60-75
Growth chamber, Dept. Plant Sciences, The University of Cambridge	12/12	22/22	80	n.d.

n.d. not determined

2.2.2 Growth of Arabidopsis in soil

A standard soil mixture containing fertilizer was used to increase seed numbers of desired plant lines and to grow Arabidopsis for transformation. A 100 L batch of soil consisted of 25 L sand, 25 L perlite, 25 L vermiculate, 25 L peatmoss, 100 g iron sulphate, 300 g Osmocote® Plus (NPK of 13.4 : 1.5 : 4.9) (Scotts, Bulkham Hills, Australia), 200 g dolomite, 50 g gypsum, 100 g agricultural lime and 40 g hydrated lime. The pH range of the soil was adjusted between 5.7 and 5.9 with KOH.

Artificial soil without fertilizer (one batch consisted of 3.6 L medium grade perlite, 3.6 L Coira and 0.25 L river sand) was used for salt stress experiments to control for the concentration of nutrients and NaCl in the soil. Plants were watered once per week with basic nutrient solution [2 mM $Ca(NO_3)2$, 15 mM KNO_3, 0.5 mM $MgSO_4$, 0.5 mM NaH_2PO_4, 15 mM NH_4NO_3, 0.025 mM NaFe(III)EDTA, 0.2 mM H_3BO_3, 1 µM Na_2MoO_3, 1 µM $NiCl_2$, 2 µM $ZnSO_4$, 4 µM $MnCl_2$, 2 µM $CuSO_4$, 1 µM $CoCl_2$, 0.005 µM $SrCl_2$, 0.5 µM Na_2SiO_3 and 0.001 µM $CdCl_2$]. Additional NaCl was supplemented as stated for each individual experiment in the respective chapters.

Moist soil was filled into standard pots (8 × 6 × 6 cm) and five to fifteen Arabidopsis seeds were spread over the soil. Pots were placed in a tray and covered with a mini-greenhouse lid (tray and lid from Smoult, Kersbrook, SA, Australia) to maintain humidity until 2 wk after seed germination. The pots were watered with reverse osmosis water as desired, approximately two to three times per wk. Excess numbers of plants were removed 2 wk after germination leaving one plant per pot for optimal growth.

2.2.3 Growth of Arabidopsis on solid Murashige and Skoog (MS) media

Surface sterilised plants were grown on solid MS media for salt stress experiments and for selection of transformed plants. Surface sterilisation of Arabidopsis seeds was carried out in 2 mL or 10 mL tubes. The desired amount of seed was poured into the tube and covered with 70 % (v/v) ethanol. The ethanol was removed after two minutes by decanting and replaced with a 50 % (v/v) bleach solution (Domestos (49.9 g L^{-1} sodium hypochlorite, Unilever Australasia, North Rocks, Australia)) and incubated for 5 min with occasional mixing. The bleach was decanted and the seeds washed at least five times with sterile ddH_2O. Seeds were immersed in H_2O for 2 d at 4 °C in the dark to reduce seed dormancy and promote even germination. Square petri dishes (100×100×20 mm, Sarstedt, Adelaide, Australia) were filled with 50 mL of sterile ½ strength MS-agar [0.22 % (w/v) MS (PhytoTechnology Laboratories, KS, USA) and 0.8 % (w/v) agar (Difco™ Agar, granulated, BD Diagnostic, Sparks, USA), pH 5.7 with KOH], from here on referred to as MS-plates. The sterilised seeds were placed individually onto the agar and the plate was sealed with 3M™ Micropore™ tape

(3M™, Pymble, Australia). If not stated otherwise, the plates were placed vertically in a growth room under short day conditions.

2.2.4 Growth of Arabidopsis in hydroponics

The set up for hydroponically grown Arabidopsis seedlings has recently been described in detail by Conn *et al.* (2013) and was used here with minor modifications (Figure 2.1). Briefly, lids of microfuge tubes were prepared with a small hole in the middle and filled with ½ strength MS-agar from the inside. Up to 3 individual seeds were placed onto the agar from the outside of the lid, in the middle of the hole, and lids were placed in the holes of a pizza tray. The pizza tray was placed in a saucer holding 2 L of liquid ½ strength MS medium. The growth solution was replaced once per week and excessive seedlings were removed after 10 days, leaving one seedling per lid. The lids containing the seedlings were transferred 3 wk after germination into an aerated 12 L hydroponics tank filled with basal nutrient solution [2 mM NH_4NO_3, 3 mM KNO_3, 0.1 mM$CaCl_2$, 2 mM KCl, 2 mM $Ca(NO_3)_2 \cdot 4\ H_2O$, 2 mM $MgSO_4 \cdot 7\ H_2O$, 0.6 mM KH_2PO_4, 1.5 mM NaCl, 50µM NaFe(III)EDTA, 50µM H_3BO_3, 50µM $MnCl_2 \cdot 4\ H_2O$, 50µM $ZnSO_4\ 7H_2O$, 50µM $CuSO_4 \cdot 5\ H_2O$, 50µM Na_2MoO_3, pH 5.6 with KOH] for another 2 wk until the start of the salt stress treatment. Salt stress application and sampling are detailed in the relevant chapter.

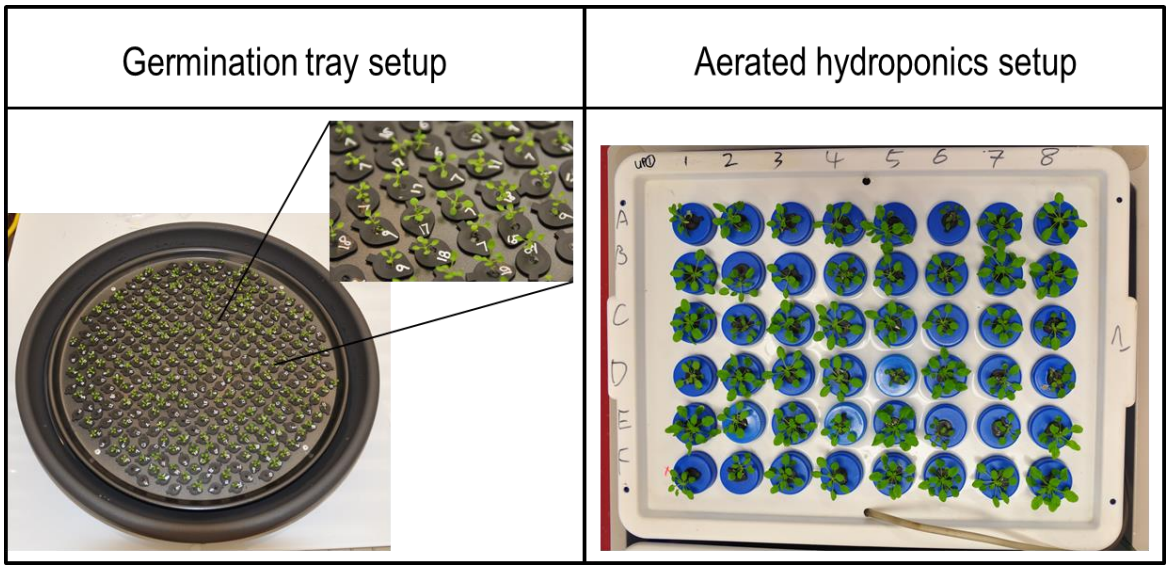

Figure 2.1: Image of germination tray and hydroponics setup.

The germination tray was made out of a pizza tray with holes, in which lids of microcentrifuge tubes were fitted. The lids were filled with ½–strength MS agar and contained a small hole in which the seed was placed. The seedling grew through the agar into the liquid media provided in the saucer underneath. After 3 wk growth, the lids were placed into aerated hydroponic tanks (pump for aeration not shown) for a further 2 wk until start of the salt stress treatment.

2.3 *Agrobacterium tumefaciens* mediated transformation of Arabidopsis

A frequently used method for transformation of Arabidopsis is the floral dipping method (Clough and Bent 1998). Immature floral buds of Arabidopsis are immersed in a solution of *A. tumefaciens*, resulting in an infection of the plant cell by *A. tumefaciens*. Parts of the plasmid DNA carried by the bacterium, containing the desired genes of interest, are inserted into the plant's chromosome. The seed produced from the siliques of the transformed floral buds, will be a mixture of transformed and non-transformed individuals. Successfully transformed seeds can be selected by germinating them on a media containing antibiotics, or spraying soil grown seedlings with a herbicide.

2.3.1 Generating chemically competent *A. tumefaciens*

The transformation of plasmid DNA into *A. tumefaciens* requires competent cells that are amenable to transformation. Chemically competent *A. tumefaciens* were generated using the protocol by Weigel and Glazebrook (2006). Briefly, laboratory stocks of *A. tumefaciens* strains AGL-1 or GV3101 were spread on solid LB media containing 50 µg/mL rifampicin and 50 µg/mL carbenicillin or 50 µg/mL rifampicin and 50 µg/mL kanamycin, respectively. A 200 mL liquid culture of LB media containing the appropriate antibiotics was inoculated with 1 mL of the chosen strain of *A. tumefaciens* and incubated at 28 ºC with vigorous agitation o/n. The culture was started in the late afternoon to be harvested the following morning when the *A. tumefaciens* culture reached an OD_{600} of 0.5-0.8. The cells were collected by centrifugation at 3000 *g* for 15 minutes at 4 °C. The pellet was then washed with sterile TE buffer (10 mM Tris-HCl, 1 mM EDTA, pH 8.0), resuspended in 20 mL of LB and distributed in 250 µL aliquots into microcentrifuge tubes. The aliquots were snap frozen in liquid nitrogen and stored at -80 °C until used for transformation.

2.3.2 Transformation of *A. tumefaciens* with plasmid DNA

The binary vectors used for *A. tumefaciens* mediated transformation were generated as described in section 2.1.10. The destination vector contains the genetic elements for amplification in *A. tumefaciens* and expression of the gene of interest *in planta.* An aliquot of *A. tumefaciens* cells was defrosted on ice before addition of 100-200 ng of plasmid DNA and incubation on ice for 15 min. The cells were snap frozen in liquid nitrogen for 5 min before incubating for 5 min in a 42 °C water bath to facilitate plasmid entry. Cells were transferred to ice for 5 min and then the entire 250 µL aliquot was spread onto solid LB media containing the appropriate antibiotics and incubated at 28 °C for 3 d. Single colonies of transformed *A. tumefaciens* were picked and analysed using colony PCR to confirm the presence of the destination vector (section 2.1.1).

2.3.3 Transformation of Arabidopsis by floral dipping

Arabidopsis plants were grown under long day conditions until flowering. The first bolt was cut back to initiate the emergence of secondary bolts, providing a large number of immature flower clusters. The best stage for floral dipping is before siliques are formed.

A positive colony of *A. tumefaciens* was used to inoculate 3 mL of LB containing 50 µg/mL rifampicin, 50 µg/mL carbenicillin and 50 µg/mL kanamycin. The culture was incubated at 30 °C with shaking (200 rpm) for 2 d and then used to inoculate 250 mL of LB containing the appropriate antibiotics, which was also incubated at 30 °C with shaking (200 rpm) o/n. The cells were collected by centrifugation at 3000 *g* for 15 min at 4 °C. The pellet was resuspended in 500 mL of 5 % (w/v) sucrose supplemented with 0.01 % (v/v) Silwet L-77 (Lehle seeds, Texas, USA). The emerging Arabidopsis flowers were submerged in this solution for 30 s to allow the bacteria to attach to the plant. The whole plant was then covered with a humidity lid and placed o/n in an area with reduced light before returning it onto the shelf in the growth room until the plant reached maturity and seeds were harvested.

2.3.4 Selection of transformed Arabidopsis

The method for selecting successfully transformed plants depended on the resistance encoded on the transformed destination vector. Plants transformed with plasmids containing the *bar* gene harbour resistance to the herbicide glufosinate (also known as BASTA®). In this case, seeds were spread evenly on soil and grown for approximately 2 wk before spraying with 0.1 % (v/v) BASTA® (Bayer CropScience, East Hawthorn, Australia) supplemented with 0.02 % (v/v) Silwet L-77 (Lehle seeds, Texas, USA). The treatment was repeated within 1 wk until senescence of untransformed plants was visible; surviving plants were transferred to individual soil pots and grown to maturity. If the plasmid conferred resistance to hygromycin or kanamycin, seeds were surface sterilised (see paragraph 2.2.3) and placed on MS-plates (as described in 2.2.3) containing 40 µg/mL hygromycin or kanamycin, respectively, and 200 µg/mL cefotaxime (to prevent growth of any remaining *A. tumefaciens)*. The surviving seedlings were taken off the plate after 2 wk and placed on wet soil and covered with a lid to maintain humidity for 2 wk, before returning to normal growth conditions.

2.4 Analysis of plant DNA

2.4.1 Extraction of genomic DNA from plant material

The DNA of plant material was used for Southern Blot analysis and genotyping. The phenol/chloroform/iso-amyl alcohol extraction method was used to obtain high quality plant DNA for genotyping with intention of subsequent Southern Blot analysis (modified from Guillemaut and Maréchal-Drouard 1992) and the Edward's buffer method was used to obtain standard purity of DNA for PCR genotyping of the plant material (modified from Kotchoni and Gachomo 2009). Both methods are briefly described below.

2.4.1.1 Phenol/chloroform/iso-amyl alcohol extraction method

Plant material was collected in 10 mL tubes, snap frozen in liquid nitrogen and ground to a fine powder by vortexing with three to five sterilised steel balls (Ø 2 mm). The powder was suspended in 1.4 mL of DNA extraction buffer [1 % (v/v) sarkosyl, 100 mM Tris-HCl, 100 mM NaCl, 100 mM EDTA, 2 % (w/v) polyvinyl-polypyrrolidone (PVPP, Sigma-Aldrich, Castle Hill, Australia), pH 8.5 with HCl] and thoroughly mixed for 1 min before addition of 1.4 mL of phenol/chloroform/iso-amyl alcohol (25:24:1). After a further 15 min mixing, the samples were centrifuged at 3600 *g* for 10 min. The aqueous phase was transferred into a 2 mL microcentrifuge tube and DNA precipitated with 100 µL of 3 M sodium acetate and 800 µL of isopropanol. The samples were left for 1 h at RT before centrifugation at 10,000 *g* for 10 min. The supernatant was removed and the pellet washed in 1 mL 70 % (v/v) ethanol. The pellet was air dried and resuspended in 100 µL of ddH_2O containing 10 mg/mL of RNase (Thermo Fisher Scientific Australia Pty Ltd., Scoresby, Australia). The obtained DNA is of high purity and was used for amplification of genes using standard PCR (section 2.1.1) with the intention to use the DNA for subsequent Southern Blot analysis.

2.4.1.2 DNA extraction with modified Edwards buffer

Plant material was collected in 2 mL microcentrifuge tubes and ground to a fine powder by vortexing with three to five metal balls (Ø 2 mm). The powder was suspended in 400 µL of modified Edward's buffer (1 % SDS, 0.5 M NaCl) and thoroughly mixed for 1 min. The mixture was left at RT for 1 h and mixed again thoroughly for 2 min before centrifugation at 10,000 *g* for 2 min. The supernatant (300 µL) was transferred to a fresh microfuge tube and DNA precipitated with 300 µL of isopropanol. The samples were left at RT for 10 min and centrifuged at 1,000 *g* for 10 min to obtain a pellet, which was then air dried and resuspended in 30 µL of ddH_2O. The obtained DNA is suitable for genotyping using standard PCR (section 2.1.1).

2.5 Analysis of plant mRNA

Plant mRNA was used to analyse transcript levels of genes of interest. For this, total RNA was extracted, containing the desired mRNA, from which cDNA was synthesised to analyse the abundance of gene transcripts using quantitative Real Time PCR (qPCR), semi-quantitative PCR (semi-qPCR) or reverse transcription-PCR (RT-PCR). The methods are detailed below.

2.5.1 Extraction and purification of RNA from plant material

Extraction of total RNA was performed following the protocol of Chomczynski (1993). Briefly, Arabidopsis leaves were collected in 2 mL microfuge tubes and frozen in liquid nitrogen. The material was ground to powder with metal balls (Ø 2 mm) before being suspended in 1 mL of TRIzol®-like reagent [38 % (v/v) phenol pH 4.3 (Sigma Aldrich®, Castle Hill, Australia), 12 % (w/v) guanidine thiocyanate (Sigma Aldrich®, Castle Hill, Australia), 7 % (w/v) ammonium thiocyanate (Sigma Aldrich®, Castle Hill, Australia), 3% (w/v) 3 M sodium acetate pH 5, 5% (v/v) glycerol)]. After 5 min, 200 µL of chloroform was added and the mixture was vigorously shaken before centrifugation at 12,000 *g* for 15 min at 4 °C. The aqueous layer at the top was transferred into a microfuge tube containing 500 µL of isopropanol to precipitate RNA. After incubation for 1 h at RT, the sample was spun at 12,000 *g* for 10 min to obtain a pellet. The supernatant was removed and the pellet washed with 1 mL of 70% (v/v) ethanol and resuspended in 25 µL of sterile water.

Contaminating DNA was removed from RNA samples using the DNA-free™ kit (Ambion®, CA, USA) according to the manufacturer's instructions. Briefly, each sample was supplemented with 2.5 µL of DNase-I buffer and 1 µL (2 U) of DNase I, gently mixed and incubated at 37 °C for 30 min. The reaction was stopped by addition of 5 µL of DNase I Inactivation reagent. After thorough mixing and 3 min incubation, the suspension was centrifuged at 10,000 *g* for 1 min to pellet the Inactivation reagent. The clear top phase containing the RNA was transferred into a fresh microfuge tube and stored at -80 °C.

In order to estimate the quantity and quality of extracted RNA, 2 µL of RNA was analysed using gel electrophoresis (section 2.1.2). Good quality RNA was used for cDNA synthesis, showing a typical double band pattern for the 28S and 18S RNA and a fainter band of lower molecular weight indicating the tRNAs. The brightness of bands is indicative of the RNA quantity and was used to confirm uniformity of RNA quantity between samples to ensure equal amounts are used for cDNA synthesis.

2.5.2 Synthesis of cDNA

Two main variations of cDNA synthesis were used. To obtain total cDNA, an oligo $d(T)_{20}$ primer was used which allows synthesis of cDNA from mRNA that contains a poly(A)-tail. Gene specific cDNA was synthesised by using a gene specific primer, as listed in the relevant chapter. The Superscript III Reverse Transcriptase kit (Life Technologies™, Mulgrave, Australia) was used with the following protocol: in a 0.5 mL microcentrifuge tube 1 µg of RNA was mixed with 1 µL of primer [either $oligo(dT)_{20}$ or gene specific primer (50 µM)], 1 µL of 10 mM dNTP and ddH_2O, to a total volume of 13 µL. The mixture was heated to 65 °C for 5 min, immediately transferred onto ice and 7 µL of the Master RT mix (4 µL 5 × first strand buffer, 1 µL 0.1 M DTT, 1 µL RNaseOUT, 1 µL 50 U reverse transcriptase) was added and mixed gently. The mixture was incubated at 50 °C for 1 h and heated to 70 °C for 15 min to terminate the reaction. The synthesised cDNA was stored at -20 °C.

2.5.3 Quantitative Real-Time-PCR (qPCR)

Quantitative Real-Time PCR (q-PCR) was performed by Neil Shirley and Ms. Yuan Li (ACPFG Pty. Ltd., Adelaide, Australia) as outlined in Burton *et al.* (2008). Briefly, the synthesised cDNA samples (section 2.5.2) were used as templates in PCR reactions to amplify a characteristic fragment of the gene of interest. Reactions were carried out in a RG6000 Rotor-Gene Real Time Thermal Cycler (Corbett Research, Sydney, Australia). The reaction mixture contained the labelling substance iQ™ SYBR® green PCR reagent (Bio-Rad Laboratories, Gladesville, Australia) to enable online detection of PCR products by fluorescence. Initially, three control genes (*Cyclophilin, GAPdH and Actin2*) were tested to normalise expression data. As *Actin2* (*At3g18780*) showed low variation between replicates, it was consequently used to normalise data in qPCR-experiments and was also chosen for semi-qPCR experiments (section 2.5.4). Primers are listed in the respective chapter.

2.5.4 Semi-quantitative PCR (semi-qPCR) and reverse transcription-PCR (RT-PCR)

Semi-qPCR is a method to estimate transcript abundance using a normal PCR reaction and visualising fragments using agarose gel electrophoresis. This method allows comparison of transcript abundance in a cost effective way. However, the data obtained with this method is more variable than qPCR results and the exact transcript copy number cannot be determined. PCR reactions were performed using Platinum® *Taq* (section 2.1.1) with synthesised cDNA as template (section 2.5.2) using a range of PCR cycles low enough not to reach reaction saturation (usually 21 to 27 cycles). The obtained PCR products were separated using agarose gel electrophoresis (section 2.1.2) and DNA was quantified by measuring the band intensity (minus background intensity) using GIMP

2.6.11 GNU Image Manipulation Program (www.gimp.org). Expression of *Actin2* was found to remain stable between replicates and was not influenced by salt treatment. It was therefore used for normalisation. Primer sequences are listed in the respective chapters.

RT-PCR is a method to determine the presence or absence of a transcript. This method also utilised a PCR reaction to amplify a fragment from cDNA and visualisation of the fragment using agarose gel electrophoresis. As opposed to semi-qPCR, the bands in RT-PCR are not quantified and only evaluated for presence or absence.

Chapter 3 **Functional characterisation of AtHKT1;1 from Col-0 and C24 in heterologous expression systems**

3.1 Introduction

Comparison of the protein sequence of AtHKT1;1 from Col-0 and C24 revealed nine amino acid changes between the two ecotypes. To test whether these amino acid changes lead to altered transport activity, the two encoded AtHKT1;1 proteins have to be studied in more detail. *In planta*, AtHKT1;1 has been linked to the retrieval of Na^+ from the stele, thus reducing the amount of Na^+ that is translocated to the shoot. A reduced function of the C24 AtHKT1;1 protein, together with lower expression levels of *AtHKT1;1* may account for the increased translocation of Na^+ to the shoot and reduced Na^+ content in the root as compared to Col-0. Heterologous expression systems are a frequently used approach to initially characterise transport properties of plant membrane transport proteins and offer the opportunity to study them individually, outside of the complex context of the plant membrane (Dreyer et al. 1999, Gilliham 2007, Tester 1997). A variety of heterologous expression systems are used to analyse properties of transport proteins. Popular systems, that have also been employed in this study, include electrophysiological characterisation of the desired protein in *Xenopus laevis* (Xenopus, African clawed frog) oocytes and functional screening using the yeast *Saccharomyces cerevisiae* or *Schizosaccharomyces pombe* (Dreyer *et al.* 1999). To a lesser extent *Escherichia coli* (*E.coli*), insect cells or mammalian cell lines can also be used for the characterisation of plant transport proteins (Dreyer *et al.* 1999). The main advantage of heterologous systems over characterisation of the protein in its native environment in a plant cell, is that the protein of interest can be analysed in isolation, thus minimising confounding effects of other endogenous plant ion transport systems. Disadvantages of these heterologous expression systems include difficulties in obtaining a functional protein, determining whether the protein has the same transport characteristics as it would in a plant cell and a possible lack of co-factors in the heterologous cells.

The two expression systems used in this study were *Xenopus laevis* oocytes and *Saccharomyces cerevisiae*. The techniques used are briefly outlined below.

3.1.1 Two electrode voltage clamp (TEVC) using *Xenopus laevis* oocytes

Xenopus expression systems can be used to analyse the properties of transport proteins using a number of techniques, such as patch clamp, biochemical analysis and two electrode voltage clamp (TEVC) (Goldin 2006). The method used in this study was TEVC. For this technique, cRNA of the gene of interest is produced by *in vitro* transcription and then microinjected into isolated Xenopus oocytes. The endogenous translation machinery within the oocytes produces the protein of interest, which is then incorporated into the membrane. An advantage of oocytes is that they are large (approximately 1 mm in diameter) and therefore allow insertion of microelectrodes to perform TEVC

studies. With TEVC, two electrodes are inserted into the oocyte, one electrode (current electrode) injects a current to maintain the membrane at a set electrical potential (voltage), while the other electrode (voltage electrode) measures the change in electrical potential as ions move across the membrane, thereby allowing the current electrode to maintain the set voltage. The amount of current applied to the oocyte is measured and recorded. The transport properties of proteins within the oocyte membrane in relation to specific ions can be measured by changing the ion composition of the bathing solution.

3.1.2 Transport functionality assays using *Saccharomyces cerevisiae*

The yeast *S. cerevisiae* is a widely used system for functional studies of plant membrane proteins (Dreyer *et al.* 1999). It has a short lifecycle and can be easily transformed with genes of interest, allowing for a relatively fast and high throughput analysis of the function of the proteins they encode. A large variety of yeast mutants exist that are deficient in defined endogenous ion transport systems which can make them more or less tolerant to ionic and nutrient conditions than wild type yeast. Transformation of these mutant and wild type strains therefore allows for the functional characterisation of the transport properties mediated by the transport protein of interest. The two strains used in this study were INVSc2 and B31. INVSc2 is considered a wild type strain with no deficiencies in ion transport capabilities and good tolerance to high levels of NaCl, while B31 is a Na^+ sensitive strain due to its defective Na^+ efflux systems in the Na^+-ATPase and a Na^+/H^+ antiporter. Further details regarding the yeast strains are listed in the materials and methods (Table 3.1).

3.1.3 Testing AtHKT1;1 transport properties using Xenopus oocytes and yeast functionality assays

The Landsberg *erecta* ecotype (L*er*) has been found to be substantially more salt tolerant than both Col-0 and C24, based on its low reduction in dry weight under stressed conditions (Jha *et al.* 2010). The *AtHKT1;1* allele from L*er* (referred to as *AtHKT1;1*-L*er* from here on) has previously been studied in the Xenopus oocyte, yeast and *E.coli* expression systems. It has four altered amino acids compared to Col-0 and 11 compared to C24, hence differences in ion transport properties of AtHKT1;1-L*er* compared to Col-0 and C24 are possible. Based on observations in Xenopus oocytes and yeast, Na^+, but not K^+ transport properties of AtHKT1;1-L*er* have been suggested (Uozumi *et al.* 2000). In *AtHKT1;1*-L*er* injected oocytes, inward currents that are dependent on Na^+, but not on K^+ were detected when exposed to a range of Na^+ (0.3 to 100 mM) and K^+ (0.3 to 100 mM) concentrations (Uozumi *et al.* 2000). When *AtHKT1;1*-L*er* was expressed in the Na^+ sensitive yeast strain G19, inhibition of growth was observed. In contrast, expression of *AtHKT1;1-Ler* could not re-

establish K^+ uptake in the K^+ deficient yeast strain CY162 (Uozumi *et al.* 2000). It should be noted, however, that *AtHKT1;1-Ler* could complement an *E.coli* strain which was defective in its K^+ uptake system, in turn indicating possible K^+ transport properties of AtHKT1;1-L*er* (Uozumi *et al.* 2000).

In this chapter, the transport properties of AtHKT1;1 from Col-0 and C24 are compared in both Xenopus oocytes and in yeast. The coding sequence of the *AtHKT1;1* allele from C24 has 22 single nucleotide polymorphisms (SNPs) compared to Col-0, resulting in 9 predicted amino acid changes in the encoded protein. To investigate potential differences in transport characteristics between the Col-0 and C24 protein, TEVC on Xenopus oocytes and yeast functional assays were performed. The two *AtHKT1;1* alleles from Col-0 and C24 are referred to as *AtHKT1;1-Col* and *AtHKT1;1-C24*, respectively from here on.

3.1.4 Aims of this study

The yeast and Xenopus oocyte heterologous expression systems were used to address the following questions:

1. Do AtHKT1;1-Col and AtHKT1;1-C24 mediate Na^+ transport?
2. Do AtHKT1;1-Col and AtHKT1;1-C24 mediate K^+ transport?
3. Does the 9 amino acid difference between AtHKT1;1-Col and AtHKT1;1-C24 alter the transport characteristics of the two proteins?

3.2 Material and methods

3.2.1 Electrophysiological characterisation using *Xenopus laevis* oocytes

3.2.1.1 Cloning of *AtHKT1;1-Col* and *AtHKT1;1-C24* into the Xenopus oocyte expression vector pGEMXho-DEST

The coding sequence of *AtHKT1;1-Col* and *AtHKT1;1-C24* were kindly provided by Dr. Joanna Sundstrom (University of Adelaide, Australia) in Gateway™ enabled pCR8 vectors. To confirm the presence of the desired genes and their sequence integrity sequencing was performed using a BigDye® reaction and capillary separation (section 2.1.11). Once confirmed, a restriction digest was performed to introduce the coding sequences of *AtHKT1;1-Col* and *AtHKT1;1-C24* into the Xenopus expression vector pGEMXho (based on pGEM-HE (Liman *et al.* 1992)), kindly provided by Dr. Aurelie Evrard (University of Adelaide, Australia) (Figure 3.1). pGEMXho and the two pCR8 vectors containing *AtHKT1;1-Col* and *AtHKT1;1-C24* were digested (section 2.1.8) with the restriction enzymes *Xho*I and *EcoR*I (New England Biolabs, Ipswich, MA, USA). The pGEMXho vector fragment was ligated to either one of the two *HKT* gene fragments using T4 DNA ligase (section 2.1.9). Positive clones containing the expression vector with the *HKT* gene of interest in the correct orientation were identified by restriction digest (section 2.1.8) and the vectors sequenced using the primer T7 to ensure no sequence errors were introduced (section 2.1.11).

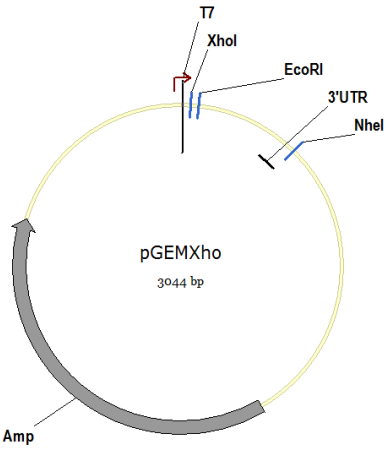

Figure 3.1: Vector map of pGEMXho vector (based on pGEM-HE (Liman *et al.* 1992)).

The pGEMXho vector was used to synthesize cRNA for use in Xenopus oocyte electrophysiology. Indicated are T7: promoter for T7 polymerase to transcribe cRNA, *Xho*I and *EcoR*I restriction sites allowing the insertion of the desired gene of interest, *Nhe*I: restriction site for linearisation of the plasmid, 3′ UTR: 3′ untranslated region which aids the expression of the plant gene in the oocyte and *Amp*: ampicillin resistance gene for selection of the plasmid in *E.coli*.

3.2.1.3 Transcription of cRNA

The pGEMXho plasmids containing the Col-0 and C24 *AtHKT1;1* coding sequence were linearised by restriction digest using *Nhe*I-HF (New England Biolabs, Ipswich, MA, USA) and were used as a template for cRNA synthesis using the mMessage mMachine 5′ capped RNA transcription kit and the lithium chloride precipitation method (Ambion, Life Technologies, Mulgrave, Australia) following the manufacturer's instructions. The quality and quantity of cRNA was determined by agarose gel electrophoresis (section 2.1.2) and using a spectrophotometer Nanodrop (Thermo Scientific, Wilmington, DE, USA). The cRNA concentration was adjusted to 500 ng/µL with RNase free water and stored at -80 °C until required for injection into oocytes.

3.2.1.4 Injection of cRNA into *Xenopus laevis* oocytes

Handling of oocytes and electrophysiological experiments were performed as described previously (Roy *et al.* 2008), with minor alterations. Oocytes were harvested by Dr. Sunita Ramesh or Ms. Wendy Sullivan (University of Adelaide, Australia) and treated with collagenase to dissociate oocytes from the ovarian lobe. Oocytes were kept at 17 °C and transferred daily to fresh ND96 [96 mM NaCl, 2 mM KCl, 5 mM $MgCl_2$, 10 mM $CaCl_2$, 2 mM pyruvic acid and 5 mM (4-(2-hydroxyethyl)-1-piperazineethanesulfonic acid (HEPES), adjusted to pH 7.6 using KOH and supplemented with 8% (v/v) horse serum, 0.1 mg/mL tetracycline, 100 U/mL penicillin and 0.1 mg/mL streptomycin] to keep the oocytes viable. Using a micro injector (Drummond 'Nanoinject II' automatic nanolitre injector, Dummond Scientific, Broomall, PA, USA) connected to a 1 µm diameter micro capillary, 46 nL (23 ng) of cRNA or nuclease free water, as control, were injected into the animal pole of 2-3 d old oocytes, close to the border of the vegetal pole. Injected oocytes were incubated in ND96 at 17 °C for 2 d prior to voltage clamp experiments to allow oocytes to recover and to allow for protein synthesis and protein integration into the membrane.

3.2.1.5 TEVC measurements on oocytes

TEVC of oocytes was performed in HMg bathing solution (6 mM $MgCl_2$, 1.8 mM $CaCl_2$, 10 mM MES and pH 6.5 adjusted with TRIS base). The bathing solution was supplemented with 1 to 50 mM of Na^+-glutamate or K^+-glutamate as indicated. Osmolarity of all solutions was adjusted to 250±10 mOsmol kg^{-1} with mannitol using a Wescor 5520 Vapour Pressure Osmometer (Logan, UT, USA). Filamented glass capillaries (1 mm outer diameter, filamented borosilicate glass capillaries (Harvard Apparatus, Edenbridge, Kent, UK)) were prepared using horizontal laser puller P-2000 (Sutter Instruments, Nowato, CA USA) and the MF-900 Microcapillary forge (Narishige, Tokyo, Japan) with a tip of 0.5 µm in diameter for the voltage electrode and 0.8 µm for the current

electrode. Capillaries were back-filled with 3 M KCl and carefully inserted into the oocyte, which remained under continuous irrigation with HMg solution in the bathing chamber. The applied voltage protocol induced membrane potentials from +40 to -120 mV over 4.5 s in 20 mV intervals, and the holding potential between ramps was -40 mV for 1.5 s (Figure 3.2). Recorded currents were amplified using a Gene Clamp 500 voltage clamp amplifier (Axon Instruments, Molecular Devices, Sunnyvale, CA, USA) and analysed using the programme Clampfit 10.0 (Axon Instruments, Molecular Devices, Sunnyvale, CA, USA). Data presented are corrected for background currents from water-injected control oocytes.

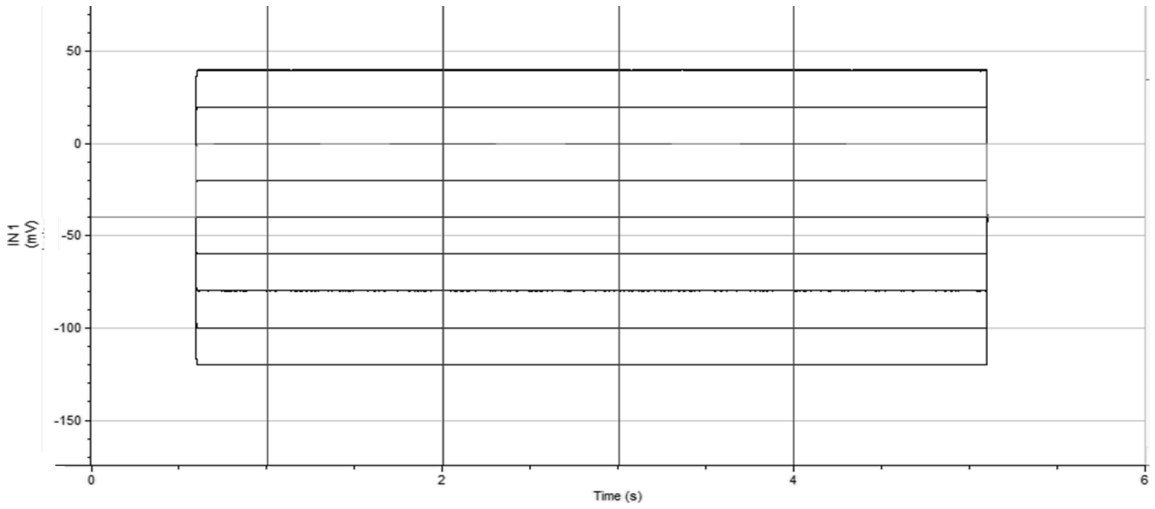

Figure 3.2: Image of voltage protocol used for two electrode voltage clamp of Xenopus oocytes.

Horizontal lines indicate the membrane potential (in mV) and the length of time (in s) it was imposed on the oocyte. The membrane potential was being ramped from +40 to -120 mV over 4.5 s in 20 mV intervals, and the holding potential between ramps was -40 mV for 1.5 s.

Data obtained from TEVC are presented as I/E-relationships with water-injected currents subtracted; the average current is determined over a 2 s interval at which the current is stable during the specified clamped electrical potential (voltage). Current traces with the corresponding voltage protocol can be found as supplementary Figures (Supplementary Figure.8.1, Supplementary Figure 8.3 and Supplementary Figure 8.2). Two important parameters can be determined from the I/E-relationship: the reversal potential (E_{rev}) and conductance (G). E_{rev} describes the electrical potential at which no net flux of ions across the membrane is measured. An approximation for E_{rev} can be determined from the intercept with the x-axis of a curve that describes the I/E-relationship for each given concentration of external ions. A shift in E_{rev} upon concentration changes of a certain ion

provides evidence for a particular selectivity of an ion transport system. The conductance (G) describes the ease with which ion flux across the membrane occurs. Approximated values for G can be obtained by determining the slope of a curve that describes the I/E-relationship just negative of E_{rev} (for the influx of a cation). An increase in conductance in response to an increased external ion concentration provides further evidence for the presence of a functioning ion-transport system (i.e. an ion transporter) in the membrane. In diagrams illustrating the I/E-relationships, the amount of external ion is generally presented as a concentration, while in diagrams displaying E_{rev} and G, the amount of ions is presented as activity. The activity refers to the portion of the ion that is freely available and is influenced by the composition of ions in the solution and the concentration. The activity of Na^+ and K^+ in each test solution was determined using the program Geochem-EZ (http://www.plantmineralnutrition.net/Geochem/Geochem%20Download.htm).

3.2.2 Yeast growth assays

3.2.2.1 Cloning of *AtHKT1;1-Col* and *AtHKT1;1-C24* into the yeast expression vector pYES2-DEST52

The previously confirmed coding sequences of *AtHKT1;1-Col* and *AtHKT1;1-C24* (section 3.2.1.1) were introduced into the Gateway™ enabled yeast expression vector pYES2-DEST52 by recombination (section 2.1.10) (Figure 3.3). Positive clones containing the expression vector with the gene of interest were identified by restriction digest using *Xba*I (section 2.1.8) and sequenced using a BigDye® reaction and capillary separation to ensure no sequence errors were introduced (section 2.1.11).

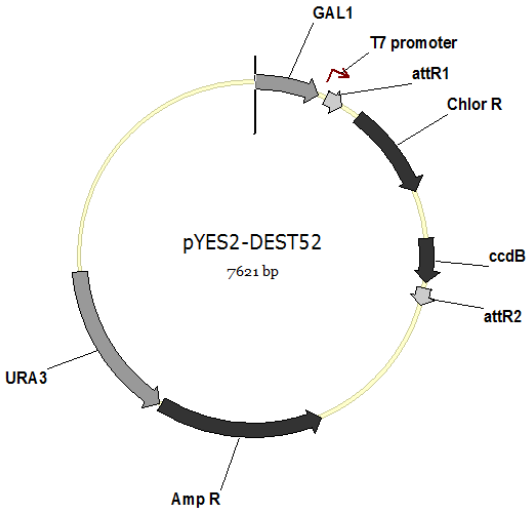

Figure 3.3: Vector map of pYes2-DEST52 vector used to express *HKT* genes in *S.cerevisiae*.

The plasmid DNA was obtained from Life Technologies (Mulgrave, Australia). Indicated are *GAL1*: galactose inducible promoter, T7 promoter: promoter for T7 polymerase, *att*R1 and *att*R2: Gateway® recombination sites, *Chlor* R: Chloramphenicol resistance gene for selection in *E.coli*, *ccd*B: gene permitting negative selection of the plasmid, *Amp R*: ampicillin resistance gene for selection of the plasmid in *E.coli* and *URA3*: gene to allow growth on uracil deficient media.

3.2.2.2 Transformation of yeast with plasmid DNA

The two yeast strains INVSc2 and B31 (Table 3.1) were used for transformation with the two *HKT* constructs and an empty vector as control. The pYES2-DEST52 vector allows selection of yeast on uracil deficient media. Yeast transformed with the empty vector, containing a sequence in the Gateway site that does not lead to a functional protein, can be used as a control as it grows under the same conditions as yeast transformed with the gene of interest. Transformation of yeast with destination vectors was performed as described previously (Gietz and Woods 2002); briefly, a 4 mL

overnight culture from a single yeast colony, grown at 30 °C in SD-Glu (Table 3.2), supplemented with the appropriate amino acids (Table 3.1) and 20 mg/mL uracil, was centrifuged to a pellet at 16,000 *g* for 30 s. The pellet was resuspended in 360 µL of transformation mix (33 % (w/v) PEG 3500, 100 mM lithium acetate, 100 µg boiled salmon sperm-Carrier DNA and 0.1 to 1 µg plasmid DNA). The suspension was incubated for 60 min in a water bath at 42°C before centrifugation at 16,000 *g* for 30 s to obtain a pellet. The supernatant was fully removed with a pipette and the pellet resuspended in 1 mL sterile ddH_2O. A 100 µL aliquot was spread onto SD-Glu-agar plates (Table 3.2) containing the appropriate amino acids (Table 3.1). The plates were incubated at 30°C for 3 to 4 d until colonies were approximately 1 mm in diameter. The presence of the gene of interest in the yeast colonies was confirmed by colony PCR (section 2.1.1). Positive yeast colonies of three independent transformation events for each construct were selected. These colonies were grown in 5 mL SD-Glu with the appropriate amino acids at 30 °C with shaking (200 rpm) for 2 d to obtain cultures for glycerol stocks. A volume of 0.75 mL of yeast culture was mixed with 0.75 mL 100 % glycerol in a 2 mL microfuge tube, snap frozen in liquid nitrogen and stored at - 80 °C. For each experiment, the glycerol stocks were used to recover yeast colonies on SD-Glu agar plates.

Table 3.1: Yeast strains used in this study with corresponding genotype, required amino acid supplements for growth and source of the yeast strain

Yeast strain	Genotype	Required amino acids in media (20 mg/L)	Source/Reference
INVSc2	*MATahis3-D1ura3-52*	L-histidine	Life Technologies (Mulgrave, Australia)
B31	*MATaade2ura3leu2his3trp1ena 1Δ::HIS3::ena4Δnha1Δ::LEU2*	L-tryptophan, adenine sulfate	(Bañuelos *et al.* 1998)

Table 3.2: Media composition of yeast media for growth and functional assays

Media	Composition	Purpose
SD-Glu	0.67% Difco™ Nitrogen Base (BD Diagnostic Systems), dropout solution*1, 2 % glucose*2	Yeast growth and control in functional assay
SD-Glu agar	As SD-Glu with 2 % Bacto agar (BD Diagnostic Systems)	Selection of transformed colonies and control in functional assay
SD-Gal	0.67% Difco™ Nitrogen Base (BD Diagnostic Systems), dropout solution*1, 2 % galactose*2	Functional assay
SD-Gal agar	As SD-Gal with 2 % Bacto agar (BD Diagnostic Systems)	Functional assay
AP-Gal	10 mM L-arginine, 8 mM phosphoric acid, 2 mM $MgSO_4$, 0.2 mM $CaCl_2$, 20 µg/L biotin, 2 mg/L calcium pantothenate, 2 µg/L folic acid, 10 mg/L inositol, 400 µg/L niacin, 200 µg/L p-aminobenzoic acid, 400 µg/L pyridoxine hydrochloride, 200 µg/L riboflavin, 400 µg/L thiamine hydrochloride, 500 µg/L H_3BO_3, 40 µg/L $CuSO_4$, 100 µg/L KI, 200 µg/L $FeCl_3$, 400 $MnSO_4$, 200 µg/L Na_2MoO_4, 400 µg/L $ZnSO_4$, dropout solution*1, 2% galactose*2	Functional assay
AP-Gal agar	As AP-Gal with 2 % Bacto agar (BD Diagnostic Systems)	Functional assay
AP-Glu agar	As AP-Gal with 2 % Bacto agar (BD Diagnostic Systems), galactose is substituted with glucose*2	Control in functional assay

*1 final concentration of dropout solution: 20 mg/L L-arginine HCL, 30 mg/L L-isoleucine, 30 mg/L L-lysine HCL, 20 mg/L L-methionine, 50 mg/L L-phenylalanine, 200 mg/L L-threonine, 30 mg/L L-tyrosine, 150 mg/L L-valine *2 40 % stock of glucose and galactose, sterile filtrated, was added after autoclaving of the remaining components to a final concentration of 2 %.

3.2.2.3 Functional assay of transformed yeast on solid media

Yeast colonies containing the desired ecotype specific *AtHKT1;1* gene were used to inoculate 5 mL of SD-Glu containing the appropriate amino acids (Table 3.2). The culture was incubated with shaking (200 rpm) at 30 °C for 2 d. For functional assays performed on plates of solid media, the yeast culture was centrifuged at 800 *g* for 1 min and the pellet resuspended in sterile water to an OD_{600} of 0.6, as determined by spectrophotometry (UV-160A, Shimadzu, Japan). The 10 µL aliquots of decimal dilutions were plated as droplets on solid SD or AP growth media containing NaCl or KCl as indicated. Three transformation events were evaluated for each construct and yeast strain and at least three technical replicate plates were performed. Plates were sealed with cling wrap, incubated at 30 °C for 2-3 d and growth phenotypes were recorded.

3.2.2.4 Functional assay of transformed yeast in liquid media

As previously, yeast colonies containing the desired ecotype specific *AtHKT1;1* gene were used to inoculate 5 mL of SD-Glu containing the appropriate amino acids (Table 3.2) in 50 mL falcon tubes and incubated for 2 d with shaking (200 rpm) at 30 °C to obtain fresh yeast cultures. To generate starting cultures for the growth assay, 200 µL of the fresh culture were used to inoculate either 5 mL of SD-Gal or SD-Glu containing the appropriate amino acids in 50 mL falcon tubes and incubated o/n with shaking (200 rpm) at 30 °C. This allows for the induction of the gene of interest in yeast cultures in SD-Gal media prior to starting growth measurements, while yeast cultures in SD-Glu provide the positive control, in which gene expression is not induced and optimal growth is expected. The OD_{600} was determined from the o/n-cultures and an aliquot of the cells grown in SD-Gal was used to inoculate 5 mL of SD-Gal containing the appropriate amino acids in 50 mL falcon tubes with either no salt, 50 mM NaCl or 50 mM KCl. An aliquot of cultures grown in SD-Glu was used to inoculate 5 mL SD-Glu containing the appropriate amino acids in 50 mL falcon tubes as a positive control. Starting OD_{600} was adjusted to be consistent at approximately 0.2-0.3. Samples of 100 µL were taken over 3 d to use for OD_{600} measurements in 1:10 dilutions. OD_{600} readings were taken in 1 mL cuvettes (Cat. # 759015, Brand, Wertheim, Germany) using a spectrophotometer (UV-160A, Shimadzu, Japan).

3.4 Results

3.4.1 Analyses of AtHKT1;1 transport characteristics in *Xenopus laevis* oocytes

3.4.1.1 Generating cRNA for expression of *AtHKT1;1-Col* and *AtHKT1;1-C24* in Xenopus oocytes

To generate *AtHKT1;1-Col* and *AtHKT1;1-C24* cRNA for injection into Xenopus oocytes, open reading frames of the two genes were ligated separately into pGEMXho vectors (Figure 3.4). The nucleotide sequence for both constructs was determined and found to be correct (data not shown). cRNA synthesis was performed using the mMessage mMachine kit (section 3.2.1.2), with transcription being initiated by the T7 promoter and discontinued as a result of linearisation at the *Nhe*I restriction site.

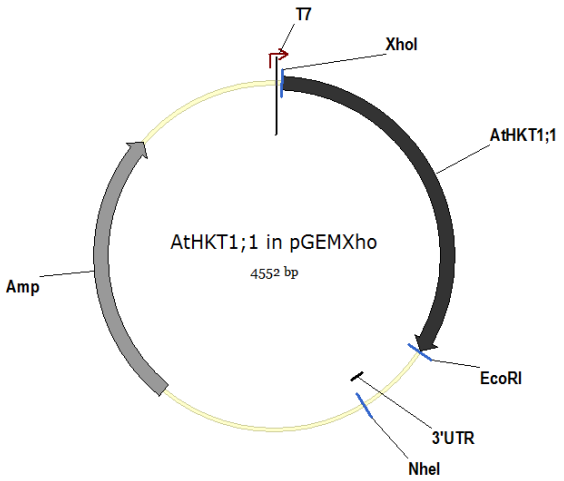

Figure 3.4: Vector map of the pGEMXho vector containing either the *AtHKT1;1-Col* or *AtHKT1;1-C24* coding sequence.

This vector was used to generate cRNA for expression in Xenopus oocytes. Features are detailed in Figure 3.1.

The transcribed cRNA was subjected to gel electrophoresis and showed one strong band with one additional faint band appearing above (Figure 3.5). The additional band might occur due to aberrantly migrating RNA in the gel because of its secondary structure. Additional bands of *AtHKT1;1* cRNA have been observed previously (Byrt 2008) and it was considered to have only minor influence during experiments as it was very faint as compared to the main band (Figure 3.5). The user manual for cRNA synthesis (mMessage mMachine) also remarks that an additional band could represent contaminating plasmid DNA, which might not have been fully digested by DNase

treatment. However, this is unlikely as a prolonged DNase treatment did not eliminate the additional band and its size did not correspond to the size of the linearized plasmid DNA (data not shown). The reference DNA ladder was presented to allow a general comparison of band intensities and ensure even migration of nucleic acid through the agarose gel. A comparison of product size with the DNA ladder is not possible because of the secondary structure of native RNA affects the overall rate of movement through the gel in a different manner to double stranded DNA.

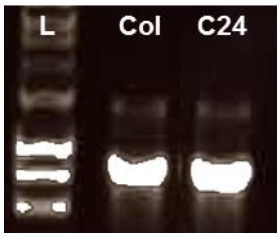

Figure 3.5: Agarose gel image of synthesised cRNA for injection into Xenopus oocytes.

cRNA *in vitro* transcribed from pGEMXho (1:10 dilution in ddH_2O). cRNA products transcribed from the coding sequences of (Col) *AtHKT1;1-Col* and (C24) *AtHKT1;1-C24*. L = 1 kb DNA ladder.

3.4.1.2 TEVC on *AtHKT1;1-Col* and *AtHKT1;1-C24* microinjected Xenopus oocytes

Only healthy looking oocytes, with a neat boundary between animal and vegetal pole, even colouring, spherical in shape and with a stable resting membrane potential were used for TEVC experiments. Up to 50 oocytes were microinjected with RNase free water as control or with cRNA encoding for *AtHKT1;1-Col* or *AtHKT1;1-C24*. The resting membrane potential of water-injected oocytes was typically between -32 and -44 mV. The resting potential can vary greatly between batches of oocytes and even between individual oocytes due to endogenous transport systems (Sobczak *et al.* 2010, Weber 1999).

The applied bathing solutions were designed to test for Na^+ and K^+ conductance in Xenopus oocytes microinjected with *AtHKT1;1* cRNA. Current densities measured in cRNA-injected oocytes were in the µA range, whereas they were in the nA range for water-injected oocytes. Data presented are corrected for currents from water-injected control oocytes.

In response to increasing external [Na^+], a shift in E_{rev} to a more positive voltage (Figure 3.6 A and B, Table 3.3) could be observed for oocytes injected with either allele of *AtHKT1;1*. A shift from -76 ± 6 mV at 1 mM Na^+ to -6 ± 1 mV at 50 mM Na^+ was measured in *AtHKT1;1-Col* injected oocytes, and similarly, a shift from -74 mV ± 7 at 1 mM Na^+ to -7 ± 2 mV at 50 mM Na^+ was measured in *AtHKT1;1-C24* injected oocytes. This positive shift of E_{rev} is in the same direction as

predicted from calculated E_{Na^+} values derived from the Nernst equation (Rubio *et al.* 1995, Rubio *et al.* 1999).

Also, in response to increasing external [K^+], a shift in E_{rev} to a more positive voltage could be observed for both *AtHKT1;1* alleles (Figure 3.6 C and D, Table 3.3). However, this shift is not as uniform as it is with the addition of Na^+. For *AtHKT1;1-Col* injected oocytes, E_{rev} does not change substantially in the range of 10 mM K^+ to 50 mM K^+, but is moderately more negative at 1 mM K^+. For *AtHKT1;1-C24* injected oocytes, shifts in E_{rev} from -73 ± 14 at 1 mM K^+ to -26 ± 9 mV at 50 mM K^+ can be observed. The positive shift of E_{rev} is in the same direction as predicted from calculated E_{K^+} values derived from the Nernst equation (Rubio *et al.* 1995, Rubio *et al.* 1999).

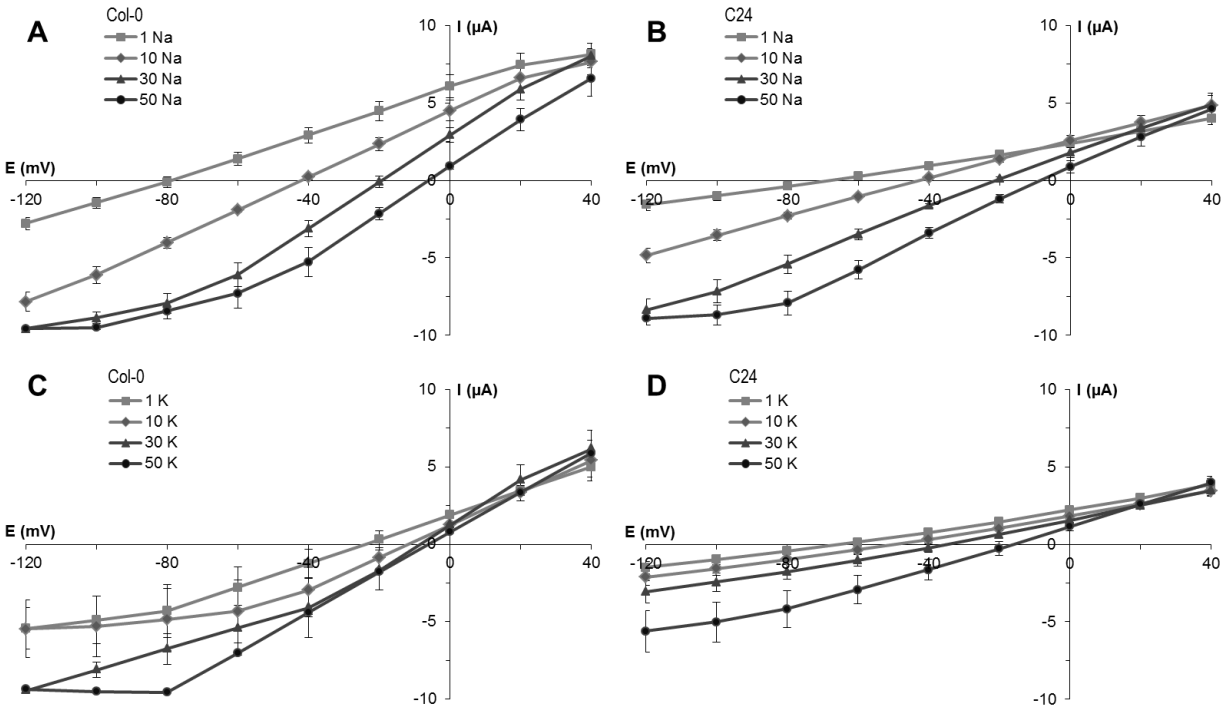

Figure 3.6: I/E-relationships of flux through Xenopus oocytes injected with *AtHKT1;1* cRNA.

cRNA derived from Col-0 (A and C) or C24 (B and D) coding sequences. Data presented are mean±S.E.M. of cRNA injected oocytes, corrected for water controls, n=3-5 oocytes with each 1-3 technical replicates. Only for panel C, the number of oocytes was 2 and 1 for concentrations 30 K and 50 K, respectively, with 3 technical replicates.

The I/E-relationships presented in Figure 3.6 are used to determine values for E_{rev} and G, which are presented in the following two figures (Figure 3.7 and Figure 3.8). It should be noted that the x-axis is referring to Na^+ and K^+ activity (in mM), not the concentration, as the activity describes the amount of ion available for transport through the transport protein and is therefore more precise than

concentration. The conductance of Na^+ and K^+ by AtHKT1;1-Col and AtHKT1;1-C24 increases with increasing Na^+ and K^+ activity (Figure 3.7 and Table 3.3). Interestingly, the conductance by AtHKT1;1-Col over a range of Na^+ and K^+ activities appear very similar, while the Na^+ and K^+ conductance by AtHKT1;1-C24 differ (Figure 3.7). The K^+ conductance by AtHKT1;1-C24 has lower values than the Na^+ conductance and does not increase as much with increasing K^+ activity (Figure 3.7 B and Table 3.3).

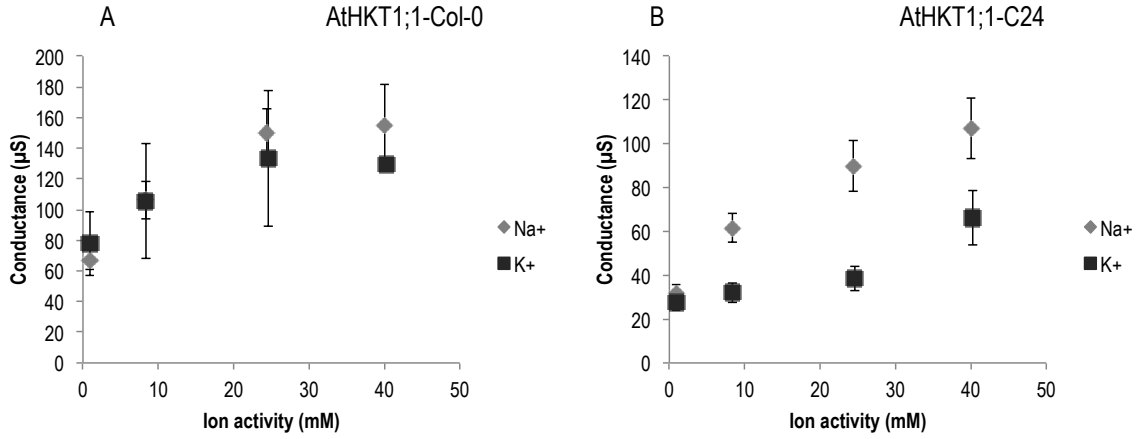

Figure 3.7: Conductance of Na^+ and K^+ by *AtHKT1;1* expressing oocytes.

Conductance (in µS) of Na^+ and K^+ (A) by *AtHKT1;1-Col* or (B) *AtHKT1;1-C24* injected oocytes in bathing solutions of differing Na^+ and K^+ activities. Data presented are mean±S.E.M. of cRNA-injected oocytes, corrected for water controls; n = 3-5 oocytes with 1-3 technical replicates.

The E_{rev} of Na^+ and K^+ in *AtHKT1;1-Col* and *AtHKT1;1-C24* expressing oocytes increases with increasing Na^+ and K^+ activity (Figure 3.8 and Table 3.3). In *AtHKT1;1-Col* expressing oocytes, the E_{rev} for Na^+ increases almost linear, and the magnitude of change in E_{rev} is greater for Na^+ (from ~ -76 mV to ~ -6 mV) than for K^+ (from ~ -34 mV to ~ -6 mV) (Figure 3.8 A). Also for *AtHKT1;1-C24* expressing oocytes E_{rev} is changing in greater magnitude for Na^+ (from ~ -74 mV to ~ -7 mV) than for K^+ (from ~ -73 mV to ~ -26 mV) (Figure 3.8 B).

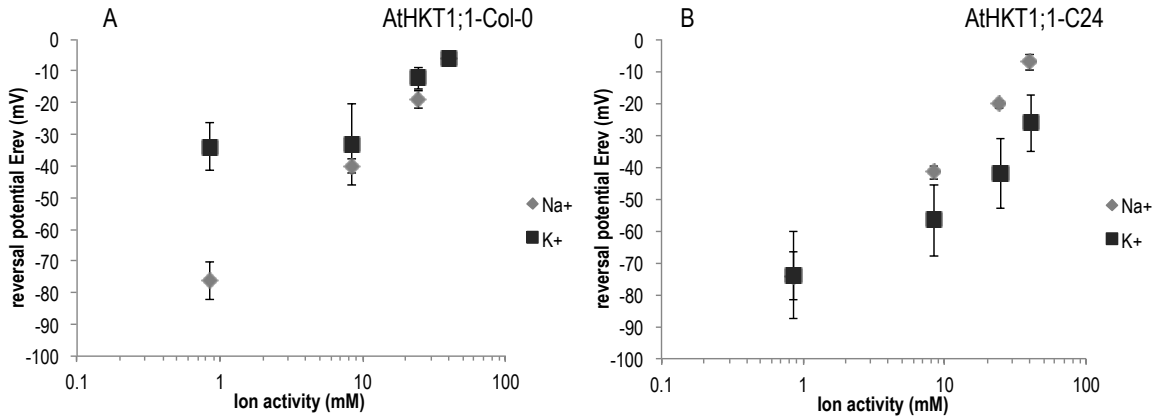

Figure 3.8: Reversal potential (E_{rev}) of Na^+ and K^+ in *AtHKT1;1* expressing oocytes

Reversal potential (in mV) of Na^+ and K^+ (A) in *AtHKT1;1-Col* or (B) *AtHKT1;1-C24* injected oocytes in bathing solutions of differing Na^+ and K^+ activities. Data presented are mean±S.E.M. of cRNA-injected oocytes, corrected for water controls; n = 3-5 oocytes with 1-3 technical replicates.

Table 3.3: Numeric values for conductance (G) and reversal potential (E_{rev}) of *AtHKT1;1-Col* and *AtHKT1;1-C24* injected oocytes in the presence of varying Na^+ and K^+ concentrations and the corresponding activity. Results are mean ± SEM, n = 3-5 oocytes with 1-3 technical replicates.

Treatment	Activity	Conductance (µS)		E_{rev} (mV)	
		HKT1;1-Col	HKT1;1-C24	HKT1;1-Col	HKT1;1-C24
1 mM Na^+	0.9 mM Na^+	67 ± 7	31±5	-76 ± 6	-74 ± 7
10 mM Na^+	8.4 mM Na^+	106 ± 12	61 ± 7	-40 ± 2	-42 ± 2
30 mM Na^+	24.5 mM Na^+	150 ± 15	90 ± 11	-19 ± 3	-20 ± 1
50 mM Na^+	40 mM Na^+	154 ± 27	107 ± 14	-6 ± 1	-7 ± 2
1 mM K^+	0.9 mM K^+	78 ± 21	28 ± 4	-34 ± 7	-73 ± 14
10 mM K^+	8.4 mM K^+	105 ± 38	32 ± 5	-13 ± 12	-57 ± 11
30 mM K^+	24.6 mM K^+	133 ± 44	38 ± 6	-12 ± 3	-42 ± 11
50 mM K^+	40.3 mM K^+	129 ± 3	66 ± 12	-6 ± 1	-26 ± 9

3.4.2 Analyses of transport characteristics in the yeast *S. cerevisiae*

3.4.2.1 Generating yeast strains expressing *AtHKT1;1-Col* and *AtHKT1;1-C24*

For expression in yeast, open reading frames of *AtHKT1;1-Col* and *AtHKT1;1-C24* were recombined from pCR8 vectors into the pYES2-DEST52 vector (Figure 3.9). The nucleotide sequences of the inserted genes were determined and were found to be correct (data not shown). The expression vector contains a galactose inducible promoter (GAL1), allowing gene expression only when galactose is the carbon source. Gene expression is not initiated in the presence of glucose. Both

yeast strains, INVsc2 and B31, were used for transformation with pYES2-DEST52 containing *AtHKT1;1-Col* or *AtHKT1;1-C24.* In addition, yeast strain INVsc2 transformed with pYES2-DEST52 containing the open reading frame of *TmHKT1;5-A,* a wheat homolog, was kindly provided by Mr. Bo Xu (University of Adelaide, Australia). *TmHKT1;5-A* expression has been shown to severely limit yeast growth on media containing Na^+ (Munns *et al.* 2012) and was therefore used as a positive control.

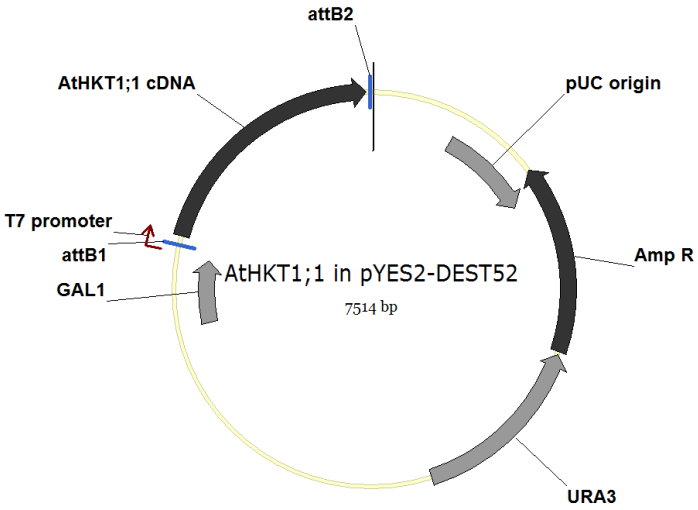

Figure 3.9: Vector map of the pYES-DEST52 vector containing either the *AtHKT1;1-Col* or *AtHKT1;1-C24* coding sequence.

The pYES2-DEST52 vector containing the coding sequence of the desired *AtHKT1;1* allele for expression of *AtHKT1;1* in *S. cerevisiae*. Features are detailed in Figure 3.3.

3.4.2.2 Growth phenotypes of *AtHKT1;1* expressing yeast on solid growth media

For yeast growth assays, decimal dilutions of wild type yeast (INVSc2) and salt sensitive B31 yeast, expressing the *AtHKT1;1* genes, were pipetted onto plates containing different growth media ± NaCl and ± KCl. To establish the optimal concentration of NaCl in solid yeast media, where inhibition of yeast growth can be observed, a range of NaCl concentrations were tested at 25 mM, 50 mM, 100 mM and 200 mM NaCl in SD-Gal agar media containing the appropriate amino acids (data not shown). It was observed that the growth of yeast was severely limited under all tested conditions; therefore, data is only shown for the addition of ± 50 mM NaCl (Figure 3.10 A). Under control conditions with glucose, which suppresses gene expression, all yeast cultures show strong growth (Figure 3.10 A), indicating that the yeast cultures are viable and suitable for growth assays. The growth of INVSc2 and B31 yeast transformed with the control empty vector on SD media containing galactose ± 50 mM NaCl, which induces gene expression, is as strong as on glucose, indicating that

the addition of 50 mM NaCl is not lethal for either yeast strain (Figure 3.10 A). INVSc2 and B31 expressing *AtHKT1;1-Col* and *TmHKT1;5-A* show entire growth inhibition in the presence of galactose, 0 mM or 50 mM NaCl on SD media (Figure 3.10 A). Interestingly, *AtHKT1;1-C24* expressing INVSc2 yeast shows moderate growth on SD-Gal 0 mM NaCl, but is also fully inhibited in the presence of 50 mM NaCl.

The inhibition of yeast growth on SD-Gal media even without additional NaCl was strong. Consequently, the Na^+ content of SD media was determined using flame photometry (model 420 Flame Photometer, Sherwood Scientific Ltd, Cambridge, United Kingdom). The Na^+ content was found to be moderately high with 2 mM Na^+, possibly causing the poor growth of yeast on SD-Gal media. Accordingly, AP media was chosen for the growth assay, as it contains only approximately 5 µM Na^+ and had previously been used for studies on HKTs (Munns *et al.* 2012). SD media is purchased as a premixed powder, based on ammonium sulphate, while AP media is based on arginine-phosphate and has all components, including vitamins, added separately, allowing for the Na^+ content to be controlled.

Strong growth of INVSc2 and B31 was also observed on AP media containing glucose as a control (Figure 3.10 B). However, while the empty vector control in INVSc2 yeast grew well on AP-Gal ± NaCl, the B31 empty vector control yeast only grew on AP-Gal with 0 mM NaCl, while 50mM NaCl was lethal to B31 yeast as complete growth inhibition was observed (Figure 3.10 B). Similarly to SD media, on AP media full growth inhibition was observed for *AtHKT1;1-Col* and *TmHKT1;5-A* expressing yeast (both INVSc2 and B31) and moderate growth could be observed for *AtHKT1;1-C24* expressing INVSc2 yeast.

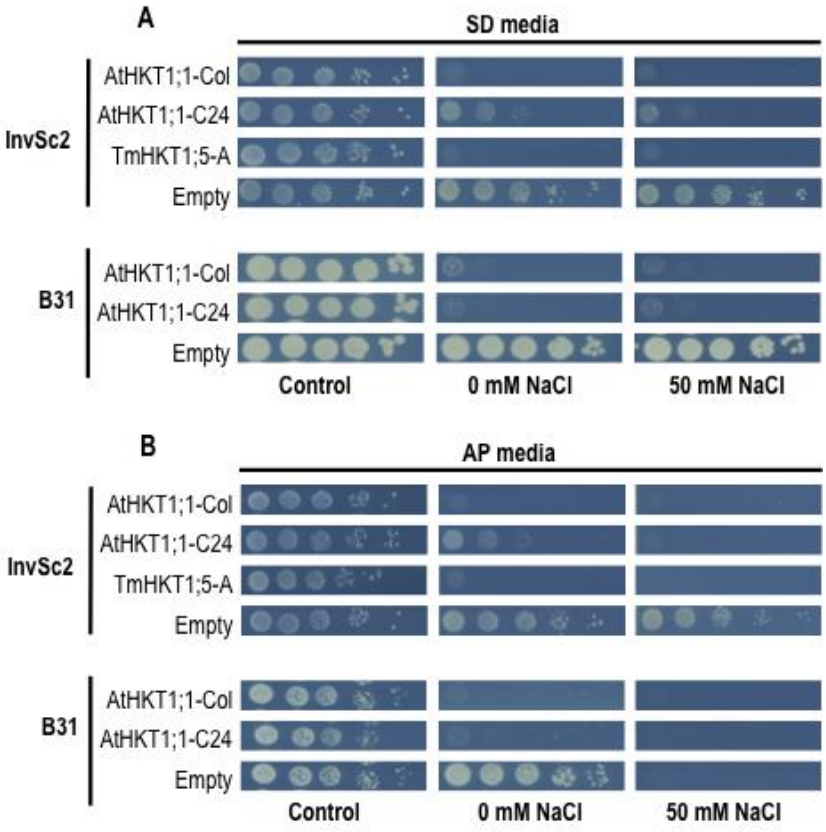

Figure 3.10: Representative growth phenotypes of *S. cerevisiae* strains InvSc2 and B31 expressing *AtHKT1;1* on media containing NaCl.

The two yeast strains InvSc2 and B31 expressing either *AtHKT1;1-Col, AtHKT1;1-C24, TmHKT1;5-A* and empty pYES-DEST52 on (A) SD or (B) AP media supplemented with ± NaCl. 10 μL of yeast were applied to the medium at an OD_{600} of 0.6 and in 4 decimal dilutions. Plates were based on SD or AP media as indicated. Control plates contained glucose as carbon source, all other plates contained galactose. Plates were supplemented with the indicated amount of NaCl. Presented data are representative of three biological replicates (independently transformed yeast colonies) and at least three technical replicates.

It is widely accepted that AtHKT1;1 proteins are important for Na^+ transport activity (Hauser and Horie 2010, Horie *et al.* 2009, Platten *et al.* 2006), however the preliminary experiments in Xenopus oocytes could also suggest a potential role for K^+ transport – at least when the protein is expressed in a heterologous system and in the absence of Na^+. This led to the decision to also evaluate the phenotype of *AtHKT1;1* expressing yeast in response to K^+ (Figure 3.11). K^+ is essential for yeast growth and not regarded as being toxic (Uozumi *et al.* 2000); therefore, K^+ uptake is not expected to inhibit yeast growth.

The phenotype of transformed yeast on glucose media and on galactose media without KCl (0 mM KCl) (Figure 3.11) is conform to previous observations for NaCl (Figure 3.10 A and B). Interestingly, it appears that with addition of 50 mM KCl, *AtHKT1;1-C24* expressing wild type yeast

has slightly improved growth, while growth of *AtHKT1;1-Col* expressing wild type yeast remains fully inhibited on both SD-Gal and AP-Gal media (Figure 3.11 A and B). In the case of the salt sensitive B31 yeast, both *AtHKT1;1-Col* and *AtHKT1;1-C24* expressing yeast show moderately improved growth with the addition of 50 mM KCl as opposed to no addition of KCl (Figure 3.11).

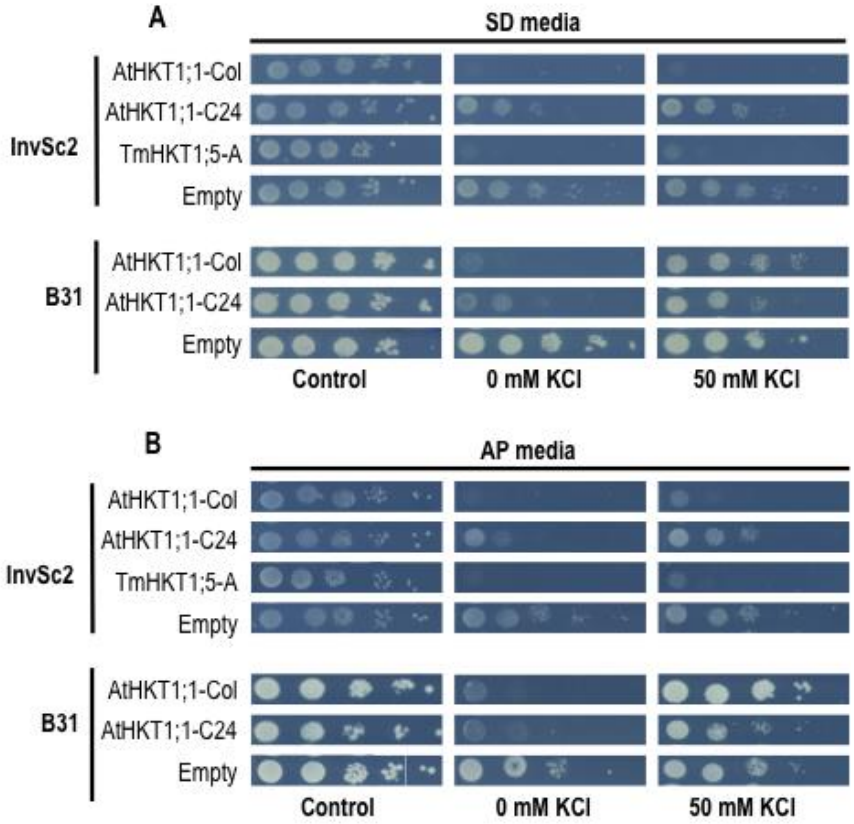

Figure 3.11: Representative growth phenotypes of *S. cerevisiae* strains InvSc2 and B31 expressing *AtHKT1;1* on media containing NaCl.

The two yeast strains InvSc2 and B31 expressing either *AtHKT1;1-Col, AtHKT1;1-C24, TmHKT1;5-A* and empty pYES-DEST52 on (A) SD or (B) AP media supplemented with ± KCl. 10 μL of yeast were applied to the medium at an OD_{600} of 0.6 and in 4 decimal dilutions. Plates were based on SD or AP media as indicated. Control plates contained glucose as carbon source, all other plates contained galactose. Plates were supplemented with the indicated amount of KCl. Presented data are representative of three biological replicates (independently transformed yeast colonies) and at least three technical replicates.

3.4.2.3 Functional assay of AtHKT1;1 expressing yeast in liquid media

In the previous section, a strong inhibition of yeast growth on plates containing SD-Gal and AP-Gal even without additional NaCl was observed (section 3.4.2.2). Therefore, an assay based on liquid yeast cultures was also performed. Any impurities contained in the agar, possibly causing growth inhibition, are excluded and growth dynamics may be better quantified.

Initially, a 96-well plate was used to measure yeast growth over time using a plate reader, which had the ability to shake the plate in between OD_{600} measurements. However, the pH of the cultures did not remain constant and dropped to approximately pH 3, even when biological buffers, such as MES, were used to buffer the solution (data not shown). The acidification of cultures may have influenced growth, as generally growth curves were not sigmoidal and OD_{600} values appeared very irregular (data not shown). The small culture volume of 100 µL and sealed compartments may not have allowed for sufficient aeration of the yeast cultures. Hence it was decided to determine growth curves in 50 mL falcon tubes and to manually determine OD_{600} values periodically over 3 d. Yeast cultures, derived from three independent transformation events per construct, were evaluated in SD media in the presence of glucose as control, and in the presence of galactose ± 50 mM NaCl and ± 50 mM KCl. The wild type strain INVSc2 (Figure 3.12) and B31 (Figure 3.13) were subject to evaluation. Only SD media was evaluated since the plate experiments had shown that results are not substantially different between SD and AP media.

Similar to growth on solid yeast media (Figure 3.10), all transformed INVSc2 yeast grew similarly in the presence of glucose, quickly reaching a plateau (Figure 3.12 A). In the presence of galactose, *AtHKT1;1-C24* expressing yeast grew similar to yeast transformed with the empty vector, while the growth of *AtHKT1;1-Col* and *TmHKT1;5-A* expressing yeast was notably reduced, also showing a greater lag phase (Figure 3.12 B). In the presence of 50 mM NaCl and 50 mM KCl, yeast transformed with the empty vector had a short lag phase and quickly reached a plateau (Figure 3.12 C and D). *AtHKT1;1-C24* expressing yeast had a moderately shorter lag phase as compared to *AtHKT1;1-Col* and *TmHKT1;5-A* expressing yeast when grown under both 50 mM NaCl and KCl, conforming with observations from solid growth media (Figure 3.12 C and D).

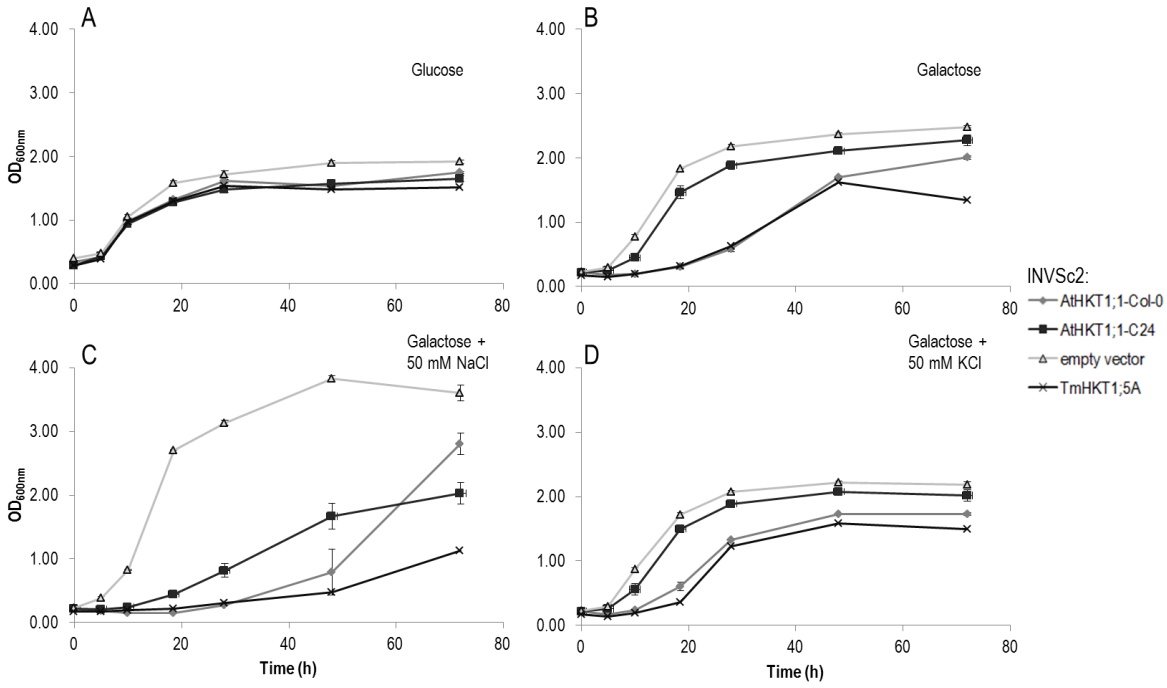

Figure 3.12: Growth curves of wild type *S. cerevisiae* (INVSc2) expressing *AtHKT1;1.*

AtHKT1;1 expressing InvSc2 yeast was grown in 5 mL SD media. Figures (A-D) display OD_{600} readings over 3 d of growth in SD media containing (A) Glucose, (B) Galactose, (C) Galactose + 50 mM NaCl and (D) Galactose + 50 mM KCl. Data presented is mean ± SEM (n=3 independently transformed yeast lines). Some error bars may be smaller than the symbols.

In agreement with solid growth media, B31 transformed yeast grew similarly in the presence of glucose, quickly reaching a plateau (Figure 3.13 A). In the presence of galactose ± 50 mM NaCl or ± KCl, yeast transformed with the empty vector grew similarly well to glucose (Figure 3.13 A-D). A strong inhibition of growth was observed for *AtHKT1;1*-C24 and *AtHKT1;1*-Col-0 expressing yeast grown in the presence of galactose ± 50 mM NaCl or ± KCl (Figure 3.13 B-D). A moderately better growth was observed for *AtHKT1;1*-C24 expressing yeast when exposed to 50 mM KCl (Figure 3.13 D).

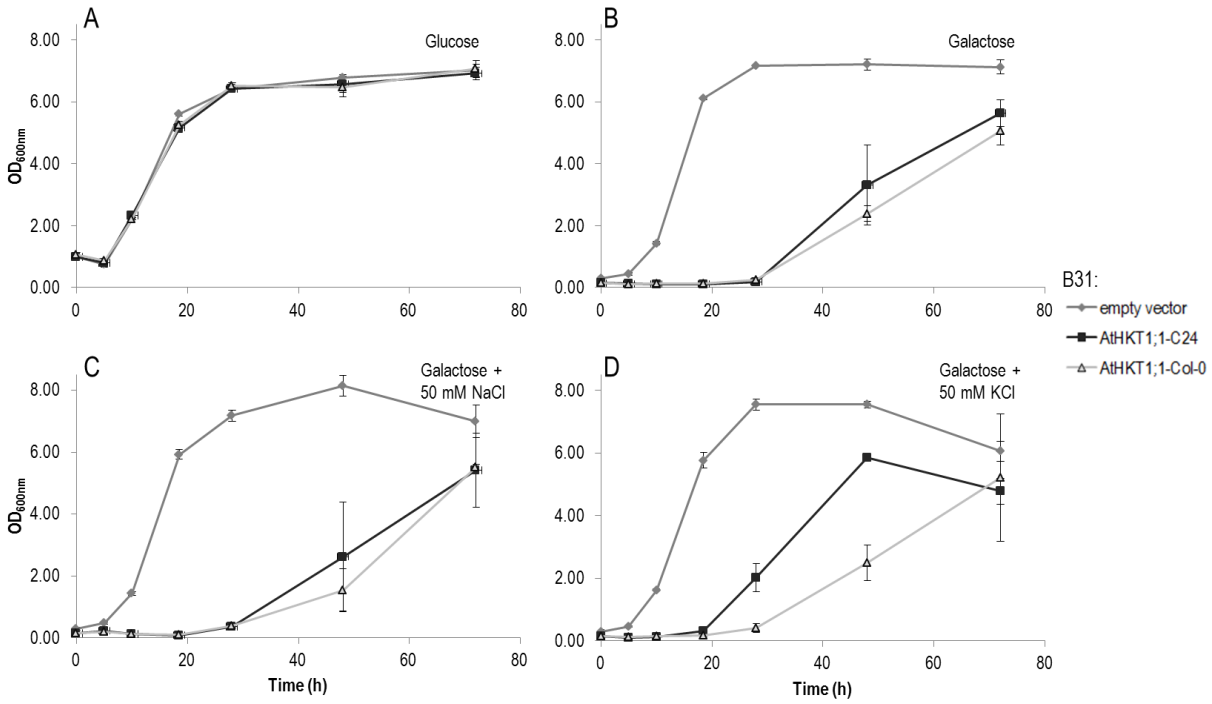

Figure 3.13: Growth curves of the salt sensitive *S. cerevisiae* (strain B31) expressing *AtHKT1;1.*

AtHKT1;1 expressing InvSc2 yeast was grown in 5 mL SD media. Figures (A-D) display OD_{600} readings over 3 d of growth in SD media containing (A) Glucose, (B) Galactose, (C) Galactose + 50 mM NaCl and (D) Galactose + 50 mM KCl. Data presented is mean ± SEM (n=3 independently transformed yeast lines). Some error bars may be smaller than the symbols.

3.5 Discussion

3.5.1 HKT1;1-Col and AtHKT1;1-C24 display Na^+ transport characteristics

To address the hypothesis that AtHKT1;1-Col and AtHKT1;1-C24 both have Na^+ transport properties, electrophysiological measurements in Xenopus oocytes and functional assays in yeast were performed. The results obtained from both expression systems suggest Na^+ transport capacities for both HKTs.

In oocytes, the increase in G and positive shift of E_{rev} with increasing [Na^+] (Figure 3.6 A and B and Figure 3.7 A) is in accordance with previous reports that AtHKT1;1 mediates Na^+ influx into Xenopus oocytes (Byrt 2008, Uozumi *et al.* 2000). Values of E_{rev} for Na^+ containing bathing solutions were in the same range as observed before by Uozumi *et al.* (2000) and Byrt (2008) and also shifted to more positive values with increasing [Na^+], which is consistent with calculated E_{Na^+} values derived from the Nernst equation. Yeast expressing the *AtHKT1;1* genes displayed a strong growth reduction even on SD media with 0 mM additional NaCl. The reduction in growth could be caused by either an increase in toxic substances in the yeast cells (for example Na^+) or due to toxicity caused by over-expression of the *AtHKT1;1* genes driven by the strong GAL1 promoter (Johnston 1987). SD media contains approximately 2 mM NaCl, which may be toxic to the cells when taken up. Consequently AP media, containing only approximately 5 μM NaCl was tested, which also led to a strong reduction in yeast growth. However, the observed growth inhibition is likely due to Na^+ toxicity, rather than toxicity due to *AtHKT1;1* over-expression, as growth of *AtHKT1;1* expressing yeast could be observed when grown on 50 mM KCl and galactose when on both SD and AP.

Although it may appear that the conductance of *AtHKT1;1-Col* expressing oocytes is greater than that of *AtHKT1;1-C24* expressing oocytes (Figure 3.7 and Table 3.3), it is not appropriate to compare the two, since the protein quantity was not determined. To further test the hypothesis that AtHKT1;1-C24 mediates less overall Na^+ transport than AtHKT1;1-Col and the observations made were not artefacts of the experimental conditions, future experiments should test whether reduced Na^+ fluxes are due to AtHKT1;1-C24 transport characteristics and not due to protein abundance in the expression system. In oocytes, care was taken to microinject with exactly the same amount of cRNA into each oocyte, however, the amount of protein that is functionally integrated into the oocyte's membrane may differ. The coding sequence between the Col-0 and C24 *AtHKT1;1* alleles differs in 22 nucleotides, which might lead to inconsistencies in expression efficiency, hence altering the amount of total AtHKT1;1 protein produced in the oocyte and yeast cell. The resulting 9 predicted amino acid changes could also influence the protein structure, affecting the efficiency with which the

protein is incorporated into the membrane. Future experiments for both systems could therefore include qPCR to ensure equal *AtHKT1;1* expression levels and an ELISA analysis or Western blot would allow to determine the total amount of AtHKT1;1 protein. The antibody for an ELISA or Western blot could be directed against the AtHKT1;1 protein itself, i.e. using the antibody generated by Sunarpi *et al*. (2005), or by using an epitope tag. AtHKT1;1 fused to epitope tags have previously been studied in Xenopus oocytes, while N-terminus GFP or FLAG tag fusions appeared to have only minor impact on Na^+ transport, C-terminal fusions were found to substantially impair Na^+ transport (Kato *et al.* 2003). Fluorescent epitope tags could also be used to analyse if the protein is correctly localised at the membrane using confocal microscopy. It should be noted that the exact size of each oocyte was not determined and therefore, the size difference was not taken into account for the analysis. Differences in oocyte size may have influenced comparison of I-E-relationships and therefore may have influenced calculated values for G and E_{rev}. Transport properties of a single AtHKT1;1 protein in an oocyte could be studied using the patch clamp technique (Methfessel *et al.* 1986).

For many proteins, posttranslational modifications are important for accurate functionality (Kwon *et al.* 2006). The nine amino acid changes, predicted in the AtHKT1;1-C24 protein compared to AtHKT1;1-Col, could alter sites of posttranslational modifications and hence result in insufficient activation. A N-glycosylation site in position N429 has been reported previously (Kato *et al.* 2001), but is not predicted to be different between the Col-0 and C24 HKT proteins (data not shown), as determined using the program NetNGlyc (Gupta *et al.* 2004). Another often occurring posttranslational modification is phosphorylation (Kwon *et al.* 2006). Phosphorylation sites were predicted using the program NetPhos2.0 (Blom *et al.* 1999). Only predicted sites that are accessible to potential kinases are of importance, therefore only sites in the cytoplasmic loops were considered (Supplementary Figure 8.4). AtHKT1;1-Col has 7 predicted phosphorylation sites in the cytosolic loops of the protein, of which AtHKT1;1-C24 is missing one (in position S384). The importance of this phosphorylation site for Na^+ transport activity may be further analysed by evaluating mutated proteins in the Xenopus oocyte and yeast expression systems. Constructs could be generated that have the phosphorylation site altered, using site directed mutagenesis, to abolish the phosphorylation site in the Col-0 version, by replacing the S384 with A384 or F384, or to potentially mimic a permanent phosphorylation in the C24 version by replacing S384 with E384 (Pearlman *et al.* 2011). These constructs could be transformed into oocytes and yeast, and the importance of the phosphorylation site on the activity of the protein determined.

In yeast, proteins can be targeted to the plasma membrane and/or the tonoplast. For *AtHKT1;1* expressing yeast cells, a reduction in growth is expected when AtHKT1;1 is localised to the plasma

membrane, mediating Na^+ uptake and therefore leading to Na^+ toxicity. It is possible that, due to the variation in amino acid sequence or protein abundance, AtHKT1;1-C24 is also localised to the tonoplast, therefore mediating less Na^+ uptake from the external media, and possibly even mediating the compartmentalisation of Na^+ into the vacuole, resulting in reduced Na^+ toxicity for the yeast cell. Future studies should therefore determine protein abundance and localisation as described above to clarify AtHKT1;1-C24 function.

An additional method to validate Na^+ uptake into yeast cells and oocytes would be the direct measurement of Na^+ flux using radiolabelled $^{22}Na^+$ (Plett *et al.* 2010). This would allow a comparison of $^{22}Na^+$ uptake by yeast cells and oocytes expressing the two *AtHKT1;1*.

3.5.2 HKT1;1-Col and AtHKT1;1-C24 also display K^+ transport characteristics

While Na^+ transport in *AtHKT1;1* expressing oocytes was expected based on previous studies (Uozumi et al. 2000, Byrt, 2008), it was not clear if currents in the presence of K^+ would be observed. It appears that at K^+ concentrations in the high mM range, K^+ currents are detected in *AtHKT1;1* expressing oocytes, while at K^+ concentrations in the low mM range only minor changes in E_{rev} and G can be observed (Figure 3.6 C and D and Figure 3.7). In Table 3.4 the different *AtHKT1;1* alleles are compared with respect to changes in E_{rev} and G in response to increasing $[K^+]$, including a comparison to two previous studies by Uozumi *et al*. (2000) and Byrt (2008). Uozumi *et al*. (2000) analysed currents in the presence different ions, at -120 mV currents were only observed in the presence of 100 mM Na^+, but not in the presence of 100 mM K^+, Rb^+, Li^+ or Cs^+. However, the oocyte bathing solution used by Uozumi *et al.* (2000) contained 88 mM Na^+ and it cannot be excluded that the Na^+ and K^+ ions influence each other for transport through AtHKT1;1. Both this study and Byrt (2008) used bathing solutions without additional Na^+ and observed currents at 50 mM K^+. It is necessary to test the combination of both Na^+ and K^+ in the same bathing solution to gain further insights into whether K^+ transport through AtHKT1;1 occurs. No strong conclusions can therefore be drawn to compare transport properties of AtHKT1;1-Col and AtHKT1;1-C24 until further experiments validate the observations. Unfortunately, it was only possible to analyse two individual batches of oocytes due to oocyte quality and time restrictions. Oocytes were harvested on a regular basis from different *X. laevis* individuals, but most batches of oocytes did not have a healthy appearance and were therefore not chosen for experiments. The reduced quality of oocytes can be associated to the old age of the frogs used in these studies. Young *X. laevis* individuals were purchased, but their arrival is to this day has been delayed due to Australian quarantine regulations.

Table 3.4: Shift of E_{rev} and conductances of *AtHKT1;1* alleles in response to increasing [K^+]

Allele	E_{rev} shift with increasing [K^+]	Conductance with increasing [K^+]
Col-0	1 to 10 mM K^+: moderately positive shift 10 to 50 mM K^+: no shift	1 to 30 mM K^+: tendency for increase 30 to 50 mM K^+: remains high
C24	1 to 50 mM K^+: positive shift	1 to 30 mM K^+: does not change 30 to 50 mM K^+: increases
L*er* (Uozumi *et al.* 2000)	1 to 10 mM K^+: no shift	1 to 10 mM K^+: no increase. No currents observed when incubated in 100 mM K^+
Col-0 (Byrt 2008)	1 to 50 mM K^+: positive shift	1 to 10 mM K^+: does not change 10 to 100 mM K^+: increases moderately

For further evidence of AtHKT1;1 mediated K^+ transport, the yeast expression system was employed. An improved growth phenotype on media containing 50 mM KCl could be observed, suggesting that AtHKT1;1 could potentially be involved in K^+ transport (Figure 3.11 and Figure 3.13). The uptake of K^+ is generally not toxic to yeast; indeed K^+ uptake is essential for yeast growth. Yeast expressing *AtHKT1;1-C24* grew better with SD media containing 50 mM KCl as compared to 0 mM NaCl/KCl, while growth of the *AtHKT1;1-Col* expressing yeast remained inhibited in the INVSc2 strain. In case of the B31 strain, both, *AtHKT1;1-C24* and *AtHKT1;1-Col* expressing yeast improved growth on 50 mM KCl as compared to 0 mM KCl. This leads to the suggestion that AtHKT1;1-C24 and possibly AtHKT1;1-Col may also be involved in K^+ transport. Unfortunately, these results are not conclusive, as the yeasts' endogenous K^+ transport systems, TRK's, could have influenced growth. Ideally, a yeast mutant defective in its K^+ uptake system, such as the CY162 mutant, which is deficient in the TRK1 and TRK2 K^+ transporters, should be used in future experiments to evaluate K^+ transport properties. This strain has been previously used to test for K^+ transport activity of AtHKT1;1-L*er*; though, it did not appear to be able to complement yeast growth (Uozumi *et al.* 2000). If *AtHKT1;1* was able to mediate K^+ uptake, it would allow the yeast strain deficient in a K^+ uptake system to grow; however, a suitable mutant was not available at the time in the laboratory. It should also be noted that the choice of construct for expression of *AtHKT1;1* in yeast might have an influence on the resulting transport properties (Haro *et al.* 2005). Further support that AtHKT1;1 mediates K^+ transport, when analysed in a heterologous expression system, is presented by Uozumi et al. (2000) who show that an *E.coli* strain defective in its K^+ uptake system was complemented by *AtHKT1;1*-L*er*. However, the bacterial expression system was not further tested in this study.

Similarly to above, an additional method to validate K^+ uptake into yeast cells and oocytes is a direct measurement of K^+ flux by using short-term measurements of radiolabelled $^{42}K^+$. This would allow a comparison of $^{42}K^+$ uptake by yeast cells and oocytes expressing *AtHKT1;1-C24 and AtHKT1;1-Col*. The yeast strain should be deficient in its K^+ transport system to minimise background signal. The Xenopus oocyte expression system could additionally be used to establish whether AtHKT1;1 is permeable for Na^+ and K^+ concurrently, and to test whether the ions influence each other with regards to transport characteristics by utilising bathing solutions with different combinations of [Na^+] and [K^+].

Besides evidence from heterologous expression systems, other evidence for K^+ transport properties of AtHKT1;1 is essential before any firm conclusions can be made. The analysis of transport proteins in isolation allows to study transport properties without the influence of endogenous transporters, however, this isolation also poses one of the greatest disadvantages - some transport proteins require activation by other proteins, such as the guard cell anion channel SLAC1, which needs to be co-localised with the protein kinases OST1 to function (Geiger *et al.* 2009). Ideally, AtHKT1;1 activity is to be measured in the intact plant cell. A very elegant study by Xue *et al.* (2011) has analysed protoplasts derived from the *athkt1;1-4* loss-of-function mutant and compared Na^+ and K^+ fluxes to wild type protoplasts using electrophysiology. In the root, *AtHKT1;1* expression is mostly limited to the stele, this restriction was overcome by using protoplasts derived from GFP labelled stelar cells for electrophysiological experiments. A lack of Na^+ transport activity in the mutant protoplasts, as opposed to the wild type protoplasts, could clearly be identified; while K^+ transport was indistinguishable between the mutant and the wild type (Xue *et al.* 2011). However, the authors point out that the lack of K^+ fluxes through AtHKT1;1 may be due to the possible down regulation of *AtHKT1;1* expression in the presence of the K^+ containing test solution (Xue *et al.* 2011). *AtHKT1;1* has very low expression levels *in planta* (Chapter 7, Jha *et al.* (2010) and Sundstrom (2011)), and additionally a number of endogenous K^+ transport systems are present (Maathuis and Amtmann 1999), which potentially limit the detection of differences in K^+ fluxes mediated by AtHKT1;1. Future investigation could include the use of the protoplast system with different solution compositions containing Na^+ and K^+ at the same time and possibly optimising the technique to obtain protoplasts with high *AtHKT1;1* expression. Other regulatory mechanisms, such as post-translational modifications to the protein, cannot be excluded and may also have major influence on *in planta* function as compared to heterologous expression systems (Xue *et al.* 2011). To further study differences in AtHKT1;1-C24 and AtHKT1;1-Col transport properties with regards to Na^+ and K^+, the *athkt1;1-4* loss-of-function mutant could be transformed with *AtHKT1;1-C24* and *AtHKT1;1-Col* and tested for complementation of Na^+ and K^+ transport.

3.5.3 Conclusion

In this chapter the heterologous expression systems Xenopus oocytes and *S. cerevisiae* were used to functionally characterise AtHKT1;1-Col and AtHKT1;1-C24. The presented data suggest that not only Na^+, but also K^+ transport may be relevant when AtHKT1;1 is analysed in the Xenopus oocyte expression system. This has to be confirmed by analysing more batches of oocytes and different Na^+ and K^+ solution compositions. Also yeast functional assays suggested Na^+ transport properties with a potential role for K^+ uptake. A strong reduction in growth was observed in *AtHKT1;1* expressing yeast in the presence of Na^+, while in the presence of K^+, yeast growth was improved as compared to control conditions. Further experiments with a yeast mutant deficient in its K^+ uptake systems are required for conclusive results.

While this chapter was focused on characterising transport properties of AtHKT1;1-Col and AtHKT1;1-C24, the following chapter will subsequently evaluate expression patterns of the *AtHKT1;1-Col* and *AtHKT1;1-C24* transcripts.

Chapter 4 **Regulation of *AtHKT1;1* expression in Col-0 and C24 by the promoter sequence**

4.1 Differences in the Col-0 and C24 *AtHKT1;1* expression pattern

The pattern of *AtHKT1;1* expression in plants has been analysed in a number of studies, using a variety of different protocols, for instance using *promoter::GUS* transgenic lines (Berthomieu *et al.* 2003, Mäser *et al.* 2002, Sunarpi *et al.* 2005). For the purpose of this thesis, the 'promoter region' refers to the intergenic region between *AtHKT1;1* and the preceding gene *At4g10300* or a fragment of the promoter is specified (i.e. 2.7 kb promoter), which refers to the genomic sequence upstream of the *AtHKT1;1* ATG start codon (in this example a fragment 2.7 kb in size immediately upstream of the ATG start codon). The intergenic region between *AtHKT1;1* and *At4g10300* is approximately 6.1 kb long in the Col-0 ecotype, but it is unknown whether this region contains the fully functional *AtHKT1;1* promoter.

Early studies of *AtHKT1;1* expression used a 837 bp promoter fragment of the Ws *AtHKT1;1* promoter sequence to drive *GUS* expression in transgenic Col-1 plants. These studies detected GUS activity predominantly in the root stele and leaf vasculature (Mäser *et al.* 2002, Sunarpi *et al.* 2005). Similarly, a 2.3 kb promoter fragment of the Col-0 ecotype was used to drive *GUS* expression, which also displayed a root stele and leaf vasculature expression pattern (Berthomieu *et al.* 2003). Additionally, AtHKT1;1 transport activity has recently been confirmed in protoplasts isolated from root stelar using electrophysiological techniques (Xue *et al.* 2011). Localisation of *AtHKT1;1* expression in the root stele is consistent with the hypothesis that AtHKT1;1 is a transport protein that retrieves Na^+ from the xylem into xylem parenchyma cells, and thereby reduces the amount of Na^+ translocated to the shoot *via* the transpiration stream.

A recent study investigated the regulatory elements in the 6 kb Col-0 *AtHKT1;1* promoter sequence, identified a small RNA binding site 2.6 kb upstream of the start codon and two repeat regions 4 kb upstream of the start codon which were hypothesised to regulate the expression of *AtHKT1;1* (Baek *et al.* 2011). A diagram of the 6.1 kb Col-0 promoter sequence is depicted in Figure 4.1.

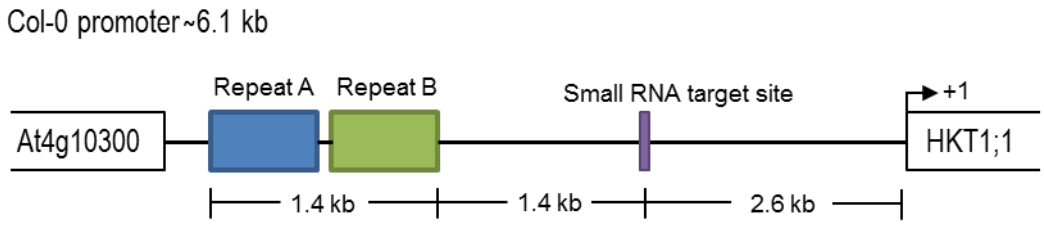

Figure 4.1: Diagram of the Col-0 *AtHKT1;1* promoter sequence.

Highlighted in the image are two 700 bp repeat regions in blue and green, positioned 4 kb upstream of the ATG start codon (marked with an arrow +1) and the small RNA target site, 2.6 kb upstream of the ATG start codon.

Various *promoter::GUS* constructs were tested in a Col-0 background and the root and shoot GUS activity was imaged in 10 d old plate grown seedlings (Summary in Table 4.1) (Baek *et al.* 2011). Strong GUS activity was observed in transgenic lines that used a 2 kb promoter fragment to drive *GUS* expression (Baek *et al.* 2011). Lower levels of GUS activity were detected in roots of transgenic lines in which *GUS* was driven by a 5.2 kb promoter fragment (containing both repeat regions and the small RNA target site), a 4.6 kb promoter fragment (only containing the region Repeat B and the small RNA target site) and a 3.9 kb promoter fragment (containing only the small RNA target site) (Baek *et al.* 2011). When specifically the small RNA target site was deleted in those listed promoter fragments, GUS activity was increased in both the shoot and root compared to constructs with intact small RNA binding site (Baek *et al.* 2011). This GUS analysis, together with methylation studies in that region, suggest that the small RNA target site is involved in regulating root and shoot *AtHKT1;1* expression, *via* small RNA mediated methylation. However, the repeat region does not appear to be important for regulating *AtHKT1;1* expression in the root, since the 5.2 kb and the 3.9 kb promoter fragments both lead to similar levels of GUS activity. Nevertheless, specifically in the *sos3* mutant background, an involvement of the repeat region in regulating *AtHKT1;1* expression is suggested (Baek *et al.* 2011); this will be outlined further in the discussion (4.7.1).

Table 4.1: Summary of results by Baek *et al*. (2011) analysing GUS activity in Col-0 seedlings transformed with various *AtHKT1;1promoter::GUS* constructs.

***AtHKT1;1* promoter fragment (in kb)**	**Repeat region present[1]**	**small RNA binding site present[1]**	**GUS activity in the root**	**GUS activity in the shoot**
5.2	yes	yes	low	weak
4.6	repeat B only	yes	low	moderate
3.9	no	yes	low	weak
5.2[2]	yes	no	moderate	strong
4.6[2]	repeat B only	no	moderate	strong
3.9[2]	no	no	moderate	strong
2	no	no	moderate	strong

[1] presence of repeat region or small RNA binding site in constructs used for *promoter::GUS* constructs (refer to Figure 4.1 for details) [2] deletion of small RNA binding site from promoter

As mentioned in the introductory chapter, previous studies have shown that *AtHKT1;1* is not expressed in C24 roots, and expression is not induced under salt stress (Jha *et al.* 2010, Sundstrom 2011). This lack of *AtHKT1;1* expression in C24 roots is hypothesised to cause the increase in shoot Na^+ content in C24 plants, as no AtHKT1;1 protein is retrieving Na^+ from the xylem, therefore allowing Na^+ to translocate to the shoot. Sundstrom (2011) confirmed the presence of the *AtHKT1;1*

gene in the C24 genome, and also detected *AtHKT1;1* transcripts in the C24 shoot, but not in the root. This chapter will investigate the role of the promoter in regulating *AtHKT1;1* expression in the root.

4.2 Col-0 and C24 display substantial differences in the *AtHKT1;1* promoter region

To investigate possible causes for the differences in *AtHKT1;1* expression between Col-0 and C24 roots, Sundstrom (2011) determined the nucleotide sequence of 6.1 kb of the Col-0 and C24 *AtHKT1;1* promoters and the *AtHKT1;1* genes. The genomic DNAs starting from the predicted preceding gene upstream of *AtHKT1;1*, *At4g10300*, to the predicted 3′ end of the *AtHKT1;1* gene were sequenced and compared between the two ecotypes (Figure 4.2). Two regions with major differences between the Col-0 and C24 promoters are highlighted. A 700 bp region, positioned approximately 4 kb upstream of the *AtHKT1;1* start codon, is repeated twice in the Col-0 *AtHKT1;1* promoter (as reported by Baek *et al.* (2011)), while the C24 promoter has only one 700 bp region. Also, a 240 bp region immediately upstream of the *AtHKT1;1* start codon is highly polymorphic between Col-0 and C24. This region just upstream of the start codon is bound by transcription and initiation factors and polymorphisms between the Col-0 and C24 sequence may result in polymorphic binding sites for these transcription factors. This could consequently cause the differential expression of the *AtHKT1;1* gene in Col-0 and C24. For instance, TATA-box and CAAT-box motifs are involved in transcription initiation (Joshi 1987, Kusnetsov *et al.* 1999). A putative TATA-box and two putative CAAT-box motifs have been identified in the Col-0 promoter (Uozumi *et al.* 2000). In C24, the polymorphisms in the 240 bp-region immediately upstream of the *AtHKT1;1* start codon result in disruption of one of the putative CAAT motifs; however, another CAAT motif is introduced at a different site due to the deletion of one base. The small RNA target site reported by Baek *et al.* (2011) is present in both ecotype's promoters in the same position.

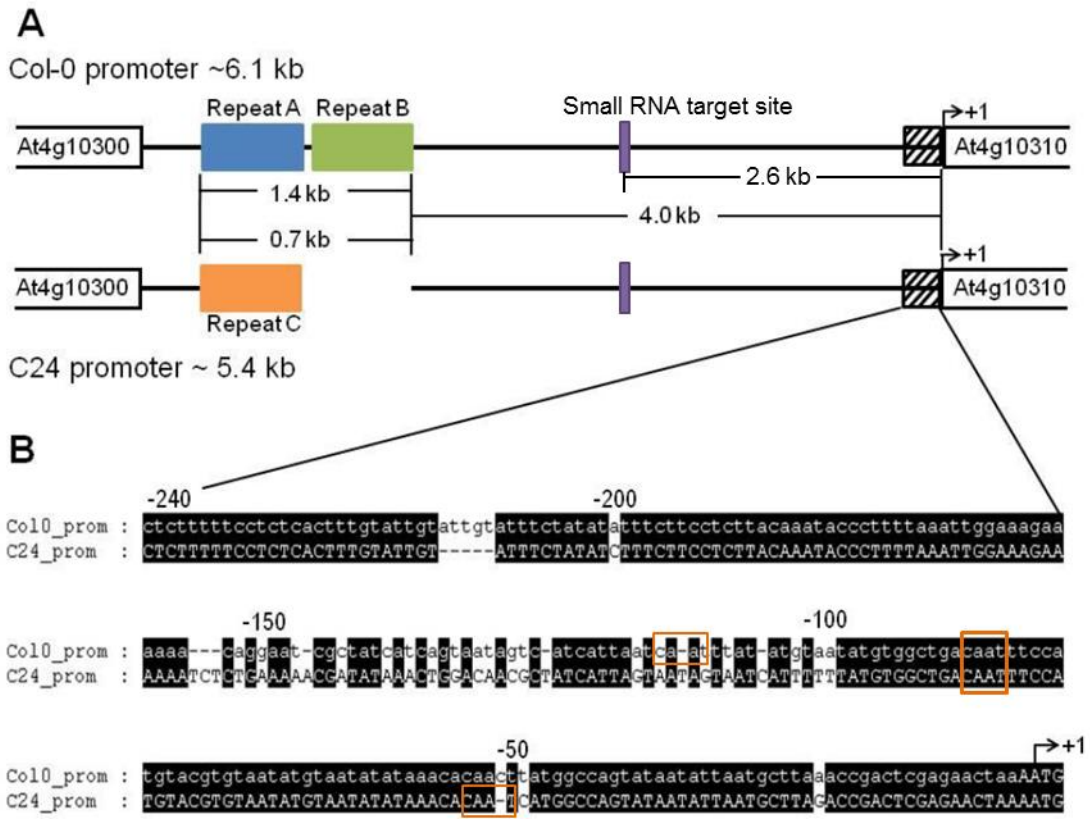

Figure 4.2: Comparison of the *AtHKT1;1* promoter sequence from Col-0 and C24 (modified from Sundstrom 2011).

(A) alignment of the Col-0 and C24 promoter sequence, highlighting in the Col-0 promoter two 700 bp repeat region with minor sequence differences (blue and green), while the C24 promoter contains only one of these regions (orange). The small RNA target site (purple) does not differ between the ecotypes. The black hashed box upstream of the *AtHKT1;1* start codon represents the 240 bp-region prior the start codon, which is shown in more detail in panel B. (B) Alignment of the 240 bp region just upstream of the *AtHKT1;1* start codon, indicated by the +1 arrow. The orange boxes mark the putative CAAT-box motifs that may be involved in transcription initiation.

The *promoter::GUS* analyses performed by Baek *et al*. (2011) suggested that the repeat region 4.0 kb upstream of the start codon has no influence on regulating expression in the root tissue, as opposed to the small RNA target site 2.6 kb upstream of the start codon, which appeared to lead to increased *AtHKT1;1* expression levels if absent. The small RNA target site is present in both Col-0 and C24, however, it is possible that altered methylation in this site causes repression of *AtHKT1;1* expression in C24. Moreover, the substantial differences identified just prior to the start codon could lead to the lack of *AtHKT1;1* expression in C24. To analyse whether the differences in the promoter cause the lack of *AtHKT1;1* expression in C24, this study tested the promoter activity *in planta*.

4.3 Approaches to test for promoter activity and expression

To analyse whether the C24 promoter causes the lack of *AtHKT1;1* expression in C24 roots, several transgenic lines were generated by Sundstrom (2011). Transgenic lines were generated in which the 2.7 kb fragments of the Col-0 or C24 *AtHKT1;1* promoter were used to drive *GFP,* or in which mixed promoters that contain the majority of the promoter from one ecotype and 250 bp, just upstream of the start codon, of the other ecotype's promoter to drive *GFP* (Figure 4.3 A). Also, transgenic lines were generated in which the 2.7 kb fragments of the Col-0 or C24 *AtHKT1;1* promoter were used to drive *AtHKT1;1* cDNA (Figure 4.3 B). The 2.7 kb promoter contains the polymorphic region just upstream of the start codon and the small RNA target site; it does not contain the repeat element, as it has not been shown to influence expression in root of transgenic Col-0 plants (Baek *et al.* 2011). Sundstrom (2011) transformed the constructs into the Col-0, C24 or Col-0 *gl1 hkt1-4* background. The Col-0 *gl1 hkt1-4* mutant has a 16 bp deletion in the third exon of *AtHKT1;1*, leading to a predicted frame shift, which would cause an altered AtHKT1;1 protein, likely to be non-functional (Rus *et al.* 2004). Consistent with the assumption that AtHKT1;1 is not functional in the Col-0 *gl1 hkt1-4* mutant, these plants accumulate an increased amount of Na^+ and have decreased root Na^+ content as compared to the background Col-0 *gl1* (Rus *et al.* 2004).

This chapter will refer mostly to the 2.7 kb fragment of the Col-0 and C24 *AtHKT1;1* promoter, hence they will be referred to as pCol-0 and pC24, respectively, and the coding sequence of *AtHKT1;1* from either ecotype will be referred to as Col-0cDNA and C24cDNA, respectively.

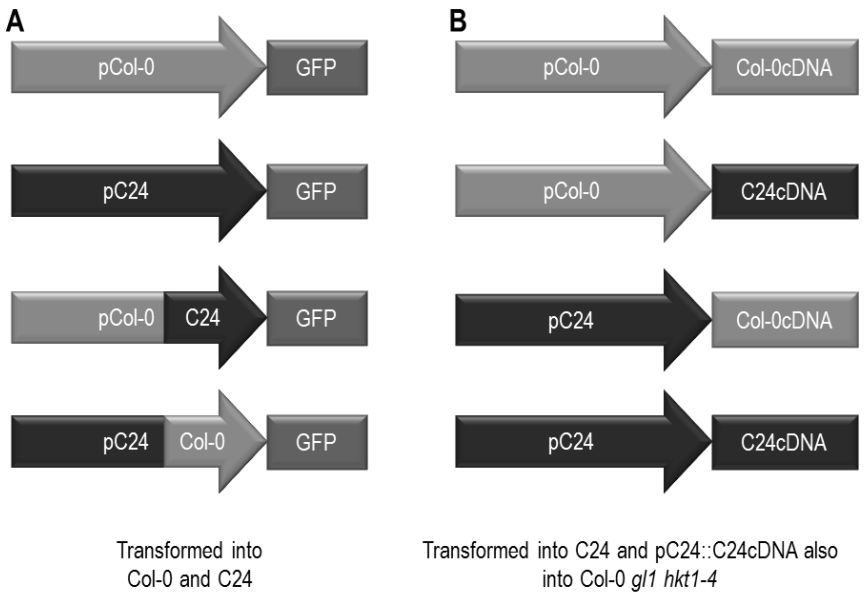

Figure 4.3: Overview of *AtHKT1;1* promoter and gene combinations of either *GFP* or *AtHKT1;1* cDNA for *in planta* analysis.

(A) *GFP* expression is driven by the 2.7 kb *AtHKT1;1* promoter of Col-0, C24 or a mixed promoter consisting of 2.24 kb of one ecotype's promoter and 250 bp of the other ecotype's promoter (just 5′ of the start codon where there are polymorphisms in the sequence between the two ecotypes). Constructs were transformed into Col-0 and C24 backgrounds for detection of *GFP* expression (B) Col-0 or C24 *AtHKT1;1* cDNA is driven by 2.7 kb of the Col-0 or C24 promoter. Constructs were transformed into C24 and the last construct, *pC24::C24cDNA* was also transformed into the Col-0 *gl1 hkt1-4* knock out mutant.

If the promoter is predominantly responsible to regulate *AtHKT1;1* expression and therefore causes the lack of *AtHKT1;1* expression in C24 roots, the analysis of *promoter::GFP* lines will provide evidence to determine if this is the case. *AtHKT1;1* expression is detectable in the stele of Col-0 roots (Berthomieu *et al.* 2003, Xue *et al.* 2011), it is therefore expected that *pCol-0* is able to drive *GFP* expression in the Col-0 background in the same cell type. Oppositely, C24 lacks native *AtHKT1;1* expression in the roots, which would lead to the hypothesis, that *GFP* expression would not be detected when driven by *pC24* in the C24 background. To test if other factors, such as small RNAs, are absent/present in C24 that suppress *AtHKT1;1* expression, transgenic lines had been generated in which *pCol-0* drives *GFP* expression in the C24 background. Similarly, to test if the C24 promoter sequence has elements missing and therefore does not lead to gene expression, constructs had been generated in which *pC24* drives *GFP* expression in the Col-0 background. Transgenic lines with mixed promoter constructs will test if the region just upstream of the ATG start codon contains regulatory elements, such as the transcription initiation site, that are interrupted in C24. The T_1 generation of *promoter::GFP* transformed lines had been tested in preliminary

experiments and GFP fluorescence was detected (Sundstrom 2011). However, these plants were subject to severe stress by the selection process, which could impact *GFP* expression resulting in false positives. A subsequent analysis of the T_2 generation on ½-strength MS media ± 100 mM NaCl did not lead to any GFP being detected using confocal microscopy (Sundstrom 2011). Plants have reduced transpiration when grown on ½-strength MS plates due to limitations in airflow and *AtHKT1;1* expression has been reported to be reduced in non-transpiring conditions as opposed to transpiring conditions (Jha *et al.* 2010, Sundstrom 2011). As *GFP* is driven by the *AtHKT1;1* promoter, it is possible that its expression is too low under non-transpiring conditions for detection. Therefore, the objective of this chapter is to test if both the Col-0 and C24 *AtHKT1;1* promoters are able to drive GFP expression in the stele of the root tissue, when grown under transpiring conditions.

Additional constructs were used to test whether the 2.7 kb promoter induces expression of the target gene in the expected tissue, the root stele, and to test whether C24 may have other regulatory molecules, such as small RNAs, that cause degradation of the *AtHKT1;1* transcript. In these constructs *pCol-0* and *pC24* are used to drive expression of the Col-0 and C24 cDNA (Figure 4.3 B). The constructs were transformed into the C24 background, as it lacks endogenous *AtHKT1;1* expression in the root (Sundstrom 2011). The lack of endogenous *AtHKT1;1* expression correlates with an increased Na^+ accumulation in the C24 shoot and reduced Na^+ content in C24 roots. It is expected that if transgenic lines express a functional *AtHKT1;1* in the expected cell type, the stele, shoot Na^+ content will decrease and the root Na^+ content will increase. Furthermore, the construct in which pC24 drives expression of the C24 cDNA was also transformed into the Col-0 *gl1 hkt1-4* background. This will demonstrate whether C24 *AtHKT1;1* is functional and able to complement the mutated endogenous *AtHKT1;1*. Successful complementation would be expected to lead to Na^+ and possibly K^+ contents comparable to the wild type Col-0. Sundstrom (2011) had tested expression of the *AtHKT1;1* transgene in the T_2 *promoter::cDNA* lines by semi-qPCR, however, the transgenic lines were previously not tested for functionality of the produced AtHKT1;1 protein by determining the Na^+ and K^+ content. These measurements will be completed in this study.

4.4 Aims of this study

The aim of this study is to characterise the putative promoter region of C24 and Col-0 *AtHKT1;1*. Since both ecotypes differ in their *AtHKT1;1* expression pattern, with C24 lacking *AtHKT1;1* transcripts in the root, the possible role of the promoter region in transcriptional regulation will be examined. For this purpose, the following points will be addressed:

1. Test if the putative C24 2.7 kb *AtHKT1;1* promoter is responsible for the lack of *AtHKT1;1* expression in C24 roots.
    a. Use *promoter::GFP* constructs to test if *pCol-0* and *pC24* are able to drive *GFP* expression in both the Col-0 and C24 background.
    b. Test if the mixed promoters, in which 240 bp have been replaced with the other ecotype's promoter fragment, are able to drive *GFP* expression.
2. Test whether the putative 2.7 kb *AtHKT1;1* promoter results in expression in previously reported cell types.
    a. Test if the *GFP* expression pattern, when driven by *pCol-0* and *pC24,* is cell type specific and consistent with previously reported stelar expression in both background ecotypes, Col-0 and C24.
    b. Transgenic lines that express *Col-0cDNA* and *C24cDNA*, under control of *pCol-0* and *pC24* in the C24 and Col-0 *gl1 hkt1-4* background are tested: (1) if functional AtHKT1;1 is produced that causes reduction of shoot Na^+ and increase in root Na^+ content compared to wild type plants and nulls when plants are exposed to salt stress and (2) if functional AtHKT1;1 is produced that has an influence on the K^+ content in the root and shoot compared to wild type plants and Nulls when plants are exposed to salt stress.

4.5 Materials and methods

4.5.1 Salt stress assay of Col-0 and C24 plants using hydroponics

Plants were grown in an aerated hydroponics system for 5 wk (chapter 2.2.4) under short day conditions (10 h light), before inducing salt stress by application of 100 mM NaCl. To maintain Ca^{2+} activity in the nutrient solution 0.8 mM $CaCl_2$ was added (determined using Visual MINTEQ 2.30). Nutrient solution was changed the day before application of salt stress and pH was monitored regularly to prevent acidification. Salt stress was applied by dissolving the desired amount of NaCl and $CaCl_2$ in a 500 mL aliquot of nutrient solution, removed from the tank, and pouring the solution back into the tank under vigorous stirring. The salt treatment was applied 1 h after the light cycle commenced. For biomass measurements, fresh weight of the whole shoot and root were recorded at time point 0, 2 d, 5 d and 7 d after salt application. The root was dried for exactly 3 sec between paper towels and the fresh weight was recorded. To determine Na^+ and K^+ content, the last fully expanded leaf was removed, its fresh weight recorded and the leaf placed in a 2 mL microfuge tube for drying at 65 °C o/n. Dried leaves were used for flame photometry to determine the Na^+ and K^+ content (section 4.5.2). Roots were washed in 10 mM $MgSO_4$ to remove nutrient solution and contaminating salt. The root was placed in a 2 mL tube and dried at 65 °C o/n. Dried samples were used for flame photometry to determine the Na^+ and K^+ content (section 4.5.2). For hydroponically grown *promoter::GFP* lines, plants were harvested after 7 d of salt treatment as follows: The last fully expanded leaf was collected, snap frozen in liquid nitrogen and stored at -80 °C for RNA extraction (section 2.5.1). One leaf was collected and stored at -20 °C for DNA extraction (section 2.4.1.2) and the root was divided laterally with one half being collected, snap frozen in liquid nitrogen and stored at -80 °C for RNA extraction (section 2.5.1), with the other half remaining attached to the shoot and being immediately subject to analysis by confocal microscopy (section 4.5.4). At least three replicate plants were kept intact for confocal analysis (no tissue removed), to ensure fluorescence was not detected as an artefact caused by taking tissue samples.

4.5.2 Measurement of Na^+ and K^+ content using flame photometry

Samples from hydroponically grown plants were harvested to determine the Na^+ and K^+ content in the youngest fully expanded leaf and the root. Dry weights of the leaf and root samples were recorded and 2 mL of 1 % (v/v) nitric acid was added to the plant tissue. Samples were digested at 65 °C o/n. For flame photometry, 1:10 dilutions of these digests were made using 2 mL sterile MQ water. The Na^+ and K^+ contents of tissue samples were determined using a model 420 Flame

Photometer (Sherwood Scientific Ltd, Cambridge, United Kingdom) calibrated to known concentrations of Na^+ and K^+.

4.5.3 Plant material: *promoter::GFP* and *promoter::*cDNA transgenic lines

Seeds of T_2 transgenic lines, transformed with constructs detailed in Figure 4.3, were obtained from Dr. Joanna Sundstrom (University of Adelaide, Australia). For *promoter*::*GFP* lines, the promoter sequences had been recombined into the expression vector pMDC107, originating from Curtis and Grossniklaus (2003), which contains the *GFP* sequence and allows selection of transformed lines on hygromycin (general vector map in Supplementary Figure 8.6). The sequences of *promoter*::*AtHKT1;1*cDNA constructs had been recombined into the expression vector pMDC100 (Curtis and Grossniklaus 2003), and allowed selection of transgenic plants on kanamycin, mediated by the *NptII* gene (general vector map in Supplementary Figure **8.7**). The destination vector was modified by Sundstrom (2011) to include a *nosT* termination sequence after the inserted gene. Plants that do not contain the transgene due to the segregation in the T_2 generation are referred to as null segregants, or nulls for short. These were identified by performing a PCR on genomic DNA (section 2.1.1) with primers amplifying a fragment of *GFP* (primers GFPi F and GFP R) or the selection maker gene *NptII* (primers listed in Table 4.2).

4.5.4 Analysis of GFP fluorescence by confocal microscopy

The roots of Col-0, C24 and T_2 *AtHKT1;1promoter::GFP* transgenic lines were imaged using a Zeiss Axioskop 2 mot plus LSM5 PASCAL laser scanning microscope, equipped with an argon laser (Carl Zeiss, Jena, Germany). To obtain an improved visualisation of cell types for localisation of GFP fluorescence, the cell walls of root tissue were stained by incubating the roots in 10 μg mL^{-1} propidium iodide at room temperature for approximately 5 min and before rinsed in H_2O for 5 to 10 min. Roots were mounted on glass slides under cover slips for imaging. Propidium iodide was detected using an excitation of 543 nm and a long pass 560 nm emission filter and displayed as red in images. GFP fluorescence was detected using an excitation of 488 nm and an emission of 505-530 nm and presented as green in images. Transmitted light images are presented in grey scale. Images were captured using PASCAL (version 4.2.0.121; Carl Zeiss Microimaging GmbH, Jena, Germany). Representative images are displayed of three hydroponics experiments with at least three independent transgenic lines per construct and a minimum of three biological replicates (unless stated otherwise).

4.5.5 Analysis of *GFP* and *AtHKT1;1* transcripts in T_2 *AtHKT1;1promoter::GFP* and *AtHKT1;1promoter::cDNA* lines

For analysis of T_2 *AtHKT1;1promoter::GFP* and *AtHKT1;1promoter::cDNA* transgenic lines, the expression of *GFP* and *AtHKT1;1-cDNA*, respectively, was detected using RT-PCR. For RT-PCR, RNA was extracted from shoot and root samples collected as described above (section 4.5.1). Total RNA was DNase treated and cDNA was synthesised using an oligo $d(T)_{20}$ primer (sections 2.5.2). To evaluate cDNA quality, a 180 bp fragment of *Actin2* transcripts was PCR amplified (using Actin2 F and R primers). To determine *GFP* expression, a 234 bp fragment of *GFP* transcripts was also PCR amplified (with GFPi F and R primers) using Platinum *Taq* DNA polymerase (section 2.1.1) and visualised using agarose gel electrophoresis (section 2.1.2). To determine *AtHKT1;1* expression, two primer-sets were used. PCR amplification of *AtHKT1;1* using the primers HKT1;1_Q_F and HKT1;1_Q_R lead to amplification of a 130 bp fragment of *AtHKT1;1* without distinguishing between the native transcript and transcripts deriving from the transgene. Additionally, PCR primers HKT1;1_Q_F and HKT1;1_transgene_R were used for amplification of a 920 bp fragment that is specific for the transgene. Primers are listed in Table 4.2. To confirm that the DNase treatment was successful and no contaminating gDNA was present in the cDNA samples, a random subset of approximately 10 % of the samples was subject to PCR using *Actin2* primers specific for genomic DNA (using Actin2 genomic F and R primers). The use of primer pair Actin 2 F and R only leads to amplification of fragments from cDNA templates, as the forward primer was designed over an exon-intron boundary. The use of the primer pair Actin2 genomic F and R leads to amplification of fragments from genomic DNA templates, as one of the primers is designed to anneal in the intron sequence.

Additionally, qPCR (section 2.5.3) was performed on pooled samples of RNA derived from a separate hydroponics experiment to verify semi-qPCR results (using primers qGFP F and R).

Table 4.2: Primers used to analyse GFP expression using semi-qPCR

Primer name	Sequence (5'-3')	Product size
Actin2 F	TGAGCAAAGAAATCACAGCACT	180 bp
Actin2 R	CCTGGACCTGCCTCATCATAC	
GFPi F	TCAAGGAGGACGGAAACATC	234 bp
GFPi R	AAAGGGCAGATTGTGTGGAC	
Actin2 genomic F	TGCCAATCTACGAGGGTTTC	544 bp
Actin 2 genomic R	GAACCACCGATCCAGACACT	
qGFP F	TGTCCTTTTACCAGACAACCATTA	104 bp
qGFP R	CAGCTGTTACAAACTCAAGAAGGA	
NptII F	AATGAACTCCAGGACGAGGCAG	612 bp
NptII R	GTCAAGAAGGCGATAGAAGGCG	
HKT1;1_Q_F	TGC AAA CTG CGG ATT TGT CC	130 bp
HKT1;1_Q_R	TGA GCA AAA CCA AGA AGC AAG G	
HKT1;1_Q_F	TGC AAA CTG CGG ATT TGT CC	920 bp
HKT1;1_transgene_R	GCTGGGTCGAATTCGCCCTTATTCTGC	

4.5.6 Northern Blot to determine *GFP* expression

Northern Blot analysis was performed to evaluate *GFP* transcript abundance. This method allows the detection of transcripts of interest by hybridising a radioactively labelled probe against a specific fragment of the transcript of interest. As opposed to qPCR, no reverse transcription is required, the transcripts are detected directly.

The RNA of salt treated plants was pooled to obtain a sufficient amount of RNA for analysis (approximately 20 μg in a volume of 5 μL).

4.5.6.1 Denaturating gel preparation

All equipment and vessels used were autoclaved twice or treated with RNAzap (Cat. # R2020, Sigma-Aldrich, Castle Hill, Australia) following the manufacturer's instructions. Samples were separated in a formaldehyde-agarose gel [1.5 % (w/v) agarose, 2 % (v/v) formaldehyde, 20 mM 3-(N-morpholino)propanesulfonic acid (MOPS), 8 mM $NaOAc \cdot 3H_2O$ and 1 mM EDTA]. The agarose-formaldehyde gel was subject to electrophoresis at 80 V for 45 min in 1x MOPS electrophoresis buffer (20 mM MOPS, 8 mM $NaOAc \cdot 3H_2O$ and 1 mM EDTA) before samples were loaded onto the gel. Once the samples were loaded, electrophoretic separation was performed at 80 V for approximately 2 h, until the RNA was sufficiently separated.

4.5.6.2 RNA sample preparation

To 5 μL of RNA 5 μL of 2 × sample buffer (50 % (v/v) deionised formamide, 0.5× MOPS, 6% (v/v) formaldehyde, 0.2 mg·mL^{-1} ethidium bromide, 10 mM EDTA, pH 8.0) was added and incubated at 65 °C for 5 min to denaturate RNA and then immediately incubated on ice for 5 min. 2 μL of blue buffer (50 % glycerol, 50 mM EDTA, 2.5 % (w/v) bromophenol-blue, 2.5 % (w/v) xylene cyanol) was added before loading the gel.

4.5.6.3 RNA transfer onto nylon membrane

RNA was transferred from the agarose formaldehyde gel onto a Biodyne® B Nylon Transfer Membrane, 0.45 μm (Cat. # 60202, Pall Corporation, Cheltenham, Australia) using the setup displayed in Figure 4.4. A sponge was soaked in 20× SSC transfer buffer (3 M NaCl, 0.3 M tri-sodium citrate) and placed in a plastic tray filled with transfer buffer. Filter paper was placed on top of the sponge, followed by a plastic screen, which has a cut-out for the gel, ensuring the transfer buffer only migrates through the gel and not directly into the tissue in the top layers. The agarose gel was placed in the hole of the screen so that it is in contact with the filter paper. The nylon membrane is carefully placed on top of the gel, followed by more filter paper. In all steps it was ensured that no air bubbles were trapped in between layers, which would interfere with the transfer. A pile of approximately 5 cm high tissue paper was placed on top to absorb the transfer buffer that migrated through the setup and covered with a heavy glass plate.

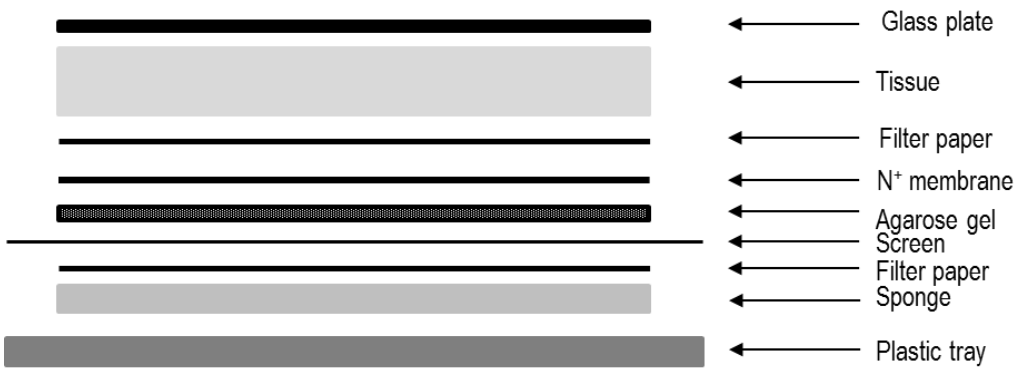

Figure 4.4: Diagram for setup of Northern Blot.

After RNA was separated in a formaldehyde-agarose gel it was transferred onto a nylon membrane by capillary action.

4.5.6.4 Hybridisation

A GFP specific probe for hybridisation was generated by PCR using Platinum *Taq* polymerase using the GFP containing pMDC107 plasmid as template (primers FW: ATGAGTAAAGGAGAAGAACTTTTCACTGG and RV: AAAGGGCAGATTGTGTGGAC (chapter 2.1.1)). Radioactive labelling of the probe, hybridisation to the membrane and detection of radioactivity was performed by Ms. Margaret Pallotta (ACPFG, Australia) following the protocol by Sambrook *et al.* (1985). Briefly, the GFP probe was oligolabelled with random primers and dCT^{32}P using DNA Polymerase I, large (Klenow) fragment. The membrane was blocked with salmon sperm and Denhardt's reagent o/n at 42 °C prior to hybridising the probe to the membrane o/n at 42 °C. The membrane was washed at least four times, then dried and placed into a developer cassette with film for 7 d at – 80 °C. The developed film was scanned for documentation.

4.6 Results

4.6.1 Salt stress assay in hydroponically grown Col-0 and C24

Previous research conducted by Shearer (2013) had tested the effect of different NaCl concentrations (50 mM and 100 mM NaCl) on Arabidopsis ecotype Col-0 grown in hydroponics. Salt treatment with 100 mM NaCl resulted in visible salt stress symptoms on Col-0 plants, but the plants were able to survive a 7 d stress period. However, the response of the ecotype C24 to a similar treatment was unknown, thus, a preliminary experiment was conducted to compare the responses between Col-0 and C24, with particular focus on whole root/shoot biomass and the root/shoot Na^+ and K^+ content after 0, 2 d, 5 d and 7 d of treatment with 100 mM NaCl (Figure 4.5 and Figure 4.6). This will identify the best time point for a more detailed subsequent analysis.

After two days of 100 mM NaCl treatment, no visible symptoms of salt damage could be detected. However, after 5 days in 100 mM NaCl solution Col-0 plants were notably smaller than 0 mM NaCl grown plants and showed symptoms of salt stress, such as darker green and purple leaves (Figure 4.5). The effect was more apparent after seven days of treatment, with the oldest leaves of Col-0 plants beginning to show symptoms of senescence (Figure 4.5). However, salt stressed C24 plants appeared healthy and visually only slightly smaller than control plants after seven days of exposure to 100 mM NaCl (Figure 4.5). Under control conditions, both Col-0 and C24 tripled their shoot (Figure 4.6A) and root (Figure 4.6B) fresh weight over the seven day period. When exposed to 100 mM NaCl, Col-0 did not significantly increase its shoot (Figure 4.6 A) and root (Figure 4.6 B) fresh weight over the seven day stress period, while C24 was able to significantly increase both shoot and root fresh weight (ANOVA, p=0.05).

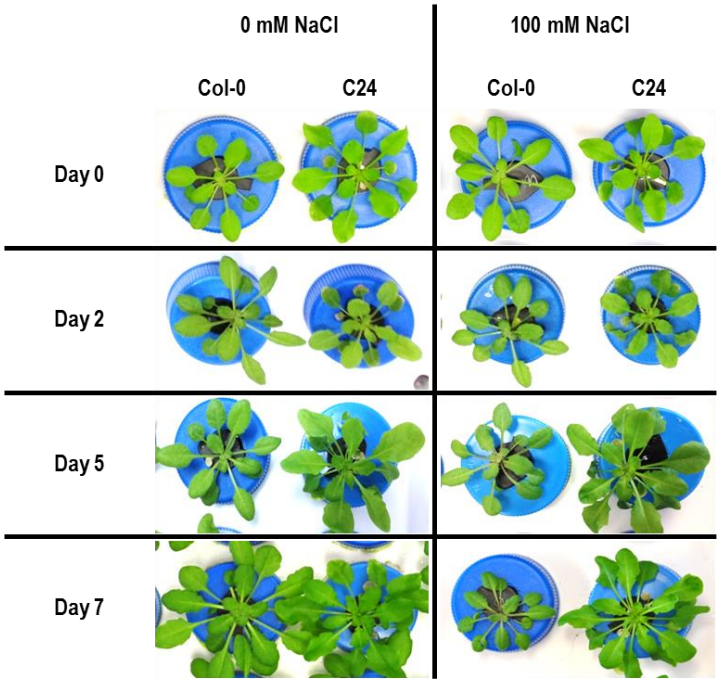

Figure 4.5: Images of hydroponically grown Col-0 and C24 plants subjected to salt stress.

Representative images of Col-0 and C24 plants grown hydroponically for 4 wk before subjected to salt treatment with ± 100 mM NaCl commencing on day 0.

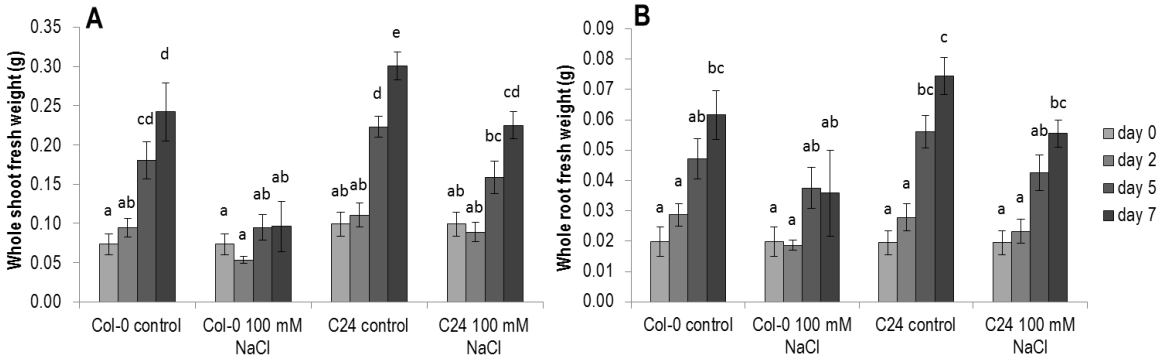

Figure 4.6: Shoot and root biomass of hydroponically grown Col-0 and C24 plants subjected to 100 mM salt stress over a 7 d period.

Fresh weights of (A) whole shoot and (B) whole root tissue of Col-0 and C24 plants, 0 d (light grey bars), 2 d (medium grey bars), 5 d (dark grey bars) and 7 d (black bars) after treatment with ± 100 mM NaCl. Values are mean±SEM (n=5). ANOVA statistical analyses were performed using Genstat and the Student-Newman-Keuls test was used for multiple comparisons. Letters indicate significance at the 0.05 level.

A minor increase in the shoot Na^+ content in Col-0 and C24 plants treated with 100 mM NaCl can be observed two days after NaCl application and is significantly increased at day 5 (Figure 4.7 A), with C24 accumulating significantly more Na^+ in the shoot at day 7 compared to Col-0 (ANOVA, p=0.05). During the same time period, the shoot K^+ content decreases under both control and salt conditions

in both Col-0 and C24 (Figure 4.7 B). There was no obvious difference between the two ecotypes for their shoot K^+ content (Figure 4.7 B). In the root, the Na^+ content significantly increases in Col-0 after only two days of 100 mM NaCl treatment and increases further by day 7 (ANOVA, p=0.05) (Figure 4.7 C). In C24, only a minor increase in root Na^+ is detected in C24 roots over 7 days of NaCl treatment (Figure 4.7 C). This increase was not significant (ANOVA, p=0.05). The overall K^+ content in the root remained consistent in C24 and increased moderately in Col-0 under both 0 mM NaCl and 100 mM NaCl during the experimental period (Figure 4.7 D).

As a significant difference in both the shoot and root Na^+ content was observed between Col-0 and C24 after 7 days of 100 mM NaCl treatment, this time point was therefore chosen for subsequent experiments. At this time point, it would be hypothesised that there is a large difference in the native expression of *AtHKT1;1*.

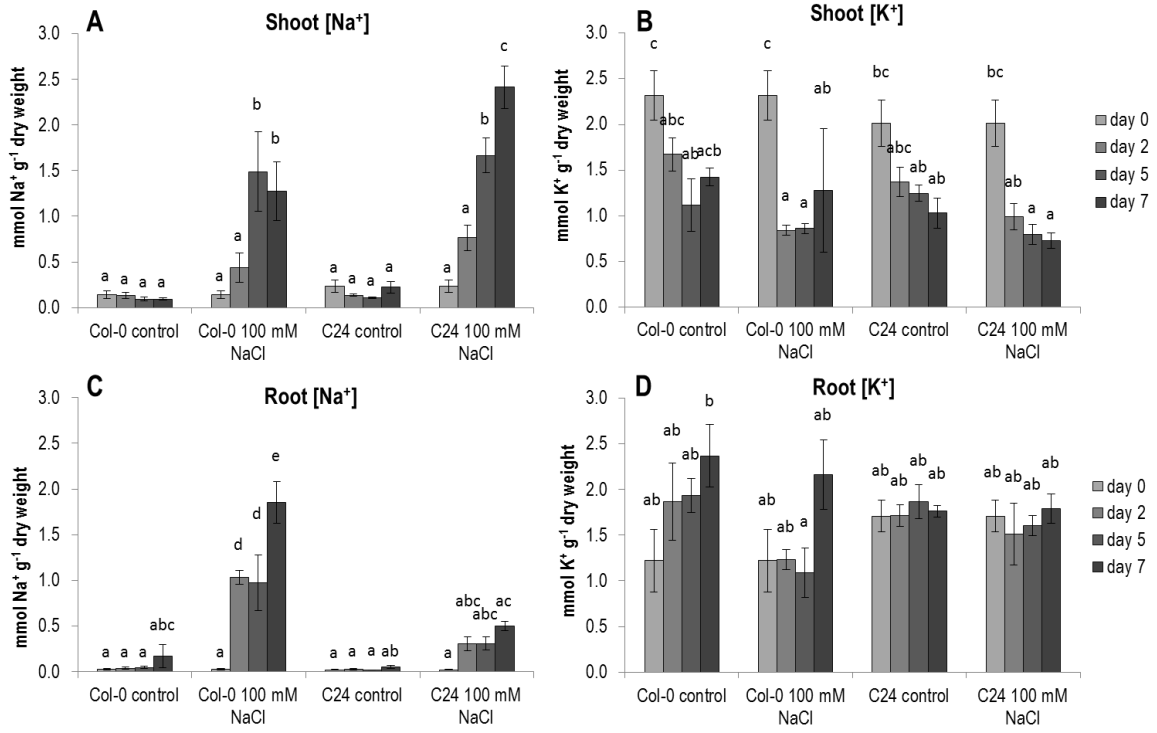

Figure 4.7: Na^+ and K^+ content in hydroponically grown Col-0 and C24 plants subjected to 100 mM salt stress over a 7 d period.

Presented are the (A) shoot Na^+, (B) shoot K^+ (C) root Na^+ and (D) root K^+ content in 6 wk old hydroponically grown Col-0 and C24 plants treated with ± 100 mM NaCl for 0 to 7 days. The youngest fully expanded leaf and whole root tissue was analysed using flame photometry at time point 0 (light grey bars), 2 d (medium grey bars), 5 d (dark grey bars) and 7 d (black bars) after treatment. Values are mean±SEM (n=5). ANOVA statistical analyses were performed using Genstat and the Student-Newman-Keuls test was used for multiple comparisons. Letters indicate significance at the 0.05 level.

4.6.3 Analysis of *GFP* expression in *AtHKT1;1promoter::GFP* transgenic lines

To test whether the putative 2.7 kb *AtHKT1;1* promoters from Col-0 and C24 are able to drive *GFP* expression in the root stele, transgenic lines had been generated in which *pCol-0* or *pC24* were fused to the coding sequence of *GFP*. Additionally, to specifically test the influence of the last 240 bp 5′ of the ATG start codon, transgenic lines were generated in which *GFP* is driven by mixed promoters, in which part of one promoter was replaced with the corresponding fragment of the other ecotype's promoter. The T_2 generation of these lines was hydroponically grown for 5 wk, followed by 7 d of ±100 mM NaCl treatment. *GFP* expression was determined using confocal microscopy to determine localisation of GFP fluorescence. Semi-qPCR was used to verify the presence of *GFP* transcripts in cases where GFP fluorescence was below the detection limit of confocal microscopy.

GFP was detected in the roots of all T_2 *AtHKT1;1promoter::GFP* transgenic lines under both 0 mM and 100 mM NaCl treatments (Figure 4.8 to Figure 4.11). Three independent transformation events were evaluated per line, where available, with three to five individuals per line. For both transgenic lines with the mixed promoters in the C24 background (*pCol-0/C24::GFP* and *pC24/Col-0::GFP* in C24), only one and two independent lines were available (Figure 4.11). While present in all lines, GFP fluorescence was occasionally very weak; therefore, imaging of wild type plants was always performed using the same microscope settings, to distinguish between what was GFP fluorescence and what was background auto-fluorescence caused by the high detector gain used on the microscope. Additionally, semi-qPCR using primers specific to *GFP* was performed to ensure the GFP fluorescence observed using the confocal was not an artefact due to the microscope settings. The images presented are from one hydroponics experiment, but similar images were recorded in three independently performed experiments.

The majority of GFP fluorescence was visible in the root stelar cells; however, some GFP also appeared to be located in the cortical and epidermal cells in all lines (Figure 4.8 to Figure 4.11). Semi-qPCR was performed on three individuals of three transgenic lines (less in lines of the mixed promoter, as indicated in Figure 4.11). Semi-qPCR demonstrates that *GFP* transcripts were detectable in all transgenic lines (Figure 4.8 to Figure 4.11), however, *GFP* transcript levels varied greatly between independently transformed transgenic lines and biological replicates within the lines (Figure 4.8 to Figure 4.11). For instance, in Figure 4.9 Panel B, for the 0 mM NaCl treatment: three independently transformed lines are presented in three separate gel images. Each gel image contains three biological replicates; for the first independently transformed line, two biological replicates show moderate band intensities for *GFP* transcripts while one is not detectable; for the second independently transformed line all three biological replicates have moderate band intensities for *GFP* transcripts and for the third independently transformed line two biological replicates have

strong band intensities, while one is not detectable. The bands indicating *Actin2* transcripts are shown below the corresponding *GFP* gel image. The *Actin2* images show camparable band intensity for all lines and replicates.

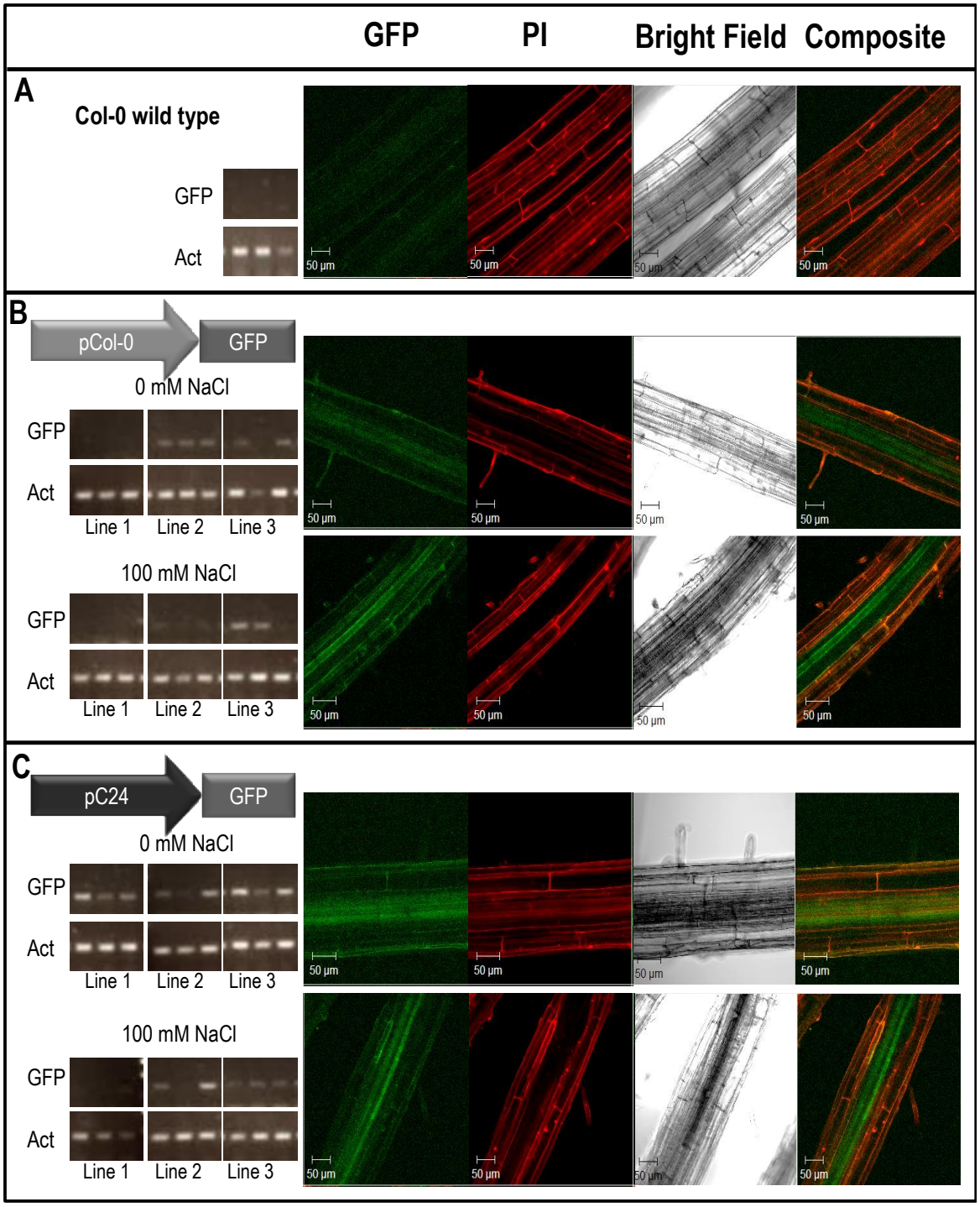

Figure 4.8: Root specific GFP fluorescence in hydroponically grown T_2 *AtHKT1;1promoter::GFP* transgenic lines in a Col-0 background.

Analysis was performed using semi-qPCR and confocal microscopy. (A) Col-0 wild type (B) Col-0 *AtHKT1;1 promoter::GFP* with control and 100 mM NaCl treatment and (C) C24 *AtHKT1;1 promoter::GFP* with control and 100 mM NaCl treatment. Representative false colour confocal images are presented from left to right: GFP fluorescence in green, propidium iodide (PI) in red, bright field in grey and composite image of GFP and PI. Gel images are of semi-qPCR on three independently transformed lines for each construct with three biological replicates per line of *GFP* and *Actin2* transcripts.

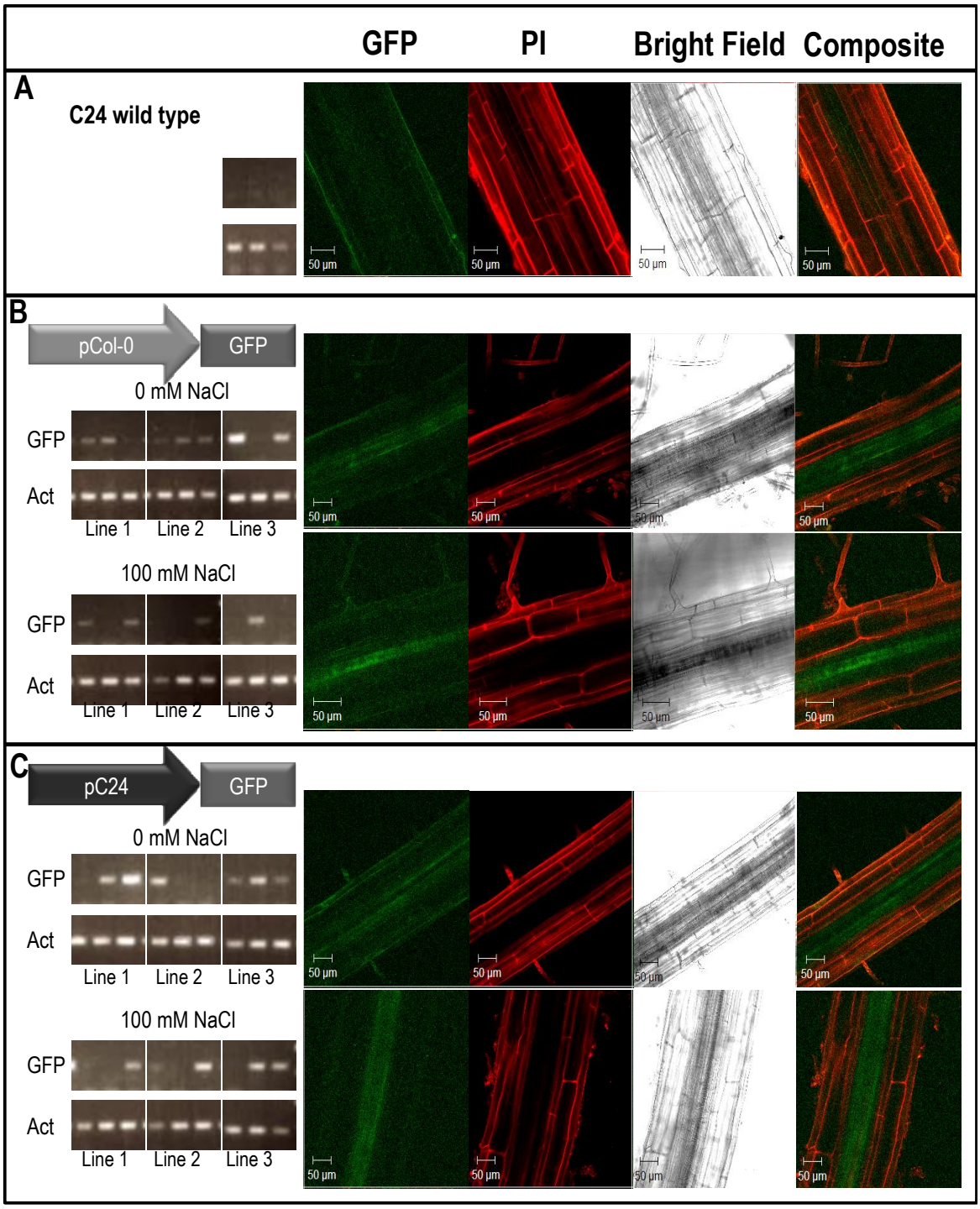

Figure 4.9: Analysis of root specific GFP fluorescence in hydroponically grown T_2 *AtHKT1;1promoter::GFP* transgenic lines in the C24 background.

Analysis was performed using semi-qPCR and confocal microscopy. (A) C24 wild type (B) Col-0 *AtHKT1;1 promoter::GFP* with control and 100 mM NaCl treatment and (C) C24 *AtHKT1;1 promoter::GFP* with control and 100 mM NaCl treatment. Representative false colour confocal images are presented from left to right: GFP fluorescence in green, propidium iodide (PI) in red, bright field in grey and composite image of GFP and PI. Gel images are of semi-qPCR on three independently transformed lines for each construct with three biological replicates per line of *GFP* and *Actin2* transcripts.

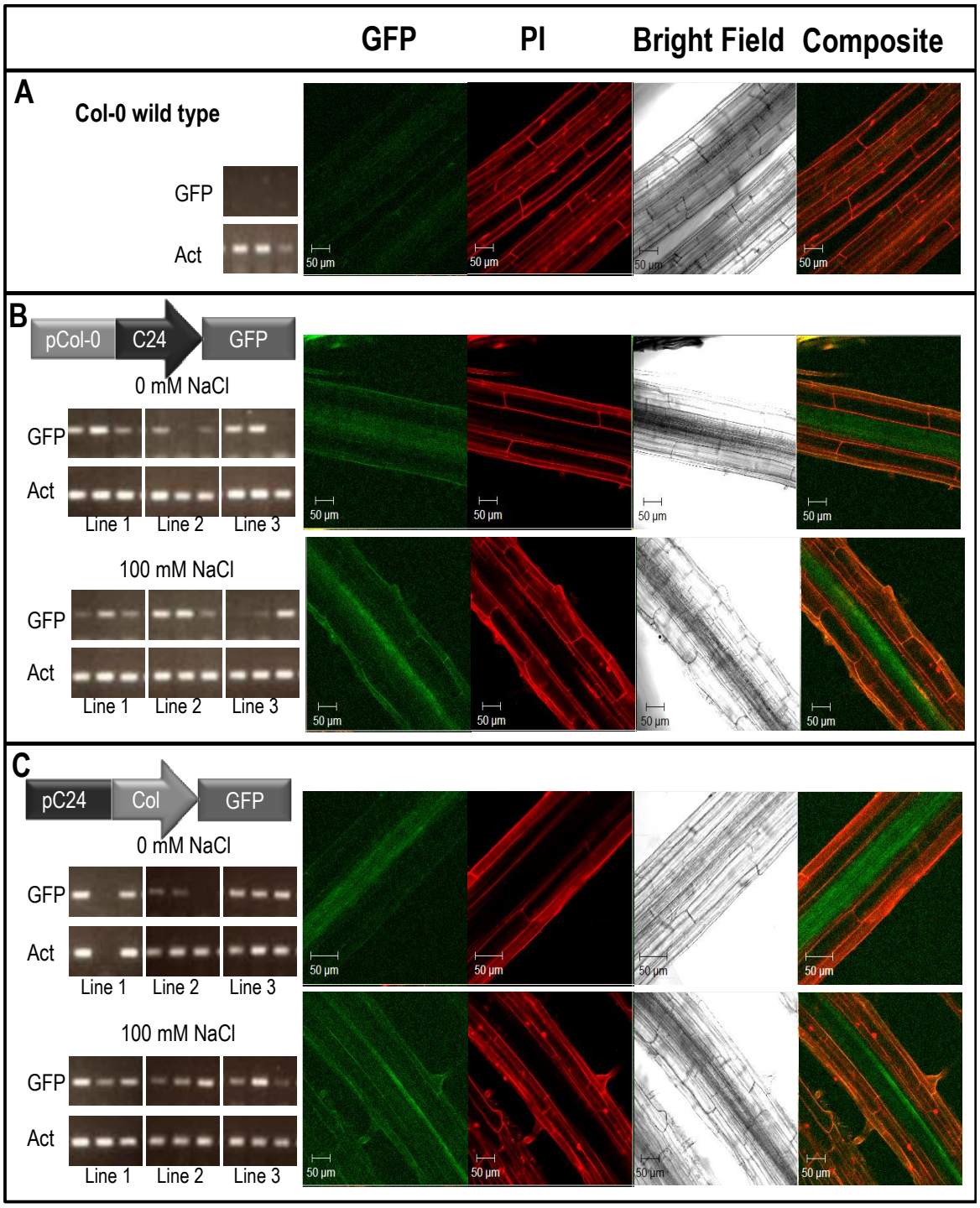

Figure 4.10: Analysis of root specific GFP fluorescence in hydroponically grown T_2 *AtHKT1;1promoter::GFP* transgenic lines in the Col-0 background.

Analysis was performed using semi-qPCR and confocal microscopy. (A) Col-0 wild type (B) Col-0/C24 *AtHKT1;1 promoter::GFP* with control and 100 mM NaCl treatment and (C) C24/Col-0 *AtHKT1;1 promoter::GFP* with control and 100 mM NaCl treatment. Representative false colour confocal images are presented from left to right: GFP fluorescence in green, propidium iodide (PI) in red, bright field in grey and composite image of GFP and PI. Gel images are of semi-qPCR on three independently transformed lines for each construct with three biological replicates per line of *GFP* and *Actin2* transcripts.

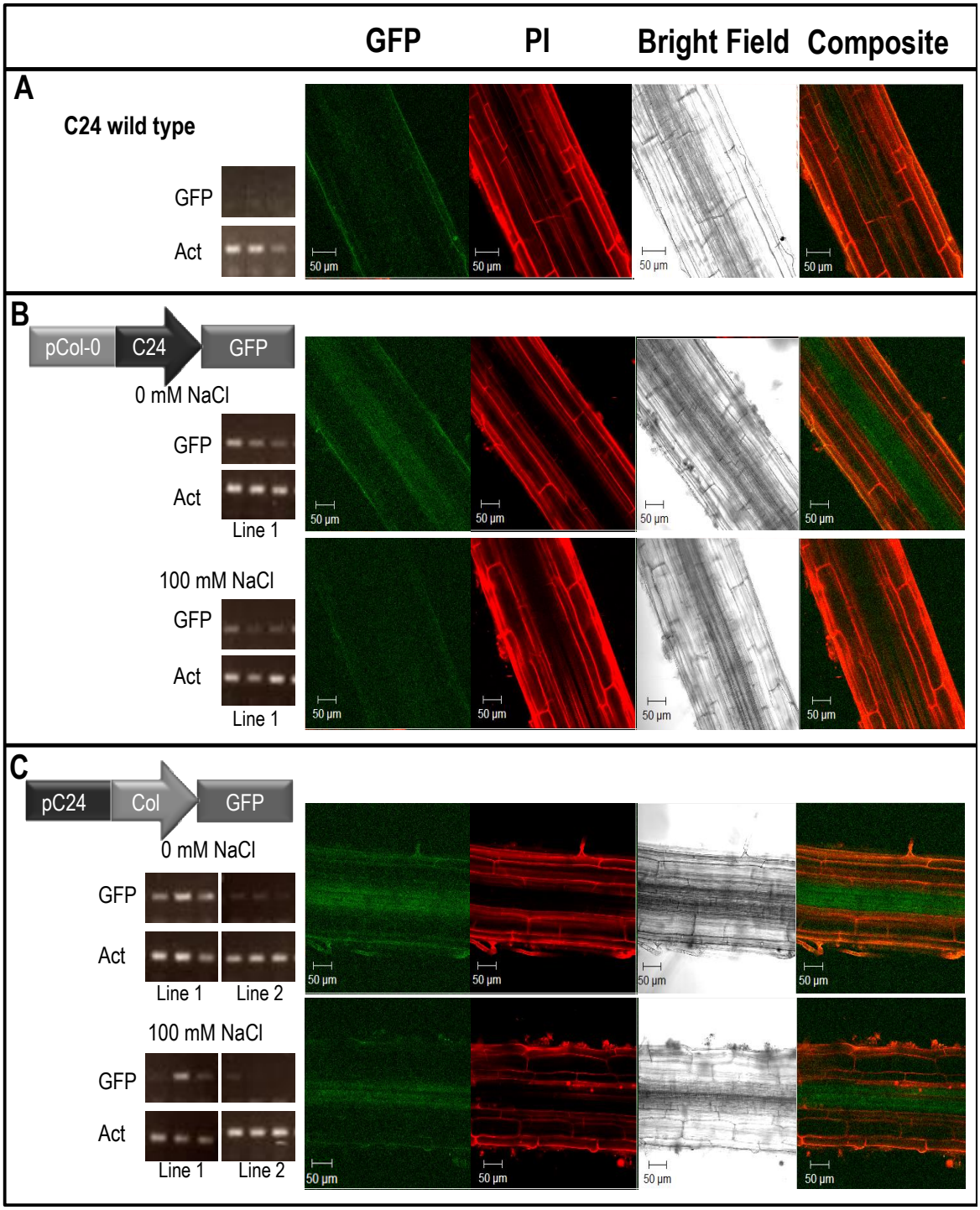

Figure 4.11: Analysis of root specific GFP fluorescence in hydroponically grown T_2 *AtHKT1;1promoter::GFP* transgenic lines in the C24 background.

Analysis was performed using semi-qPCR and confocal microscopy. (A) C24 wild type (B) Col-0/C24 *AtHKT1;1 promoter::GFP* with control and 100 mM NaCl treatment and (C) C24/Col-0 *AtHKT1;1 promoter::GFP* with control and 100 mM NaCl treatment. Representative false colour confocal images are presented from left to right: GFP fluorescence in green, propidium iodide (PI) in red, bright field in grey and composite image of GFP and PI. Gel images are of semi-qPCR on three independently transformed lines for each construct with three biological replicates per line of *GFP* and *Actin2* transcripts.

Additionally to semi-qPCR and confocal microscopy, *GFP* transcripts were confirmed by qPCR and Northern Blot analysis in pooled root RNA samples of salt stressed plants carrying the *pCol::GFP* and *pC24::GFP* construct in the Col-0 and C24 background (Figure 4.12). Northern blot and qPCR analyses show that both 2.7 kb promoters are able to drive *GFP* expression in the Col-0 and C24 backgrounds. The Northern Blot shows strongest signals for *GFP* transcripts for *pCol-0::GFP* in Col-0, *pC24::GFP* in Col-0 and *pC24::GFP* in C24 (Figure 4.12 A). Lower levels of *GFP* transcripts were detected in *pCol-0::GFP* in C24 (Figure 4.12 A). Total RNA levels were comparable in all lanes to ensure the observed intensity of the Northern Blot GFP bands were not due to differences in amount of RNA loaded (Figure 4.12 B). *GFP* expression determined by qPCR showed highest transcript abundance in *pCol-0::GFP* in Col-0 and lower for the remaining three transgenic lines (Figure 4.12 C).

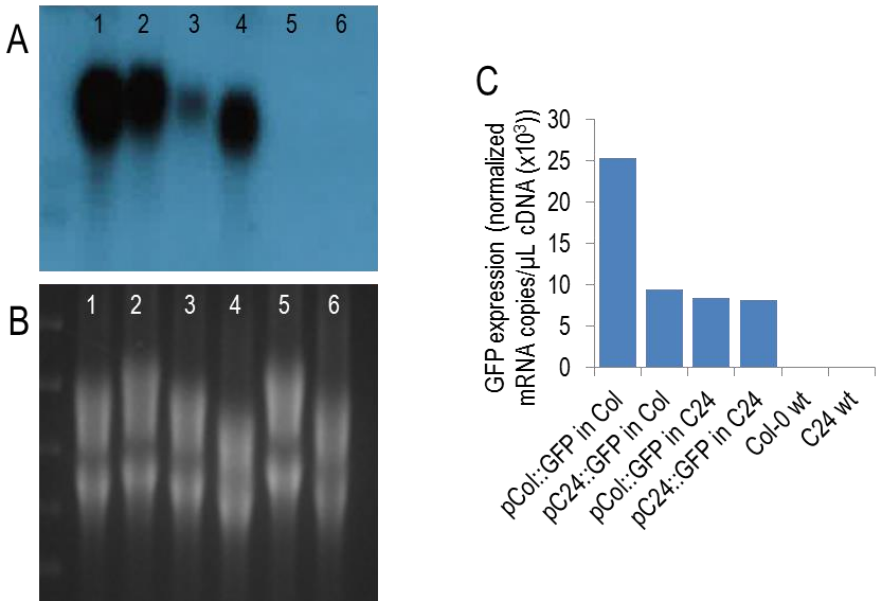

Figure 4.12: Quantification of *GFP* transcripts in *AtHKT1;1promoter::GFP* transgenic lines.

(A) Northern Blot analysis was performed using a GFP probe on (B) pooled samples of root RNA obtained from 5-10 plants, 6 wk old and exposed to 100 mM NaCl for 7 days. The same samples were used for (C) qPCR analysis of *GPF* expression. (1) *pCol-0*::*GFP* in Col-0 (2) *pC24*::*GFP* in Col-0 (3) *pCol-0*::*GFP* in C24 (4) *pC24*::*GFP* in C24 (5) Col-0 wt (6) C24 wt.

4.6.4 Analysis of *AtHKT1;1promoter::cDNA* transgenic lines

To test for the ability of the Col-0 and C24 *AtHKT1;1* promoters to drive the expression of the *AtHKT1;1* coding sequence in different ecotypes, a selection of T_2 *AtHKT1;1promoter::cDNA* lines were obtained from Dr. Joanna Sundstrom (University of Adelaide, Australia). The T_2 plants of these lines had been tested for transgene expression by RT-PCR by Sundstrom (2011) and all transgenic lines were found to express the *AtHKT1;1* transgene. Two accessions of Arabidopsis were used

which lack native expression of *AtHKT1;1* in the root: The ecotype C24 and the Col-0 *gl1 AtHKT1;1* mutant *hkt1-4*. Since the transgenic lines were of the T_2 generation, and therefore segregating for the transgene, individuals were first genotyped using a PCR amplification of the selectable marker gene *NptII.* Root and shoot tissue of the individual plants were then analysed for Na^+ and K^+ content. This allows separating the Na^+ and K^+ values of transgenic individuals belonging to the same line from the values of individuals that do not have the transgene present (the nulls). It is hypothesised that transgenic C24 and Col-0 *gl1 hkt1-4* lines expressing functional *AtHKT1;1,* localised in the root stele, would show a reduction in shoot Na^+ and increase in root Na^+ content compared to the respective wild types and nulls. Three lines transformed with *pCol-0::Col-0cDNA* in C24, one line with *pCol-0::C24cDNA* in C24, five lines with *pC24::ColcDNA* in C24, six lines with *pC24::C24cDNA* in C24 and three lines with *pC24::C24cDNA* in Col-0 *gl1 hkt1-4* were tested.

To determine the Na^+ and K^+ content in both the transgenic lines and in the reference plants, plants were grown hydroponically for a total of six weeks, including one week of ± 100 mM NaCl treatment. For each line, three to five plants with control and three to five plants with NaCl treatment were analysed and measurements corresponding to the same construct were averaged. Nulls were identified using PCR amplification of the selectable marker *NptII* (Table 4.3). In most lines, a number of nulls were identified, indicating that lines are segregating for the transgene, as is expected for the T_2 generation of lines that have a low number of inserts. Some lines were identified as being made up solely as nulls, showing that the T-DNA insert has been completely removed through segregation.

Table 4.3: Genotyping of T_2 *AtHKT1;1promoter::cDNA* lines using the selectable marker *NptII* Lane legends: *pCol-0::Col-0* and *pCol-0::C24*: *HKT1;1promoter* from Col-0 driving *HKT1;1cDNA* from Col-0 or C24, respectively; *pC24::Col-0* and *pC24::C24*: *HKT1;1promoter* from C24 driving *HKT1;1cDNA* from Col-0 or C24, respectively; background accession is indicated by either C24 or Col hkt (referring to Col-0 *gl1 hkt1-4*).

Transgenic line	# of line	Plant transgenic or null	# of plants
C24 *pCol-0::Col-0*	1	transgenic	2
		null	7
	2	transgenic	6
		null	0
	3	transgenic	3
		null	6
C24 *pCol-0::C24*	1	transgenic	7
		null	0
C24 *pC24::Col-0*	1	transgenic	3
		null	4
	2	transgenic	2
		null	5
	3	transgenic	7
		null	2
	4	transgenic	5
		null	2
	5	transgenic	4
		null	3
C24 *pC24::C24*	1	transgenic	5
		null	6
	2	transgenic	4
		null	2
	3	transgenic	6
		null	2
	4	transgenic	8
		null	1
	5	transgenic	0
		null	9
	6	transgenic	6
		null	1
Col-0 *hkt* *pC24::C24*	1	transgenic	3
		null	4
	2	transgenic	5
		null	1
	3	transgenic	3
		null	4
Col-0	1	transgenic	0
		null	6
C24	1	transgenic	0
		null	6

Na^+ and K^+ measurements for nulls were combined and averaged for comparison with the transgenic plants. C24 and Col-0 wild type plants were included in the experiment to allow comparison to transgenic lines and nulls. In the shoot, no significant differences in Na^+ content were detected in all lines (Figure 4.13 A). In the C24 background, three out of four transgenic lines have a marginally reduced shoot Na^+ content, while one line, *pCol-0::Col-0* has a trend for increased shoot Na^+ content (Figure 4.13 A). In the Col *gl1 hkt1-4* mutant, the line transformed with the *pC24::C24* construct also had a decrease in shoot Na^+. None of the transgenic lines had a shoot Na^+ content as low as the Col-0 wild type control did. In the root, two of the transgenic lines have a significantly higher Na^+ content, *pCol-0::C24* and *pC24::Col-0* in the C24 background (Figure 4.13 B). However, the root Na^+ content of the other two lines in the C24 background is not significantly different (Figure 4.13 B). In the Col *gl1 hkt1-4* mutant, the line transformed with the *pC24::C24* construct also had a slight increase in root Na^+. The shoot and root Na^+ content of NaCl treated independent transformed lines can be found in Supplementary Figure 8.5.

The K^+ content in the shoot of NaCl treated plants is decreased in all lines compared to control conditions (Figure 4.14 A), while the overall K^+ content in the root remains unchanged in all lines and treatments (Figure 4.14 B). Interestingly, the same lines that showed altered root Na^+ content, also show significantly altered shoot K^+ content. With *pC24::Col-0* having higher shoot K^+ content (towards values observed for the Col-0 wild type) and *pCol-0::C24* having significantly lower shoot K^+ content (towards levels observed for the Col-0 *gl1 hkt1-4* mutant).

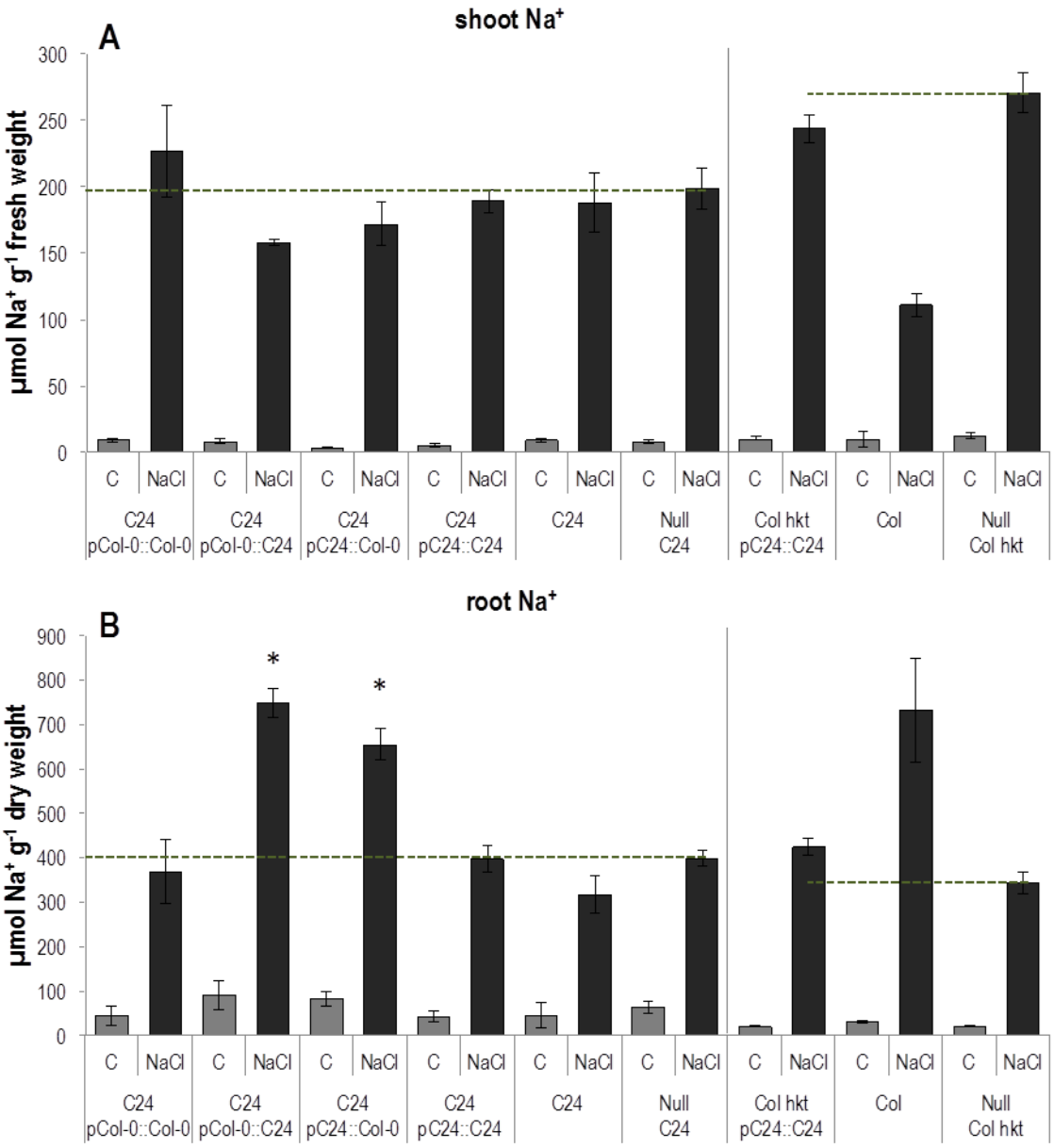

Figure 4.13: Na⁺ content in T_2 transgenic *AtHKT1;1promoter::AtHKT1;1cDNA* lines (C24 and Col-0 *gl1 hkt1*-4 background).

(A) Na⁺ content of the youngest fully expanded leaf and (B) the root were determined using flame photometry from 6 wk old hydroponically grown plants that had been treated for 7 d with ± 100 mM NaCl. C: control treatment; NaCl: 100 mM NaCl treatment; measurements corresponding to the same construct were averaged across the lines. *pCol-0::Col-0* and *pCol-0::C24* has the *AtHKT1;1promoter* from Col-0 driving *AtHKT1;1cDNA* from Col-0 or C24, respectively; *pC24::Col-0* and *pC24::C24* has the *AtHKT1;1promoter* from C24 driving *AtHKT1;1cDNA* from Col-0 or C24, respectively. These constructs were transformed into either the ecotype C24 or Col hkt (referring to Col-0 *gl1 hkt1-4*). Transgenic and null plants were determined by PCR genotyping using the *NptII* marker. Values deriving from the control treatment are presented in light grey bars and salt treatment in dark grey bars. The green dashed line indicates the mean of the null background ecotype for easier comparison to transgenic lines. Values are mean ± SEM (n=3-16), asterisk indicates significance on the 0.05 level to the corresponding null genotype as determined using students t-test.

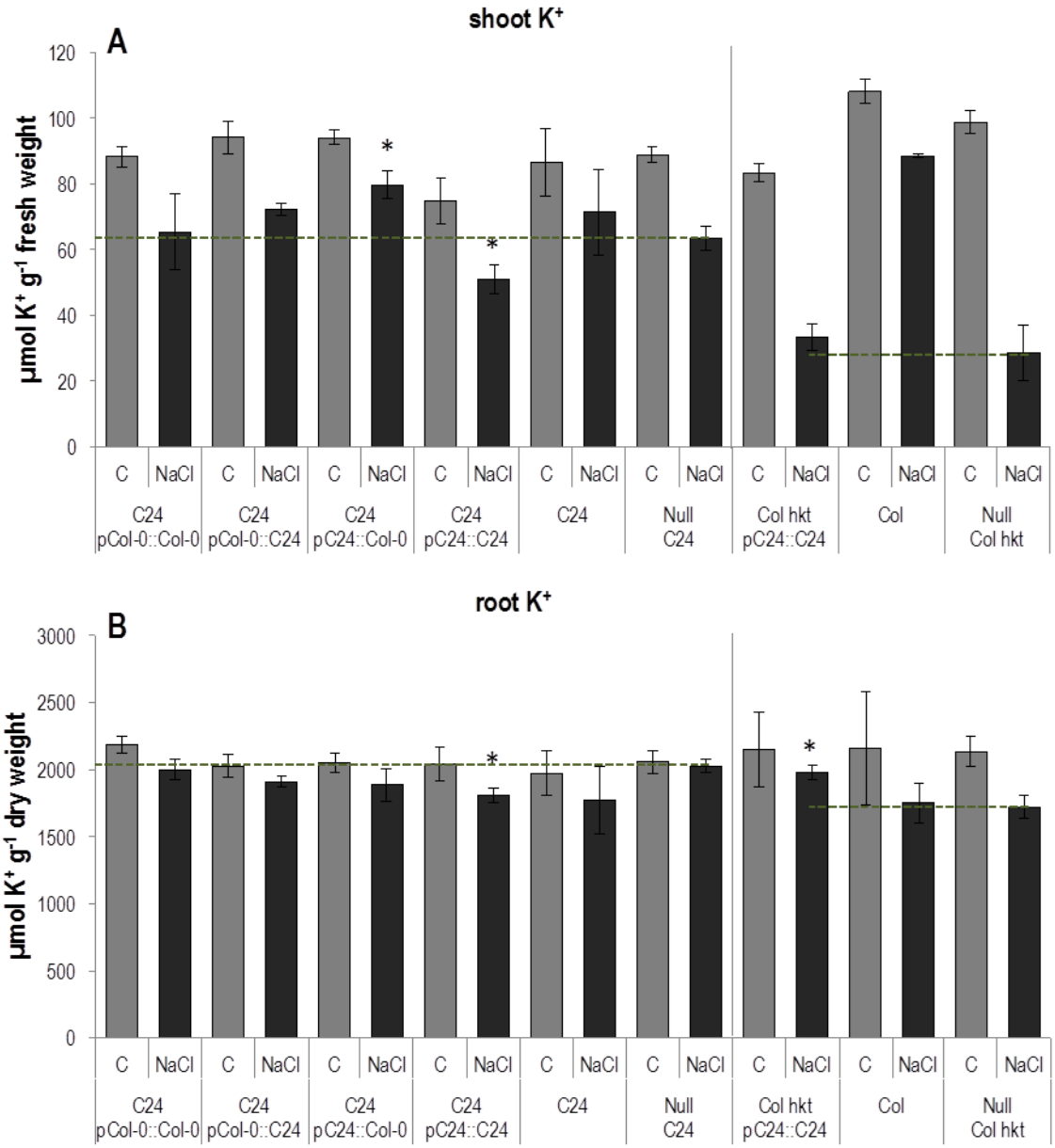

Figure 4.14: K^+ content in T_2 transgenic *AtHKT1;1*promoter::*AtHKT1;1*cDNA lines (C24 and Col-0 *gl1 hkt1-4* background).

(A) K^+ content of the youngest fully expanded leaf and (B) the root were determined using flame photometry from 6 wk old hydroponically grown plants that had been treated for 7 d with ± 100 mM NaCl. C: control treatment; NaCl: 100 mM NaCl treatment; measurements corresponding to the same construct were averaged across the lines. *pCol-0::Col-0* and *pCol-0::C24* has the *AtHKT1;1promoter* from Col-0 driving *AtHKT1;1cDNA* from Col-0 or C24, respectively; *pC24::Col-0* and *pC24::C24* has the *AtHKT1;1promoter* from C24 driving *AtHKT1;1cDNA* from Col-0 or C24, respectively; These constructs were transformed into either the ecotype C24 or Col hkt (referring to Col-0 *gl1 hkt1-4*). Transgenic and null plants were determined by PCR genotyping using the *NptII* marker. Values deriving from the control treatment are presented in light grey bars and salt treatment in dark grey bars. The green dashed line indicates the mean of the null background ecotype for easier comparison to transgenic lines. Values are mean ± SEM (n=3-16), asterisk indicates significance on the 0.05 level to the corresponding null genotype as determined using students t-test.

The results obtained for Na^+ and K^+ measurements of transgenic lines were not conclusive. For instance, a decrease in shoot Na^+ was expected in transgenic lines compared to the respective null, however, some lines showed an increase in shoot Na^+. Siblings of the same generation were tested for the presence of the transgene and also for the presence of transcripts by Sundstrom (2011). To ensure expression of *AtHKT1;1* is still present in the transgenic lines, the expression of the transgene was retested. For expression analysis, plants were grown hydroponically for 3 wk, and root and shoot tissue of 3-10 plants per line pooled to obtain sufficient material for analysis. Transcripts for *Actin2* were observed in most root and shoot samples (Figure 4.15 A), indicating that the cDNA synthesis and PCR reactions were functioning. The PCR '*AtHKT1;1*' results in amplification of both native *AtHKT1;1* transcripts and the transgene. Therefore, bands corresponding to 130 bp DNA fragments are expected in all shoot and root tissue samples of the transgenic lines and the Col-0 wild type. This band is not expected to be present in the root tissue of C24 wild type plants, as these lack *AtHKT1;1* expression in the root. The PCR for 'transgene specific *AtHKT1;1*' results in amplification of a DNA fragment specific of the transgene. Faint bands corresponding to '*AtHKT1;1'* (endogenous and transgene) transcripts were only detected in a few of the lines: one shoot sample, a C24 line transformed with *pC24::C24cDNA*, and 6 root samples, corresponding to one C24 line transformed with *pC24::Col-0cDNA*, two C24 lines transformed with *pC24::C24cDNA*, two lines of the Col-0 *gl1 hk1-4* mutant transformed with *pC24::C24cDNA* and the Col-0 wild type. The PCR for 'transgene specific *AtHKT1;1*' did not amplify any DNA fragments of the transgenic lines, indicating that no transcripts of *AtHKT1;1* derived from the transformed construct is present. It should be noted that PCR conditions and primers were tested on plasmid controls to ensure correct PCR conditions for proper amplification of DNA project (data not shown). Different concentrations of cDNA, annealing temperatures as well as extension times were used in an attempt to further optimise the assay. The repeat of PCRs for '*AtHKT1;1'* resulted in bands being present in other plant samples, and were overall very inconsistent and untrustworthy. It is necessary to repeat the experiment where the exact same plants are used to determine the Na^+ and K^+ content, for analysis of the genotype (presence and absence of the transgene) and for analysis of the expression levels of native and transgene specific *AtHKT1;1*. This would allow to better group lines that express *AtHKT1;1* and correlate expression to Na^+ and K^+ contents in the root and shoot. However, this was not possible in the timeframe of this PhD.

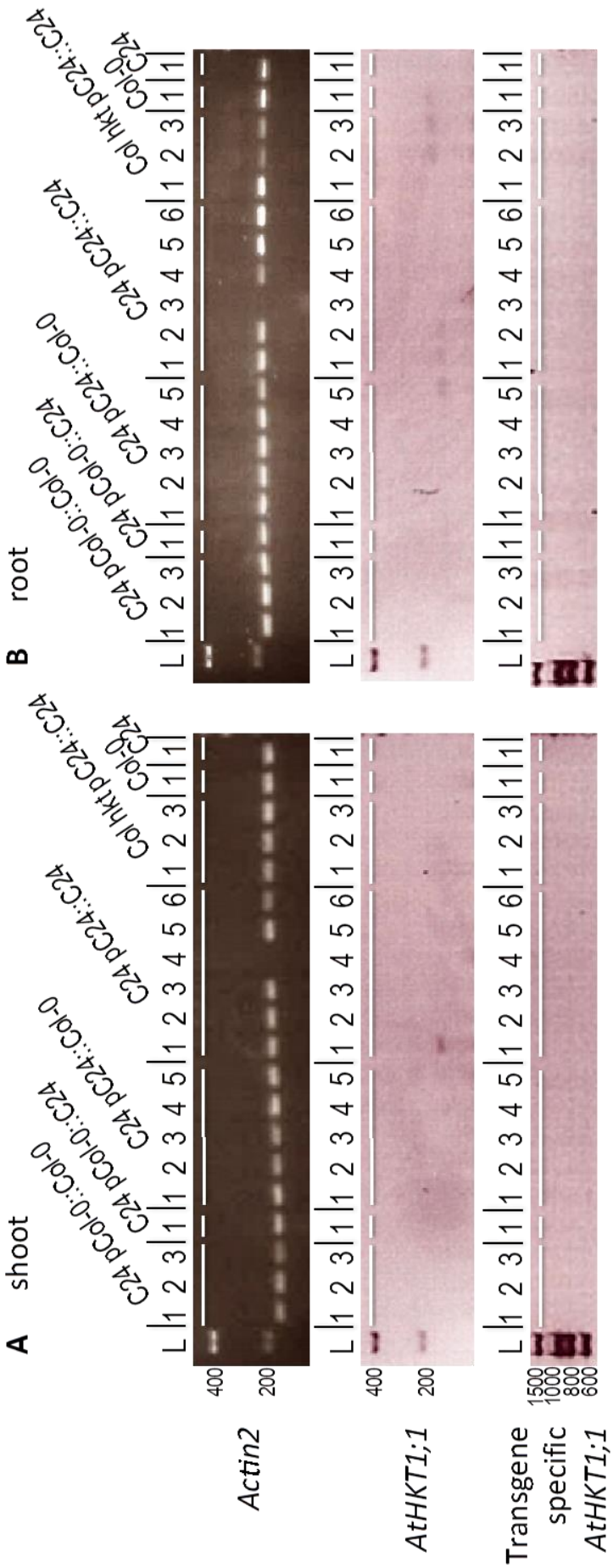

Figure 4.15: Analysis of *AtHKT1;1* expression in 3 wk old hydroponically grown T_2 *HKT1;1promoter::cDNA* lines.

(A) Shoot and (B) root tissue of 3-10 plants per line were pooled for generation of cDNA, which was used for RT-PCR. Transcripts were analysed of *Actin2* as control, native *AtHKT1;1* and transgene specific *AtHKT1;1*. Lane legends: *pCol-0::Col-0* and *pCol-0::C24*: *HKT1;1promoter* from Col-0 driving *HKT1;1cDNA* from Col-0 or C24, respectively; *pC24::Col-0* and *pC24::C24*: *HKT1;1promoter* from C24 driving *HKT1;1cDNA* from Col-0 or C24, respectively; background accession is indicated by either C24 or Col hkt (referring to Col-0 *gl1 hkt1-4*). Line # as indicated in Table 4.3.

4.7 Discussion

4.7.1 The putative 2.7 kb *AtHKT1;1* promoter from Col-0 and C24 is able to drive *GFP* expression

GFP transcripts and fluorescence were detected in all *promoter::GFP* transgenic lines (Figures Figure 4.8 to Figure 4.11). This suggests that both the Col-0 and the C24 promoter have the necessary nucleotide sequence to drive *AtHKT1;1* gene expression (*GFP* and *AtHKT1;1 cDNA*) in both Col-0 and C24 (Figure 4.8 to Figure 4.11). Fluorescence was mainly detected in the stele, which is consistent with the proposed function of AtHKT1;1 in Na^+ retrieval from the xylem and agrees with previous localisation studies (Berthomieu *et al.* 2003, Mäser *et al.* 2002, Sunarpi *et al.* 2005, Xue *et al.* 2011). No fluorescence was observed in these tissues in wild type plants. Very low fluorescence was also detected in the cortical and epidermal cells, however, it is possible that this is due to auto fluorescence, which was also observed in roots from wild type plants, as the confocal detector gain was set high to detect faint GFP signals (Figure 4.8 to Figure 4.11). It is therefore not possible to draw conclusions on *AtHTK1;1* promoter activity in those cell types. The presence of the *GFP* transcript was confirmed by semi-qPCR, qPCR and Northern blot. The amount of *GFP* cDNA transcript observed in this experiment (7-25 × 10^3 copies per μL) are comparable to the amount of *AtHKT1;1* transcript in wild type plants under salt stress (Jha *et al*., 2010).

Sundstrom (2011) had proposed that a 240 bp region just upstream of the start codon, with high polymorphism between Col-0 and C24, might be responsible for the lack of *AtHKT1;1* expression observed in C24 roots. The present study tested all combinations of the mixed promoter, where the main proportion of the promoter derived from one ecotype and the 240 bp region from the other ecotype's promoter, in both ecotype backgrounds. All promoters were able to drive *GFP* expression, indicating that this highly polymorphic sequence, with the altered CAAT motif, does not cause the lack of *AtHKT1;1* expression in C24 roots.

Variation in *GFP* transcript levels is expected between individuals belonging to one transgenic line as the T_1 generation was not screened for single insert lines and the resulting T_2 generation is segregating for the transgene. Some lines and individuals would contain multiple inserts of the transgene, while others are nulls. The number of inserts is not of importance for this experiment, as its aim was to test qualitatively for *GFP* expression. Expression levels of *AtHKT1;1* are very low in roots of Col-0 plants driven by its native promoter, therefore, it was expected that also *GFP* would be expressed at low levels when driven by the *AtHKT1;1* promoter. An attempt to quantify GFP fluorescence so close to the detection limit would not be appropriate. Therefore, this assay was set

up to test for presence or absence of *GFP* expression driven by both the Col-0 and C24 promoter. It was shown that the Col-0 and C24 promoter can drive expression of the downstream gene, therefore, the lack of *AtHKT1;1* expression in C24 roots is not due to the promoter, but potentially due to other transcriptional or posttranscriptional reasons. These factors could include small RNAs targeting the *AtHKT1;1* transcript in C24 or methylation preventing transcription. This was further investigated in the following chapter 5.

In addition to the polymorphic region 5′ of the start codon, another major difference between the Col-0 and C24 promoter is the repeat element approximately 4 kb upstream. This 700 bp region is repeated twice in the Col-0 ecotype. In the C24 ecotype, it appears that a deletion occurred between the repeats, leaving only one of the 700 bp regions. A similar scenario has been proposed for the two ecotypes Ts-1 and Tsu-1, found in the coastal region of Spain and Japan, respectively (Rus *et al.* 2006). These accessions, similarly to C24, accumulate significantly more Na^+ than Col-0 in the shoot and are more salt tolerant (Rus *et al.* 2006). Mapping of the genomic region conferring these traits, identified *AtHKT1;1* as the likely candidate gene responsible for the phenotype (Rus *et al.* 2006). Similarly to C24, *AtHKT1;1* expression in the root of Ts-1 and Tsu-1 accessions is very low/absent, while it can be detected in the shoot (Rus *et al.* 2006). Rus *et al.* (2006) determined the promoter and most of the genomic sequence and identified major polymorphisms in the promoter region. It was found that the repeat element that is present twice in Col-0, is only present once in the accessions Ts-1 and Tsu-1, and it was hypothesised that this region is responsible for the lack of *AtHKT1;1* expression in the root, however, direct experimental evidence has not yet been presented (Rus *et al.* 2006). Other features of the promoter may be important in controlling root expression. Constructs with *pCol-0* and *pC24* that were used in this study contained the sequence of a small RNA target site that had been identified by Baek *et al.* (2011). This small RNA site was hypothesised to be involved in regulating *AtHKT1;1* expression by small RNA mediated methylation. In the results presented here, both 2.7 kb promoters (which contain this small RNA binding site) were able to drive *GFP* expression in the C24 and Col-0 background. Therefore, it is unlikely that the lack of *AtHKT1;1* expression in C24 roots is caused by altered small RNA mediated methylation of this target site in the promoter, as suggested by Baek *et al.* (2011).

The 700 bp repeat element that is present in the Col-0 promoter region (~ 5.4 kb upstream of the ATG start codon), which is present only once in C24, is not hypothesised to cause the lack of *AtHKT1;1* expression in C24 roots. A previous study has shown that different *AtHKT1;1* promoters, which have the repeat region present or absent, are able to drive the expression of the reporter gene *GUS* and that the presence or absence of the repeat region does not lead to altered GUS staining in

Col-0 roots (Baek *et al.* 2011). Consequently, the absence of this repeat region in the C24 promoter is also not thought to cause the lack of *AtHKT1;1* expression in C24 roots.

However, it appears that both the repeat region and the target site for small RNA binding are of importance for regulation of *AtHKT1;1* expression, specifically in the *sos3* mutant background. Baek *et al.* (2011) conducted the majority of their analysis in the *sos3* mutant, as the initial *AtHKT1;1* mutants were discovered in the *sos3* mutant background (Rus *et al.* 2001). In the *sos3* mutant background, the 5.2 kb promoter appears necessary to obtain full expression levels of *AtHKT1;1* (Baek *et al.* 2011), while the small RNA binding site is primarily important for *AtHKT1;1* expression in the shoot (Baek *et al.* 2011). The influence of various promoter fragments on *AtHKT1;1* expression in the *sos3* mutant background seems complex and may be influenced by a multitude of factors. This network of interactions has not been further described yet.

Given that *AtHKT1;1* expression is altered in *sos3* mutants, a connection between *AtHKT1;1* and *SOS3* expression is possible. In the study presented here, it was therefore verified that *SOS3* is expressed in C24 plants. *SOS3* expression in C24 roots was confirmed by qPCR at levels similar to Col-0 (data not shown). SNPs in the nucleotide sequence between Col-0 and C24 *SOS3* alleles (sequences obtained from Clark *et al.* (2007)) do not suggest that frame shifts or non-sense mutations are present in C24, however one amino acid was altered from S205 in Col-0 to R205 in C24, which may compromise a potential phosphorylation site (data not shown).

From the presented evidence in this thesis, it can subsequently be concluded that the lack of *AtHKT1;1* expression in C24 roots is not caused by the polymorphisms present in the 2.7 kb *AtHKT1;1* promoter (compared to the Col-0 promoter). And together with evidence provided by Baek *et al*. (2011) it is also not likely that the lack of expression is caused by the absence of the repeat element 5.4 kb upstream of the *AtHKT1;1* start codon. Therefore other reasons for regulating gene expression must be investigated (Chapter 5)

4.7.2 Lack of *AtHKT1;1* expression in C24 can partially be complemented with *AtHKT1;1promoter::AtHKT1;1cDNA* lines

The Na^+ content in the shoot had the tendency to be lower in four out of the five analysed transgenic *promoter::cDNA* lines (*pCol-0::C24cDNA* in C24, *pC24::Col-0cDNA* in C24, *pC24::C24cDNA* in C24 and *pC24::C24cDNA* in Col-0 *gl1 hkt1-4*) compared to the respective nulls and wild type after salt stress; however, the reduction was not significant. In the root, the Na^+ content of two transgenic lines was significantly increased, compared to the nulls and the C24 wild type when grown for 7 days in 100 mM NaCl, almost to levels comparable to the Col-0 wild type, suggesting that AtHKT1;1 may be

functional in these lines. Interestingly, the two lines were *pCol-0::C24cDNA* and *pC24::Col-0cDNA* (the same lines that also showed slightly reduced shoot Na^+). These results could indicate that both promoters are able to drive target gene expression and produce functional AtHKT1;1 proteins which are able to reduce shoot Na^+. Not all independently transformed lines displayed the same effect on root and shoot Na^+ content (Supplementary Figure 8.5), which could be explained by variations in insert number of the transgene, expression levels and location of the insert(s) in the genome. At least one independently transformed line per construct had altered distribution of root and shoot Na^+ content, possibly indicating the presence of functional AtHKT1;1 in these lines. However, the individual plants that were analysed for Na^+ and K^+ content were not tested for number and location of transgene insertion. The location of the transgene could disrupt the function of other genes important for Na^+ and K^+ distribution and endogenous *AtHKT1;1* expression may have been affected by the presence of the transgene, produced mRNA or protein.

Interestingly, significant alterations were observed in the shoot K^+ content of the *pC24::Col-0cDNA* line and *pCol-0::C24cDNA*. With *pC24::Col-0cDNA* having higher shoot K^+ content than the C24 wild type and *pCol-0::C24cDNA* having a lower K^+ content than the C24 wild type. Although the difference is statistically significant, the overall levels are similar. However, it could be hypothesised that this difference may be explained by AtHKT1;1 transport properties that were observed in the previous chapter 3. Besides Na^+ transport activity, a potential K^+ transport activity was detected for AtHKT1;1-C24 (see chapter 3). Under native conditions, no *AtHKT1;1* transcript can be found in the C24 roots (Jha *et al.*, 2010), however, in the transgenic line expressing the *AtHKT1;1* from C24, the AtHKT1;1-C24 protein may retrieve K^+, as well as Na^+ from the stele and therefore prevent K^+ from reaching the shoot, leading to reduced shoot K^+ levels. While in the transgenic line expressing *AtHKT1;1* from Col-0 in the C24 background the increase in shoot K^+ may be due to an indirect effect. It has been previously proposed that the membrane depolarisation caused by Na^+ influx through AtHKT1;1, activates K^+ channels and provides the driving force for K^+ release (Horie *et al.* 2009, Sunarpi *et al.* 2005, Xue *et al.* 2011).

It should be noted for the above discussion that the expression of the *AtHKT1;1* transgene could not be confirmed or disproved, which makes analysis of these plants difficult. To ensure the altered Na^+ and K^+ content resulted from *AtHKT1;1* transgene expression driven by the Col-0 and C24 promoter, the individual plants should have been tested for transgene expression, and not pooled plants of the same line in a subsequent experiment. Ideally, single insert homozygous lines should be used for this analysis. This would allow comparison of transgene expression levels to native expression levels in the Col-0 wild type. Together with data for root and shoot Na^+ content, this would determine if the 2.7 kb promoter is sufficient to obtain the expression pattern and levels that are characteristic for

Col-0, in the C24 background. Furthermore, all combinations of *promoter::cDNA* constructs should be transformed into Col-0 *gl1 hkt1-4* mutants to test if both *AtHKT1;1* cDNAs are able to complement the mutant when expressed under the 2.7 kb promoter.

With the 2.7 kb *AtHKT1;1* promoter fragment from C24 being able to drive *GFP* expression in C24, it remains to be discovered what causes the lack of *AtHKT1;1* expression in C24 roots. A sequence comparison of the Col-0 and C24 *AtHKT1;1* alleles (Figure 1.3) had shown there was a large difference in the second intron, with C24 containing an additional 1.6 kb of sequence. As introns can be involved in the regulation of gene expression through a number of mechanisms (introduced in chapter 5), the subsequent focus of the thesis was on analysing the insertion in the second intron in the C24 gDNA and its effect (if any) on the expression of the *AtHKT1;1* gene. This line of investigation will be subject of the following chapter.

4.7.3 Conclusion

In summary, the results from this chapter show that the 2.7 kb *AtHKT1;1* promoter from C24 is able to drive *GFP* and *AtHKT1;1* cDNA expression in both the Col-0 and C24 background. The repeat element further upstream in the promoter was not included in the constructs used in this study, and was therefore not tested for its effect on gene expression. However, *promoter::GUS* studies by Baek *et al.* (2011) indicate that expression is not altered when the promoters with and without this repeat element were analysed in the Col-0 background. This suggests that the promoter is not causal for the lack of *AtHKT1;1* expression in C24 roots. It also shows that the 2.7 kb promoter is able to drive *GFP* expression specifically in the stele in both Col-0 and C24, consistent with previous findings (Berthomieu *et al.* 2003, Mäser *et al.* 2002, Sunarpi *et al.* 2005, Xue *et al.* 2011). These results also suggest that C24 possesses the required transcriptional regulators for the promoter region, such as transcription factors or small RNAs, necessary for *AtHKT1;1* expression in the root.

Chapter 5 **The role of the second intron in *AtHKT1;1* expression**

5.1 Introduction

In the previous chapter it was shown that the 2.7 kb *AtHKT1;1* promoter from C24 is able to drive *GFP* expression in both Col-0 and C24. This indicates that this promoter sequence is not causing the lack of *AtHKT1;1* expression in C24 roots. Hence, another regulatory mechanism is hypothesised to explain the lack of *AtHKT1;1* expression in C24 roots. Sequencing the *AtHKT1;1* gene from genomic DNA identified an additional 1.6 kb of repetitive sequence is present in the second intron of the *AtHKT1;1* gene in C24 (Sundstrom 2011). Given the results obtained from *AtHKT1;1promoter::GFP* expressing lines, it is therefore hypothesised that this insertion in the intron may be responsible for the lack of *AtHKT1;1* expression in C24 roots. A diagram indicating the location of the second intron is provided in Figure 5.1.

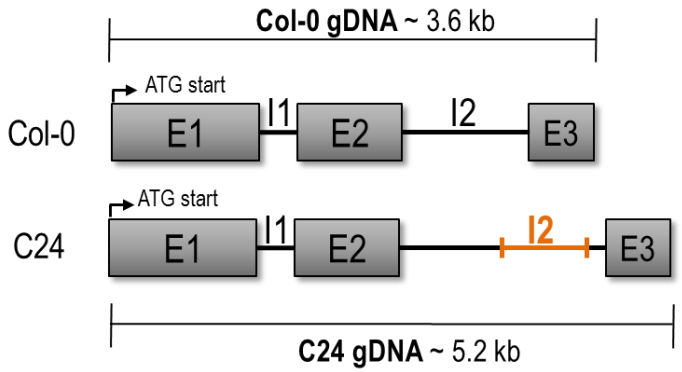

Figure 5.1: Comparison of the *AtHKT1;1* genomic sequence from Col-0 and C24.

Alignment of the Col-0 and C24 sequence, highlighting the 1.6 kb insertion (in orange colour) in the second intron (I2) of the C24 sequence. The start of the coding sequence is indicated by the arrow labelled ATG start (E) indicates an exon and (I) stands for intron.

This chapter investigates the second intron of *AtHKT1;1* and its potential to regulate gene expression. Based on the current literature, the following mechanisms were identified in which introns can influence expression of genes. A brief explanation is also given in each section as to how this mechanisms may have implications for *AtHKT1;1* expression.

5.2 Mechanisms by which introns can regulate gene expression

5.2.1 Intron mediated enhancement (IME)

Introns can be involved in the enhancement of gene expression, referred to as intron mediated enhancement (IME), which was first identified in maize (Callis *et al.* 1987, Vasil *et al.* 1989). IME has been shown to increase gene expression from less than 10-fold to up to 1,000-fold or more (Callis *et al.* 1987, Curie *et al.* 1993, Zhang *et al.* 1994). In Arabidopsis it has been shown that the intron of the *Polyubiquitine* gene, *UBQ10*, results in a three-fold increase in gene expression (Norris *et al.* 1993). Although a number of genes containing introns that are involved in IME have been identified in Arabidopsis, the mechanisms of IME are still largely unknown (Morello and Breviario 2008, Rose 2008). It is suggested that IME is more likely to involve introns that are found at the beginning of the gene and short conserved DNA sequences have been identified that may act as signals to enhance expression, enabling the prediction of introns that may be involved in IME (Morita *et al.* 2012, Parra *et al.* 2011, Rose *et al.* 2008). Most of the studies for IME involve transient or stable expression assays using the *GUS* reporter or firefly *luciferase* (*LUX*) genes fused to the intron sequence.

AtHKT1;1 expression may be subject to IME, leading to enhanced *AtHKT1;1* expression in the roots of the Col-0 ecotype. The 1.6 kb insertion in the second intron of *AtHKT1;1* in C24 may disrupt these elements that enhance root specific *AtHKT1;1* expression, resulting in the lack of *AtHKT1;1* expression in the C24 root. To date, there are no reports in the current literature as to whether the *AtHKT1;1* genomic sequence was specifically analysed for elements that mediate IME.

5.2.2 Intron dependent spatial expression (IDSE)

Some introns not only enhance expression by IME, but are also involved in tissue specificity of expression. An example where IDSE occurs is the gene *Profilin2* (*PRF2*), one of five members of the profilin family. *GUS* expression under control of the *PRF2* promoter is observed in vascular bundles, while expression of *PRF2promoter::intron::GUS* (construct containing the first intron of the *PRF2* gene) showed constitutive and strong expression throughout the vegetative tissue (Jeong *et al.* 2006). When the first intron of *PRF2* was placed after the *PRF5* promoter, which usually drives expression specifically in to reproductive tissues, GUS reporter activity was observed in the vegetative tissue, indicating that the *PRF2* intron mediates specificity for the vegetative tissue (Jeong *et al.* 2006). Other examples of IDSE have been recently outlined (Morello and Breviario 2008, Morello *et al.* 2011).

IDSE could be combined with IME and could explain why *AtHKT1;1* expression is observed in the root of Col-0, while the insertion of DNA in the second intron may lead to the lack of root specific *AtHKT1;1* expression in C24.

5.2.3 Rapid degradation of mRNA (small RNA independent pathways)

Alternative splicing occurs in many plant mRNAs (Campbell *et al.* 2006, Wang and Brendel 2006) and may lead to the formation of premature termination codons (PTC). This can cause the initiation of none-sense mediated decay (NMD), in which mRNA is degraded through mechanisms involving deadenylation, decapping of the 5′ end and/or a 3′ to 5′ decay (reviewed by Chiba and Green 2009). A recent review describes substrates for NMD, which have mostly been identified in yeast and mammalian systems (Kervestin and Jacobson 2012). An example for NMD in plants includes the rice *WAXY* gene. In a *waxy* mutant that contains a PTC, the fully spliced mRNA is subject to degradation by the NMD pathway, while transcripts that retain the first intron are not subject to decay (Isshiki *et al.* 2001). Recently it has also been shown for plants that the presence of large 3′ UTR regions induce NMD, causing degradation of aberrant transcripts (Nyikó *et al.* 2013).

Similar processes are plausible for the transcript produced from C24 *AtHKT1;1.* Due to the insertion in the second intron of *AtHKT1;1* in C24, which is close to the 3′ end of the gene, the intron itself or alternative splicing may lead to the formation of PTCs, which in turn could lead to degradation of the transcript by activation of NMD. For this mechanism to explain the lack of *AtHKT1;1* expression specifically in the root tissue of C24, the factors for recognition of PTCs or degradation would have to be shoot and root specific.

5.2.4 Introns may affect pre-mRNA structure, potentially causing faulty poly(A)-tailing

Polyadenylation (poly(A)) of the messenger RNA is an important step during its maturation, whereby a poly(A)-sequence is added to the 3′-end of the transcript. The pre-mRNA structure appears to be of importance as it influences poly(A)-signals and accessibility of trans-acting factors that add the poly(A) sequence (Loke *et al.* 2005). Additionally, it has been raised that AU-rich introns close to the 3′ end of the transcript may also influence poly(A)-signals in mammals, which in turn affect the interplay between polyadenylation and splicing (Tian *et al.* 2007).

Alternative splicing or repetitive (AU-rich) sequences in the C24 *AtHKT1;1* transcript may cause the RNA to fold into an alternate structure and/or it could shift the location of poly(A)-signals, which may alter polyadenylation. On the plant level, it is unlikely that the produced mRNA without functional

poly(A)-tail will be further processed to produce a functional AtHKT1;1 protein. Also, the detection of transcripts using qPCR or RT-PCR involves reverse transcription of the RNA to cDNA, utilising the mRNA's poly(A) tail, which is the target site of the primer. Without the functional poly(A)-tail on the *AtHKT1;1* transcript, the RNA would not be transcribed into cDNA and, consequently, the presence of the transcript would not be detected in subsequent PCR amplifications. Current literature does not describe if the second intron of *AtHKT1;1* contains AT-rich regions or if the corresponding transcript is AU-rich. Similarly to above, for this mechanism to explain the lack of *AtHKT1;1* expression specifically in the root tissue of C24, the factors that are involved in adding the poly(A)-sequence would have to be specific to the shoot and the root tissue.

5.2.5 Introns can be target sites of small RNAs

Small RNAs, such as microRNAs (miRNAs), have been found to play an essential role in regulating gene expression by mediating the decay of transcripts. Intron regions of genes can contain transposons, repetitive elements or other sequences that may be involved in the transcription of small RNAs and/or these sequences may be target sites of small RNAs, which could result in a reduction of gene expression. The following will briefly introduce types of small RNAs, their general function and how the silencing function may be related to intron sequences.

A recent review by Rogers and Chen (2013) covers in detail the miRNA biogenesis, turnover and repression of miRNA targets in plants. For miRNA biogenesis, the respective miRNA gene is transcribed into primary-miRNA (pri-miRNA) by a RNA polymerase. After a two-step cleavage by Dicer-like (DCL), pri-mRNA is processed into precursor-miRNA (pre-miRNA) and then into miRNA. The miRNA is then incorporated into the Argonaute (AGO) component of an RNA-induced silencing complex (RISC). This complex is then guided to transcripts containing highly complementary recognition sites and the target is destabilised. It has been proposed that most miRNA targets in plants undergo destabilisation by slicing, as opposed to destabilisation by decapping and deadenylation (Rogers and Chen 2013). It has also been shown in plants that the RISC can cause inhibition on the translational level by interfering with polysomes at the endoplasmic reticulum (Li *et al.* 2013). The regulation of gene expression by miRNA does not only occur on the post-transcriptional or translational level, but may also occur on the transcriptional level *via* RNA-directed DNA methylation (RdDM) (Wu *et al.* 2010). Wu *et al.* (2010) show that some miRNA are able to direct methylation in *cis,* at its own locus, as well as in *trans,* at target loci.

As mentioned above, miRNAs are transcribed from the genome, and are initially one RNA molecule that is self-complimentary and therefore forms a hairpin, resulting in double stranded RNA, which is then processed to miRNA. Small interfering RNAs (siRNAs), on the other hand, originate from

double stranded RNA precursors. A recent review details the different classes of small RNAs, their biogenesis and functions (Axtell 2013). A number of siRNA classes can be described: heterochromatic siRNAs are the most abundant class of small RNAs deriving from intergenic transposon loci and repetitive genomic regions (Wu *et al.* 2010). Transcripts of transposon loci or repetitive DNA are thought to be transcribed by Pol IV, a plant-specific DNA-dependent RNA polymerase (Herr *et al.* 2005, Kanno *et al.* 2005, Onodera *et al.* 2005). From these transcripts, double stranded RNA is produced by the RNA-dependent RNA polymerase (RDR2) (Xie *et al.* 2004). This double stranded RNA is then processed by DCL into siRNAs (Xie *et al.* 2004), and incorporated into AGO proteins (Li *et al.* 2006, Qi *et al.* 2006, Zheng *et al.* 2007, Zilberman *et al.* 2003). This complex then recruits RNA-directed DNA Methylation (RdDM) at target DNA loci, often resulting in silencing of transposons and genes in proximity to the transposon or transposable element (Axtell 2013, Law and Jacobsen 2010, Matzke *et al.* 2009). Another class of siRNAs are secondary siRNAs, whose precursor is meditated by upstream small RNAs, such as degradation products of double stranded RNA that was target of a RISC (Allen *et al.* 2005, Axtell 2013). Other classes of siRNAs are natural antisense transcript siRNAs (natsiRNAs), *trans*-acting siRNAs (tasiRNAs) and piwi-interacting RNAs (piRNAs). NatsiRNA and tasiRNA are involved in the post-transcriptional regulation of transcripts, while piRNA appears to be involved in the suppression of transposons and repeat elements (Axtell 2013, Borsani *et al.* 2005, Chapman and Carrington 2007).

The eukaryotic genome contains numerous transposable elements (TEs) and many of them have been identified in intron regions (Nekrutenko and Li 2001). In plants, regions of transposons and TEs have been linked to DNA methylation on a genome wide basis (Zhang *et al.* 2006a). It is possible that the *AtHKT1;1* intron in C24 contains a transposon, or transposable element, which is methylated. The methylation may then spread into the *AtHKT1;1* gene itself and silence expression on a transcriptional level. A similar case has been reported where a Long Interspersed Element (LINE), a non-LTR retrotransposon, leads to methylation of the adjacent *BONSAI* (*BNS)* gene and subsequently induces silencing (Saze and Kakutani 2007). Also, a *Mutator*-like TE has been identified in the first intron of the *FLOWERING LOCUS C* (*FLC*) in the ecotype L*er* (Michaels et al. 2003). The TE is target of siRNAs generated by homologous TEs, leading to methylation and transcriptional silencing of *FLC* and consequently leads to early flowering of the ecotype (Liu *et al.* 2004). Another region adjacent to the promoter region of FLC has been identified, which is methylated in the L*er* ecotype, but not in Col-0 (Zhai *et al.* 2008). It has been shown that L*er* has high levels of the corresponding siRNA, leading to methylation, as opposed to Col-0 (Zhai *et al.* 2008). This variation in siRNA abundance was also found to affect the methylation status of other

genes that contain the specific siRNA target site (Zhai *et al.* 2008). Similarly, it is possible that C24 and Col-0 vary in the abundance of specific siRNAs that target TEs in other regions of the *AtHKT1;1* genomic sequence, again leading to ecotype specific silencing of *AtHKT1;1* expression.

If the C24 *AtHKT1;1* contains a TE it could also be post-transcriptionally silenced. The transcript may be the target site of small RNAs, which may lead to slicing of the whole transcript and therefore silenced *AtHKT1;1* gene expression.

The tissue specificity of methylation or abundance of siRNAs is not well understood, particularly when comparing root and shoot tissue. Therefore, it would be difficult to explain the lack of *AtHKT1;1* expression specifically in the C24 root, while expression is present in low levels in the shoot. It has been described that TEs can be activated pollen tissue specifically. The methylation of TEs is reduced in vegetative nuclei of mature pollen, leading to the transcriptional activation of TEs (Slotkin *et al.* 2009). The selective loss in siRNAs causes the absence of methylation and therefore activation of TEs (Slotkin *et al.* 2009). A similar process of root specific expression of siRNA may be present in the root of C24. The siRNAs that target *AtHKT1;1* may be transcribed from a homologous TE, which is located in a genomic region that mediates root specific expression.

5.3 Investigating the *AtHKT1;1* sequence of other ecotypes

Recently, the genomic sequence of 19 Arabidopsis ecotypes has been determined (Gan *et al.* 2011). With the correct bioinformatic tools, this allows searching for genes of interest, such as the genomic *AtHKT1;1* sequence. For some of these ecotypes, information regarding Na^+ accumulation or salinity tolerance is also available (Baxter *et al.* 2010). C24 has the 1.6 kb insertion in the second intron of *AtHKT1;1*, it accumulates more Na^+ than Col-0, has an increased salinity tolerance compared to Col-0 and no *AtHKT1;1* expression in the root. The two ecotypes Ts-1 and Tsu-1 also accumulate high levels of Na^+, have an increased salinity tolerance compared to Col-0 and have low levels of *AtHKT1;1* expression in the root (Rus *et al.* 2006). Rus *et al*. (2006) also reported difficulties in obtaining the sequence of the last 157 bp of the second intron, the region containing the additional sequence in C24. Furthermore, a study by Baxter *et al.* (2010) had investigated a vast number of Arabidopsis ecotypes for their shoot Na^+ accumulation and showed that some ecotypes that are found close to the sea or other saline areas, accumulate more shoot Na^+. A comparison of the C24 *AtHKT1;1* to the *AtHKT1;1* of the other 19 ecotypes may yield additional information regarding the genomic structure of *AtHKT1;1*, which may correlate with available data for shoot Na^+ content and salinity tolerance.

5.4 Testing for the role of the second intron in regulating *AtHKT1;1* expression *in planta*

In this study, a series of constructs are designed to investigate if the genomic *AtHKT1;1* DNA regulates gene expression, in particular the second intron, hypothesised to cause the lack of *AtHKT1;1* expression in C24 roots (Table 5.1). Transgenic *promoter::gDNA* lines were designed to test for *AtHKT1;1* transgene expression. The 2.7 kb promoters of Col-0 and C24, again referred to as pCol-0 and pC24, that were used in the previous chapter to drive *GFP* and *AtHKT1;1* cDNA expression were also used in this study to drive *AtHKT1;1* gDNA and *intron::GFP* and *intron::GUS* constructs. Constructs containing the Col-0 and C24 *AtHKT1;1* gDNA, referred to as *Col-0-gDNA* and *C24-gDNA*, under control of the 2.7 kb promoter were designed to test if expression of the transgene is detected when transformed into the Na^+ accumulating, low root *AtHKT1;1* expressing ecotype C24, and the Na^+ accumulating Col-0 *gl1* mutant line, *hkt1-4* which has no expression of *AtHKT1;1*. These transgenic lines would also be tested for altered shoot and root Na^+ content compared to the wild type, as expression of *AtHKT1;1* has been correlated with a reduction in shoot Na^+ and an increase in root Na^+ (Møller *et al.* 2009). Additionally, the influence of the second intron was directly investigated by generating transgenic lines containing *promoter::intron::reporter-gene* constructs. The hypothesis is that the intron will influence the expression of the reporter gene, *GFP* or *GUS*. Similar experiments have been performed by Baek *et al.* (2011), in which part of the *AtHKT1;1* promoter, the repeat element located 4 kb upstream of the start codon, was fused between the minimal 35S promoter and *GUS* to analyse stably transformed lines for *GUS* expression. Both the *GFP* and *GUS* reporter genes were included in this study. *GFP* has been shown to be expressed under control of pCol-0 and pC24 in the previous study (chapter 4), while GUS activity is detected by an enzymatic reaction, facilitating detection even if *GUS* is expressed in low levels (Jefferson *et al.* 1987, Mantis and Tague 2000).

Table 5.1: Components of expression vectors to examine if the difference in *AtHKT1;1* genomic sequence, specifically the second intron, results in different expression patterns in Col-0 and C24. The expected phenotype is based on the hypothesis that the second intron in the C24 *AtHKT1;1* reduces root expression of *AtHKT1;1*

***Promoter::gene* combination**	**Destination vector**	**Arabidopsis background**	**Expected phenotype**
pCol-0::Col-0-gDNA	pMDC100	C24	Expression in root, reduced shoot Na^+ and increased root Na^+
		Col-0 *gl1 hkt1-4*	Expression in root, reduced shoot Na^+ and increased root Na^+
pCol-0::C24-gDNA	pMDC100	C24	No expression in root, Na^+ unchanged
		Col-0 *gl1 hkt1-4*	No expression in root, Na^+ unchanged
pC24::Col-0-gDNA	pMDC100	C24	Expression in root, reduced shoot Na^+ and increased root Na^+ than background ecotype
		Col-0 *gl1 hkt1-4*	Expression in root, reduced shoot Na^+ and increased root Na^+ than background ecotype
pC24::C24-gDNA	pMDC100	C24	No expression in root, Na^+ unchanged
		Col-0 *gl1 hkt1-4*	No expression in root, Na^+ unchanged
pCol-0::Col-0intron	pMDC107 (GFP)	Col-0	GFP signal in root
		C24	GFP signal in root
pCol-0::C24intron	pMDC107 (GFP)	Col-0	No GFP signal in root
		C24	No GFP signal in root
pC24::Col-0intron	pMDC107 (GFP)	Col-0	GFP signal in root
		C24	GFP signal in root
pC24::C24intron	pMDC107 (GFP)	Col-0	No GFP signal in root
		C24	No GFP signal in root
pCol-0::Col-0intron	pMDC162 (GUS)	Col-0	Signal in root
		C24	Signal in root
pCol-0::C24intron	pMDC162 (GUS)	Col-0	No GUS signal in root
		C24	No GUS signal in root
pC24::Col-0intron	pMDC162 (GUS)	Col-0	Signal in root
		C24	Signal in root
pC24::C24intron	pMDC162 (GUS)	Col-0	No GUS signal in root
		C24	No GUS signal in root

5.5 Aims of this study

The aim of the chapter is to determine if the second intron of *AtHKT1;1* has the potential to cause the differences in the *AtHKT1;1* expression pattern, that is observed in Col-0 and C24. In particular, the focus will be on the 1.6 kb insertion in the second intron and if it may cause the lack of *AtHKT1;1* expression in C24 roots. Different mechanisms of how introns may regulate *AtHKT1;1* gene expression were introduced above, to this end, available information from the literature and databases will be used to narrow down likely mechanisms of regulation. The aim is also to combine *in planta* analyses, such as transgenic lines, along with bioinformatics approaches to determine if the second intron mediates regulation of *AtHKT1;1* expression in C24 roots. The following points will be addressed:

1. Use available bioinformatics tools and current literature to gather information regarding the second intron, particularly the 1.6 kb insertion in the C24 *AtHKT1;1*.
2. Generate constructs designed to test if the sequence corresponding to the insertion in the second intron reduces *AtHKT1;1* and reporter gene expression *in planta*.

5.6 Materials and methods

5.6.1 Bioinformatics analyses

Basic bioinformatics analysed were performed using the BLAST tool (Altschul *et al.* 1997).

General BLAST searches were performed using the nucleotide BLAST (blastn suite) available from the National Center for Biotechnology Information (NCBI, http://blast.ncbi.nlm.nih.gov). Sequences were obtained from The Arabidopsis Information Resource (TAIR10, http://www.arabidopsis.org/) and information visualised using the Generic Genome Browser version 2.55 (gbrowser, http://tairvm17.tacc.utexas.edu/cgi-bin/gb2/gbrowse/arabidopsis/). TAIR contains genetic and molecular data specifically for Arabidopsis. It contains a wealth of sequence information, such as the location of T-DNA inserts in knockout lines, polymorphisms between Col-0 and other ecotypes, and the presence of transposable elements. The TAIR database is regularly updated with the latest information published.

The SIGnAL Arabidopsis Methylome Mapping Tool was used to show the methylation pattern of the genomic region in question (Zhang *et al.* 2006a). Two methods were used to capture methylated DNA, methylcytosine Immunoprecipitation (mCIP) and methylcytosine binding domain (MBD) (Zhang *et al.* 2006a). The captured DNA was then identified using an Arabidopsis single-chip tiling microarray (Zhang *et al.* 2006a). Genome wide methylation patterns were analysed in two methylation deficient mutant backgrounds *met1* and *drm1 drm2 cmt3* (ddc) as they eliminate different methylation patterns, CG methylation and non-CG methylation (Zhang *et al.* 2006a). This tool also displays small RNA signatures (Gustafson *et al.* 2005, Lu *et al.* 2005). Labelling of the individual traces can be found in the Supplementary Table 8.1.

The Repbase Update program is a website based program, which searches repetitive sequences by homology (Jurka *et al.* 2005).

The genomic sequences of 19 Arabidopsis genomes (Bur-0, Can-0, Ct-1, Edi-0, Hi-0, Kn-0, Ler-0, Mt-0, No-0, Oy-0, Po-0, Rsch-4, Sf-2, Tsu-0, Wil-2, Ws-0, Wu-0 and Zu-0) were obtained from http://mus.well.ox.ac.uk/19genomes/ (Gan *et al.* 2011) and were made searchable by Mr. John Toubia, B.Sc. Bioinformatics (ACPFG, Adelaide, Australia) in the Batch BLAST Portal available at the ACPFG.

5.6.2 Analysis of *AtHKT1;1* transcripts by semi-qPCR

To analyse the presence of *AtHKT1;1* transcripts in more detail, gene specific primers were used in a reverse transcription reaction to obtain gene specific cDNA, as opposed to using oligo $d(T)_{20}$ primers to obtain total cDNA. Two *AtHKT1;1* gene specific primers were designed for cDNA synthesis, one which bound in the third exon 3′ of the second intron and a second primer which bound in the second intron 5′ of the second intron.

cDNA synthesis was performed as described previously (section 2.5.2), with the only difference that gene specific primers listed in Table 5.2 were used and 200 U reverse transcriptase enzyme. Approximately 500 ng of RNA, derived from roots of 6 wk old hydroponically grown Col-0 and C24 plants subject to 7 d of ± 100mM NaCl treatment, in three biological replicates, was used for cDNA synthesis.

Table 5.2: Primers used for *AtHKT1;1* specific cDNA synthesis

Primer name	Sequence (5'-3')	Annealing location (approximate distance from ATG start codon)
HKT1;1-exon 3_R	GATTCTTTACCCCTCGTCTTCCTAA	Annealing at the end of Exon 3 (1.5 kb)
HKT1;1-exon 2_R	ATTTTGCCTTTCGGTGATTG	Annealing at the end of Exon 2 (1.2 kb)

RT-PCR was also performed as described previously (section 2.5.4) with primers listed in Table 5.3. DNA fragments were visualised using agarose gel electrophoresis (section 2.1.2).

Table 5.3: Primer pairs used for RT-PCR using *AtHKT1;1* specific cDNA

Primer name	Sequence (5'-3')	Annealing location
Semi-q-HKT_Pair1	TGGCTCTGTGTTGCTTCTTG TTGAGGGATTAGGAGCCAGA	Amplification of 200 bp within Exon 1
Semi-q-HKT_Pair2	GGTTTCACTACCGGGTACA TGGCTGTGAACTGCTTAAACC	Amplification of 150 bp within Exon 2

5.6.3 Generation of constructs for *in planta* analyses

To test the effects of the second intron sequence on *AtHKT1;1* expression, various constructs were designed for *in planta* analysis. The plasmids containing the 2.7 kb promoters (*pCol-0* and *pC24*) in the pCR8 vector were kindly provided by Dr. Sundstrom (University of Adelaide, Australia). The genomic *AtHKT1;1* DNA sequences were cloned as described in the following.

Table 5.4: Combination of *AtHKT1;1* 2.7 kb promoters and *AtHKT1;1* sequences with corresponding destination vectors for *in planta* analyses of the second intron and its influence on regulating *AtHKT1;1* expression

2.7 kb *AtHKT1;1* promoter	*AtHKT1;1* sequence	Destination vectors
Col-0	Col-0-gDNA	pMDC100nosT
Col-0	C24-gDNA	pMDC100nosT
C24	Col-0-gDNA	pMDC100nosT
C24	C24-gDNA	pMDC100nosT
Col-0	Col-0 intron	pMDC107 (GFP) and pMDC162 (GUS)
Col-0	C24 intron	pMDC107 (GFP) and pMDC162 (GUS)
C24	Col-0 intron	pMDC107 (GFP) and pMDC162 (GUS)
C24	C24 intron	pMDC107 (GFP) and pMDC162 (GUS)

5.6.3.1 Template DNA to amplify genomic *AtHKT1;1* sequences

To amplify the Col-0 *AtHKT1;1* genomic sequence, total genomic plant DNA was purified from leaf material as described in section 2.4 and used as a template in PCR reactions.

Sundstrom (2011) was unable to determine the full genomic *AtHKT1;1* sequence from C24 plant genomic DNA. A Bacterial Artificial Chromosome (BAC), ATC24016B6 (obtained from Professor June Nasrallah (Cornell University, Ithaca, NY, USA)), containing the C24 genomic sequence was utilised to determine the C24 genomic *AtHKT1;1* sequence (Sundstrom 2011). To clone the full length genomic region of *AtHKT1;1* in the present thesis, this BAC clone was obtained from Dr. Sundstrom and used as template for PCR reactions. BAC plasmid DNA was purified following the protocol below:

A single colony of the BAC clone was used to inoculate 10 mL of LB with chloramphenicol (12.5 µg mL^{-1}) and the solution incubated at 37 °C o/n. The cell pellet from this bacterial culture was resuspended in 200 µL of P1 (re-suspension solution from Qiagen, Chadstone Centre, Australia, Cat. #19051). The cells were lysed by the addition of 400 µL of 1 % (w/v) SDS/0.2 M NaOH and incubated on ice for 5 min. Cell debris was precipitated by addition of 300 µL of neutralisation buffer P3 (Qiagen, Cat. #19053) and a further incubation of 10 min on ice. After centrifugation at 16,000 *g* for 15 min at 4 °C, nucleic acids were precipitated by the addition of 550 µL of 100% (v/v) isopropanol to the remaining supernatant. A pellet of nucleic acid was formed by centrifugation for 5 min at 16,000 *g* in a bench top centrifuge. The pellet was washed with 70% (v/v) ethanol and air dried. The plasmid DNA was resuspended in 30 µL of MQ-water and used for subsequent PCR amplification of the C24 *AtHKT1;1* fragments.

5.6.3.2 PCR amplification of Col-0 and C24 *AtHKT1;1* gDNA

A number of different PCR conditions were tested to determine the optimal conditions for amplification of the Col-0 and C24 genomic DNA. The following polymerases were tested as recommended by the manufacturer's instructions: Elongase® (Life Technologies™, Mulgrave, Australia, Cat. #10480010,), Phusion® High-Fidelity DNA Polymerase (New England Biolabs, Ipswich, MA, USA, Cat. #M0530), FailSafe™ PCR Test kit (EPICENTRE® Biotechnologies, Madison, WI, USA, Cat. #FSP995), Platinum® *Pfx* DNA polymerase (Life Technologies™, Mulgrave, Australia, Cat. #11708013), Phire Hot Start II DNA polymerase (Thermo Scientific, Wilmington, DE, USA, Cat. #F-122) and FastStart High Fidelity PCR System (Roche, Castle Hill, Australia, Cat. #03553426001). Annealing temperatures between 50 °C to 60 °C were tested in 2 °C increments. Amplification of the full sequence in one single PCR using the above mentioned polymerases was not successful; therefore a different cloning strategy was applied. The sequence was divided into smaller fragments, which contain at either side unique restriction sites that occur naturally in the *AtHKT1;1* sequence for ligation of the fragments in the correct order to obtain the full length *AtHKT1;1* gDNA. The advantage is that the smaller fragments are less likely to incorporate sequence errors during amplification and can be sequenced separately before ligation. The Col-0 gDNA was divided into two fragments and the C24 gDNA was divided into three fragments. Again, a number of PCR conditions were tested to obtain the DNA fragments without sequence errors. The use of various Failsafe™ buffers have shown to be most successful for these PCR amplifications. Different FailSafe™ buffers contain varying amounts of $MgCl_2$ and FailSafe PCR enhancer.

The general workflow to obtain full length *AtHKT1;1* gDNA fragments is depicted in Figure 5.2 and described below:

1) Primer design using Primer 3 and Netprimer (section 2.1.1) with unique restriction sites that occur naturally in the *AtHKT1;1* sequence for ligation of the fragments; 2) amplification of DNA fragments using PCR (section 2.1.1); 3) analysis of PCR products using agarose gel electrophoresis (section 2.1.2); 4) purification of PCR products from agarose gel (section 2.1.3); 5) addition of an A-overhang to PCR fragments to enable TA-cloning (section 2.1.4) into pCR8 vectors; 6) TA-cloning of PCR fragments into the pCR8 vector (section 2.1.4); 7) transformation of pCR8 vector containing DNA fragments into TOP10 cells and colony analysis by extracting plasmid DNA, restriction digest and agarose gel electrophoresis (sections 2.1.7, 2.1.8 and 2.1.2); 8) sequencing of positive clones with primers GWI and GWII, which anneal on the pCR8 vector either side of the inserted DNA fragment, if necessary additional sequencing using gene specific primers to ensure sequence is without errors (section 2.1.11); 9) digest of correct fragments using desired restriction enzymes and separation of fragments using agarose gel electrophoresis, followed by purification; 10) fragment ligation and 11) transformation of the vector into TOP10 cells, colony selection and sequence analysis (from step 7 onwards). After completion, the correct genomic *AtHKT1;1* DNA fragments were in Gateway® enabled vectors that can be used for LR reactions to obtain destination vectors (section 2.1.10).

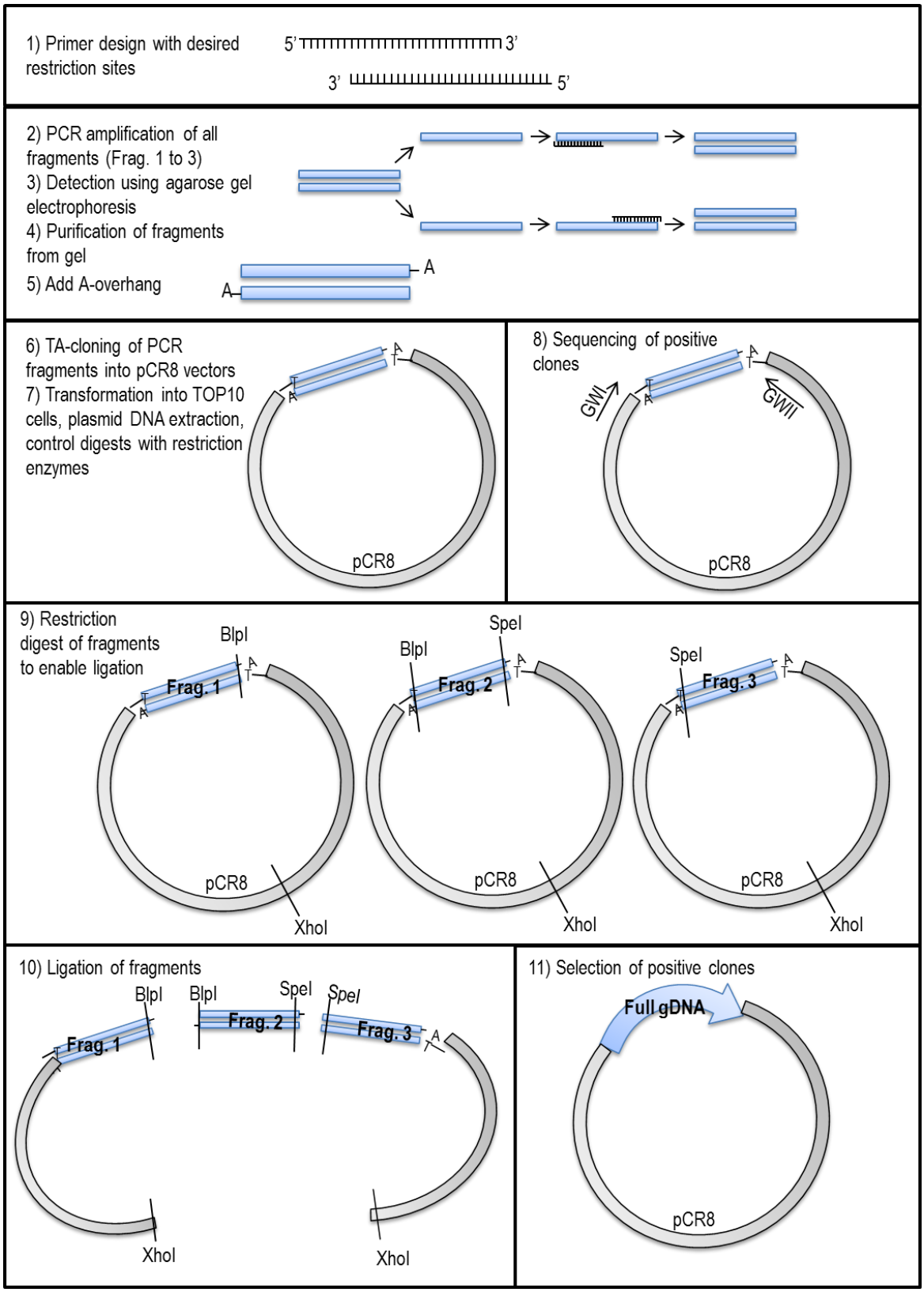

Figure 5.2: Diagram illustrating workflow for cloning of *AtHKT1;1* genomic DNA fragments.

Depicted is the workflow of constructing the full length *AtHKT1;1* genomic DNA from C24. The Col-0 *AtHKT1;1* gDNA was generated similarly but only using two fragments. Details regarding individual steps can be found in the text.

Once the full length genomic DNA or intron fragments with the correct sequence were obtained, they were ligated behind the *AtHKT1;1* promoter sequence in pCR8 (Figure 5.3). For this, 1) the pCR8 vectors containing the *AtHKT1;1* gene sequence and promoter sequence were digested using the restriction enzyme *Xho*I. The fragments were separated using agarose gel electrophoresis and purified as described previously (sections 2.1.2 and 2.1.3). 2) The desired DNA fragments were then ligated (section 2.1.9), transformed into TOP10 cells and colonies were selected for restriction digest analysis. As indicated in Figure 5.3 also the plasmid backbone contains an *Xho*I restriction site, which is undesirable as it is therefore possible for the fragments to ligate in an undesired orientation. Unfortunately, it was not possible to use another restriction enzyme so restriction digestion of the ligated *promoter::gene* pCR8 constructs was performed to identify those plasmids with the incorrect assembly and these were excluded. 3) Positive clones were selected and sequenced to ensure all fragments were present in the correct order and orientation using GWI and GWII (section 2.1.11).

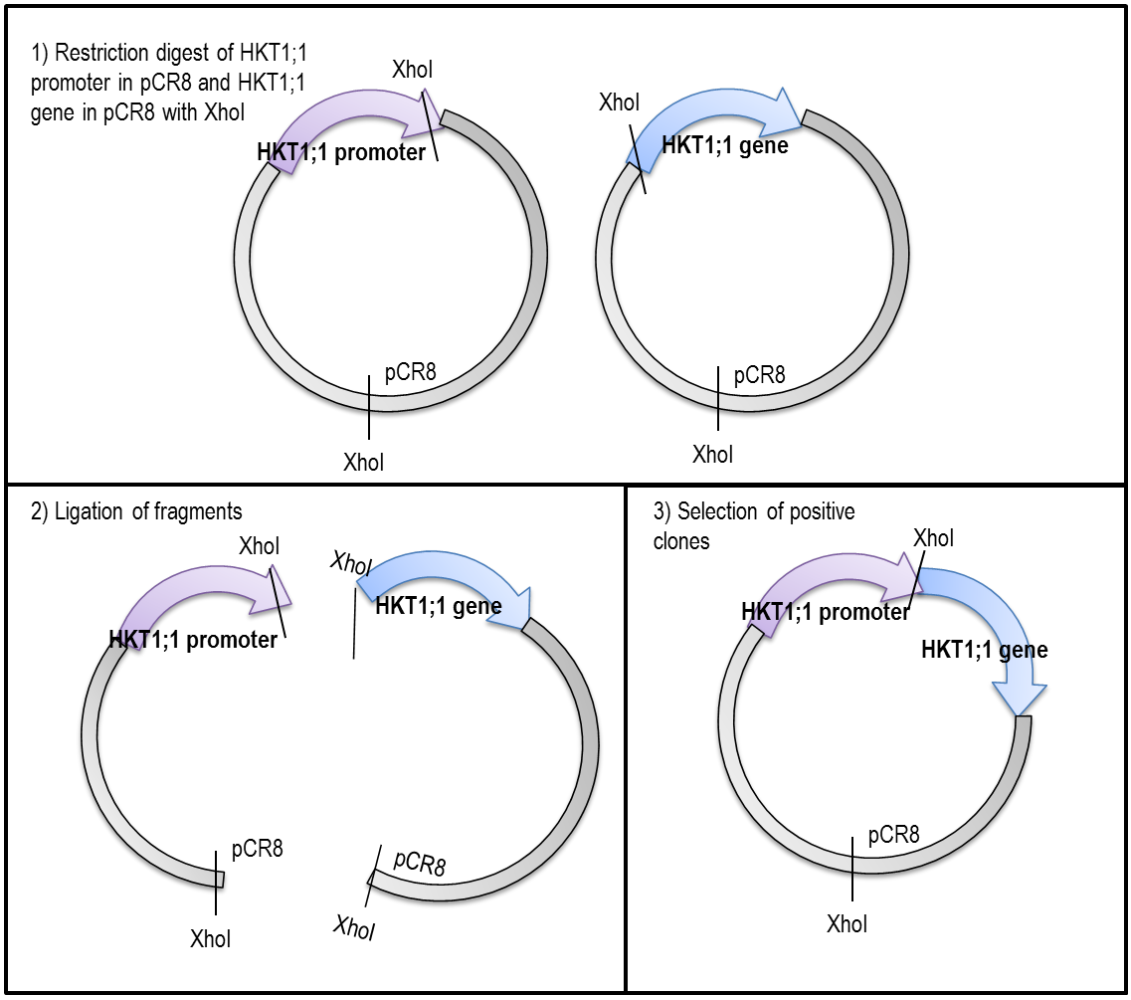

Figure 5.3: Diagram illustrating cloning strategy to ligate *AtHKT1;1* promoter fragments with gene fragments.

Fragments were generated using *Xho*I restriction digest and then ligated to the final entry vector.

Once the desired *AtHKT1;1* promoter and *AtHKT1;1* gene sequence were in the pCR8 vector, they were recombined into the desired destination vector by LR recombination (section 2.1.10) as outlined in Figure 5.4.

The destination vectors pMDC107 and pMDC162 were available as laboratory stocks, originating from Curtis and Grossniklaus (2003), while pMDC100nosT vector was modified by Sundstrom (2011). pMDC107 and pMDC162 contain a *GFP* and *GUS* reporter gene, respectively, downstream of a Gateway enabled cloning site which can be used to insert a desired gene promoter to test its activity. The vector pMDC100nosT does not contain a promoter for driving the expression of a gene of interest. It only contains a *nosT* sequence downstream of the Gateway® enabled entry site which allows the termination of the transcript of an inserted gene of interest. pMDC100nosT therefore allows the expression of a gene of interest under the control of a promoter of interest. As indicated, all three vectors are Gateway® enabled, allowing the insertion of the gene of interest from a pCR8 entry vector by LR recombination (section 2.1.10). These vectors also contain the required genes for amplification in *A. tumefaciens* (section 2.3), mediate expression and transgene selection in Arabidopsis (section 2.3.4).

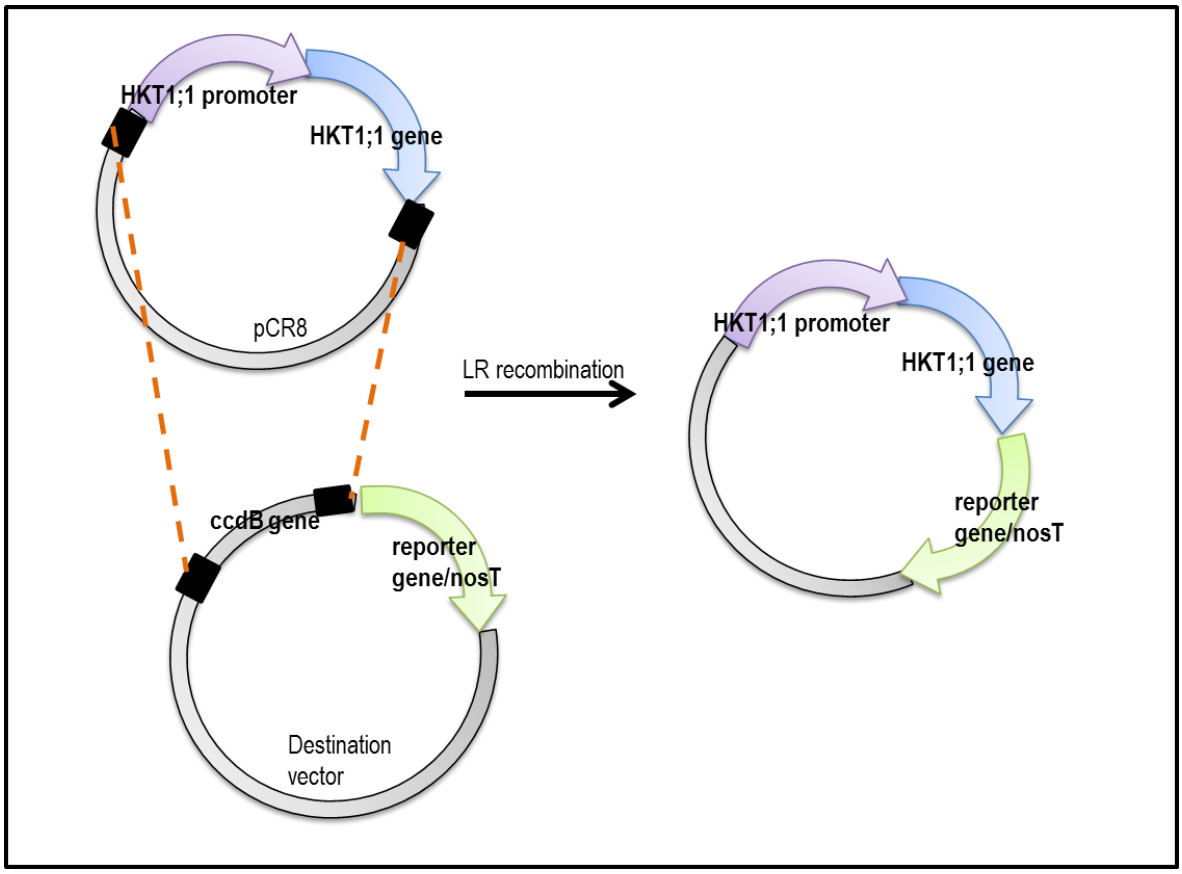

Figure 5.4: Diagram illustrating the recombination of the *AtHKT1;1* promoter and gene sequences from the pCR8 vector into the desired destination vector.

Gateway® recombination sites are marked in black boxes and mediate the replacement of the *ccdB* gene, which facilitates negative selection in bacteria, with the DNA sequence of interest, in this case the *AtHKT1;1* promoter and gene sequences (indicated by orange dashes).

5.7 Results

5.7.1 Identifying regulatory elements in the second intron of *AtHKT1;1*

Intron mediated enhancement (IME) has been identified in a number of genes in Arabidopsis. Genes with known IME have often been described as having overrepresentation of short nucleotide sequence repeats in their first introns. The two known sequences are (1) GATCTG (Morita *et al.* 2012, Rose *et al.* 2008) and (2) CGATT (Parra *et al.* 2011). While (1) GATCTG was not present in the *AtHKT1;1* genomic DNA sequence of Col-0 or C24, (2) CGATT was present in the second intron in both Col-0 and C24. In C24, the motif was found approximately 30 bp upstream of the 1.6 kb insertion, which is hypothesised to be involved in regulating *AtHKT1;1* expression. Since the motif is present in both ecotypes' *AtHKT1;1*, there is not an overrepresentation of the sequence, and the motif is located in the second intron, it seems unlikely that IME is causing the lack of *AtHKT1;1* expression in C24 roots. However, this mechanism cannot be excluded without empirical testing.

Another mechanism that is known to regulate gene expression is non-sense mediated decay (NMD). The degradation of transcripts by NMD containing PTCs has not yet been described to be tissue specific, which would make this mechanism unlikely to be the cause for the lack of *AtHKT1;1* expression in the root of C24 plants. However these mechanisms have been primarily studied in the mammalian and yeast system and studies have not yet analysed tissue specificity of NMD in plants. Unfortunately, no additional information is available to judge if NMD may be responsible for the decay of *AtHKT1;1* transcript in C24 roots and, therefore, this mechanism cannot be excluded.

The lack of *AtHKT1;1* transcript in roots of C24 may result from insufficient addition of poly(A)-sequence to the end of the RNA transcript. The *AtHKT1;1* transcript sequence of Col-0 and C24 was not determined in this study, which would enable the quantification of the actual AU content, however, the AT content of *AtHKT1;1* was determined on the basis of the genomic DNA (Table 5.5). The AT-content of the *AtHKT1;1* second intron is higher in Col-0 (80 %) compared to C24 (70 %), while the 1.6 kb insertion in the second intron in C24 is even lower (65 %). It has been previously reported that the average AU-content of introns in Arabidopsis is approximately 70 % (Ko *et al.* 1998), which is similar to the *AtHKT1;1* AT content. AU rich sequences in the intron close to the 3′-end of transcripts have been linked to alterations in poly(A)-signals, inhibiting the addition of the poly(A)-tail in mammals (Tian *et al.* 2007). Yet, it does not appear that an unusually high AU content is present in the second intron of the *AtHKT1;1* transcript which may interfere with the addition of a poly(A)-tail. However, the intron region in C24 appears to have repetitive elements, which may in turn lead to alternate folding of the transcript, which may interfere with addition of the poly(A)

sequence. Therefore, this mechanisms cannot be excluded to be causing the lack of *AtHKT1;1* transcript in C24 roots.

Table 5.5: AT-content of *AtHKT1;1* genomic Col-0 and C24 DNA fragments located towards the 3' end of the gene

Fragment of genomic DNA (approximate length)	~ % AT content
Full length Col-0 second intron (~ 0.8 kbp)	80
Full length C24 second intron (~ 2.4 kb)	70
DNA insertion in second intron of C24 (~ 1.6 kb)	65
Col-0 third exon (~ 0.2 kb)	55
C24 third exon (0.2 kb)	52

Studies and mechanisms described in the current literature did not lead to conclusive evidence whether or not *AtHKT1;1* expression in C24 roots is controlled by IME, NMD or insufficient poly(A)-sequence addition. Therefore, bioinformatics databases were consulted.

5.7.2 Bioinformatics analysis of the genomic DNA sequence, in particular the second intron

5.7.2.1 Col-0 *AtHKT1;1* contains transposable elements in the second intron

To investigate if the regulation of *AtHKT1;1* is influenced or controlled by elements in the genomic DNA, particularly elements present in the second intron, a range of databases containing sequence and transcript data were consulted. TAIR was searched for *AtHKT1;1*, *At4G10310*, to obtain information concerning the ecotype Col-0 (Figure 5.5). A subset of the database was selected containing the desired information (referred to as tracks) for *AtHKT1;1*. As expected, the predicted gene model confirmed *AtHKT1;1* is composed of three exons and two introns. Interestingly, analysis of the database indicated the presence of a large transposable element, ATHPOGON1 in the second intron of the Col-0 *AtHKT1;1* gene (Figure 5.5 Track 1, A). Two smaller transposable elements, ATREP11 and BRODYAGA1, were also identified within the second intron (Figure 5.5 Track 3, B). Additionally, a number of small RNA binding sites were identified in the region of the large transposable element (Figure 5.5 Tracks 4-6, C). To investigate whether the region of the genome containing *AtHKT1;1* is subject to methylation, the SIGnAL Arabidopsis Methylome Mapping Tool

was used (Figure 5.6). It should be noted that the methylation status was determined in floral tissue and methylation may be different in shoot or root tissue. Little methylation was found in the genomic region of *AtHKT1;1*; however, strong methylation was detected in the promoter region, approximately 2.4 kb upstream of the *AtHKT1;1* start codon (Figure 5.6 Track 2, A). Within the *AtHKT1;1* promoter (approximately 3 kb to 6 kb upstream of the AtHKT1;1 start codon) there were also a large number of small RNA binding sites (Figure 5.6 Track 3, B), along with a smaller number in the second intron (2.5 kb to 3.4 kb in the *AtHKT1;1* genomic sequence) (Figure 5.6 Track 3, C).

5.7.2.2 Insertion in the second intron in C24 corresponds to transposon SIMPLEHAT2

Since the second intron in Col-0 contains a large transposable element, the additional sequence present in C24 was subjected to a BLAST search to investigate if the insertion is a transposable element itself. The query was subject to a BLAST search using the tool blastn in the nucleotide database of *Arabidopsis thaliana* and optimising for highly similar sequences (megablast). A graphical overview of BLAST results indicates the similarity of sequences identified (Figure 5.7 A). The length and position of the identified sequences (lines in red) are presented relative to the query sequence (numbered red line at the top). The colour of the bands indicates that the identified sequences have a high bit score, which is a normalised measurement of sequence similarity. The table underneath contains a list of identified loci that have a similar sequence to the second intron of *AtHKT1;1* in C24 (Figure 5.7 B). It provides a brief description of the identified loci, for example on which chromosome the sequence was identified and the E-value. The E-value indicates how likely it is that this sequence alignment would be obtained by chance, the smaller the E-values the less likely the sequences are similar by chance. The column headed “Ident” indicates the percent identity of the match of the sequences and the “Accession” column leads to experimental details in which the sequence was identified. These BLAST results were used to investigate if the sequence has been annotated elsewhere in the genome.

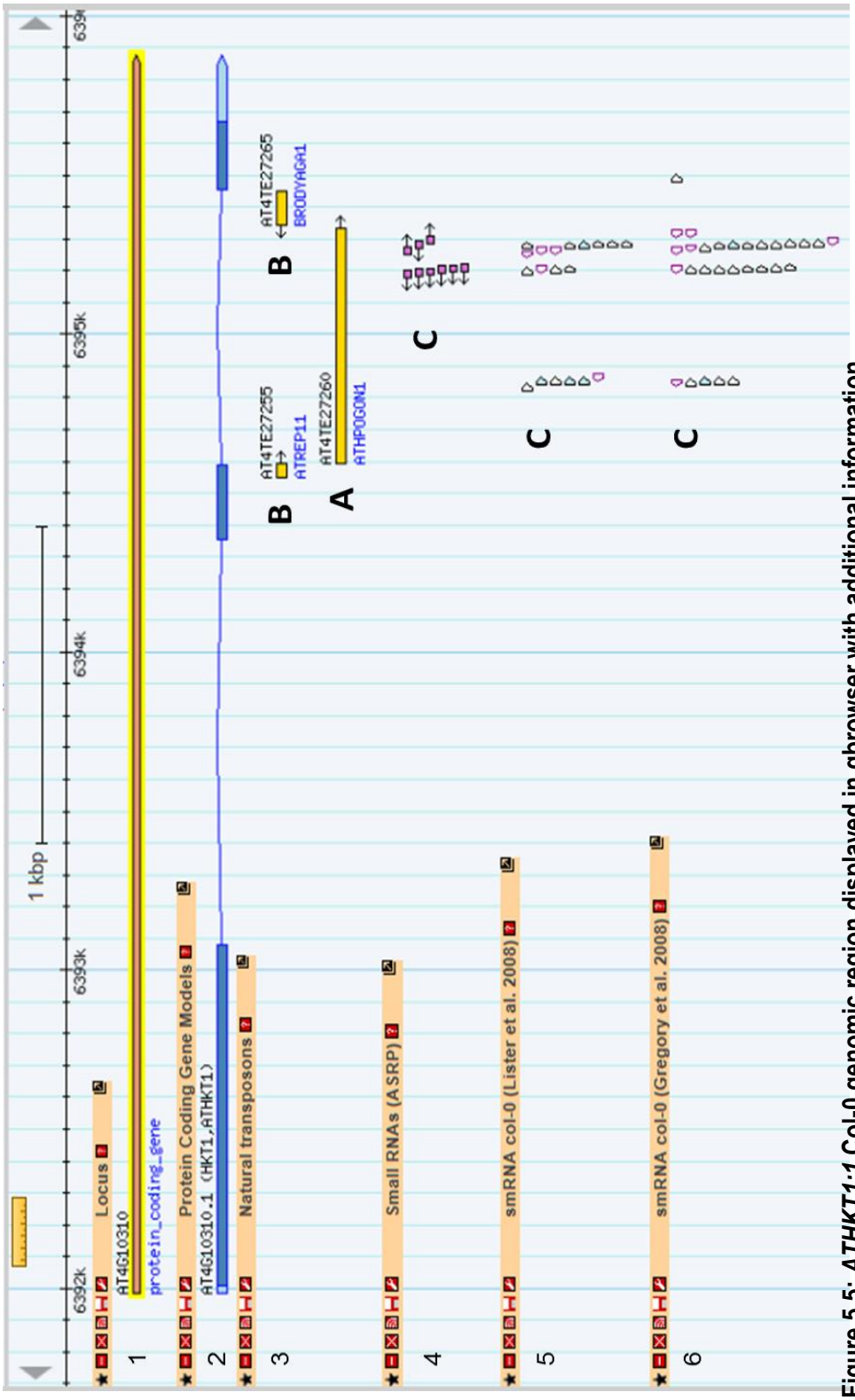

Figure 5.5: *ATHKT1;1* Col-0 genomic region displayed in gbrowser with additional information.

Tracks included are (1) At4g10310 locus (AtHKT1;1), (2) the gene model indicating three exons (solid blue box) and two introns (lines between boxes), (3) natural transposons annotated from TAIR and a variety of external sources including TIGR and the Quesneville group (Buisine et al. 2008) highlighting the (A) ATHPOGON1 transposon and (B) ATREP11 and BRONDYAGA1 transposons; and tracks (4), (5) and (6) display small RNA binding sites identified by different sources as indicated, highlighted with (C).

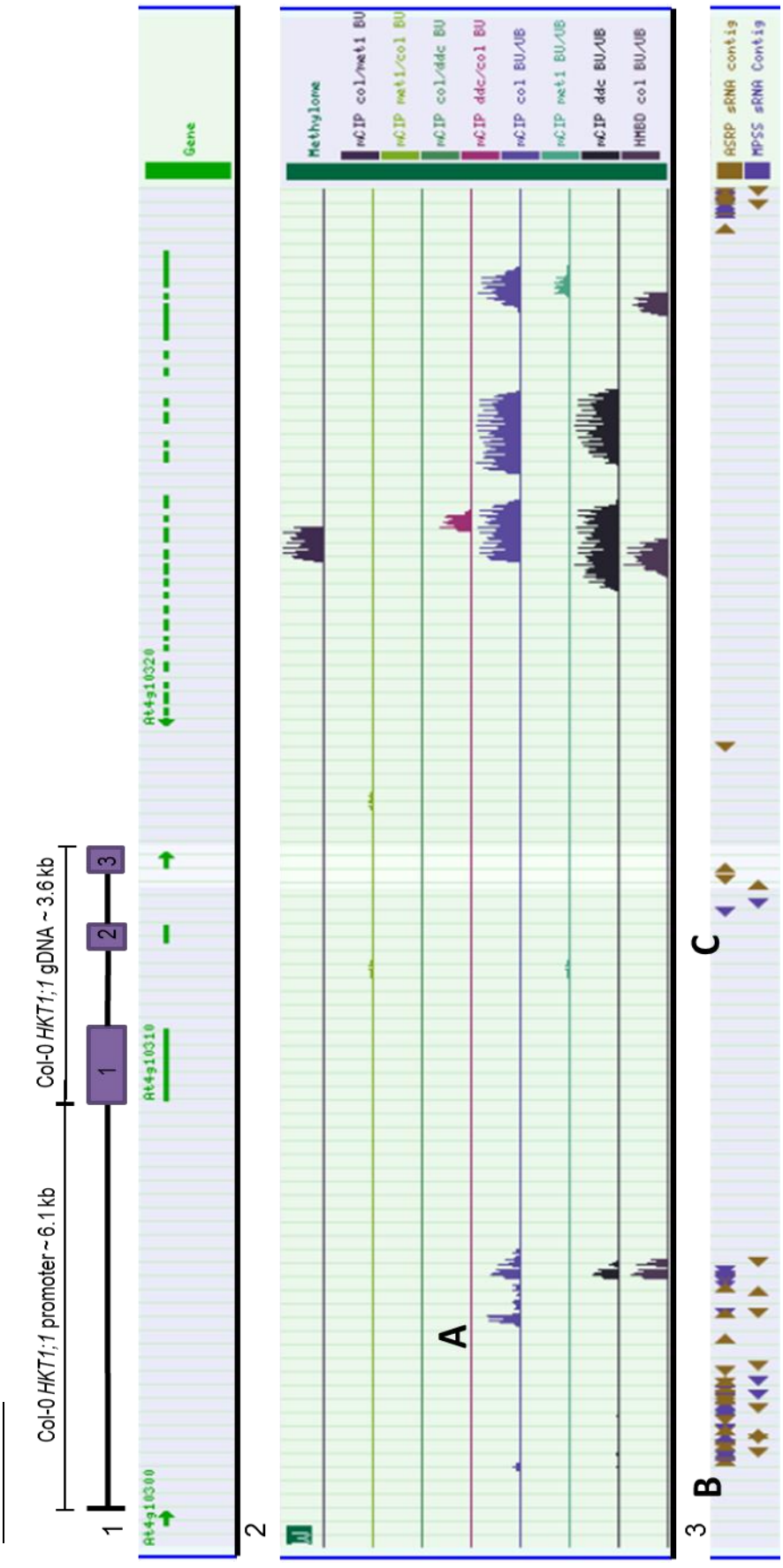

Figure 5.6: Methylation and small RNA signatures in Col-0 *ATHKT1;1*, identified using The SIGnAL Arabidopsis Methylome Mapping Tool.

Track (1) indicates the genomic region, with exons in green: At4g10310 (*ATHKT1;1*) is in the middle of the window, the upstream gene At4g10300 to the left and the downstream gene At4g10320 to the right. Tracks in (2) indicate the methylated DNA regions as determined by mCIP and MBD with two methylation deficient mutant backgrounds *met1* and *drm1 drm2 cmt3* (ddc) (Zhang *et al.* 2006a). In (3) indicating small RNA binding sites from ASRP (Gustafson *et al.* 2005) or MPSS databases (Lu *et al.* 2005, Nakano *et al.* 2006). The white shaded area is marked by the program and only indicates the middle of the analysis window. (A) highlightes methylated region upstream of HKT1;1, also highlighted are(B) small RNA binding sites found (B) upstream of *ATHKT1:1* and (C) small RNA binding sites in the second intron of *ATHKT1:1*.

A

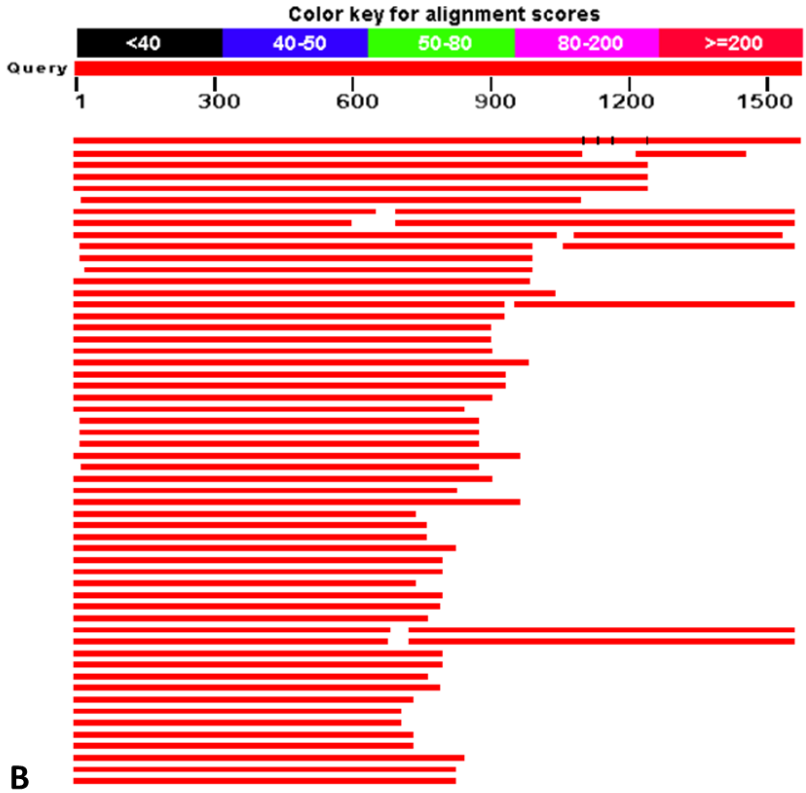

B

	Description	E value	Ident	Accession
☐	Arabidopsis thaliana chromosome 5, complete sequence	0.0	89%	CP002688.1
☐	Arabidopsis thaliana genomic DNA, chromosome 5, P1 clone:MAC9	0.0	89%	AB010069.1
☐	Arabidopsis thaliana chromosome 1, complete sequence	0.0	86%	CP002684.1
☐	Genomic sequence for Arabidopsis thaliana BAC F1L3 from chromosome I, complete sequence	0.0	86%	AC022492.5
☐	Arabidopsis thaliana chromosome I BAC F28G4 genomic sequence, complete sequence	0.0	86%	AC007843.6
☐	Arabidopsis thaliana genomic DNA, chromosome 5, BAC clone:F16F17	0.0	88%	AB028606.1
☐	Genomic Sequence For Arabidopsis thaliana Clone F15F15, Chromosome V, complete sequence	0.0	93%	AC007627.3
☐	Arabidopsis thaliana BAC F14I23 from chromosome V near 69 cM, complete sequence	0.0	93%	AC007399.1
☐	Arabidopsis thaliana chromosome I BAC F6A14 genomic sequence, complete sequence	0.0	88%	AC011809.2
☐	Arabidopsis thaliana chromosome 3, complete sequence	0.0	90%	CP002686.1
☐	Arabidopsis thaliana DNA chromosome 3, BAC clone F13I12	0.0	90%	AL133292.3
☐	Arabidopsis thaliana chromosome 1 BAC T2K10 sequence, complete sequence	0.0	89%	AC005966.2
☐	Arabidopsis thaliana chromosome I BAC F12K8 genomic sequence, complete sequence	0.0	89%	AC006551.6
☐	Arabidopsis thaliana genomic DNA, chromosome 3, P1 clone:MMG15	0.0	87%	AB028616.1
☐	Arabidopsis thaliana BAC F6I13	0.0	90%	AF262044.1
☐	Arabidopsis thaliana genomic DNA, chromosome 5, TAC clone:K21B8	0.0	90%	AB025611.1
☐	Arabidopsis thaliana chromosome 1 BAC F21N10 genomic sequence, complete sequence	0.0	90%	AC027033.3
☐	Arabidopsis thaliana genomic DNA, chromosome 3, TAC clone:K17E7	0.0	90%	AP000736.3
☐	Arabidopsis thaliana chromosome 1 BAC F2P9 genomic sequence, complete sequence	0.0	90%	AC016662.7
☐	Arabidopsis thaliana BAC F1I21 from chromosome 1, near 59 cM, complete sequence	0.0	88%	AC005687.1
☐	Arabidopsis thaliana BAC F21J6 from chromosome V, containing KNAT3 and mapping near 60.5 cM, complete sequence	0.0	88%	AC006259.1
☐	Arabidopsis thaliana BAC F18G18 from chromosome V near 60.5 cM, complete sequence	0.0	88%	AC006258.1

Figure 5.7: Results of a BLAST search (blastn) in the *Arabidopsis thaliana* nucleotide selection using the 1.6 kb intron sequence that is present in C24 *AtHKT1;1*, but not in Col-0.

(A) Graphical overview of results and (B) list of results with corresponding E-values, % identity and Accession. Further details are provided in the text (5.7.2.2).

The BLAST search identified a number of highly similar sequences to the second intron of *AtHKT1;1* in C24. The first result in the list suggests that a sequence is present on Arabidopsis (Col-0) chromosome 5 that is highly similar to the insertion in the second C24 intron (Figure 5.7). The sequence on chromosome 5 corresponding to the C24 insertion is in position 24818790 – 24819893 bp, upstream of the gene *At5g61770*. The sequence is annotated as *At5TE89325*, a SIMPLEHAT2 transposon (Figure 5.8). A number of other similar sequences in the list of BLAST returns (Figure 5.7) were investigated and were also found to be SIMPLEHAT2 transposons. From the annotation in TAIR, it can be seen that the SIMPLEHAT2 transposon contains a large number of binding sites for small RNAs (Figure 5.8). Only one of the references for small RNA binding sites as described by Gustafson *et al.* (2005), was included in Figure 5.8 due to space limitations; however, the other two sources, Lister *et al*. (2008) and Gregory *et al*. (2008), showed a similar distribution of small RNA binding sites. All RNA binding sites in the SIMPLEHAT2 transposon were annotated to be bound by the same RNA class - small RNA 131. Methylation of this region was analysed using SIGnAL, however, only weak methylation was detected in the region of *At5TE89325.* The results from SIGnAL complemented the results from TAIR by indicating that a large number of small RNA binding sites have been identified (Figure 5.9).

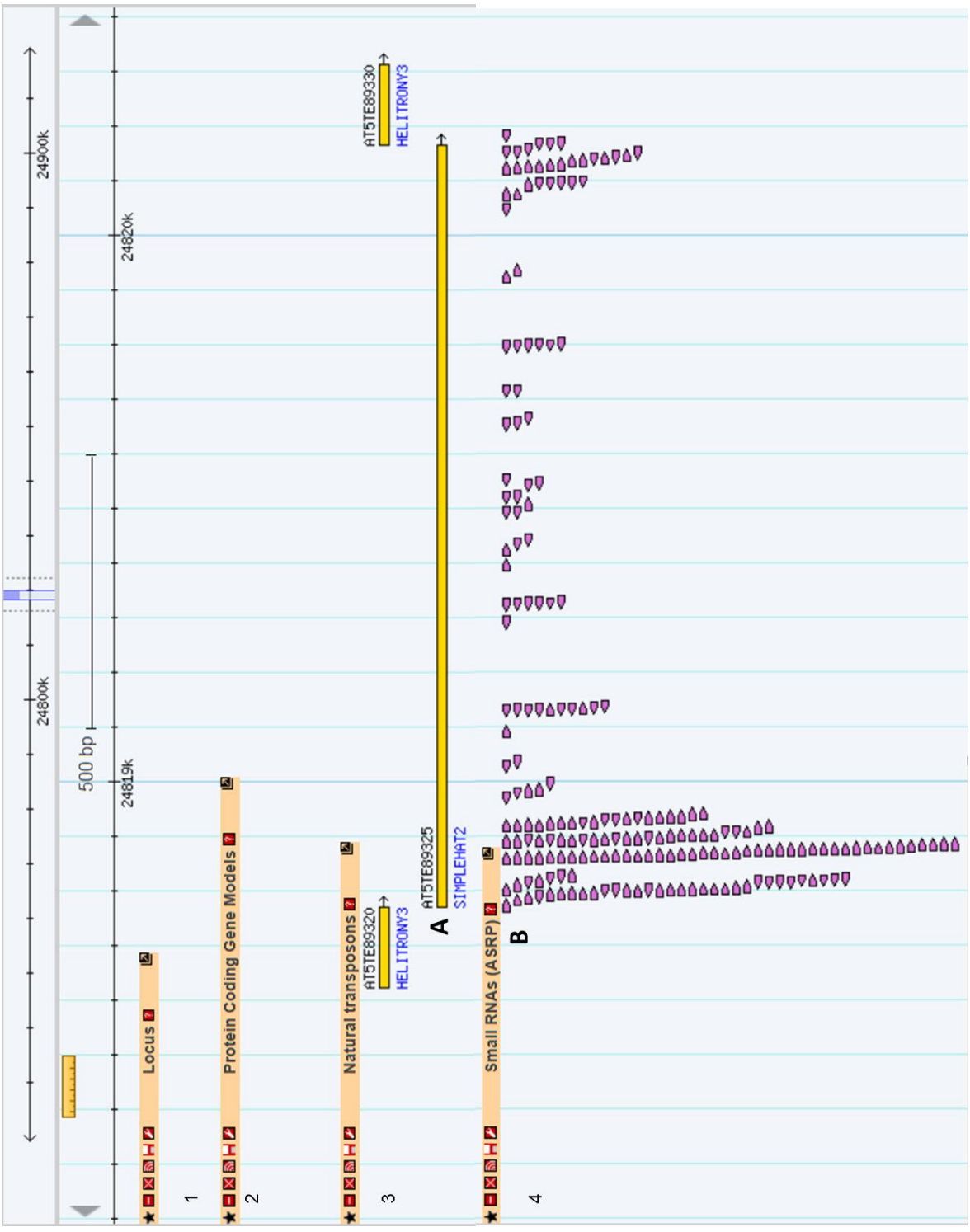

Figure 5.8: SIMPLEHAT2 region, *At5TE89325*, on Chromosome 5, displayed in gbrowser with additional information.

Tracks included are (1) *At5TE89325* genomic region, (2) the protein coding model, (3) natural transposons annotated from TAIR and a variety of external sources including TIGR and the Quesneville group (Buisine *et al.* 2008), (4) small RNA binding sites identified by the ASRP. Highlighted regions are the (A) SIMPLEHAT transposon and (B) small RNA binding sites.

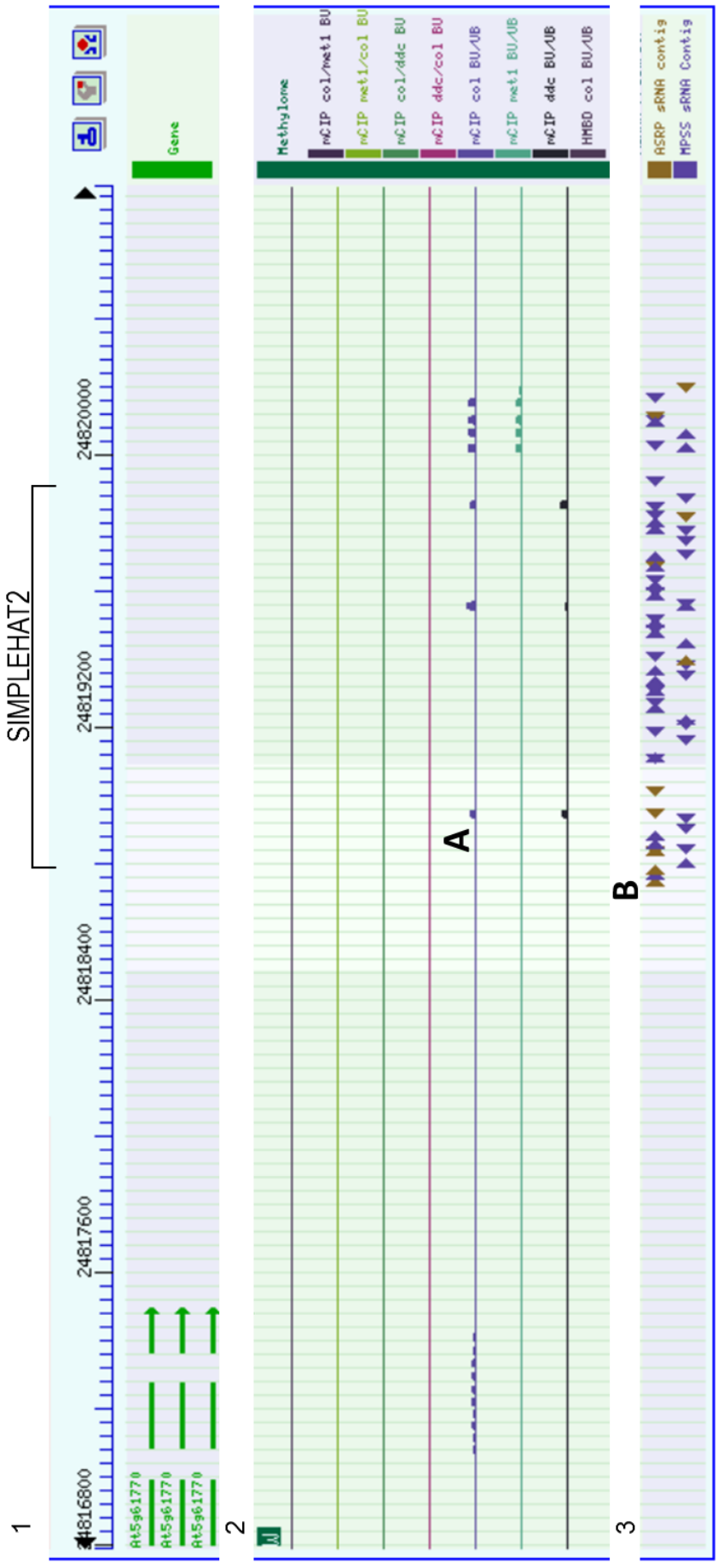

Figure 5.9: Methylation and small RNA signatures in the genomic region of *At5TE89325*, SIMPLAHAT2 (approximate position marked in figure), containing SIMPLEHAT2, identified using The SIGnAL Arabidopsis Methylome Mapping Tool.

Track (1) indicates the genomic region, with exons in green. Tracks in (2) indicate the methylated DNA regions as determined by mCIP and MBD with two methylation deficient mutant backgrounds *met1* and *drm1 drm2 cmt3* (ddc) (Zhang *et al.* 2006a). In (3) indicating small RNA signatures from ASRP (Gustafson *et al.* 2005) or MPSS databases (Lu *et al.* 2005, Nakano *et al.* 2006). Highlighted are (A) small methylation signatures and (B) small RNA binding sites in the SIMPLEHAT2 transposon region.

To further determine whether the insertion in the second intron can be attributed to the transposon SIMPLEHAT2, the Repbase Update program was utilised with the full length Col-0 and C24 *AtHKT1;1* sequences as query sequences (Figure 5.10 to Figure 5.12). The Col-0 sequence returned eight predicted repetitive regions across the length of the gene, with most of them having a size of less than 100 bp (Figure 5.10). The largest transposable element, with the highest score, is ATHPOGON1 in the second intron, which was also annotated in the TAIR database, displayed in Figure 5.5. Again, the transposable element SIMPLEHAT2 was identified as being in the region of the insertion in the second intron in the C24 *AtHKT1;1* (Figure 5.11 and Figure 5.12). Interestingly, there were not many similarities between repeat elements within the C24 and Col-0 *AtHKT1;1* genes (Figure 5.11). Besides the repeats Copia-66_Aly-I and ATHPOGON1, there is no conformity between Col-0 and C24.

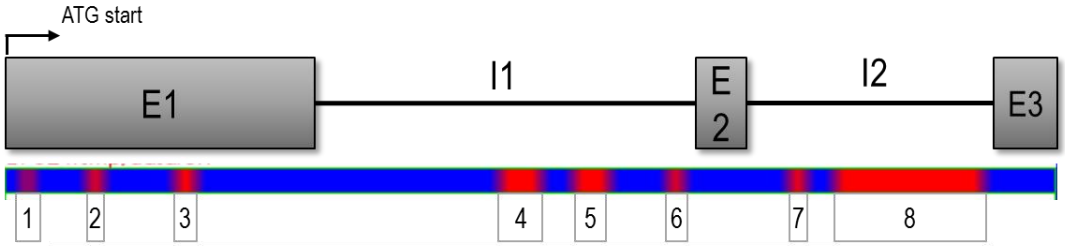

	From	To	Name	From	To	Class	Dir	Sim	Score
1	64	101	TREP60	57	94	Simple/Sat/MSAT	c	0.8421	220
2	285	338	Mariner-1_GM	2751	2804	DNA/Mariner	d	0.7407	250
3	582	654	DIRS-1_NGr	322	393	LTR/DIRS	c	0.7260	217
4	1683	1827	EHINV1	350	488	Interspersed_Repeat	c	0.7630	207
5	1932	2062	Gypsy7-VV_I	9485	9625	LTR/Gypsy	c	0.6985	304
6	2257	2310	Copia-66_ALY-I	1474	1527	LTR/Copia	d	0.8077	260
7	2669	2725	Tx1-7_Crp	3916	3973	NonLTR/Tx1	c	0.7586	245
8	2820	3329	ATHPOGON1	1	528	DNA/Mariner	d	0.8872	3155

Figure 5.10: Repbase Update output for the full length 3.6 kb Col-0 *AtHKT1;1* sequence.

The gene *AtHKT1;1* model was added to the figure to locate repeat element in relation to the exon-intron-structure of *AtHKT1;1*. The heat map indicates in blue the sequences without repeat elements and in red repeat elements that are listed with the corresponding number in the table below. The first two columns (From/To) indicate the position of the repeat element in the *AtHKT1;1* sequence in bp from the ATG start codon, followed by (Name) the name of the repeat element and (From/To) which part of the sequence of the repeat element matches the *AtHKT1;1* sequence. (Class) refers to the transposon class as specified in the repeat annotation and (Dir) indicates the direction, 'd' for direct and 'c' for complementary. (Sim) contains a value for similarity (with value 1 meaning identical) and (Score) is the alignment score obtained from BLAST.

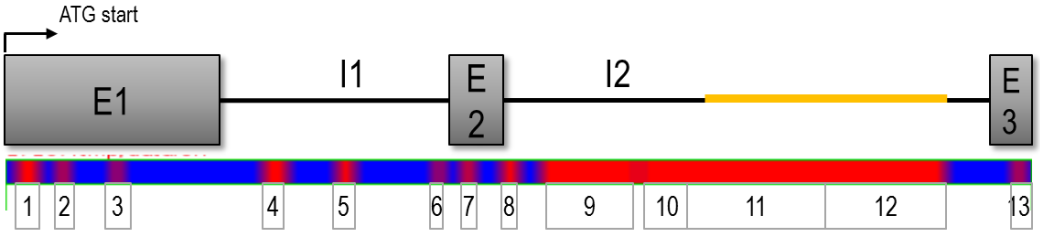

	From	To	Name	From	To	Class	Dir	Sim	Score
1	60	186	BovB_La	1290	1408	NonLTR/RTE	c	0.6803	253
2	276	336	MuDR-3_STu	7325	7385	DNA/MuDR	d	0.6885	201
3	562	616	Crack-5_AAe	1472	1529	NonLTR/Crack	c	0.7321	236
4	1362	1494	Transib-12_HM	292	440	DNA/Transib	c	0.7333	204
5	1743	1848	hAT-14_SM	2506	2588	DNA/hAT	c	0.7865	209
6	2257	2310	Copia-66_ALY-I	1474	1527	LTR/Copia	d	0.8077	260
7	2402	2477	Copia-9_GM-I	820	888	LTR/Copia	d	0.7324	203
8	2614	2712	MtPH-E-Ia	88	180	DNA/Harbinger	c	0.7447	234
9	2819	3330	ATHPOGON1	1	528	DNA/Mariner	d	0.8932	3222
10	3340	3371	ENSPM2_VV	257	288	DNA/EnSpm/CACTA	c	0.9375	211
11	3372	4301	SIMPLEHAT2	1	933	DNA/hAT	d	0.9378	7457
12	4304	4956	SIMPLEHAT2	543	1208	DNA/hAT	d	0.9330	5120
13	5312	5374	CR1-66_HM	1858	1920	NonLTR/Crack	c	0.7903	225

Figure 5.11: Repbase Update output for the full length 5.4 kb C24 *AtHKT1;1* sequence.

Details as in Figure 5.10. Additionally, in the *AtHKT1;1* gene graphic, the 1.6 kb insertion present in the second intron is marked in orange colour.

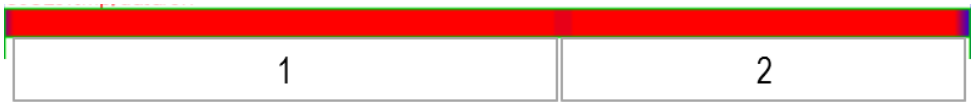

	From	To	Name	From	To	Class	Dir	Sim	Score
1	1	910	SIMPLEHAT2	21	933	DNA/hAT	d	0.9376	7292
2	913	1565	SIMPLEHAT2	543	1208	DNA/hAT	d	0.9330	5120

Figure 5.12: Repbase Update output for the sequence corresponding to the 1.6 kb insertion in the second intron of the C24 sequence.

Table references as in Figure 5.10.

The annotation of SIMPLEHAT2 provided by the Repbase Update database is shown in Figure 5.13. It is a class II, non-autonomous DNA transposon of the hAT superfamily. SIMPLEHAT2 siRNA was linked to AGO4 and AGO6, two components in the RISC, which again is involved in methylation of target genes and slicing of transcripts (Qi *et al.* 2006, Zheng *et al.* 2007). The discussion section contains further information on possible mechanisms of how SIMPLEHAT2 may be involved in regulating *AtHKT1;1* gene expression.

Annotation of Repbase Sequences

```
ID   SIMPLEHAT2  repbase;    DNA;    PLN; 1208 BP.
XX
AC   .
XX
DT   07-MAY-2001 (Rel. 6.04, Created)
DT   21-DEC-2005 (Rel. 11.01, Last updated, Version 2)
XX
DE   SIMPLEHAT2 is a non-autonomous DNA transposon - a consensus.
XX
KW   hAT; DNA transposon; Transposable Element;
KW   8-bp target site duplication; hAT superfamily; SIMPLEHAT2; TIR;
KW   minisatellite; nonautonomous DNA transposon.
XX
NM   SIMPLEHAT2.
XX
OS   Arabidopsis thaliana
OC   Eukaryota; Viridiplantae; Streptophyta; Embryophyta; Tracheophyta;
OC   Spermatophyta; Magnoliophyta; eudicotyledons; core eudicotyledons;
OC   rosids; malvids; Brassicales; Brassicaceae; Camelineae;
OC   Arabidopsis.
XX
RN   [1]
RP   1-1208
RA   Kapitonov V.V. and V.V. .;
RT   "A non-autonomous hAT-type element.";
RL   Direct Submission to Repbase Update (MAY-2001).
XX
DR   [1] (Consensus)
XX
CC   SIMPLEHAT2 is a non-autonomous DNA transposon.
CC   Its individual copies are ~94% identical to the consensus and
CC   there are about 50 copies of SIMPLEHAT2 scattered in the
CC   A.thaliana
CC   genome. They are bordered by 8 bp-long target site duplications
CC   and
CC   have 19-bp terminal inverted repeats.
CC   Internal portion of SIMPLEHAT2 is composed of a 28-bp
CC   minisatellite repeat (21 copies of the minisatellite repeat are
CC   present
CC   in the consensus sequence). Related 27- and 28-bp minisatellites
CC   have been propagated also by the SIMPLEHAT1, SIMPLEGUY1 and
CC   ATREPX1
CC   transposons.  Updated by J. Jurka, Dec. 2005.
XX
```

Figure 5.13: Annotation of SIMPLEHAT2 provided by the Repbase Update database.

5.7.2.3 Other Arabidopsis ecotypes do not contain insertions in the second intron

To analyse the *AtHKT1;1* gene composition of other ecotypes, sequence information of 19 ecotypes were obtained from Gan *et al.* (2011) and made searchable using BLAST by Mr. John Toubia, B.Sc. Bioinformatics (University of Adelaide, Australia). The *AtHKT1;1* genes were then identified by performing a BLAST search using the Col-0 *AtHKT1;1* sequence as a query. The sequences were extracted from the dataset and aligned (Figure 5.14). The alignment shows in black the highly conserved sequences, with the lighter grey regions indicating areas of polymorphisms. Alignment analysis indicates that only C24 contains a 1.6 kb insertion in the second intron (Figure 5.14 bottom panel). The high shoot Na^+ accumulating, low *AtHKT1;1* expressing ecotype Tsu-1 is highlighted in the alignment (purple arrow), but it does not contain the 1.6 kb transposon in the second intron. Interestingly however, it appears that a number of ecotypes do not contain a sequence of approximately 500 bp in the first intron, marked with an orange box in Figure 5.14. C24, Bur-0, Can-0, Ct-1, Rsch-4, Tsu-0, and Zu-0 all contain the 500 bp region (indicated by light grey bars in the alignment), while the ecotypes Edi-0, Hi-0, Kn-0, Ler-0, Mt-0, No-0, Oy-0, Po-0, Sf-2 Wil-2, Ws-0, Wu-0 do not contain this sequence (indicated by a single line in the alignment) (Figure 5.14). The ecotype Col-0 also contains the 500 bp sequence, but is not included in the alignment. An alignment of the C24 and Col-0 sequence can be found in the supplementary material (Supplementary Figure 8.8). Information regarding Na^+ accumulation and natural habitats is available from Baxter *et al*. (2010) and was compared for the available ecotypes sequenced (Table 5.6). With the exception of Ws-0, all ecotypes that do contain the 500 bp fragment in the first intron contain a high leaf Na^+ content of more than 700 mg/kg, while ecotypes that no not have the 500 bp fragment in the first intron have a lower leaf Na^+ content of under 700 mg/kg. However, no clear correlation between the presence or absence of the 500 bp sequence in the first intron with habitat proximity to saline areas could be identified.

Table 5.6: Comparison of the presence of a 500 bp fragment in the first intron (sequencing data by Gan *et al.* (2011)) to corresponding leaf Na^+ data and distance to saline areas from Baxter *et al.* (2010)

Ecotype	Presence of 500 bp sequence in first intron	Leaf Na^+ (mg/kg)	Distance to saline area (km)
Mt-0	N	406	39.1
Edi-0	N	542	4.3
Oy-0	N	563	2.7
Hi-0	N	610	n.d.
Wil-1	N	659	n.d.
Can-0	Y	703	4.1
Rsch-4	Y	751	433.4
Col-0	Y	914	n.d.
Ct-1	Y	951	10.9
Ws-0	N	1418	n.d.
Ts-1	Y[1]	2504	13.5
Bur-0	Y	2958	14.8
Tsu-1	Y	High[1]	Close[1]
C24	Y	High[1]	n.d.

[1] data from Rus et al. (2006)

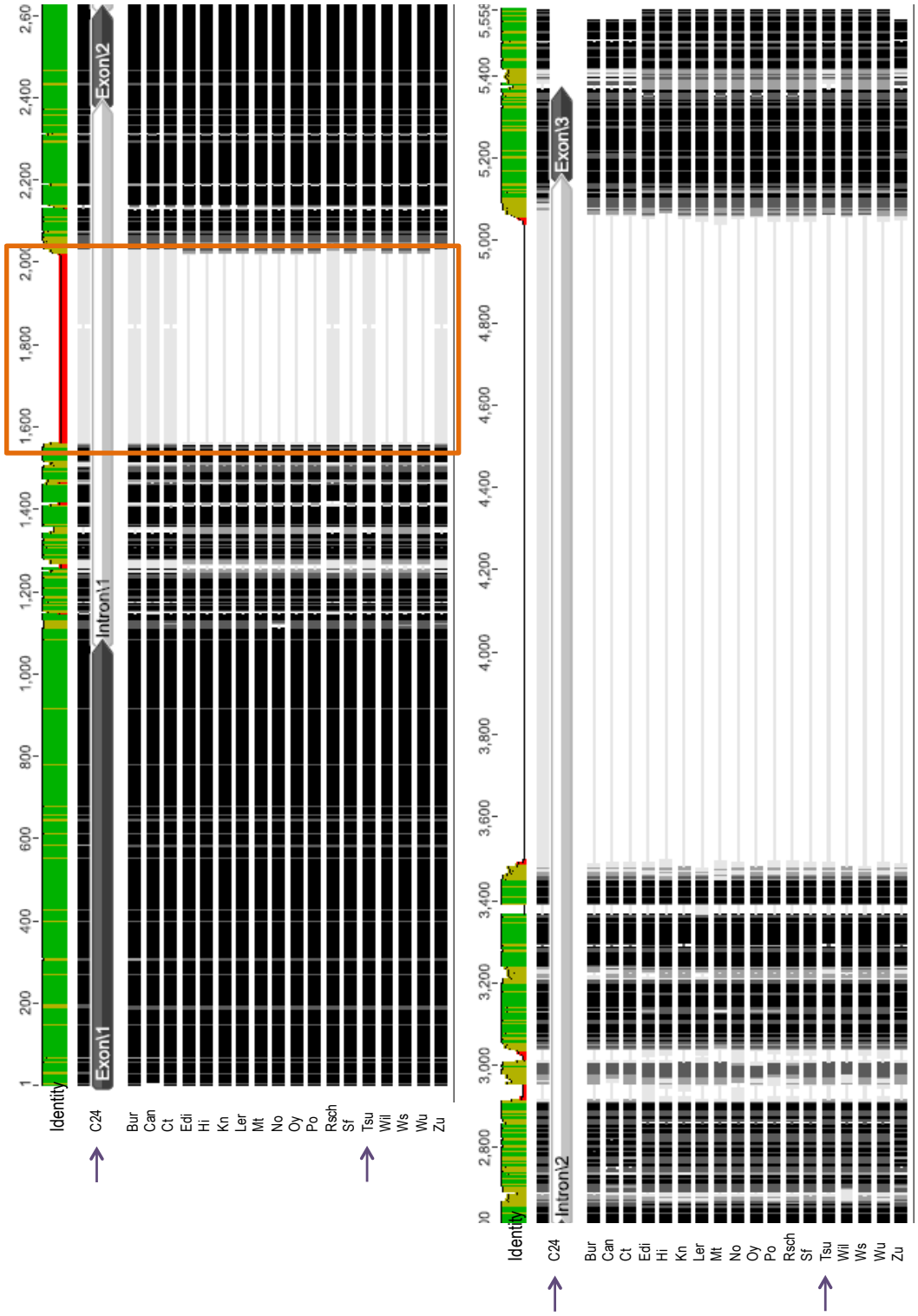

Figure 5.14: Alignment of genomic *AtHKT1;1* sequences from 19 Arabidopsis ecotypes to the C24 *AtHKT1;1* sequence.

The sequence alignment was divided into two parts for appropriate illustration, the top panel contains the first part of the alignment up to the end of exon 2, the bottom panel contains the remaining alignment from intron 2 to the end. Two ecotypes of particular interest, C24 and Tsu-1, are marked with a purple arrow and the polymorphisms in the first intron are marked with an orange box. The identity score is presented above the alignment (high identity in green colour and lower identity in red). C24 sequence was obtained from Sundstrum (2011), all other sequences from Gan *et al*. (2011)

5.7.3 Analysis of *AtHKT1;1* transcripts by semi-qPCR

To determine if there are differences in alternative splicing between Col-0 and C24, gene specific RT-PCR was performed using primers for different regions of the *AtHKT1;1* coding sequence. cDNA synthesis had previously been performed using an Oligo $d(T)_{20}$ primer to obtain cDNA from all mRNA containing poly(A)-tails. However, if the poly(A)-tail is not present in C24 *AtHKT1;1* transcripts in the root, for instance due to differences in splicing or RNA folding, these transcript would not be detected by regular RT-PCR. This may explain the observed qRT-PCR results in other studies where little *AtHKT1;1* expression was detected in the roots of C24 (Jha *et al.* 2010, Sundstrom 2011). RNA was derived from roots of 6 wk old hydroponically grown Col-0 and C24 plants subjected to 7 d of ± 100mM NaCl treatment (labelled control and salt). The location of the gene specific primers used for cDNA synthesis and subsequent RT-PCR analysis are indicated in Figure 5.15.

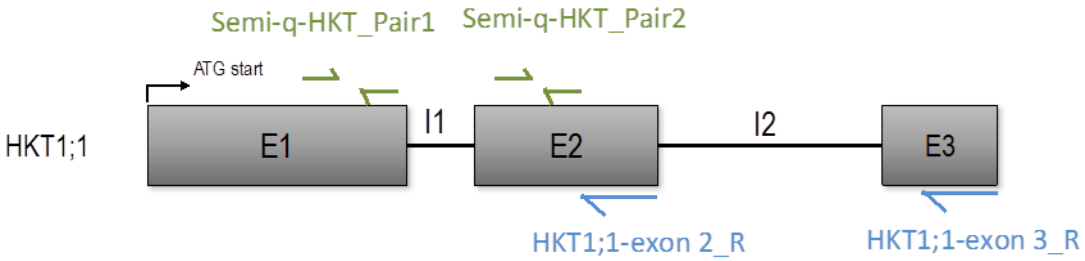

Figure 5.15: Diagram of gene specific RT-PCR on *AtHKT1;1* transcripts.

AtHKT1;1 specific cDNA was produced using primers AtHKT1;1-exon 2_R and AtHKT1;1-exon3_R (indicated in blue), while the subsequent PCR reaction was performed using Semi-q-HKT_Pair1, resulting in a 200 bp fragment, and Semi-q-HKT_Pair2, resulting in a 150 bp fragment of DNA (primer pairs indicated in green).

AtHKT1;1 transcripts were detected in samples of cDNA derived from roots of Col-0 plants (control and salt treated), while no transcripts were detected for cDNA derived from C24 roots (Figure 5.16). Specifically, bands are visible in two out of three replicates of control and salt treated Col-0 samples, where a fragment of exon 1 was amplified in cDNAs (Figure 5.16 A). Weaker bands were visible in samples corresponding to Col-0 salt treated plants with cDNA generated using AtHKT1;1-exon3_R (Figure 5.16 A). No bands were displayed in samples derived from C24 (Figure 5.16). The primer pair used to amplify a fragment in exon 2 (150 bp) also displays primer dimers, which may be visible as shadows in the lower part of the images. However, PCR products were clearly distinguishable on the agarose gel. Bands for amplicons of exon 2 are visible in images corresponding to Col-0 control and salt treated cDNA samples generated using AtHKT1;1-exon3_R, while only one band is visible

in Col-0 cDNA generated using AtHKT1;1-exon2_R (2nd biological replicate under salt stress; Figure 5.16B). No bands are visible in any C24 samples (Figure 5.16 B).

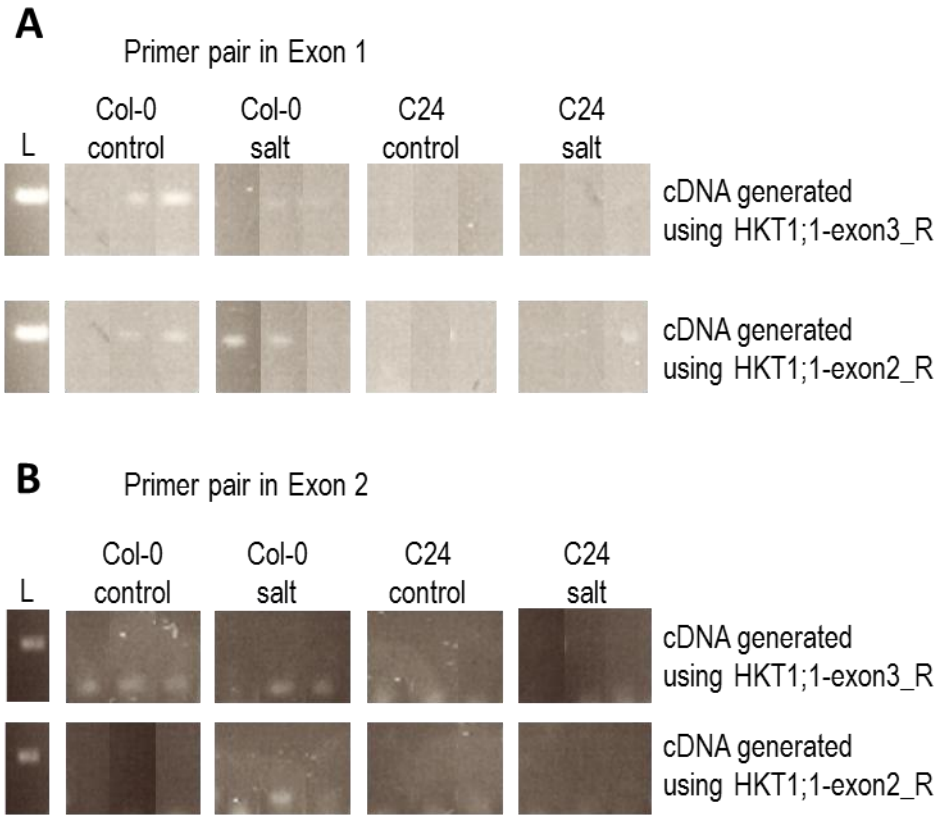

Figure 5.16: Agarose gel images of RT-PCR on *AtHKT1;1* specific cDNA.

(A) Primer set Semi-q-HKT_Pair1 was used to amplify a 200 bp fragment in the first exon of *AtHKT1;1* cDNA. (B) Primer set Semi-q-HKT_Pair2 was used to amplify a 150 bp fragment in the second exon of *AtHKT1;1* cDNA. cDNA was generated using a primer that annealed in the third exon (HKT1;1-exon3_R) or one that anneals in the second exon (HKT1;1-exon2_R). (L) Ladder represents fragment with a size of 200 bp. Agarose gel images of three biological replicates were rearranged to facilitate suitable labelling.

5.7.4 Generation of expression vectors for *in planta* analyses

To test if the *AtHKT1;1* genomic sequence, in particular the second intron of C24, influences *AtHKT1;1* expression levels *in planta*, a number of constructs were designed. Although various polymerases and amplification variables were tested, amplification of the full length Col-0 or C24 *AtHKT1;1* gDNA without sequence errors was not successful. Therefore, a different approach was taken, in which the Col-0 and C24 gDNA was amplified in two and three fragments, respectively, and the fragments ligated to form the full length gDNA. Primers were designed that enable the amplification of the fragments and subsequent ligation (Table 5.7). The primer sequence contained

restriction sites that occur naturally and only once in *AtHKT1;1* to enable digest and ligation. Amplification of the fragments was proving to be difficult and a variety of annealing temperatures, combination of polymerases and buffers were tested for optimal, error-free amplification. The final conditions that were used to amplify the fragments are listed in Table 5.8.

Table 5.7: Primers used to amplify the *AtHKT1;1* genomic sequence from Col-0 and C24. Underlined nucleotides indicate restriction sites used to ligate fragments using *XhoI*. NNNN are random nucleotides that were included to facilitate restriction digest.

Fragment name	Primer name	Sequence (5'-3')	~Product size (bp)
Col-0 HKT 1st half	AtHKT1-gene_F[1]	ACCGACTCGAGAACTAAAATGGACA	2100
	AtHKT1_Col_1st _R	NNNNTTAATTAATGGTTAATATAGATATAT	
Col-0 HKT 2nd half	AtHKT1_Col_2nd_F	NNNNTTAATTAAGGAACCTACAAGAGAATG	1500
	AtHKT-gene_R[1]	NNNCTGCAGTTAGGAAGAGGGGTAAAG	
C24 HKT 1st third	AtHKT1-gene_F[1]	ACCGACTCGAGAACTAAAATGGACA	1600
	AtHKT1_C24_1st_R	NNNNGCTAAGCTGATTAATTGGTG	
C24 HKT 2nd third	AtHKT1_C24_2nd_F	NNNNGCTTAGCAATTGAAAGC	1700
	AtHKT_C24_2nd_R	NNNGGGACTAGTGTAAAAAATGAC	
C24 HKT 3rd third	AtHKT1_C24_3rd_F	NNNNACTAGTCCCAACTCGG	2150
	AtHKT-gene_R[1]	NNNCTGCAGTTAGGAAGAGGGGTAAAG	
Col-0 intron	AtHKT_Intron_F	NNNNCTCGAGACCGAAAGGCAAAATCTAC	1200
	AtHKT_Intron_R	ACCATCGATGATATCCA	
C24 intron	AtHKT_Intron_F	NNNNCTCGAGACCGAAAGGCAAAATCTAC	2700
	AtHKT_Intron_R	ACCATCGATGATATCCA	

[1]obtained from Sundstrom (2011)

Table 5.8: PCR setup and cycling conditions to amplify *AtHKT1;1* genomic DNA and intron fragments. Part (A) shows the general PCR mix and cycling conditions. Components varying between amplifications are marked in bold and indicated with "X"; refer to (B) for the specific conditions used for amplifying each DNA fragment.

A

Component	µL
Failsafe buffer X	25
Primer F	0.75
Primer R	0.75
Polymerase X	**X**
Template DNA X	**X**
MW-water	to 50

Cycling conditions		
1	94 °C	2 min
2	94 °C	30 sec
3	**Annealing temperature X**	30 sec
4	68 °C	**Extension time X**
6	68 °C	10 min
5	Repeat step 2	29 times
7	15 °C	∞

B

PCR fragment	Failsafe buffer	Polymerase	Template DNA	Annealing temperature (°C)	Extension time (min)
Col-0 HKT 1st half	E	Elongase/Phusion (0.5/0.5 µL)	Col-0 gDNA (1 µL)	50	2:20
Col-0 HKT 2nd half	B	Elongase (1 µL)	Col-0 gDNA (1 µL)	53	2
C24 HKT 1st third	F	Elongase (1 µL)	C24 BAC DNA (0.5 µL)	53	3
C24 HKT 2nd third	G	Elongase (1 µL)	C24 BAC DNA (0.5 µL)	53	3
C24 HKT 3rd third	F	Elongase (1 µL)	C24 BAC DNA (0.5 µL)	55	3
Col-0 Intron	E	Elongase (1 µL)	Col-0 gDNA (1 µL)	50	3
C24 Intron	G	Elongase/*Pfx* (1/0.1 µL)	C24 BAC DNA (0.5 µL)	50	3

The DNA fragments obtained by PCR (Figure 5.17 and Figure 5.18) were purified, an A-overhang was added to the fragments and they were ligated into pCR8 for amplification in *E.coli*. Correctness of constructs was ensured by sequencing. The fragments "C24 HKT 3rd third" (Figure 5.17) and "C24

intron" (Figure 5.18) were particularly difficult to amplify, as they contain a large number of repetitive sequences, compromising the polymerase's fidelity. These repetitive regions also complicated the analysis of sequencing reactions, as the sequencing outputs were usually short. To obtain the full Col-0 and C24 gDNA, the desired DNA fragments (Figure 5.17 A and B, respectively) were subjected to restriction digest with the indicated enzymes and were ligated.

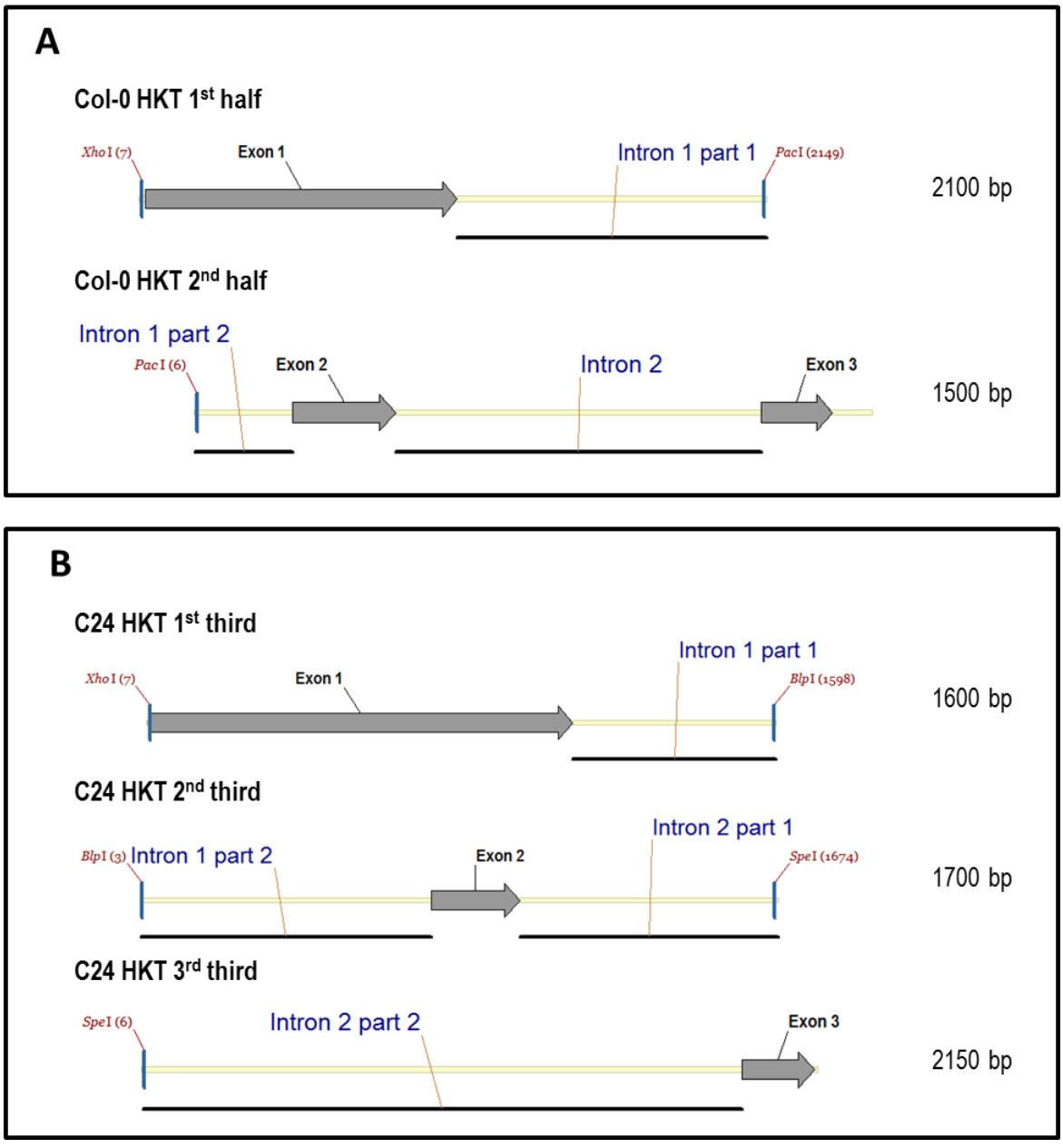

Figure 5.17: Amplified DNA fragments of the (A) Col-0 gDNA and (B) C24 gDNA.

Illustrated are the DNA fragments used for ligation to obtain the full length *AtHKT1;1* gDNA. Restriction sites used for the ligation process are indicated. Images are not to scale, fragment sizes are indicated on the right hand side.

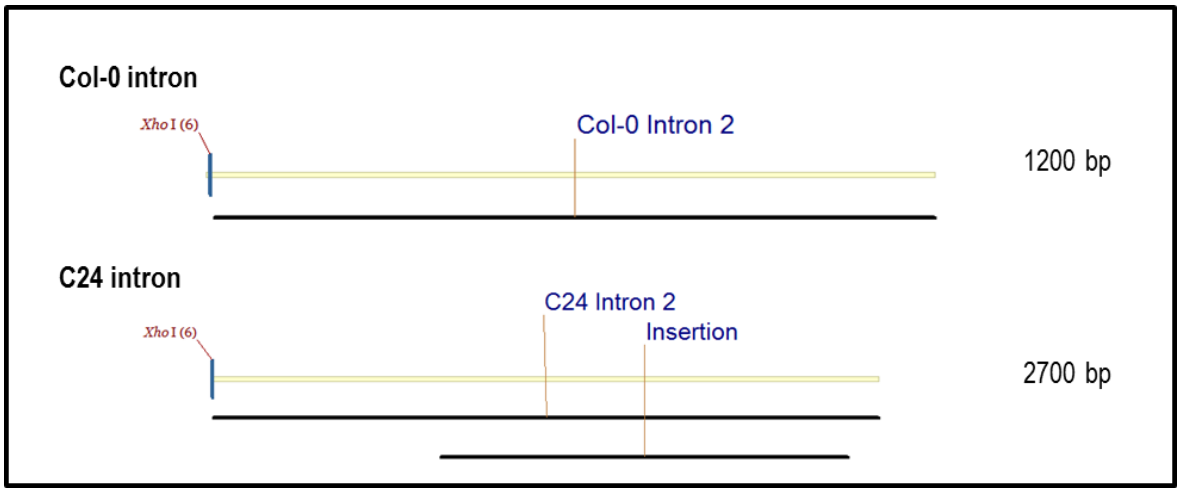

Figure 5.18: Amplified DNA fragments containing the second intron of Col-0 and C24.

Images are not to scale, fragment sizes are indicated on the right hand side and the location of the insertion in the C24 intron is marked. *Xho*I restriction sites required for ligation to the promoter fragments are indicated.

The two plasmids containing DNA fragments forming Col-0 *AtHKT1;1* gDNA (Figure 5.17 A) were successfully ligated and were verified to contain the correct sequence. This plasmid was further processed for recombination with the destination vector as will be outlined below. However, ligation of the three DNA fragments comprising of the C24 *AtHKT1;1* gDNA (Figure 5.17 B) into the pCR8 entry vector was not successful. The expected sizes after *BsrGI* restriction digest of the pCR8 vector containing the C24 gDNA sequence are 1.6 kb, 2.7 kb and 3.7 kb. However, one of the DNA bands was consistently sized below 1.5 kb, at approximately 1.3 kb. Figure 5.19 shows a representative example of a restriction digest obtained for C24 gDNA, the shorter than expected size for the third fragment - 200 bp of the sequence is absent. Sequencing of a number of clones from different ligation reactions elucidated that part of the repetitive region in the second intron (towards the 3′ end of the intron) was absent from all. The initial three C24 DNA fragments were retested using both restriction digests and sequencing which confirmed that they originally contained the expected nucleotide sequence prior to ligation. A number of different DNA ligation conditions were trialled to ensure it was not the interaction between fragments that prohibited correct ligation. Variations on the ligation protocol included: shortening the ligation time from 1 h to 15 min, extending of the ligation time to 2 d, incubating the ligation at different temperatures (21 °C, 25 °C and 4 °C), different ratios of the three DNA fragments and different DNA ligases. Unfortunately, for reasons unknown, it was not possible to obtain the correct clone containing full length C24 gDNA.

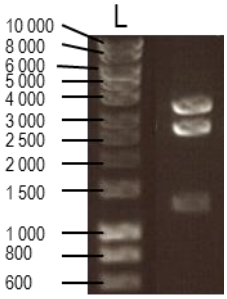

Figure 5.19: Representative agarose gel image of a *Bsr*GI restriction digest of the pCR8 plasmid containing C24 *AtHKT1;1* gDNA.

The image of the digest did not show the expected restriction fragments with sizes of 1.6 kb, 2.7 kb and 3.7 kb. (L) Molecular weight ladder in bp as reference.

Subsequently, GeneScript (Piscataway, NJ, USA) was used to artificially synthesis the full length of the *AtHKT1;1-C24* gene, including the long second intron. GenScript, likewise, reported difficulties in synthesising the sequence, and had to change the restriction sites anticipated for cloning. Eventually, after several attempts GeneScript were able to provide a full length version of the C24 *AtHKT1;1* gene. However, even after multiple attempts it was not possible to transfer the synthesised gene sequence into the pCR8 vector by restriction digest and ligation within the time frame of the PhD candidature.

While the C24 *AtHKT1;1* gDNA fragments were not successfully ligated, the Col-0 *AtHKT1;1* gDNA had been successfully ligated and the correct sequence was obtained. This Col-0 gDNA sequence was now cloned behind the *AtHKT1;1* promoter as presented in the cloning strategy in Figure 5.3. While it was not possible to clone the full gDNA sequence of C24 *AtHKT1;1* it was possible to clone the complete sequence of the second intron from both Col-0 and C24 behind the *AtHKT1;1* promoter using the same strategy presented in Figure 5.3. The *AtHKT1;1* promoter was fused to both the gDNA and second intron sequences by digesting the pCR8 vectors containing the desired sequences with the restriction enzyme *Xho*I. The fragments were then purified and ligated. After verification of correct fragments and orientation, the *promoter::gene* combinations were recombined into the destination vectors required for *in planta* analysis. The vectors containing the *AtHKT1;1* gDNA were recombined into pMDC100nosT vectors that enable expression of the *AtHKT1;1* gDNA *in planta* and the constructs containing the second intron were recombined to pMDC107 and pMDC162 for visualisation of GFP fluorescence and GUS activity. Table 5.9 lists the completed destination vectors and sizes of fragments expected by restriction digest shown in Figure 5.20.

Table 5.9: List of constructs in final destination vector with corresponding enzyme for control digests and fragment pattern.

#	Final destination vector description	Restriction enzyme and resulting sizes of fragments for control digest (in kb)
S1	pCol-0::Col-0-gDNA in pMDC100nosT	*Xho*I 6.8+4.8+2.8+0.9
S3	pC24::Col-0-gDNA in pMDC100nosT	*Xho*I 6.8+5.0+2.8+0.9
S5	pCol-0::Col-0intron in pMDC107 (GFP)	*Xho*I 9.6+2.1+1.1+1.0
S6	pCol-0::C24intron in pMDC107 (GFP)	*Xho*I 9.6+2.6+2.1+1.1
S7	pC24::Col-0intron in pMDC107 (GFP)	*Xho*I 9.6+2.1+1.1+1.0
S9	pCol-0::Col-0intron in pMDC162 (GUS)	*EcoR*I 9.0+3.8+2.2
S10	pCol-0::C24intron in pMDC162 (GUS)	*EcoR*I 9.0+5.4+2.2

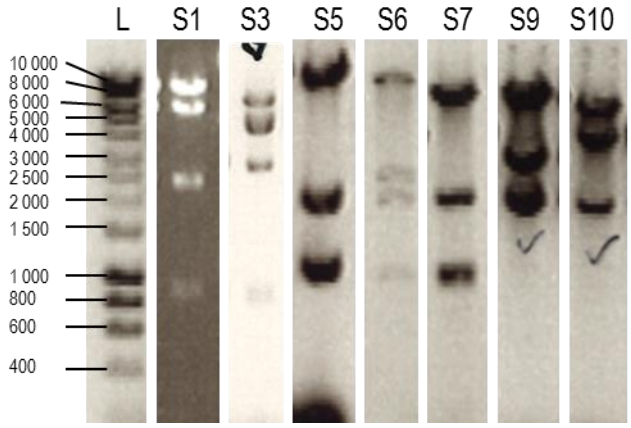

Figure 5.20: Images of agarose gels after restriction digests of fully cloned destination vectors listed in Table 5.9.

The labelling corresponds to the numbering in Table 5.9. Images were taken from different gels and sizes of images were adjusted to fit the (L) molecular weight ladder showing fragment sizes in bp as reference.

The completed destination vectors were transformed into *A. tumefaciens* for Arabidopsis transformation (section 2.3). Again, difficulties were experienced in recombining the vector containing the C24 intron fragment into destination vectors. An overview in Table 5.10 illustrates which constructs were successfully completed, recombined into destination vectors, transformed into *A. tumefaciens* and subsequently transformed into Arabidopsis (section 2.3).

Table 5.10: Overview of vectors constructed, the generation of the required destination vector, and the success of transforming the destination vector into *A. tumefaciens* and Arabidopsis.

#	Vector construct		Destination vector		In *A.tumefaciens*	In Arabidopsis
S1	pCol-0::Col-0-gDNA	✓	pMDC100nosT	✓	✓	✓
S2	pCol-0::C24-gDNA	X	pMDC100nosT	X	X	X
S3	pC24::Col-0-gDNA	✓	pMDC100nosT	✓	✓	✓
S4	pC24::C24-gDNA	X	pMDC100nosT	X	X	X
S5	pCol-0::Col-0intron	✓	pMDC107 (GFP)	✓	✓	✓
S6	pCol-0::C24intron	✓	pMDC107 (GFP)	✓	✓	✓
S7	pC24::Col-0intron	✓	pMDC107 (GFP)	✓	✓	✓
S8	pC24::C24intron	✓	pMDC107 (GFP)	X	X	X
S9	pCol-0::Col-0intron	✓	pMDC162 (GUS)	✓	X	X
S10	pCol-0::C24intron	✓	pMDC162 (GUS)	✓	X	X
S11	pC24::Col-0intron	✓	pMDC162 (GUS)	X	X	X
S12	pC24::C24intron	✓	pMDC162 (GUS)	X	X	X

✓: stage completed, X: stage not completed

Unfortunately, the *in planta* analysis was not completed within the candidature due to time constrains and the cloning difficulties outlined above.

5.8 Discussion

5.8.1 Transposable elements present in *AtHKT1;1* sequence

The aim of this chapter was to investigate the genomic sequence of *AtHKT1;1*. The particular focus was the second intron, which contains a 1.6 kb insertion in the C24 ecotype. This insertion was hypothesised to regulate *AtHKT1;1* expression, resulting in the lack of *AtHKT1;1* expression in C24 roots.

The Col-0 *AtHKT1;1* genomic sequence contains a number of transposable elements (Figure 5.5 and Figure 5.10) with one of them, ATHPOGON1, being the target of small RNAs. The mode of action of small RNAs are predominantly mediating methylation and/or slicing. As this genomic area is not methylated (Figure 5.6), the small RNAs may cause some degradation of the *AtHKT1;1* transcript, resulting in overall low expression levels of *AtHKT1;1* in Col-0 as previously reported (Jha *et al*. 2010), particularly when compared to other important salt tolerance genes, such as *AVP1*. In C24, the 1.6 kb insertion in the second intron has been identified as a SIMPLEHAT2 transposon (Figure 5.7, Figure 5.8, Figure 5.11 and Figure 5.12). A SIMPLEHAT2 transposon on chromosome 5, which has a high identity to the sequence found in the C24 *AtHKT1;1* intron, is the target of a large number of small RNAs (Figure 5.8 and Figure 5.9), implying the transposon found in the C24 *AtHKT1;1* intron may also be the target of small RNAs. Only minor methylations have been identified in SIMPLEHAT2 on chromosome 5 (Figure 5.9). Small RNAs may mediate the degradation of transcripts, resulting in reduced AtHKT1;1 protein production. This could explain the phenotypic difference in Na^+ accumulation between Col-0 and C24. Tissue specificity of small RNA mediated silencing has not been researched intensely yet, as most research is focussed on the aerial parts of the plant. However, it has been shown that small RNA mediated silencing is altered in the pollen tissue, regulated through gene expression encoding for small RNA interacting proteins (Slotkin *et al.* 2009). Furthermore, grafting experiments show that siRNA can move from the root to the shoot, and *vice versa*, and cause methylation (Molnar *et al.* 2010). A similar mechanism may be mediating root specific silencing of *AtHKT1;1* expression in C24. It is also possible that tissue specific expression of *AtHKT1;1* is caused by the methylation present in the promoter region (Figure 5.6), the region in which small RNA binding sites have been identified previously (Baek *et al.* 2011). It has been reported that there is a positive correlation between methylated regions in the promoter sequence and tissue specific expression patterns, and also between methylated areas in the gene region and high expression levels of the gene (Zhang *et al.* 2006a). Future research should test the C24 *AtHKT1;1* gene and promoter regions for the presence of methylation to investigate whether the SIMPLEHAT2 transposon or other regions are methylated. The methylation status can be

determined gene specific using bisulfite genomic DNA sequencing in combination with PCR, as has been used previously for *AtHKT1;1* in Col-0 by Baek et al. (2011). For instance methylation of a small RNA binding site has been identified by Baek *et al*. (2011) and was further analysed using *promoter::GUS* experiments. A number of different *AtHKT1;1* promoter fragments, ± the small RNA binding site, were fused to *GUS* for expression analysis in stable Col-0 transformants; however, it cannot be judged from the images showing whole seedlings if tissue specificity is affected. Microscope images showing a cross section of the root of these transgenic *promoter::GUS* lines may be suitable to investigate tissue specificity.

To determine if differences in alternative splicing between Col-0 and C24 led to undetectable *AtHKT1;1* transcripts, other parts of the *AtHKT1;1* transcript were used for RT-PCR analysis (Figure 5.16), but no fragments were PCR amplified from gene specific cDNA that was obtained from C24 root samples. Fragments were amplified from Col-0 gene specific cDNA, serving as a positive control (Figure 5.16). It may be that either the C24 *AtHKT1;1* is not transcribed at all, or that the transcripts are rapidly degraded below the detection limit. It is also possible that alternative splicing of the first intron is influencing the transcript. This could be tested by performing additional gene specific RT-PCR, where cDNA synthesis is performed with a primer that is located closer to the 5′ end of the gene, upstream of the first intron.

SIMPLEHAT2 matches abundant small RNAs that are associated with AGO4 and AGO6, which are components of the silencing complex RISC (Qi *et al.* 2006, Zheng *et al.* 2007). In the *ago6* and *ago4* mutants, a reduction in methylation in the SIMPLEHAT2 locus has been detected, suggesting that RdDM is mediated by small RNAs that are associated with AGO4 and AGO6 (Qi *et al.* 2006, Zheng *et al.* 2007). AGO4 also comprises a catalytic domain mediating slicing of target RNA, which in turn produces siRNAs (Qi *et al.* 2006), hence having the potential to silence target gene expression. This may be an explanation for silencing of *AtHKT1;1* in C24. To verify the involvement of small RNAs associated with AGO4 or AGO6 in the silencing of *AtHKT1;1*, it could be tested if *AtHKT1;1* transcripts are present in the *ago6* and *ago4* single and in the *ago6 ago4* double mutants in the C24 background. The single mutants *ago6* and *ago4* and the double mutant *ago6 ago4* in the C24 background may be generated by T-DNA insertion or by crossing the characterised and available T-DNA insertion mutants (Zheng *et al.* 2007) with the C24 background, followed by backcrossing to obtain both the *ago* mutant genotype and the C24 *AtHKT1;1* allele in the same line. A knock down approach using an RNAinterference may not be suitable, since the AGO genes share some sequence similarity which may enhance the effect of unwanted siRNA mediated RNAinterference on other *AGO* transcripts. The presence of the *AtHKT1;1* transcript could then be tested in the *ago* mutants as described earlier using gene specific RT-PCR. Furthermore, *AtHKT1;1* transcripts could

be tested in an *AGO4-DDH* mutant (Qi *et al.* 2006), which is deficient in activity of the catalytic domain involved in slicing of the target RNA in a similar way as described above. Since similarities between C24 and Tsu-1 have been identified, such as Na^+ accumulation and lack of *AtHKT1;1* expression in the root, it was hypothesised that Tsu-1 may also contain the 1.6 kb transposon in the second intron, but a comparison of the genomic DNA did not suggest that the transposon is present in Tsu-1. Also, the comparison of *AtHKT1;1* genomic DNA sequences of 18 other ecotypes did not indicate that these contain the SIMPLEHAT2 transposon in the second intron. Therefore, this transposon does not appear to be conserved in *AtHKT1;1* and in other ecotypes the expression of *AtHKT1;1* may be influenced by other control elements.

5.8.2 Cloning of the *AtHKT1;1* sequences, containing transposable elements, prove difficult

To get *in planta* evidence that the C24 intron is responsible for the lack of *AtHKT1;1* expression in C24 roots, constructs were designed to test *in planta AtHKT1;1* and *GUS/GFP* reporter gene expression.

Unfortunately, it was not possible to obtain the full list of constructs and transform these into Arabidopsis for analysis (Table 5.10). The identified transposon in the second intron of the C24 *AtHKT1;1* sequence is comprised of highly repetitive sequences, which have caused difficulties in both the traditional cloning approach and synthesis by a commercial provider, GenScript. GenScript is used regularly by other groups at the ACPFG and has been known to deliver accurate gene synthesis products and no problems had been experienced before with the synthesis of other genes. Since both approaches had difficulties during cloning the C24 *AtHKT1;1* genomic DNA sequence, there appears to be an inherent problem with this specific sequence of DNA. Furthermore, it cannot be excluded that additional problems are caused by the transposon once the constructs are transformed into plants. If more time was available, the full list of constructs would be completed using the cloned sequence by GenScript. Additional drawbacks in obtaining transformed plants were a number of growth chamber break downs that led to loss of plant material. Surveillance systems have been installed in the growth rooms that should reduce the risk of losing plant material due to breakdowns in the future.

An approach using transient expression in Arabidopsis root protoplasts was considered, however these were not carried out as important constructs for comparison were missing, such as the full length C24 gDNA sequence and destination vectors containing the C24 intron sequence. Furthermore, difficulties using a root protoplast system would be expected as expression under

control of pCol-0 and pC24 has been shown to be predominantly located in the stele (chapter 4), presumably limiting the success rate of detecting the signal.

5.9 Conclusion

It was possible to sequence, clone and identify the 1.6 kb insertion in the second intron of C24 as a SIMPLEHAT2 transposon. This transposon may be involved in methylation of the *AtHKT1;1* DNA and degradation of the transcript RNA, possibly resulting in undetectable *AtHKT1;1* expression in C24 roots. The *in planta* analyses were incomplete as major difficulties in the cloning procedure were experienced. With the now synthesised C24 genomic *AtHKT1;1* sequence by GenScript, it should be possible to complete the cloning processes and obtain stably transformed Arabidopsis for evaluation of *GFP/GUS* and *AtHKT1;1* transgene expression.

Chapter 6 **Comparing NaCl induced alterations in the cytosolic free calcium concentration ($[Ca^{2+}]_{cyt}$) in Col-0 and C24**

6.1 Introduction

The following chapter has been prepared for submission to the peer reviewed journal FEBS letters and is attached in the required submission format. The research described in this chapter has been conducted at The University of Cambridge, United Kingdom, in collaboration with Dr. Alex Webb, and was funded by the Barr Smith Travel Scholarship for Agriculture, the Brenda Nettle Award and by the Waite Research Institute.

The focus of previous chapters was to further analyse the role and control of *AtHKT1;1* from Col-0 and C24. The ecotypes had become of interest because C24 accumulates more Na^+ in the shoot compared to Col-0 and a major QTL had been identified over the genomic region containing *AtHKT1;1* (Roy *et al*., unpublished). Additionally, other observations had been made, including that despite accumulating more Na^+, the C24 ecotype has an increased salt tolerance index, based on shoot dry weight (Jha *et al.* 2010). C24 also appeared to have a reduced response to salt stress, as it does not change the gene expression of some salt responsive genes, hence it had been suggested that C24 might not be able to detect salt (Jha *et al.* 2010). In this chapter the reduced responsiveness of C24 is studied further. In this chapter, an assay using Aequorin based bioluminescence, was developed to compare the responses in the stress inducible calcium signalling pathways of Col-0 and C24 seedlings when exposed to salt stress. Excitingly, C24 was found to be missing part of the calcium signature observed in the salt responsive plant Col-0. This suggests that C24 does not detect the ionic component of salt stress, potentially providing a suitable screening methodology for the identification of yet unknown components in the early stages of the salt signalling pathway.

6.2 Aequorin bioluminescence to measure cytosolic free calcium concentrations $[Ca^{2+}]_{cyt}$

Aequorin mediates bioluminescence and originates from the jellyfish *Aequorea victoria.* The protein, Apo-aequorin, is approximately 22 kDa in size and contains three EF-hand loops; it binds the prosthetic group, coelenterazine, with oxygen to form functional Aequorin (Charbonneau *et al.* 1985, Kendall and Badminton 1998). Binding of calcium ions to the EF-hand loops of the protein induces oxidation of coelenterazine to coelenteramide and emission of blue light, with a wavelength of $\lambda_{max} = 470$ nm (Kendall and Badminton 1998). This photon emission can be monitored using a variety of techniques and equipment, allowing the indirect detection of Ca^{2+}. The system can be used in plants, for instance by using transgenic lines constitutively expressing Apo-aequorin and external application of coelenterazine, allowing the detection and quantification of cytosolic free calcium

concentration $[Ca^{2+}]_{cyt}$ without imposing toxic effects on the plant (Knight *et al.* 1991). The double logarithmic relationship between $[Ca^{2+}]_{cyt}$ and the remaining Aequorin at completion of the experiment allows the determination of the quantity of $[Ca^{2+}]_{cyt}$ at any point in time (Knight *et al.* 1996 and references therein). The total remaining Aequorin can be determined by addition of excess Ca^{2+}, which discharges the system and values for $[Ca^{2+}]_{cyt}$ can be obtained using an empirically derived calibration equation optimised for the system (Knight *et al.* 1996 and references therein).

6.3 Luminometer setup

A purpose-built luminometric setup was employed for the detection of photons that are emitted when calcium is bound by Aequorin (Figure 6.1). Apo-aequorin expressing Arabidopsis seedlings, grown on plates (Figure 6.1 A), were carefully placed into cuvettes and fully immersed into the base solution supplemented with 10 µM coelentrazine overnight for reconstitution of functional Aequorin (Figure 6.1 B). To determine the plant Ca^{2+} response to a variety of stimuli the cuvette was inserted into the brass chamber, which allowed the detection of photons in a light tight surrounding (Figure 6.1 C). A test solution containing different nutrients, ions and osmotica can be applied directly through an inlet tube to the cuvette using a syringe with needle (indicated by the arrow, Figure 6.1 C). The luminometer can then be used to record the amount of total light being emitted from the plant.

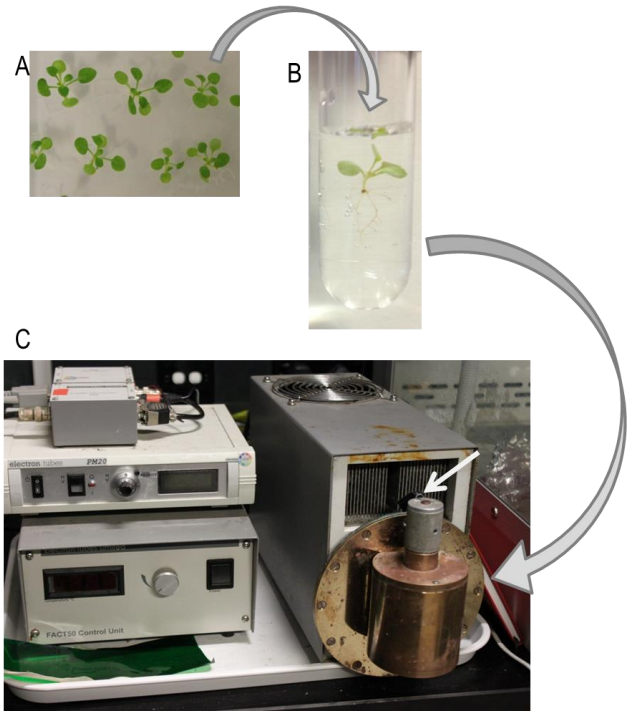

Figure 6.1: Image of purpose-built luminometer setup.

(A) Apo-aequorin expressing Arabidopsis seedlings were grown on plates for 13 d to 15 d before (B) placing them o/n into cuvettes containing base solution supplemented with 10 µM coelentrazine for reconstitution of functional Aequorin. (C) The cuvette containing the seedling was placed into the light tight brass housing for detection of photons by a photon multiplier tube (Electron tubes, UK). In picture (C) in the bottom left is the cooling device to maintain the equipment temperature at -21 °C and on top a CT2 time module to process photon counts. Test solutions were applied to the cuvette through the inlet tube using a syringe with needle, indicated with a white arrow.

Two base solutions, in which the Arabidopsis seedlings were placed for reconstitution and measurements, were tested. Both solutions have been tested in a previous study and their simple composition has been deemed suitable for Aequorin bioluminescence measurements (Tracy *et al.* 2008): A hyperpolarising solution containing 1 mM $CaCl_2$, 0.1 mM KCl, 5 mM 2-(N-morpholino)-ethansulfonic acid (MES), adjusted to pH 5.5 with NaOH; and a depolarising solution containing 1.4 mM $CaCl_2$, 20 mM KCl, 5 mM MES, adjusted to pH 5.5 with NaOH. The overall trend between the two base solutions was comparable, with depolarising solution having slightly more distinct peaks (alterations of $[Ca^{2+}]_{cyt}$ in hyperpolarising solution are depicted in Supplementary Figure 8.9); therefore, presented data is focused on depolarising solution. Stress stimuli such as NaCl induce a depolarisation of the plasma membrane and depolarisation activated Ca^{2+} channels are thought to be involved in stress signal transduction (Cakirlar and Bowling 1981, Shabala *et al.* 2003, White 2000). The use of a depolarising base solution may increase the open probability of depolarisation-activated Ca^{2+} permeable channels, therefore enhancing $[Ca^{2+}]_{cyt}$ peaks.

6.4 Imaging of Aequorin bioluminescence

In the luminometer setup, the whole Arabidopsis seedling is exposed to the stimulus and therefore Aequorin bioluminescence may be detected from all tissues. To evaluate which tissue specifically responds to NaCl treatment, images of seedlings were taken using an ICCD225 photon-counting camera system (Photek, Hastings, UK) (Figure 6.2). For this, plants were grown vertically on ½ strength MS plates in a 12 hr light/dark cycle for 10 d. The seedlings were sprayed with depolarising solution supplemented with 10 µM coelentrazine and incubated overnight for Aequorin reconstitution. The plate with seedlings was placed into the imaging chamber, imaging commenced and the treatment solution was applied after approximately 30 seconds using a syringe that connected to the plate from the outside of the imaging chamber. A volume of 30 mL was applied to ensure the plate was fully covered and seedlings were submerged in the treatment solution. The software Photek IFS32 (Photek, Hastings, UK) was used for image acquisition and processing.

Most of the bioluminescence was detected in the root and the leaf tips (Figure 6.2). Only very little photons were detected when only base solution was applied, indicating that a touch response has only a minor influence (Figure 6.2 A). In response to 200 mM NaCl, photons were first emitted around the root tip, then the signal migrated towards the shoot and after approximately one minute, photon emission was also detected from leaf tips (Figure 6.2 B, video not shown). In response to 400 mM sorbitol, which has the same osmotic strength as 200 mM NaCl, it appeared that photons were detected in all parts of the root at the same time (Figure 6.2 C). No substantial differences between Col-0 and C24 bioluminescence were detected using the imaging system. This is likely due to the substantially reduced sensitivity of the photon counting camera detection system compared to the luminometer setup (section 6.3).

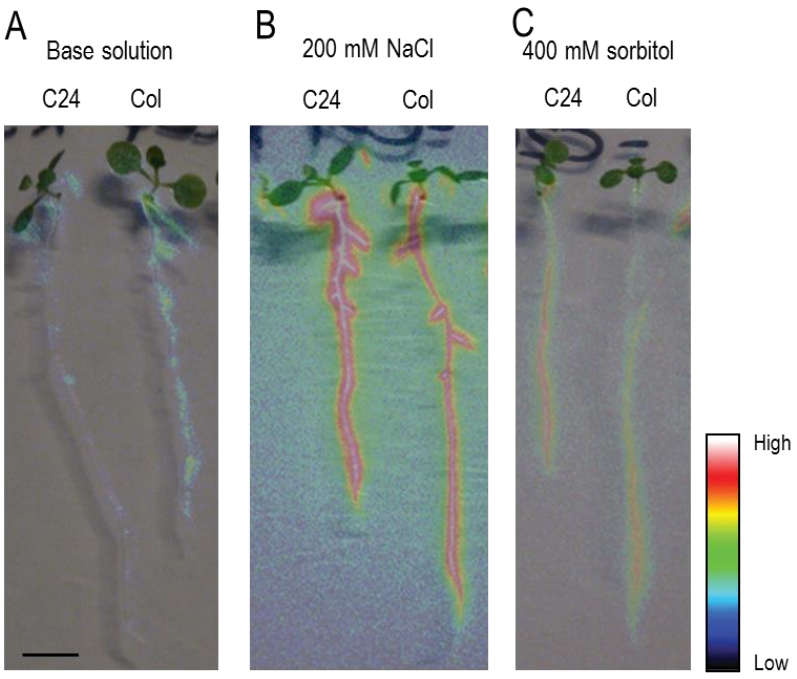

Figure 6.2: Representative images of aequorin bioluminescence of 10 d old Col-0 and C24 Arabidopsis seedlings in response to (A) base solution, (B) 200 mM NaCl and (C) 400 mM sorbitol.

Images are overlays of the bright field image and the 8-bit false-colour image representing cumulative photon density over 200 s. Colour scale is arbitrary, cold colours (blue and green) indicate low photon counts and warm colours represent high photon counts. Bioluminescence images were taken using a photon counting imaging system (Photek, Hastings, UK). Scale bar indicates 1 cm.

6.5 Detecting the calcium signature using a plate reader

In this chapter it is suggested that the difference in Col-0 and C24 calcium signatures might offer a suitable screening methodology for QTL analysis in a Col-0xC24 mapping population in order to identify genes that are important in the early salt signalling pathway. The luminometer setup is not suitable for a high throughput screening as manual handling is necessary (approximately 5 min per sample) and only one seedling can be measured at a time. Use of a 96-well plate reader based system for high throughput screening is suggested instead, as it allows the automated measurement of dozens of samples without substantial manual handling and measurements to run over night.

A plate reader setup was tested to evaluate the response of Col-0 and C24 seedlings in response to NaCl (Figure 6.3). For the plate reader assay, plants were grown on ½ strength MS plates horizontally in a 12 hr light/dark cycle. 13 d to 15 d old seedlings were taken off the plate with forceps and placed carefully in to a 96-well plate – the roots had been carefully wound together to facilitate the transfer. Seedlings were submerged in 100 µL of depolarising solution supplemented with 10 µM

coelentrazine and incubated overnight. The plate reader recorded photon counts every 4 s and 187.5 mM NaCl was applied to the wells after 30 s (Figure 6.3).

For both ecotypes, an immediate increase in $[Ca^{2+}]_{cyt}$ can be observed after stimulus application (Figure 6.3). For C24, the signal declines, while for Col-0 a secondary rise in $[Ca^{2+}]_{cyt}$ is detected. This type of signature corresponds to what can be detected using the luminometer (see following manuscript). However, as discussed in the manuscript, it is necessary to obtain measurements with high temporal resolution, ideally every second, as the first peak is very narrow and occurs immediately after application of the treatment. The temporal variability in the secondary rise in $[Ca^{2+}]_{cyt}$, as observed in Col-0 seedlings, results in large error bars when the average of the individual traces is displayed (Figure 6.3), therefore in the manuscript the data from individual plants is presented and not averaged. Preliminary experiments have been performed using the plate reader system and it may provide a promising methodology for screening a ColxC24 mapping population. However, further optimisation is required with regards to temporal resolution of measurements and NaCl concentration, optimal to detect secondary elevations in $[Ca^{2+}]_{cyt}$. Further work on developing analysis software that can automatically detect the second peak in Ca^{2+} in the Col-0 background is also required.

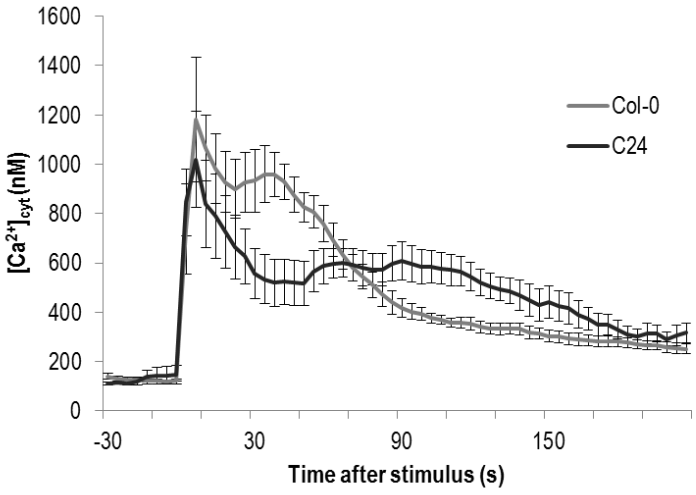

Figure 6.3: Response of *Apoaequorin* expressing Col-0 and C24 seedlings to 187.5 mM NaCl in a plate reader system.

Treatment was applied at time point 0. Traces represent the mean of 6 seedlings, error bars represent ±SEM, n=6

6.6 Calcium signature in response to $CaCl_2$ stimulus

Figure 6.7 in the following manuscript points towards potential components in the salt signalling pathway that may be altered between Col-0 and C24. Hence 150 mM $CaCl_2$ was also tested on Apo*aequorin* expressing Arabidopsis as a stimulus to obtain more information regarding the role of Ca^{2+} in the process of how the calcium signature is formed in Col-0 and C24. Interestingly, besides the first general response peak, a second increase in $[Ca^{2+}]_{cyt}$ can be observed in Col-0 between 90 and 120 s after stimulus application (Figure 6.4 A). The overall shape of the response appears very similar in all individual traces. In C24 however, no additional peaks to the first general response peak are observed (Figure 6.4 B). This suggests that components of the calcium dependent signalling network may be altered in C24. Both $CaCl_2$ and NaCl are chloride salts, however, the response to $CaCl_2$ appears different to NaCl induced alterations in $[Ca^{2+}]_{cyt}$, making it unlikely that Cl^- is the main ion provoking the alterations. This can be further tested by using other chloride salts, such as KCl, $MgCl_2$ and RbCl. The manuscript provides a model of the early stages of the salt signalling pathway (Figure 6.7). Depicted are potential calcium stores from which Ca^{2+} may be released into the cytosol. The difference in Ca^{2+} response between the two ecotypes to $CaCl_2$ may be that Ca^{2+} is released from different compartments in C24 or the activation of calcium conductances is altered between Col-0 and C24.

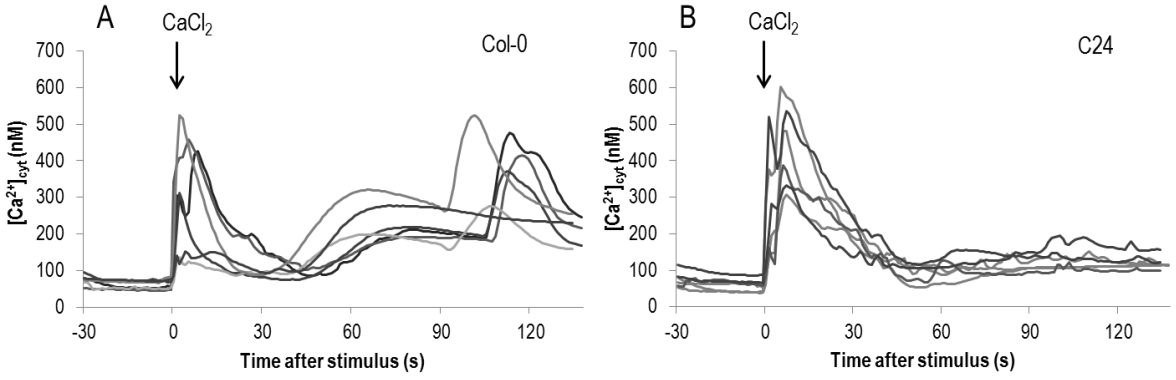

Figure 6.4: Luminometric measurements of whole Arabidopsis seedlings, constitutively expressing *Apoaequorin* subjected to $CaCl_2$ stimulus.

Alterations of $[Ca^{2+}]_{cyt}$ induced by 150 mM $CaCl_2$ in *Apoaequorin* expressing (A) Col-0 and (B) C24 in depolarising solution. Each panel contains data from six representative individual seedlings. Stimulus was applied at time point 0.

To determine the compartments from which Ca^{2+} is released into the cytosol, inhibitory substances, targeting calcium conductances, have been employed in previous studies in the ecotype Col-0

(Knight *et al.* 1997, Tracy *et al.* 2008). However, results were inconclusive due to a lack of specificity of inhibitors influencing a number of channels/transporters or having undetectable effects (Tracy *et al.* 2008).

Further experiments should include the thorough testing of other Na^+- and Cl^-- salts to obtain further information regarding Na^+ and/or Cl^- specificity in $[Ca^{2+}]_{cyt}$ alterations. Also, other Arabidopsis ecotypes should be tested to determine the extent of phenotypic variation. Other ecotypes may have even more contrasting calcium signatures in response to NaCl or other stimuli offering a valuable genetic resource for gene discovery.

Title

Comparing NaCl induced calcium signatures in the *Arabidopsis thaliana* ecotypes Col-0 and C24 - a genetic tool to dissect the salt signalling pathway?

Running title

NaCl induced $[Ca^{2+}]_{cyt}$ alterations in Col-0 and C24

Author list

Sandra M. Schmöckel[1], Alex A.R. Webb[2], Bettina Berger[3], Mark Tester[4], Stuart J. Roy[1*]

[1]Australian Centre for Plant Functional Genomics and The University of Adelaide, PMB1, Glen Osmond, SA 5064, Australia

[2]Department of Plant Sciences, The University of Cambridge, Downing Street, Cambridge CB2 3EA, United Kingdom

[3]The Plant Accelerator and The University of Adelaide, Hartley Grove, Urrbrae, SA 5064, Australia

[4]Division of Biological and Environmental Sciences and Engineering, King Abdullah University for Science and Technology, Saudi Arabia

[*] Corresponding author: stuart.roy@acpfg.com.au, tel: +61 8 8313 7159 fax: +61 8 8313 7102

Abstract

A common feature of stress signalling pathways are alterations in cytosolic free calcium ($[Ca^{2+}]_{cyt}$), allowing the specific and rapid transmission of stress signals, including salinity stress in plants. Here, we used an Aequorin based bioluminescence assay to compare the calcium signatures of the salt responsive Arabidopsis ecotype Col-0 to the non-responsive ecotype C24. We show that C24 lacks the salt specific component of the calcium signature compared to Col-0. This phenotypic variation could be exploited as a screening methodology for the identification of yet unknown components in the early stages of the salt signalling pathway.

Keywords

Salinity tolerance, salt sensing, Ca^{2+} imaging, Ca^{2+} signalling, Aequorin

Abbreviations

$[Ca^{2+}]_{cyt}$ - Cytosolic free calcium concentration

Highlights

- NaCl induces specific alterations in cytosolic free calcium $[Ca^{2+}]_{cyt}$
- Ecotype C24 lacks salt specific component of calcium signature compared to Col-0
- Aequorin bioluminescence as a tool to dissect the NaCl signalling pathway is proposed

Introduction

Worldwide approximately 20 % of the irrigated agricultural land is affected by soil salinity (FAO 2008). This leads to a significant decrease in crop yield, ultimately impacting revenue and food security. In many crop species salinity stress is predominantly due to high levels of sodium chloride (NaCl) in the soil. NaCl will hereby be referred to as salt.

Plant salinity stress can be categorised into two phases, the initial shoot ion independent osmotic stress and the later ionic stress (Munns and Tester 2008). Osmotic stress occurs as soon as the plant encounters salt in the soil and results in an immediate reduction in the shoot growth rate (Munns and Passioura 1984). Ionic stress is caused by the accumulation of ions such as Na^+ and Cl^- in the cytosol of cells in the shoot and results in the inhibition of cellular processes and induces premature leaf senescence. Plant responses to the osmotic component of salt stress occur in the shoot prior to the accumulation of toxic concentrations of ions in cells. This suggests that a signalling pathway exists whereby perception of salt at the root/soil interface is communicated to the shoot, before the onset of ionic stress.

Currently, the transmission of NaCl induced stress signals in plants is only partially understood. In both animal and plant signalling pathways, calcium ions (Ca^{2+}) play an important role as second messengers, mediating the response to developmental and environmental stimuli. Ca^{2+} is involved in a variety of plant

signalling pathways such as abiotic stress responses (Kudla *et al.* 2010, McAinsh and Pittman 2009), control of stomatal aperture (Allen *et al.* 2001, Ng *et al.* 2001) and interactions with pathogenic and symbiotic microorganisms (Ma and Berkowitz 2007, Oldroyd *et al.* 2009). It has been hypothesised that alterations in the cytosolic free Ca^{2+} concentration ($[Ca^{2+}]_{cyt}$) follow a spatial and temporal pattern (referred to as calcium signature), inducing a stimulus specific response (Allen *et al.* 2001, Dodd *et al.* 2010, McAinsh and Pittman 2009). This hypothesis is further supported by Whalley and Knight (2013) who used electrical stimulation to induce a variety of different calcium oscillations and could link those oscillations to specific changes in gene expression.

Changes in $[Ca^{2+}]_{cyt}$ have also been linked to the salt stress signalling pathway. Immediate increases of $[Ca^{2+}]_{cyt}$ can be observed when a plant is challenged with NaCl (Kiegle *et al.* 2000, Knight 2000, Knight *et al.* 1997, Tracy *et al.* 2008). This elevated $[Ca^{2+}]_{cyt}$ can be perceived by calcium sensing proteins such as Calcium dependent protein kinases (CDPKs), Calmodulines (CaM), calcineurin B-like proteins (CBLs) and Calmodulin-like proteins (CMLs) (Batistič and Kudla 2012, Kudla *et al.* 2010). In *Arabidopsis thaliana* several components of a signalling pathway for salt stress have been identified by the characterisation of *salt overly sensitive* (*sos*) mutants (Wu *et al.* 1996, Zhu 2000). NaCl-initiated increases in $[Ca^{2+}]_{cyt}$ are detected by Salt Overly Sensitive 3 (SOS3; AtCBL4) and the binding of Ca^{2+} facilitates the interaction of SOS3 with SOS2 (CBL-interacting protein kinase 24, AtCIPK24) (Halfter *et al.* 2000, Zhu 2000). This complex has been shown to activate the Na^+/H^+-antiporter SOS1 by phosphorylation, resulting in the transport of Na^+ out of the cell and the reduction of $[Na^+]_{cyt}$ (Quintero *et al.* 2002, Shi *et al.* 2000). Early speculations arose that SOS1 could possibly act as a sensor for NaCl due to the protein's long C-terminus and other characteristics (Zhu 2002), however no evidence supporting this hypothesis has been put forward.

It appears that many rapidly responding genes are common to different abiotic stress treatments, while genes that are expressed differently at later time points appear stress specific (Kilian *et al.* 2007). Interestingly, a study examining the expression profiles of salt responsive genes in different ecotypes of Arabidopsis identified the ecotype C24 as being less responsive to salt stress when compared to Col-0 (Jha *et al.* 2010). A possible explanation for this finding is that the ecotype C24 has an alternate or defective Ca^{2+} signalling pathway (Jha *et al.* 2010). Given

that changes in expression levels of salt responsive genes are downstream of the salt signalling pathway, how salt stress is initially perceived by plant cells and the initiation of intracellular signalling pathways, require further investigation. One possibility is to investigate the stress activated calcium signalling pathway, which generates stress specific calcium signatures, given that Ca^{2+} is known to play a key role in the early stages of the salt stress response.

Calcium signatures can be analysed using the Aequorin bioluminescence reporter system. *Apo-aequorin* encodes for a precursor protein that is localised in the cytosol and forms functional Aequorin when supplemented with the prosthetic group, coelentrazine (Montero *et al.* 1995). In this system, cytosolic Ca^{2+} binds to Aequorin, leading to the emission of photons that can be measured using a luminometer, thereby giving an indication of total $[Ca^{2+}]_{cyt}$ present at any given time. It has been used previously to measure increases in $[Ca^{2+}]_{cyt}$ to analyse the response of Arabidopsis seedlings to abiotic stresses such as drought, cold and salt stress (Kiegle *et al.* 2000, Knight *et al.* 1997, Tracy *et al.* 2008, Zhu *et al.* 2013).

Here we show that the analysis of calcium signatures in response to salt stress might offer an opportunity to further investigate components of the salt signalling pathway. We provide evidence that calcium signatures evoked by salt treatment vary between the responsive ecotype Col-0 and the less-responsive ecotype C24. In addition, the importance of the temporal aspect of alterations in $[Ca^{2+}]_{cyt}$ will be discussed.

Material and Methods

Plant material and growth conditions

Luminometric experiments were performed using the *Arabidopsis thaliana* ecotypes Col-0 and C24 expressing *APOAEQUORIN* under control of the CaMV-35S promoter (Knight *et al.* 1991). Seeds were surface sterilised with 70 % (v/v) ethanol and sown onto petri dishes containing ½ strength MS (Duchefa, Harlem, Netherlands) supplemented with 0.8 % (g/v) Bacto agar (Becton, Dickson and Company, Sparks, MD, USA) (adjusted to pH 5.7 with KOH). The plates were incubated horizontally in a growth chamber under 12/12 h light/dark regime, at 22°C and 80 µM m^{-2} s^{-1} light intensity.

Measurement of $[Ca^{2+}]_{cyt}$

Seedlings were grown for 13 d to 15 d and developmentally alike seedlings were placed into luminometer cuvettes (51 mm high × 12 mm diameter, Sarstedt, Leicester, UK) containing 300 µL reconstitution solution [1.4 mM $CaCl_2$, 20 mM KCl, 5 mM 2-(N-morpholino)-ethansulfonic acid (MES) and 10 µM coelentrazine (Prolume, Pinetop, AZ, USA), adjusted to pH5.5 with NaOH]. The experiments were conducted in this depolarising base solution because of its simple composition, as described previously (Tracy *et al.* 2008), and its ability to impose a membrane potential similar to that of MS growth solution, -40 mV for depolarising base solution and -55 mV for MS (Maathuis and Sanders 1993). Treatment solutions consisted of base solution (1.4 mM $CaCl_2$, 20 mM KCl, 5 mM MES) supplemented with the nominated amount of NaCl or sorbitol. Ca^{2+} activity in NaCl containing treatment solutions was maintained by addition of $CaCl_2$ as determined using the programme Visual MINTEQ (version 3.0, http://www2.lwr.kth.se/English/OurSoftware/ Vminteq/). The osmolarity of solutions was measured using a Wescor 5520 Vapour Pressure Osmometer (Logan, UT, USA) following the manufacturer's instructions. The osmolarity of sorbitol solutions was adjusted to the osmolarity of NaCl solutions.

The setup of the luminometer and conversion of photon counts into $[Ca^{2+}]_{cyt}$ has been described elsewhere (Kiegle *et al.* 2000, Knight *et al.* 1997). Briefly, the luminometer cuvette was placed into a purpose-built brass housing connected to a photon multiplier tube (Electron tubes, UK), (kept at -21°C) and a CT2 time module to process photon counts. Data were recorded in one second intervals using the P10232 photon counting package (version 1.0.2) by Electron tubes. An inlet in the sample housing allowed the injection of solutions using a light tight syringe. Calibration was performed by discharging all remaining Aequorin within the plant by the addition of 2 M $CaCl_2$ (in 20 % (v/v) ethanol) thereby allowing the conversion of photon counts into values of $[Ca^{2+}]_{cyt}$. The following empirically derived equation was used for conversions: $pCa = 0.332588(-\log k) + 5.5593$, where k is the quotient of luminescence counts per second over total luminescence counts (Knight *et al.* 1996).

Data analysis

Statistical analysis was performed on at least three biological replicates, error bars indicate the standard error of the mean (S.E.M.). Statistical significance was determined using Student's t-test, * $P<0.05$ and ** $P<0.01$.

Results and Discussion

Many processes in the plant are rapidly altered upon addition of salt to the roots, including the activation/deactivation of genes and proteins. Previous research identified the *Arabidopsis thaliana* ecotype C24 as not substantially changing the expression of several key salt responsive genes and, therefore, appears less responsive to salt treatment as compared to the ecotype Col-0 (Jha *et al.* 2010). It was hypothesised that C24 has a dysfunctional or alternate salt signalling pathway. To investigate the early stages of this pathway, we compared the calcium signatures of Col-0 and C24 using the Aequorin bioluminescence reporter system. Luminometric measurements were performed on whole Col-0 and C24 seedlings constitutively expressing *Apoaequorin* using a luminometer with high sensitivity and high temporal resolution.

NaCl triggers a distinct calcium signature

When *Apoaequorin* expressing Col-0 and C24 were challenged with 200 mM NaCl, 400 mM sorbitol or cold (9 °C), an instantaneous increase in $[Ca^{2+}]_{cyt}$ of similar magnitudes could be observed for both ecotypes (Figure 6.5). This signal quickly declined within a few minutes to a base level. Treatment with 200 mM NaCl resulted in a peak with a magnitude of 800±39 nM and 855±66 nM $[Ca^{2+}]_{cyt}$ in Col-0 and C24, respectively (Figure 6.5 A and D). The same strength of osmotic stress was imposed using 400 mM sorbitol resulting in peak magnitudes of 737±58 nM and 750±50 nM $[Ca^{2+}]_{cyt}$ in Col-0 and C24, respectively (Figure 6.5 B and E). Cold treatment was used to compare the response to a different abiotic stress; it also resulted in an instantaneous increase in $[Ca^{2+}]_{cyt}$ with magnitudes of 1052±52 nM and 914±93 nM $[Ca^{2+}]_{cyt}$ in Col-0 and C24, respectively (Figure 6.5 C and F). For all stress treatments tested, there are no significant differences in the magnitude of the first peak between ecotypes. These results are broadly in

agreement with previous research (Kiegle *et al.* 2000, Knight *et al.* 1997, Tracy *et al.* 2008).

The magnitudes of the initial NaCl and sorbitol induced $[Ca^{2+}]_{cyt}$ increase are dependent on stimulus strength. The amplitudes of the first peak increases with increasing concentrations of NaCl and sorbitol, but were not significantly different between ecotypes (data not shown). The amplitude of the first peak was determined over 13 NaCl and sorbitol concentrations in Col-0 and C24, ranging between 0 to 1 M NaCl and respective sorbitol concentrations of 0 to 2 M (data not shown in manuscript, but are in thesis supplementary material, Supplementary Figure 8.9). Over this range of concentrations, the amplitudes of sorbitol induced peaks are smaller than those of NaCl induced peaks. This suggests that the NaCl response is partially due to the osmotic and partially due to the ionic component of NaCl treatment. This is in agreement with other studies in which a small number of selected NaCl and sorbitol concentrations were tested (Kiegle *et al.* 2000, Knight *et al.* 1997, Tracy *et al.* 2008, Zhu *et al.* 2013). The correlation between stimulus strength and amplitude of the first $[Ca^{2+}]_{cyt}$ peak indicates that touch response is not the major contributor to $[Ca^{2+}]_{cyt}$ increases.

Col-0 and C24 have different calcium signatures in response to NaCl

Interestingly, there is a pronounced difference in NaCl induced $[Ca^{2+}]_{cyt}$ alterations between Col-0 and C24 (Figure 6.5 A and D). While the calcium signatures for salt treated Col-0 seedlings are biphasic, the signatures in C24 only contain the initial peak. Comparison of individual $[Ca^{2+}]_{cyt}$ traces of NaCl treated Col-0 seedlings indicate that the secondary rises in $[Ca^{2+}]_{cyt}$ all have a similar amplitude, which is always smaller than the first peak (Figure 6.5 A). Notably, the timely occurrence of the secondary rise in $[Ca^{2+}]_{cyt}$ differs in individual seedlings (Figure 6.5 A); therefore, $[Ca^{2+}]_{cyt}$ traces were not averaged as this would mask the biphasic appearance.

To test whether differences in $[Ca^{2+}]_{cyt}$ alterations were significant between Col-0 and C24, the secondary rises in $[Ca^{2+}]_{cyt}$ were compared, assessing the bimodal characteristics. For the purpose of determining values of peak amplitudes, the first peak was defined as the local maximum that occurs within the first 30 seconds after stimulus onset, while the second peak was defined as the local maximum that occurs beyond 30 seconds after stimulus application. The amplitude of the

second peak is significantly different between the ectypes Col-0 and C24 when challenged with 200 mM NaCl, with values of 656±60 nM $[Ca^{2+}]_{cyt}$ and 383±46 nM $[Ca^{2+}]_{cyt}$, respectively (Figure 6.6 A). To analyse whether this characteristic only occurs at 200 mM NaCl, a further 12 different NaCl concentrations (0 M to 1 M) were tested and the amplitudes of the second peak for each [NaCl] is depicted in Figure 6.6 B. The described differences in amplitude of the second peak occur over a wide range of [NaCl], and this difference is significant for all concentrations up to 800 mM NaCl (Figure 6.6 B).

It has previously been suggested by Tracy *et al.* (2008) that the second peak is NaCl specific, as it does not occur when the same strength of osmotic stress is applied using sorbitol. The presented results support this hypothesis by displaying the biphasic characteristics of NaCl induced $[Ca^{2+}]_{cyt}$ alterations and monophasic sorbitol induced $[Ca^{2+}]_{cyt}$ alterations for the Col-0 ecotype (Figure 6.5 A and B). The hypothesis is further supported by taking into account that another abiotic stress, cold treatment, also induces monophasic $[Ca^{2+}]_{cyt}$ alterations (Figure 6.5 C).

Previous research has focussed on describing $[Ca^{2+}]_{cyt}$ alterations predominantly based on the amplitude of the first peak and signatures were often averaged (Kiegle *et al.* 2000, Knight *et al.* 1997, Tracy *et al.* 2008, Zhu *et al.* 2013). Secondary peaks would have been masked by averaging the signature due to the variability of the time of occurrence. The bimodal characteristics of NaCl-induced $[Ca^{2+}]_{cyt}$ increases in Col-0 seedlings were also not detected using an imaging based screening system, where luminescence values of 100 seedlings were integrated over a 40 s period (Zhu *et al.* 2013); this would restrict the detection of secondary peaks. When analysing events that are related to single cell oscillations, such as circadian oscillations in guard cells, not only the time resolution is important, but also the spatial resolution of Aequorin bioluminescence needs to be considered. Signals received from whole seedlings might not represent oscillation events that occur on a single cell level for reasons such as overlapping oscillations and delays in response (Dodd *et al.* 2006, Plieth 2010). However, when analysing salt signalling based on the Aequorin bioluminescence system, the focus lies on observing the transmission of signals in the whole seedling, with an emphasis on resolving the temporal resolution of the $[Ca^{2+}]_{cyt}$ signature.

What might cause the difference in calcium signatures between Col-0 and C24?

NaCl induced calcium signatures in Col-0 and C24 seedlings are substantially different as measured using the Aequorin bioluminescence system. The observed differences provide evidence that the early stages of the salt signalling pathway differ in these ecotypes. The salt signalling pathway is triggered by a NaCl stimulus and initiates a signalling cascade, which results in the influx of Ca^{2+} into the cytosol and thereby forming the calcium signature (Figure 6.7). This calcium signature is then thought to encode for the stimulus specific response. Consequently, the salt sensor, the signalling molecules, the calcium influx system or a yet unidentified component could be dysfunctional or absent in C24, leading to an altered calcium signature and thus reducing the responsiveness of C24 as measured by gene expression.

Details related to the components of the early salt signalling pathway are not well understood. The very first step of the pathway, the perception of NaCl stress, remains elusive. From observations such as immediate salt specific responses in form of calcium oscillations and salt specific activation of gene expression, it can be assumed that a sensor that perceives salt stress exists. So far, the molecule acting as a sensor, for instance a protein, has not been identified and it remains speculative if it might be membrane bound or located in the cytosol. C24 could be missing the function of the salt sensor. This is one possibility, considering the calcium signature in C24 seedlings only forms the first peak, which could be attributed to the general stress response, which is also present during osmotic and cold stress. A dysfunctional salt sensor could result in the absence of the secondary, salt specific, calcium peak.

The next step in the signalling pathway is transmission of the stress signal from the sensor to effectors. While such transmitting signalling molecules, for instance inositol trisphosphate, have been well studied in animal systems (Martin 1998), their identity in signalling cascades in plants is not well understood (Munnik and Testerink 2009). Inositol phosphates have been found to rapidly increase upon salt and osmotic stress and they were also linked to calcium signalling events (DeWald *et al.* 2001, Takahashi *et al.* 2001). Inositol phosphates could therefore serve as molecules transmitting the salt stress signal from the sensor to effectors such as calcium channels (DeWald *et al.* 2001). Alterations in inositol phosphates or other

signalling molecules in C24 could result in altered or non-activation of the salt specific calcium influx system, resulting in an altered calcium signature.

The calcium influx system is crucial to form calcium signatures. Ca^{2+} enters the cytosol from compartments such as the vacuole, the endoplasmic reticulum (ER) and mitochondria or across the plasma membrane (PM). A review by Hetherington and Brownlee (2004) provides comprehensive details on different types of calcium channels, their subcellular location and potential role in calcium signalling. The molecular identity of calcium channels mediating the salt response, however, is vastly unknown. NaCl induced $[Ca^{2+}]_{cyt}$ changes are potentially mediated by Ca^{2+} entry *via* the plasma membrane and from the vacuole through inositol phosphate activated calcium channels (Knight *et al.* 1997, Muir and Sanders 1997). The tonoplast localised transporter TPC1 was a candidate for NaCl induced Ca^{2+} release, but analysis of *tpc1-2* mutants suggests that it is not the major contributor to NaCl, cold and osmotic stress induced $[Ca^{2+}]_{cyt}$ alterations (Ranf *et al.* 2008). C24 has, at least in parts, a functioning calcium influx system, as alteration in $[Ca^{2+}]_{cyt}$ are not completely abolished in response to other stress stimuli. However, it is possible that the influx system from a certain compartment is dysfunctional. For example, a bimodal $[Ca^{2+}]_{cyt}$ response has been analysed in tobacco cell lines treated with distilled water, inducing a hypo-osmotic shock (Cessna *et al.* 1998). In this study the use of inhibitors identified that the first $[Ca^{2+}]_{cyt}$ peak is originating from external Ca^{2+} pools and the second peak from internal compartments (Cessna *et al.* 1998). These tobacco cell lines also show a bimodal response to salt and hyper-osmotic stress with mannitol (Pauly *et al.* 2001). Inhibitor studies on NaCl stressed Arabidopsis seedlings, however, are inconclusive. The inhibitor gadolinium chloride had significant effects on the amplitude of $[Ca^{2+}]_{cyt}$ increases in Col-0 seedlings, suggesting that calcium influx occurs at least in parts across the PM, however, a long incubation time was necessary to obtain effects and therefore other inhibitory effects could influence the measurements (Knight *et al.* 1997, Tracy *et al.* 2008). Also neomycin significantly reduced $[Ca^{2+}]_{cyt}$ increases, suggesting a role for inositol phosphate activated calcium channels (Knight *et al.* 1997, Tracy *et al.* 2008). The molecular identity of the calcium influx system that mediates NaCl induced $[Ca^{2+}]_{cyt}$ alterations remains to be investigated. If it is hypothesised that a bimodal response might occur due to activation of different calcium influx systems, such as influx across the PM results in the first peak and

calcium from the vacuole forms the second peak, C24 might lack the latter influx system, causing only a monophasic response. The comparison of Col-0 and C24 might offer a genetic tool to yield insights into the molecular identity of such a calcium influx system.

Any of the three main stages in the early signalling pathway that are depicted in Figure 6.7 offer an explanation for the differences in calcium signatures in Col-0 and C24. However, the molecular identity of the salt sensor, signal transmission molecules and the calcium influx systems are poorly understood and it cannot be excluded that a completely different mechanism is underlying these differences in $[Ca^{2+}]_{cyt}$ alterations. On the other hand, it is of great advantage that the genomes of Col-0 and C24 have been fully sequenced (Cao *et al.* 2011), making a genetic approach a useful tool to investigate the early stages of the salt signalling pathway.

Can calcium signatures of Col-0 and C24 be used as a genetic tool to dissect salt signalling?

Previous work has shown a difference in salt induced gene expression between Col-0 and C24 seedlings, with C24 showing little response to salt stress (Jha *et al.* 2010). Here, we show that differences in NaCl induced responses between the two ecotypes occur earlier in the salt detection pathway as indicated by the lack of a NaCl-specific secondary Ca^{2+} peak in C24. Therefore, the hypothesis of a dysfunctional or alternate salt signalling pathway in C24 is maintained.

The herein used luminometer is highly sensitive, providing reproducible calcium signatures and importantly, the photon counts can be calibrated to obtain values of $[Ca^{2+}]_{cyt}$. However, it only allows the measurement of one seedling at a time and is therefore not suitable for high throughput genetic screenings. An imaging based system, allowing for high throughput, has recently been used to screen *Apoaeqorin* expressing T-DNA mutants for increased and decreased luminescence upon H_2O_2 and NaCl treatment to identify novel candidate genes involved in the signalling pathway (Pan *et al.* 2012). However, there were issues with the identification of false positives and problems with varying amounts of aequorin within each transgenic plant. Using a system similar to what is described in the study here, with a high temporal resolution and the ability to calibrate the total amount of Aequorin in a plant, gives an opportunity to further dissect these

Ca^{2+} signalling pathways. This method of luminometric measurements with high throughput capabilities can be performed in a 96-well plate reader with the appropriate emission filter and an injection capacity. A high temporal resolution is recommended to allow the detection of rapid $[Ca^{2+}]_{cyt}$ changes and to permit detection of the secondary peak with its variability in temporal occurrence. A high throughput genetic screen of a Col-0 x C24 population, based on the Aequorin bioluminescence system, could lead to the identification of yet unknown components in the early stages of the salt signalling pathway.

Acknowledgements

We would like to thank Dr. Marc Knight for providing *Arabidopsis thaliana* ecotypes Col-0 and C24 expressing *Apoaequorin* as well as Mr. Matthew Stancombe for technical support. We would also like to thank the Australian Centre for Plant Functional Genomics as well as The Waite Research Institute, the Barr Smith Travel Scholarship in Agriculture and the Brenda Nettle Travel Award for financial support.

References

The list of references in this manuscript have been included in the thesis reference section.

Figures and legends

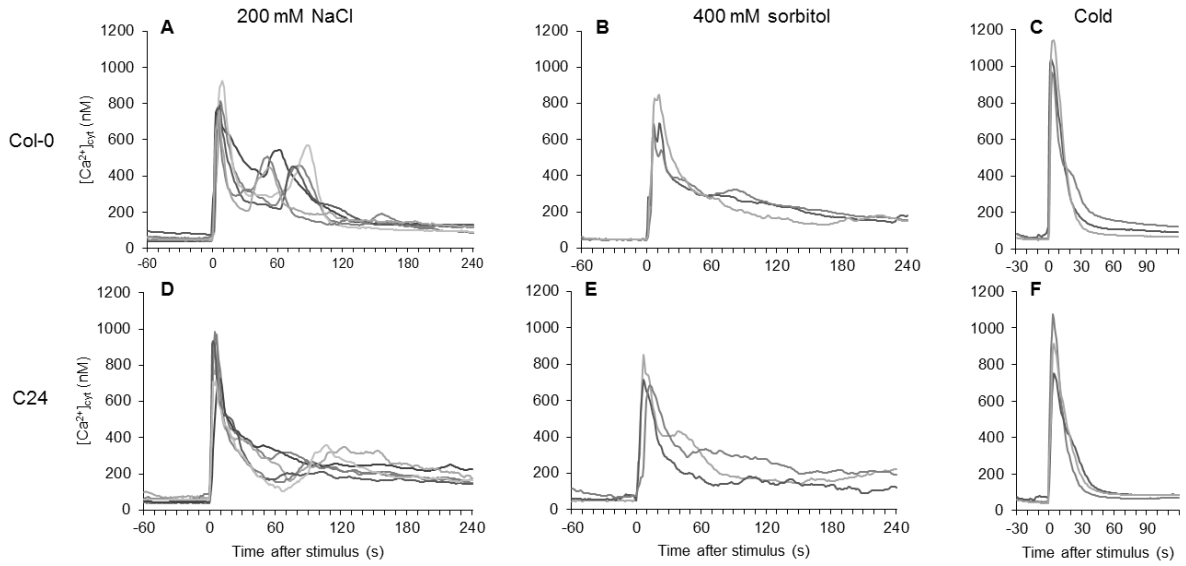

Figure 6.5: **Luminometric measurements of whole Arabidopsis seedlings, constitutively expressing *Apoaequorin*.**

Alterations of $[Ca^{2+}]_{cyt}$ induced by (A) 200 mM NaCl, (B) 400 mM sorbitol or (C) 9 °C cold treatment in ecotype Col-0 and (D) 200 mM NaCl, (E) 400 mM sorbitol or (F) 9 °C cold treatment in ecotype C24. Each panel contains data from three to six representative individual seedlings. Stimulus was applied at time point 0.

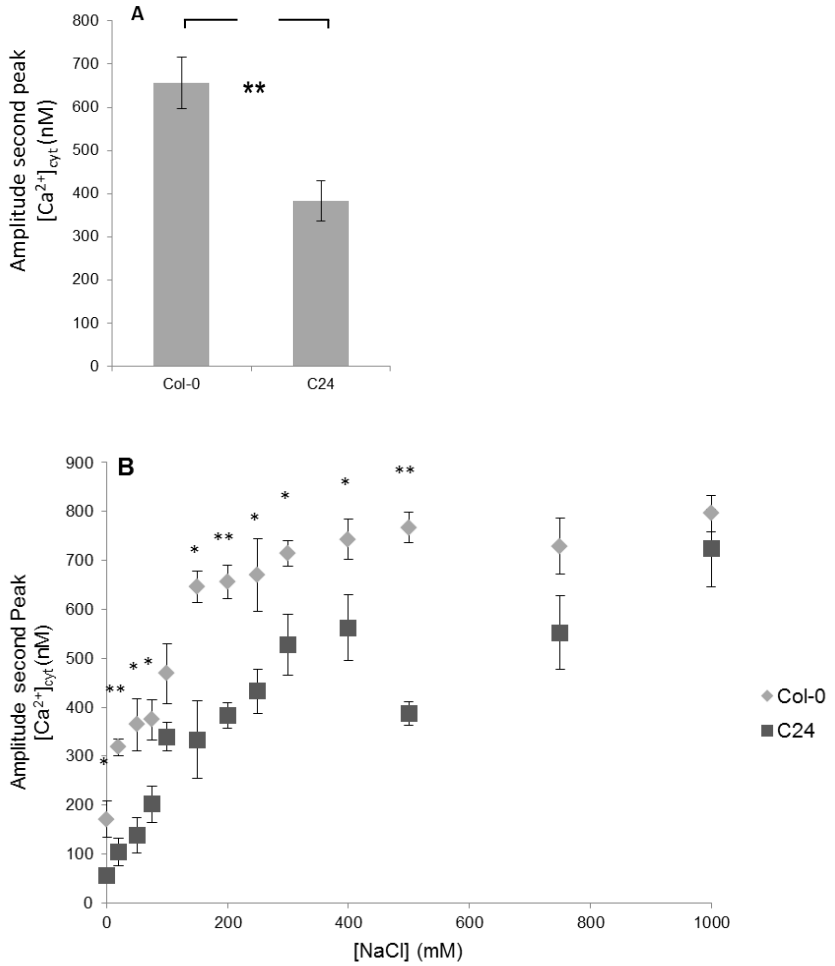

Figure 6.6: **Amplitude of second $[Ca^{2+}]_{cyt}$ peak in response to [NaCl] treatment.**

Col-0 and C24 seedlings constitutively expressing *Apoaequorin* treated with (A) 200 mM NaCl and (B) a range of NaCl concentrations. Each point represents the average peak height of the second $[Ca^{2+}]_{cyt}$ peak of three replicates, error bars indicate the standard error of the mean (S.E.M.). Asterisk indicates the significance based on a T-test. With *: $p<0.05$ and **: $p<0.01$.

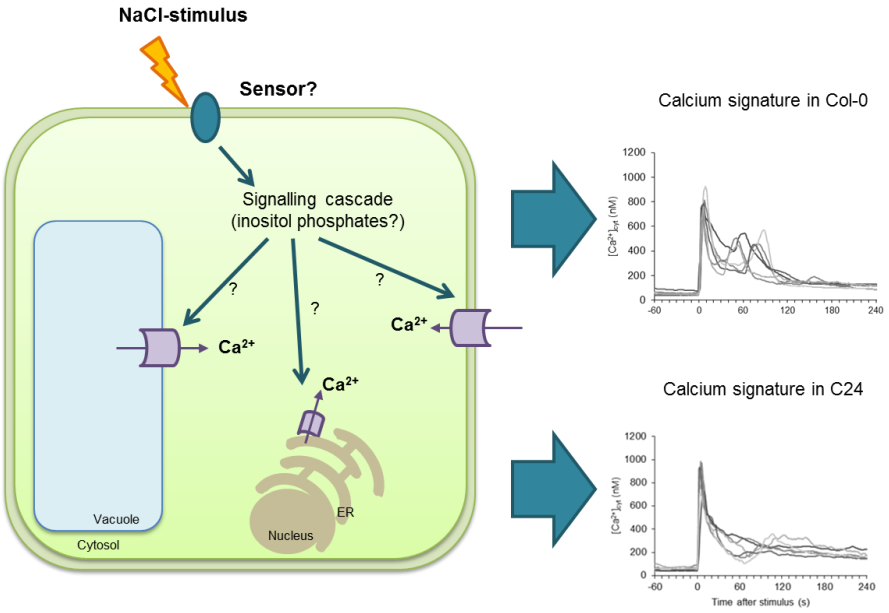

Figure 6.7: **Formation of NaCl induced $[Ca^{2+}]_{cyt}$ alterations.**

A NaCl stimulus is perceived by the plant, probably by a sensor protein, and initiates the signalling cascade. The molecules transmitting the signal could be inositol phosphates, which then activate the calcium influx system. Ca^{2+} enters the cytosol from vacuolar stores, the endoplasmic reticulum or across the plasma membrane and subsequent alterations in $[Ca^{2+}]_{cyt}$ can be measured using the Aequorin bioluminescence system. Characteristic calcium signatures are depicted in the panel on the right hand side. The calcium signature in Arabidopsis ecotype Col-0 is biphasic, while it is monophasic in C24. The question marks point to potential stages in the salt signalling pathway that could cause the difference in calcium signatures between Col-0 and C24. Further details are provided in the text.

Chapter 7 **Analysing NaCl-induced responses in Col-0 and C24**

7.1 Introduction

In the previous chapter alterations in $[Ca^{2+}]_{cyt}$ of Col-0 and C24 seedlings were analysed in response to NaCl, sorbitol and cold treatment. While in Col-0 the $[Ca^{2+}]_{cyt}$ alterations in response to NaCl were biphasic, they were monophasic in C24 seedlings. It has been hypothesised that the cause for differences in the calcium signature between the ecotypes lies in the early stages of the signalling pathway. This difference provides a unique opportunity to identify the as yet unknown components involved in the early detection of NaCl at the cell membrane. To identify the genetic cause for the difference in sensing response it was proposed to use a forward genetics approach. However, to analyse the calcium signature between Col-0 and C24 using a forward genetic approach such as QTL mapping, a transgenic Col-0 × C24 mapping population, which contains the reporter gene *Apoaequroin* would be required. To generate such a mapping population a homozygous Col-0 or C24 plant for the *Apoaequorin* gene would have to be crossed with the reciprocal parent. From the F_1 offspring, only plants containing *Apoaequorin* would be selected for selfing to generate the next generation. This process would be repeated until a recombinant inbred population would be produced (usually 7-8 selfing events). Unfortunately it would not be possible to transform pre-existing Col-0 × C24 recombinant inbred lines (RILs) with *Apoaequorin*, due to the different integration sites of *Apoaequorin* potentially having an effect on aequorin fluorescence and plant response. Generating a mapping population containing *Apoaeqorin* would require a large amount of time and would not be feasible in the time scale of this thesis. Hence, another phenotyping assay was considered to utilise an existing Col-0 × C24 mapping population that is available in the laboratory.

It had previously been observed that in addition to differences in the calcium signature between Col-0 and C24, C24 also appeared to have a reduced response to salt stress, as it does not change the gene expression of salt responsive genes (Jha *et al.* 2010). In this chapter the reduced responsiveness of C24 as measured by reduced induction of salt responsive genes is studied further to determine if a robust assay measuring expression profiles of salt responsive genes could be used as a phenotype for QTL analysis in a Col-0 × C24 mapping population. The aim of this study was to assess the altered responsiveness of C24, and to consequently set up a screening assay for a QTL analysis of a Col-0 × C24 mapping population. The basics of QTL mapping are introduced below.

7.2 QTL mapping

Quantitative trait loci (QTL) are genomic regions linked to a specific phenotypic trait (Sax 1923, Thoday 1961). QTL analyses are commonly carried out on mapping populations produced from a cross between two parents which are known to be different in respect to a certain trait or phenotype

(bi-parental mapping). The aim is to discover the genomic sequence associated with the variation and from there to identify the underlying gene important for the phenotype. This approach is called forward genetics, because the gene is identified on the basis of an observed phenotype.

Another mapping approach is genome wide association (GWA) mapping or genome wide association study (GWAS); here, a population consisting of individuals of the same species that are not related to each other are studied for phenotypic variation and genetic loci linked to that trait identified. A useful population can be established using Arabidopsis, because of its large number of natural accessions. For instance a salinity study using 300 Arabidopsis accessions was recently performed and identified the *AtHKT1;1* locus to be linked to shoot Na^+ content (Baxter *et al.* 2010). For a comprehensive review on GWAS in Arabidopsis see Korte and Farlow (2013). A brief comparison of advantages and disadvantages of both mapping approaches is given in Table 7.1

Table 7.1: Comparison of advantages and disadvantages of GWAS and mapping using bi-parental RILs in Arabidopsis

Mapping approach	Advantages	Disadvantages
GWAS	- Arabidopsis collections usually readily available. - 1,300 accessions have been genotyped for 250,000 SNPs. - Very fine mapping resolution	- Dense marker map is required. - If phenotype is caused by rare variant of an allele, or small phenotypic effects are caused, there may be difficulties in detecting the locus.
Mapping using RILs	- Inbred lines allow the repeated testing of the population. - The effect of rare variants is enhanced, because only two parents are used, facilitating detection of locus.	- Mapping resolution is dependent on amount of recombination occurred during crossing. - Only allelic diversity segregating between the parents can be assayed.

Although it is possible that a GWAS approach would have been successful in identifying important parts in the salt signalling pathway, a bi-parental QTL mapping approach was considered for this project for two main reasons. If the non-responsiveness to salt that was observed in C24 is caused by a missing salt sensor, it is possibly a rare variant in Arabidopsis. Therefore GWAS is not an ideal approach to detect this variant. Also, the desired trait had already been observed between Col-0 and C24 and a Col-0 × C24 mapping population had been produced previously (Törjék *et al.* 2003, Törjék *et al.* 2006), which was available in the laboratory.

There are a vast number of studies, which use QTL analysis on bi-parental populations to identify loci important for a large range of phenotypes. A number of QTL related to salt tolerance have

already been identified - Table 7.2 shows a selection of QTL for salinity tolerance traits identified in species other than Arabidopsis by bi-parental mapping.

Table 7.2: List of QTL analyses for salinity tolerance on bi-parental mapping populations in species other than Arabidopsis.[1]

Species	Reference
Barley (*Hordeum* ssp.)	(Ellis *et al.* 2002, Ellis *et al.* 1997, Mano and Takeda 1997, Nguyen *et al.* 2013, Rivandi *et al.* 2011, Shavrukov *et al.* 2010, Xu *et al.* 2012a, Xue *et al.* 2009, Zhou *et al.* 2012)
Rice (*Oryza* ssp.*)*	(Alam *et al.* 2011, Ammar *et al.* 2009, Bonilla *et al.* 2002, Cheng *et al.* 2012, Ghomi *et al.* 2013, Gong *et al.* 2001, Haq *et al.* 2010, Koyama *et al.* 2001, Lee *et al.* 2007, Lin *et al.* 2004, Prasad *et al.* 2000, Thomson *et al.* 2010, Tian *et al.* 2011, Wang *et al.* 2012a, Wang *et al.* 2012b, Zhang *et al.* 1995)
Wheat (*Triticum* ssp.)	(Byrt *et al.* 2007, de León *et al.* 2011, Genc *et al.* 2013, Genc *et al.* 2010, Lindsay *et al.* 2004, Ma *et al.* 2007, Quarrie *et al.* 2005, Xu *et al.* 2013b, Xu *et al.* 2012b)
Citrus grandis and *Poncirus trifoliata*	(Tozlu *et al.* 1999a, Tozlu *et al.* 1999b, Tozlu *et al.* 2002)
Mimulus guttatus	(Lowry *et al.* 2009)
Soybean (*Glycine max*)	(Ha *et al.* 2013, Hamwieh *et al.* 2011, Hamwieh and Xu 2008, Tuyen *et al.* 2010, Tuyen *et al.* 2013)
Tomato (*Solanum* ssp.)	(Asins *et al.* 2010, Villalta *et al.* 2008)
Cucumber (*Cucumis sativus*)	(Kere *et al.* 2013)
Chickpea (*Cicer arietinum*)	(Vadez *et al.* 2012)
Medicago trunculata	(Arraouadi *et al.* 2012, Arraouadi *et al.* 2011)

[1] List includes selected studies only.

Arabidopsis is a good organism to perform QTL analyses due to the ease of generating mapping populations and the ease to design new markers as the genome of multiple ecotypes has now been sequenced. A vast number of QTL analyses have been performed in Arabidopsis for different abiotic stresses, such as salt, drought, light and temperature; a comprehensive review was carried out by Lefebvre (2009). QTL analyses regarding salinity tolerance traits in Arabidopsis have for example been performed by (Buescher *et al.* 2010, DeRose-Wilson and Gaut 2011, Quesada *et al.* 2002, Ren *et al.* 2010, Roy *et al.* 2013).

These examples show that QTL analysis is a successful method, but for the approach to work, there are several key factors required: 1) A measurable, quantifiable phenotype; 2) two accessions or closely related species which can interbreed to produce a large number of mapping lines; 3) The

ability to differentiate between the DNA of the two parents using DNA markers and the ability to locate those markers on either a genetic or physical map; and 4) a strong QTL analysis algorithm to identify the loci significantly linked to the desired phenotype. These factors are briefly described below.

7.2.1 Phenotype for QTL analysis

QTL analysis is based on evaluating phenotypes in a population. The investigated phenotype must be heritable and measurable as a quantitative phenotype using interval numbering. Many morphological phenotypes such as height, grain number (Xiao *et al.* 1995), fruit size (Frary *et al.* 2000) or floral characteristics, such as petal or sepal length (Juenger *et al.* 2000), to name just a few, have been used to identify QTL and underlying genes. Morphological data were initially used in these experiments, as they are easy to access and easy to measure quantitatively. For studies in salinity tolerance phenotypes such as shoot Na^+ concentration (Shavrukov *et al.* 2010) and biomass (Genc *et al.* 2010) are often used. Recently, expression QTL (eQTL) mapping has been used to identify important loci. eQTL mapping makes use of large amounts of transcriptional data as the quantitative phenotype to compare with the genetic map. Particularly the use of microarray data has been shown useful for eQTL studies, and is not just limited to plants (Doerge 2002, Gibson and Weir 2005, Jansen and Nap 2001, Schadt *et al.* 2003). Large sets of microarray data from Arabidopsis and barley have been used for eQTL analysis for a variety of traits (Keurentjes *et al.* 2007, Potokina *et al.* 2008, West *et al.* 2007). The variation in gene expression between organisms, ecotypes and species is abundant, heritable and can be complex (Brem and Kruglyak 2005, Brem *et al.* 2002, Morley *et al.* 2004, Schadt *et al.* 2003), giving numerous opportunities to study transcript abundance, that do not have to result in a morphological measurable phenotype.

7.2.2 Mapping populations for QTL analysis

QTL analysis also relies on a good quality mapping population. Recombinant inbred lines (RILs), F_2, doubled haploid lines and backcrossed inbred lines can be used as mapping populations (Yano 2001). A broad list of recombinant inbred lines and F_2 populations for Arabidopsis are listed by the Institut National de la Recherche Agronomique, France (Sennesal, http://dbsgap.versailles.inra.fr/vnat/). RILs are widely used for QTL mapping as this kind of mapping population is considered to be most useful. Members from the same recombinant inbred line are genetically identical, thereby allowing comparison of the exact same genotype in different treatments as well as the opportunity to repeat experiments and multiply seed material. RILs are produced by crossing two parent ecotypes, followed by the creation of inbred lines from the resulting F_1 through

single line decent, so that the marker-QTL linkage is in linkage disequilibrium (Kearsey 1998). Linkage disequilibrium describes the non-random association of genes (alleles), which leads to the observation that some gene- (allele-) combinations are seen more or less frequently than expected when randomly inherited (Li 1955). It is important when producing a RIL population to have a large number (hundreds) of individual lines. The more lines in the population, the more chances of recombination in the genome are possible and the more precise the QTL can be mapped to the location of the gene of interest.

To link the phenotype observed in the plant to regions in the genome, a set of genetic markers is required. Individual organisms and species all differ slightly in their genomic sequence. Genetic markers which recognise these differences can be used to distinguish between the genomes of two individuals (Tanksley 1983). For QTL analysis, genetic markers are used to identify the parental origin of the genomic region in the individuals of the RIL. A genetic map can then be made of each individual, identifying from which parent the fragments of DNA came from. The most commonly used genetic markers for Arabidopsis are DNA markers, which occur as insertion/deletions (indels), single nucleotide polymorphisms (SNPs) or simple sequence repeats (SSRs). High resolution melt PCR (Liew *et al.* 2004) or Kompetitive Allele Specific PCR (KASP) (Semagn *et al.* 2013) are fast and efficient technologies to detect for differences like SNPs in DNA sequences. Other approaches include cleaved amplified polymorphic sequence (CAPS) and derived cleaved amplified polymorphic sequence (dCAPS) markers. These allow SNPs to be identified as a result in a loss or gain of a restriction enzyme recognition site in a PCR amplified DNA fragment (Konieczny and Ausubel 1993, Neff *et al.* 1998). Simple sequence repeats (SSR) are PCR amplified and distinguished by the size of the PCR fragment (Litt and Luty 1989) and allele-specific primer-PCR (ASP-PCR) uses primers that amplifies DNA parent specific (Hirotsu *et al.* 2010). Other markers such as random-amplified polymorphic DNA (RAPD), amplified fragment length polymorphism (AFLP) and restriction fragment length polymorphisms (RFLP) are known, but not adequate for this purpose as random sequences are amplified (Collard *et al.* 2005), resulting in the whole DNA being examined instead of obtaining information for a specific genomic region.

To design markers, the genomic data of a species is determined using, for example, DNA libraries or deriving information from related species (Liu 1997). This information is used to design markers, to neutral regions of DNA which are polymorphic between the parents analysed. Recombination frequencies of the analysed markers are subsequently used to determine the order of markers and generate linkage maps (Collard *et al.* 2005). For Arabidopsis, the genome sequence of a number of accessions has been determined and genome wide SNP analyses have been performed for most accessions, allowing the straightforward generation of SNP markers (Törjék *et al.* 2003). Markers

based on SNPs are simple to use, but have the disadvantage that the sequence information of the DNA region needs to be known before the markers can be designed. In the case of Arabidopsis, the SNPs of many accessions are known (Clark *et al.* 2007), enabling the design of new markers without the need for re-sequencing.

7.2.3 Detection of QTL with computer programs

The amount of data processing which is necessary for QTL identification is vast; therefore, the analysis is done by computer programs, which may use three different analysis methods: single-marker analysis, simple interval mapping and composite interval mapping, which are outlined by Liu (1998) and Doerge (2002). The difference between the methods lies in the algorithm used to map the QTL and in their precision and ability to detect a QTL. Single-marker analysis is the simplest method and simply compares the phenotype with the genotype at that marker. It has the advantage that information regarding the position of the marker on the genetic map or its relation to other markers is not required. The disadvantage is that if the gene responsible for the desired phenotype is some distance between markers then a QTL may not be detected. Simple interval mapping (SIM) is statistically more powerful, as it tests for QTL in multiple analysis points between adjacent markers. This has the advantage over single marker analysis as it can detect QTL, which are some distance between markers, however, the disadvantage is that the order of markers along a chromosome (linkage group) must be known. Composite interval mapping (CIM) is a more powerful version of SIM, however, it also includes markers in other positions of the genome in the analysis to take into account the influence of other genomic regions on the plant phenotype. This further improves the detection of QTL and often results in more narrow defined intervals than those observed with SIM. As with SIM, CIM requires the location of markers on a linkage map for the analysis to take place.

Two programs commonly used for QTL mapping are MapManagerQTX (Manly *et al.* 2001) and WinQTLCartographer (Wang *et al.* 2010). The graphic visualisation of the QTL analysis is similar for both programs – a graph with the distance along the chromosome plotted against the level of significance that the region on the chromosome is significantly related to the phenotype of the plant. In more recent years the open-source software package R has been commonly used, due to its flexibility and ability to handle complex mapping population structures, such as advanced backcrossed double haploid populations.

Two scores are commonly used to evaluate a QTL, both of which are a statistical estimate of the region of DNA in question being associated with the phenotype by chance. First, the likelihood of the ratio statistic (LRS) and, second, the logarithm of odds (LOD), which is LOD = LRS ÷ 4.6 (Liu 1997). The LOD depends on the possibility of recombination and is therefore dependent on the genome

size and the type of mapping population (van Ooijen 1999). A genome-wide significance level of 5 % (p= 0.05) is usually applied which results in a threshold LOD of 2.1-2.5 for a typical Arabidopsis recombinant inbred mapping population (Lisec *et al.* 2009).

In addition to indicating regions of DNA significantly linked to the observed phenotype, QTL mapping programs also give other useful information (Manly and Olson 1999):

1) The additive effect contains information about the parent from which the QTL comes from. Depending on whether the value is positive or negative the trait is caused by one or the other parent. Accordingly, the additive effect can be expressed as:

[(mean of occurrence allele parent one) – (mean of occurrence allele parent two)] /2 (Manly and Olson 1999).

2) The heritability (H) of the trait, which is defined as the ratio of genotypic and phenotypic variance and describes the genetic influence on the phenotype.

3) The % phenotypic variation describes how much of the phenotype is explained by the QTL in question. One or more QTL can be obtained along the chromosomes from the analysis.

7.2.4 Fine mapping of the QTL interval

The outcome of a QTL analysis is the identification of an interval on the genome, spanning from a few hundred to thousands of genes. To identify the candidate gene, this interval needs to be narrowed down, which is done by further analysing the DNA region in that interval by introducing more parent specific markers. Key to the success of fine mapping is having mapping lines with recombination across the QTL interval. As a 1 centi Morgan (cM) genetic distance is essentially a 1% chance of having a recombination event within that interval, mapping populations in the region of 400 RILs are often required to fine map to genetic distances of 0.25 cM. For Arabidopsis, a large number of genes are already annotated (The Arabidopsis Information Resource database (www.arabidopsis.org)), potentially facilitating the selection of candidate genes from a large interval if further fine mapping is not possible, due to having insufficient lines. If the interval has be narrowed down further, it may be necessary to produce more RILs or to backcross selected RILs to one of the parents in order to obtain near isogenic lines (NILs), which ideally introduces more recombination in the interval of interest. Further phenotyping and genotyping would be required. This systematic decrease in genetic distance is done until a candidate gene within that interval can be selected, which is likely to be the gene responsible for the observed trait.

7.3 Chapter aims

The aims of this chapter are to 1) develop a screening assay based on alterations in gene expression to determine whether C24 is non-responsive when compared to Col-0 after salt application; 2) develop an assay which allows the fast, robust and reliable screening of a mapping population to perform QTL analysis.

Approach 1: Analysing changes in the transcription levels of salt responsive genes

- Identification of candidate genes expression is up- or down-regulated upon salt treatment

- Performing salt stress experiments in soil, on MS plates and in hydroponics and test candidate genes with semi-qPCR

Approach 2: Analysing germination of Col-0 and C24 on saline MS media

Approach 3: Analysing root growth when in contact with salt

7.4 Material and methods

7.4.1 Salt stress application in soil grown plants

To evaluate the changes in gene expression that are induced by a short salt stress in soil grown Col-0 and C24, plants were grown for 5 wk in soil without fertilizer as described in section 2.2.4. Watering was discontinued 3 d prior to salt treatment to ensure the soil moisture is low, but the soil contains enough moisture to avoid drought stress. The treatment was applied by flooding the tray containing the pots, with 0 mM, 50 mM, 100 mM or 150 mM NaCl. After exactly 24 h, three of the last fully expanded leaves were removed from the plant using tweezers and collected in 10 mL tubes. The tubes were snap frozen in liquid nitrogen and stored at -80 °C until required (section 7.4.5).

7.4.2 Salt stress application for plants grown on MS-plates

Three different methods of exposing Arabidopsis to salt stress on plates containing ½ strength MS-agar (MS-plates) were tested. 1) to determine the change in gene expression upon salt stress, plants were transferred as 2 wk old seedlings onto MS-plates supplemented with salt; 2) to compare the germination rate between ecotypes, seeds were directly placed onto MS-plates containing various amounts of NaCl; and 3) to compare the growth of roots when growing towards NaCl containing MS-media, seedlings were grown on MS-plates for 10 d, then the bottom half of the plate was replaced with MS-agar containing various amounts of NaCl. The three methods are described in further detail below:

7.4.2.1 Transfer of Arabidopsis seedlings onto MS-plates containing NaCl

Col-0 and C24 plants were grown for 2 wk vertically on MS-plates in a short day growth room (see section 2.2.3). To apply the salt treatment, seedlings were carefully removed from the plate with bent tipped tweezers, to avoid tissue damage, and positioned on MS-plates supplemented with or without 150 mM NaCl and 1.725 mM $CaCl_2$. The addition of $CaCl_2$ is necessary to maintain Ca^{2+} activity which is reduced by the presence of Na^+. The required amount of additional Ca^{2+} was calculated using Visual MINTEQ 2.30 (KTH, Department of Land and Water Resources Engineering, Stockholm, Sweden, http://www.lwr.kth.se/English/OurSoftware/vminteq/download.html). This method of transfer was chosen, as opposed to using nylon mesh or similar techniques, to allow direct contact of the roots with the salt containing media. Accordingly, plates had to be placed vertically to allow roots to grow on the agar surface without penetrating the agar. The entire shoot and root were collected after 24 hours of salt treatment in 2 mL microcentrifuge tubes, snap frozen in liquid nitrogen and stored at -80 °C until required (section 7.4.5)

7.4.2.2 Germination of Arabidopsis on MS-plates containing NaCl

Col-0 and C24 seeds were germinated on MS-plates, supplemented with 0, 25, 50, 75, 100, 125 and 150 mM NaCl (7.5.2) and the appropriate amount of $CaCl_2$ to maintain Ca^{2+} activity (section 7.4.2.1). Plates were placed into a short day growth room and germination was evaluated after 7 d. For each NaCl concentration, 20 to 50 seeds were sown.

7.4.2.3 Growth of roots towards NaCl containing media

Surface sterilised seeds of Col-0 and C24 were placed onto MS-plates (section 2.2.3) and incubated vertically in a short day growth room. Seedlings were imaged using a scanner 4 d after germination. A NaCl gradient was generated by removing the media in the bottom half of the plate with a spatula (diagonally across the plate) and replacing it with ½ strength MS-agar supplemented with 0 mM, 50 mM, 100 mM or 150 mM NaCl and the appropriate amount of $CaCl_2$ (section 7.4.2.1) (Figure 7.1). Plates were returned to the growth chamber and growth phenotypes were recorded 12 d after germination for Col-0 and 14 d after germination for C24. For each NaCl concentration and ecotype, two plates with each 10 seedlings were assessed.

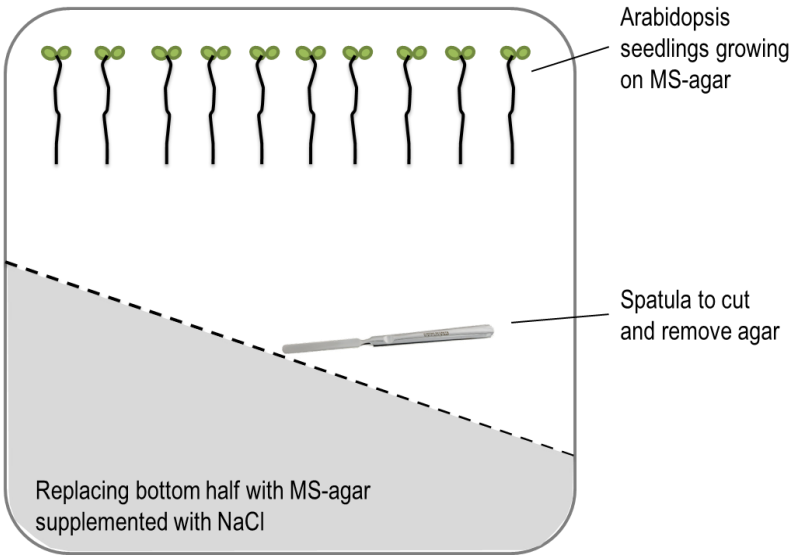

Figure 7.1: Diagram of Arabidopsis root growth assay on salt.

Arabidopsis seedlings were grown vertically on MS-agar for 4 d after germination, then the bottom half of the agar was removed using a spatula and replaced with MS-agar containing 0, 50, 100 or 150 mM NaCl and the appropriate amount of $CaCl_2$. Plants were grown for further 12 to 14 d before evaluating root growth towards the NaCl containing area.

7.4.4 Assessing Col-0 and C24 using hydroponics

Col-0 and C24 were grown hydroponically as described previously (section 2.2.4). 100 mM NaCl salt stress was applied by dissolving the desired amount of NaCl and $CaCl_2$ (section 7.4.2.1) in 500 mL of growth solution, which was taken out of the tank, and poured back into the tank under stirring. The salt treatment was applied 1 h after the light cycle commenced. The last fully expanded leaf was removed and snap frozen in liquid nitrogen for RNA analysis. Roots were washed in 10 mM $MgSO_4$ to remove nutrient solution and contaminating salt, dried for exactly 3 sec between paper towels and snap frozen in liquid nitrogen for RNA analysis. Samples for RNA analysis were taken at 0, 30 min, 12 h, 24 h and 2 d after stress application. RNA extraction and cDNA synthesis were performed as described previously (section 2.5) and qPCR as described below (section 7.4.5).

7.4.5 Processing of samples with semi-qPCR or qPCR

Tissue samples, collected as described above (7.4.1, 7.4.2 and 4.5.1), were used for RNA extraction (section 2.5.1), followed by cDNA synthesis (section 2.5.2). A very important step during cDNA synthesis for qPCR is to ensure RNA is present in equal amounts. This will reduce the variation between samples, i.e. in transcript abundance of control genes such as *Actin2* and improves reliability of semi-qPCR. This was done by determining the concentration of RNA using agarose gel electrophoresis and spectrophotometry using a NanoDrop instrument (Thermo Fisher Scientific Australia Pty Ltd., Scoresby, Australia).

Semi-qPCR and qPCR were performed as described previously (section 2.5.3 and 2.5.4) with primers listed in Table 7.3. An example of a semi-qPCR image is presented in Figure 7.2. From this image the band intensities were measured using the image analysis program GIMP 2.6.11 GNU Image Manipulation Program (www.gimp.org). An example of pixel analysis is presented in Figure 7.3. The result section will show values of normalised band intensities. These values are obtained by dividing the band intensity corresponding to the gene of interest by the band intensity corresponding to the control gene at a given PCR cycle where band intensities increase linearly. Therefore, this window of linear increase in band intensity had to be determined for every gene of interest and treatment separately.

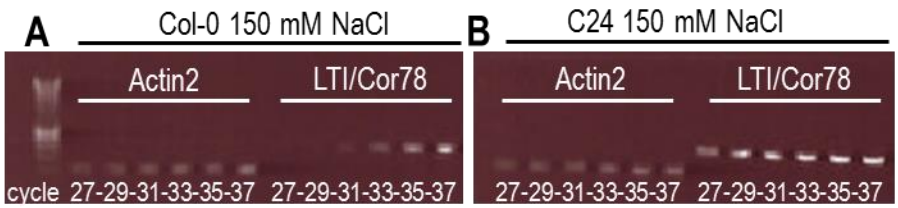

Figure 7.2: Example of agarose-gel image resulting from semi-qPCR of transcripts of cDNA derived from salt treated Col-0 and C24 shoot tissue.

Amplified fragments correspond to transcripts of *Actin2* and *LTI/Cor78* with different PCR cycles as indicated by the numbers below the bands. This is a subset of the image used for analysis presented in Figure 7.3.

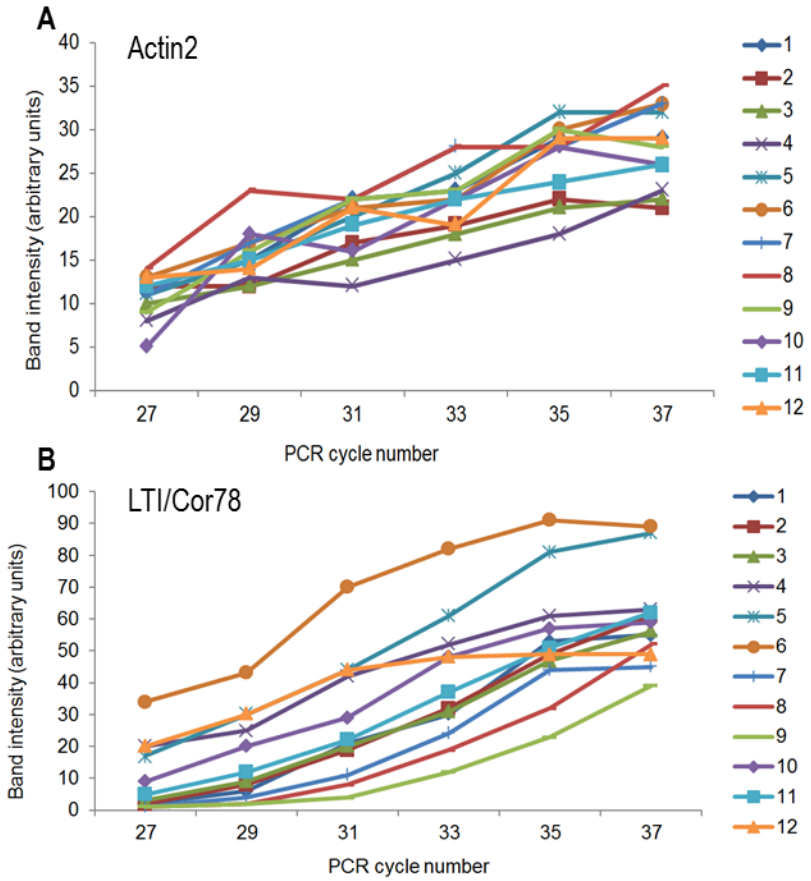

Figure 7.3: Example of semi-qPCR analysis of transcript of cDNA derived from salt treated Col-0 and C24 shoot tissue.

Col-0 and C24 seedlings were grown on MS plates for 2 wk before transfer onto plates containing MS- agar ±150 mM NaCl. Shoot tissue was used for cDNA synthesis analysed by semi-qPCR. PCR products of (A) *Actin2* and (B) *LTI/Cor78* transcripts, derived from a range of cycle numbers, were subject to gel electrophoresis. Values for band intensities were extracted from the obtained agarose gel image using the image analysis program GIMP 2.6.11. Background signals were subtracted. Sample legends 1-3: Samples derived from Col-0 seedlings with control treatment, 4-6: Samples derived from Col-0 seedlings with 150 mM NaCl treatment, 7-9: Samples derived from C24 seedlings with control treatment and 10-12: Samples derived from C24 seedlings with 150 mM NaCl treatment.

7.5 Results

7.5.1 Transcription analyses of salt responsive genes

7.5.1.1 Identification of candidate genes

The aim of this section was to identify candidate genes from the literature that are up- or down-regulated during salt treatment and are appropriate to be used in a screening assay for a mapping population using semi-qPCR. The transcript abundance of genes, differentially expressed during salt stress, is being used as a marker to evaluate the salt responsiveness of the two ecotypes Col-0 and C24.

Previously, the expression of a number of genes (*AtAVP1, AtNHX1, AtSOS1 and AtHKT1;1*) were found to be substantially changed in the ecotype Col-0, but not in C24 (Jha *et al.* 2010). These genes were initially used to test for responsiveness and the list was extended to other candidate genes from the literature (Table 7.3). The primer pairs were chosen towards the 3′ end of the open reading frame and located on either side of an intron (intron spanning) so that if contaminating gDNA was present, a larger fragment was amplified. Alternatively one of the primers was located over an exon-intron-exon boundary, meaning that the primer cannot anneal to genomic DNA because of the presence of the intron - the primer can still anneal to cDNA since introns are not present.

The gene analysis tool Genevestigator (Zimmermann *et al.* 2004) was used to investigate the salt responsiveness of candidate genes. A selected subset of Genevestigator results is presented in Figure 7.4. It contains information from a microarray study by Kilian *et al.* (2007) where the Arabidopsis ecotype Col-0 was grown hydroponically for 18 days before application of 150 mM NaCl; root and shoot samples were then collected at six time points over an 24 h period and used for microarray analysis using an Affymetrix ATH1 (22 K) chip (Kilian *et al.* 2007). The 24 hour time point is depicted in Figure 7.4 for the candidate genes in Table 7.3. The Genevestigator “Sample tool” was used to display gene expression strength under the tested conditions. Besides illustrating the fold change in gene expression it also indicates the overall level of expression (low, medium or high). This provides information that can be incorporated into semi-qPCR analysis. For instance, a gene with low expression will need a higher number of PCR cycles to be visible on an agarose gel as compared to a gene with high expression.

Table 7.3: List of genes and corresponding primers that were used for semi-qPCR and qPCR to test for salt responsiveness. Source describes whether the primers were already available at the ACPFG or had to be designed using Primer 3

Gene locus	Other name	Primers (forward (FW) and reverse (RV))	Source	Reference
At1g78920	*AtAVP1*	FW: GCAGCTCTTAAGATGGTTGAA RV: AGAGGTGTGAGCATGACAAGG	ACPFG qPCR Database	(Jha *et al.* 2010)
At2g01980	*AtSOS1*	FW: CTGCTTGCTACATTTCTGCTG RV: TGCTTCCTCTCCTTCCTTTTC	ACPFG qPCR Database	(Jha *et al.* 2010)
At5g27150	*AtNHX1*	FW: ACTCATAAGCTACCTATTACCG RV: GGTCTCGAGTTACTAAGATCAGG AGGGTTTCTC	ACPFG qPCR Database	(Jha *et al.* 2010)
At4g10310	*AtHKT1;1*	FW: TGCAAACTGCGGATTTGTCC RV: TGAGCAAAACCAAGAAGCAAGG	ACPFG qPCR Database	(Jha *et al.* 2010)
At5G52310	*LTI/Cor78*	FW: CAAAGTTACTGATCCCACCAAAGAAG RV: CGGCGAATCCTTACCGAGAA	designed using Primer 3	(Kreps *et al.* 2002)
At1g78070		FW: GCTGAGCCAGCGGACTTTGT RV: CGAGTGGTTTCGCTTCCTGTT	designed using Primer 3	(Takahashi *et al.* 2004)
At5g15970	*Kin1*	FW: TATAAACCATTAAGCCCACATCTC RV: TCCTTCACGAAGTTAACACCTC	designed using Primer 3	(Takahashi *et al.* 2004)
At3g18780	*Actin2*	FW: TGAGCAAAGAAATCACAGCACT RV: CCTGGACCTGCCTCATCATAC	ACPFG qPCR Database	(Roy *et al.* 2008)

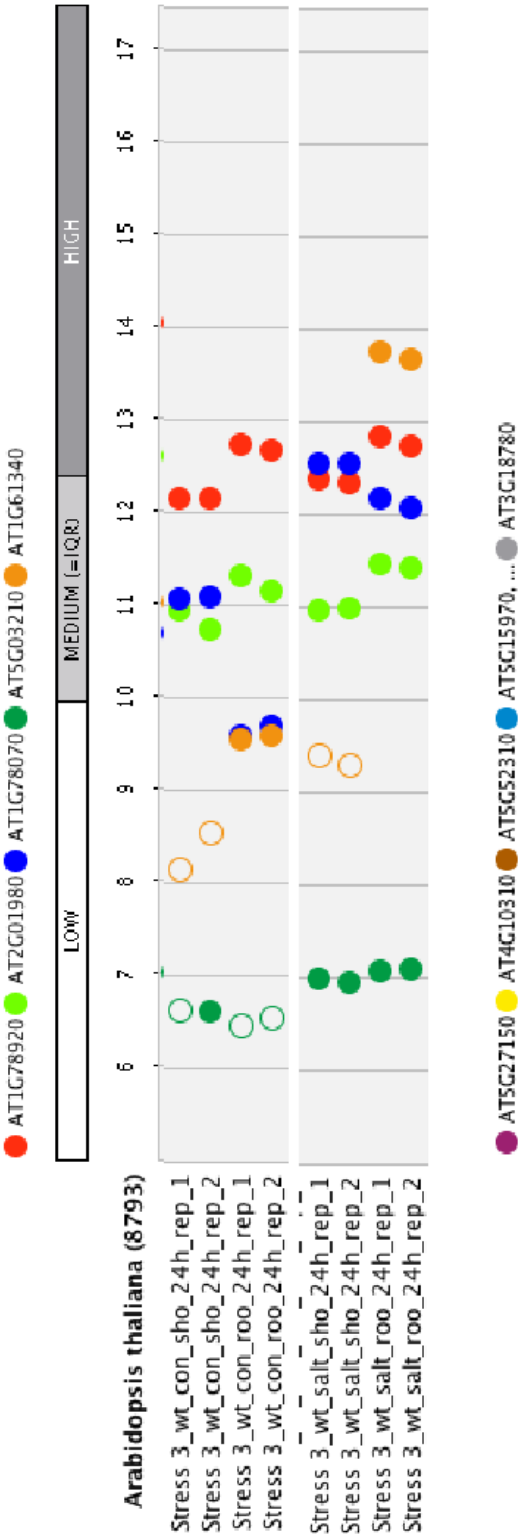

Figure 7.4: Output of Genevestigator analysis for candidate genes using the built in application "Sample".

The selected reference study by Kilian et al. (2007) used 18 d old hydroponically grown Col-0 (wt) seedlings, for treatment with 0 mM NaCl as control (con) or 150 mM NaCl (salt). Shoot (sho) and root (roo) samples were analysed separately. Full circles indicate the signal is "present" and empty circles indicate the signal in close to the background and therefore called "absent". *At1g78920* is *AtAVP1*, *At2g01980* is *AtSOS1*, *At5g27150* is *AtNHX1*, *At4g10310* is *AtHKT1;1*, *At5G52310* is *LTI/Cor78*, *At1g78070* has no other name and *At5g15970* is *Kin1*.

7.5.1.2 Testing candidate genes in salt stressed plants grown in soil

A number of salt responsive candidate genes were identified from the literature (section 1.3.1). To confirm whether these genes were similarly salt responsive in the experimental setup in this study, a short NaCl treatment time of 24 hours was chosen for the experiments. A longer NaCl treatment time could result in accumulation of Na^+ in the shoot and root tissue, initiating other effects such as ionic stress, which will compound issues with analysis. In the chapter 4 it was shown that after only 2 d of NaCl treatment, Na^+ is accumulating in the plant (section 4.6.1).

The aim of this chapter is to develop an easy and robust screening assay, and the assessment of soil grown plants allows for reasonable high throughput analysis of a mapping population and easy handling. A favourable method to evaluate transcript abundance is semi-qPCR, because of its low cost compared to qPCR. However, for optimal semi-qPCR performance a large difference in transcript abundance between treatments and also between ecotypes is desirable. NaCl treated soil grown plants were subject to semi-qPCR analysis using primers for the two genes *AtSOS1* (Figure 7.5) and *AtAVP1* (Figure 7.6). The band intensity is representative of transcript abundance of the analysed gene. For Col-0, transcript levels of *AtSOS1* are lower at 0 mM NaCl as compared to NaCl treated samples (Figure 7.5). For C24, *AtSOS1* levels do not appear to change substantially (Figure 7.5). When *AtAVP1* expression is analysed, transcript abundance only increases marginally after salt treatment for both ecotypes. Since no clear difference in transcript levels was observed using semi-qPCR, qPCR was performed validating that expression levels of *AtAVP1* did not change substantially (Figure 7.7). The gel image (Figure 7.8) illustrates transcript abundance of other selected genes after 150 mM salt treatment in Col-0 and C24. Transcript levels of the control gene *Actin2* appear equal in both treatments, but no substantial difference in transcript abundance of other genes can be observed when comparing salt treated Col-0 and C24 plants.

The differences in expression levels for *AtAVP1* and *AtSOS1* were inconclusive in soil grown Col-0 and C24 plants treated with NaCl for 24 h. QPCR results obtained for *AtAVP1* transcript abundance are not consistent with semi-qPCR results, indicating that that this system is not suitable for use as a screening assay and another method of salt stress was considered, where plants are grown on plates containing MS-agar and are transferred onto media supplemented with NaCl.

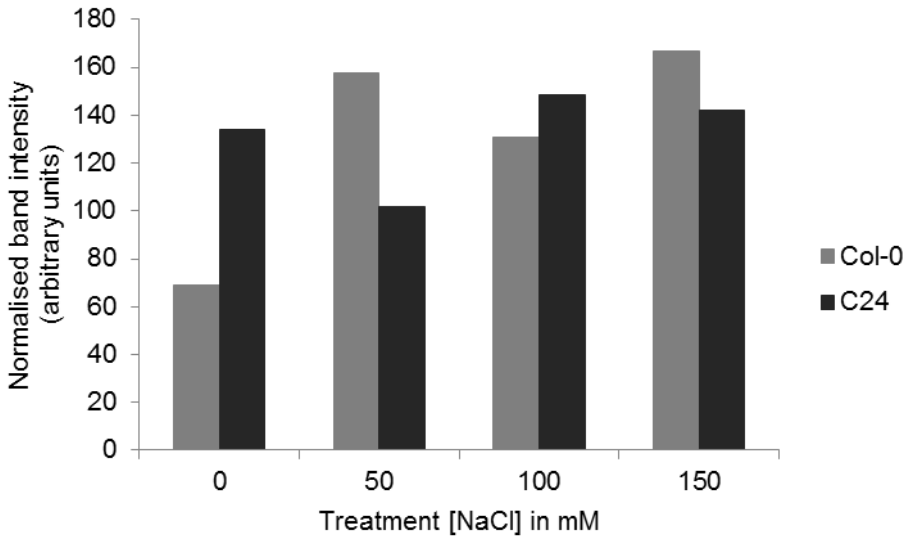

Figure 7.5: *AtSOS1* transcript abundance using semi-qPCR, in soil grown Col-0 and C24 plants subjected to 24 h of 150mM NaCl.

AtSOS1 transcript abundance determined from Col-0 (light grey bars) and C24 (dark grey bars) soil grown plants treated with NaCl for 24 h using semi-qPCR. Data presented correspond to the band intensity of the PCR product present at cycle 29, normalised with the band intensity corresponding to the abundance of *Actin2* transcripts. Presented are data for one biological replicate.

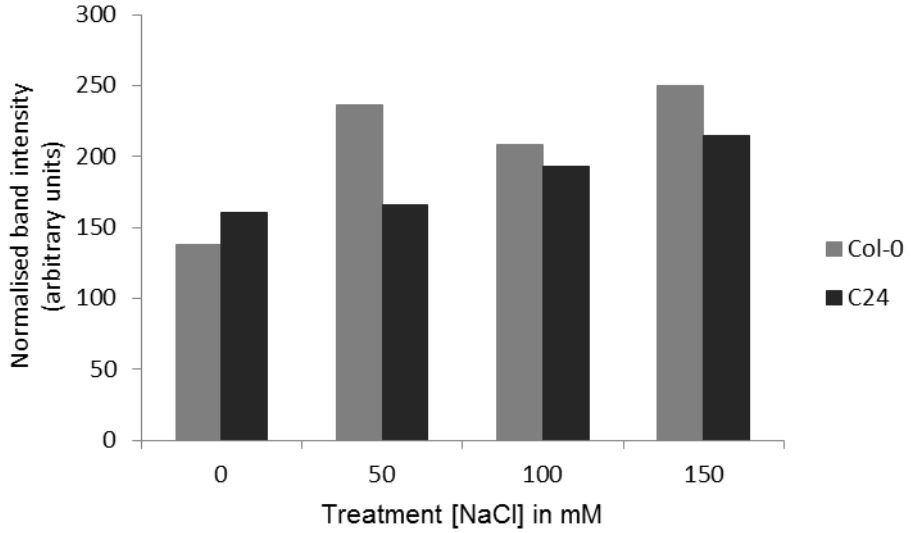

Figure 7.6: *AtAVP1* transcript abundance using semi-qPCR, in soil grown Col-0 and C24 plants subjected to 24 h of 150mM NaCl.

AtAVP1 transcript abundance determined from soil-grown Col-0 (light grey bars) and C24 (dark grey bars) plants treated with NaCl for 24 h using semi-qPCR. Data presented correspond to band intensity of PCR product present at cycle 27, normalised with band intensity corresponding to abundance of *Actin2* transcripts. Presented are data for one biological replicate.

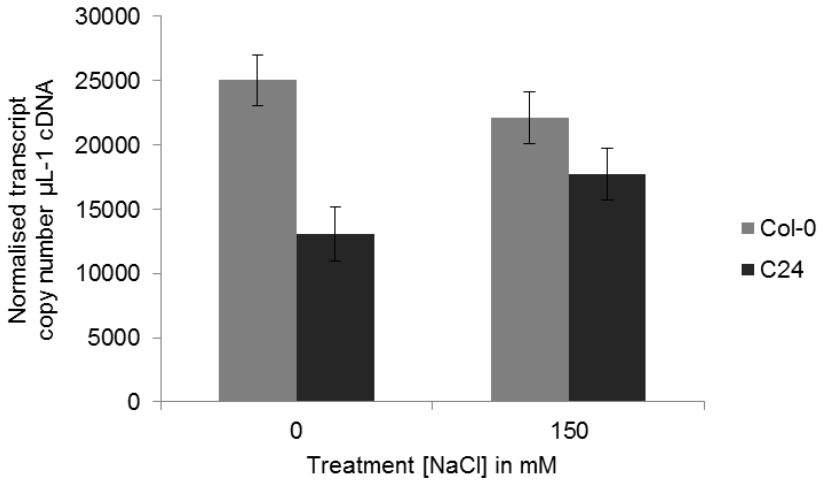

Figure 7.7: *AtAVP1* transcript abundance using qPCR, in soil grown Col-0 and C24 plants subjected to 24 h of 150mM NaCl.

QPCR analysis of *AtAVP1* expression in soil-grown Col-0 (light grey bars) and C24 (dark grey bars) plants under control treatment (0 mM NaCl) and salt treatment (150 mM NaCl) for 24 h. Error bars indicate SD of three biological replicates.

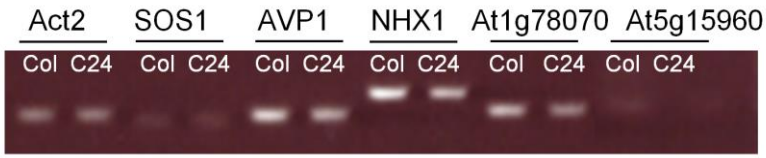

Figure 7.8: Gel image of semi-qPCR on samples derived from soil-grown Col-0 and C24 plants treated with 150 mM NaCl for 24 h.

Transcript levels tested for genes indicated above the corresponding bands. No substantial difference in transcript levels of NaCl treated Col-0 and C24 plants visible.

7.5.1.3 Testing candidate genes in salt stressed plants grown on MS agar plates

Results from the previous section (7.5.1.2) have shown that the treatment of soil grown plants with up to 150 mM NaCl for 24 h did not lead to a conclusive results regarding induction of gene expression in Col-0 or C24. The advantage of using MS-agar plates for application of salt stress is that the roots come in direct contact with the media containing NaCl immediately upon transfer. It also allows the analysis of root and shoot tissue for induction of salt responsive genes, as opposed to soil grown plants, where the use of root tissue would involve thorough cleaning, which may impact root RNA integrity.

QPCR analysis for the four genes *AtAVP1, AtSOS1, AtHKT1;1* and *LTI/Cor78* was performed on root and shoot samples of control and salt treated seedlings (Figure 7.9). No substantial differences in *AtAVP1* gene expression (Figure 7.9 A) are visible when comparing control and salt treatments in Col-0 and C24 in the shoot and root. Gene expression for *AtSOS1* (Figure 7.9 B) is doubled in Col-0 shoot samples after NaCl treatment but does not change substantially in C24. Expression of *AtHKT1;1* (Figure 7.9 C) is substantially decreased in Col-0 and C24 shoot samples after NaCl treatment. It has to be noted that overall expression levels of *AtHKT1;1* (Figure 7.9 C) are very low and values around 500 copy numbers per µL of cDNA are within background levels. Expression of *LTI/Cor78* (Figure 7.9 D) is substantially different in Col-0 and C24 shoot and root in response to salt treatment. While expression levels under control conditions are below 20,000 transcripts per µL of cDNA, they are over 900,000 transcripts per µl in Col-0 shoots after salt treatment.

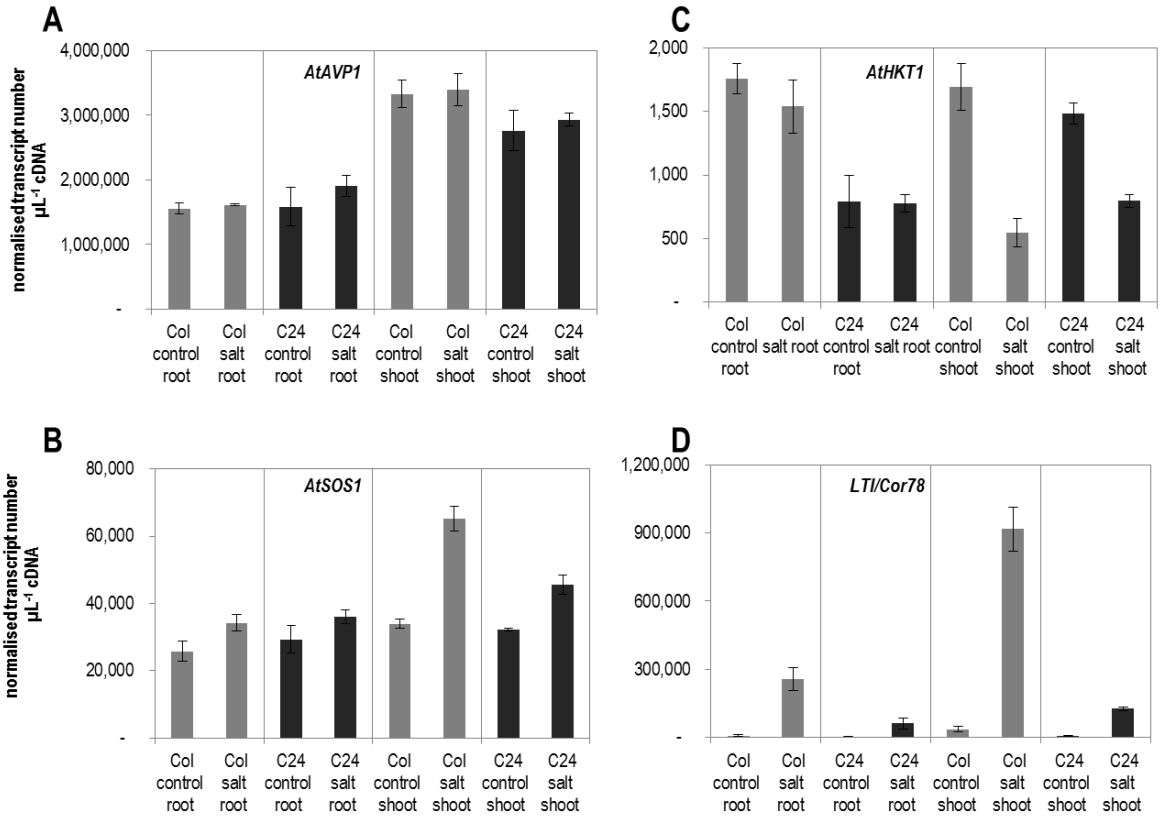

Figure 7.9: QPCR analysis on root and shoot samples of plate grown Col-0 and C24 plants treated with ± 150 mM NaCl for 24 h.

Control treated Col-0 (light grey) and C24 (dark grey) plants (0 mM NaCl) and salt treated plants (150 mM NaCl) were tested for expression of *AtAVP1* (A), *AtSOS1* (B), *AtHKT1;1* (C) and *LTI/Cor78* (D). Error bars indicate SD of three biological replicates.

A substantial induction of *LTI/Cor78* expression can also be found using semi-qPCR on Col -0 shoot samples ±150 mM NaCl treatment (Figure 7.10). The difference between three salt treated Col-0 and C24 seedlings is substantial, but not significant, based on a t-test with three biological replicates that resulted in a *p*-value of 0.0505.

Given the large responsiveness of *LTI/Cor78* expression in Col-0 after salt treatment, this gene was used to test a subset of a Col×C24 mapping population for their salt responsiveness.

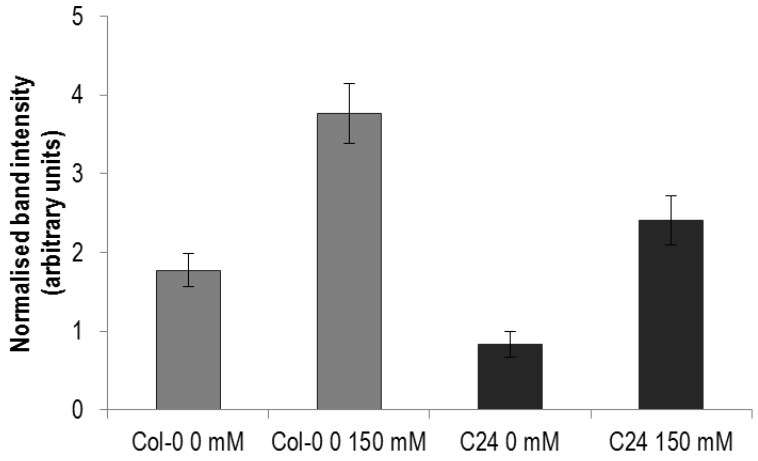

Figure 7.10: *LTI/Cor78* transcript abundance using semi-qPCR, in plate grown Col-0 and C24 plants subjected to 24 h of 150mM NaCl.

LTI/Cor78 transcript abundance in plate-grown Col-0 (light grey) and C24 (dark grey) shoot, as determined using semi-qPCR, in plants treated with ± 150 mM NaCl. Data presented correspond to band intensity of PCR product present at cycle 33, normalised with band intensity corresponding to abundance of *Actin2* transcripts. Error bars indicate S.E.M., n=3.

7.5.1.4 Expression analysis of the candidate gene *LTI/Cor78* in a subset of a Col-0 × C24 mapping population

The gene *LTI/Cor78* was identified as a candidate gene to compare the responsiveness of Col-0 and C24 (section 7.5.1.3), when the plants were subject to 24 h of salt stress on MS-plates and transcript analysis was performed with semi-qPCR. To investigate the genomic locus conferring the non-responsiveness trait in C24, a forward genetic approach was considered. A F_{10} Col-0 × C24 mapping population is available consisting of 209 Col-0 × C24 and 214 C24 × Col-0 recombinant inbred lines, genotyped using 110 evenly distributed framework single nucleotide polymorphism (SNP) markers (Törjék *et al.* 2003, Törjék *et al.* 2006). Both populations are referred to as Col × C24 mapping population. NaCl induced *LTI/Cor78* expression was analysed on a subset of this mapping

population to determine if this provides a suitable, robust screening assay to perform QTL analysis on the entire mapping population.

A subset of the mapping population containing 30 lines was selected based on the following two criteria: selected lines should have a proportion of 50% of the markers from the Col-0 parent and 50% from the C24 parent; and, for each of the 110 loci 15 plants should have the Col-0 genotype and 15 lines should have the C24 genotype.

Out of the subset, four lines were randomly selected, grown on MS-plates, treated with 150 mM NaCl and analysed for changes in *LTI/Cor78* gene expression using semi-qPCR as suggested by the previous section (7.5.1.3). This experiment was repeated several times in the same growth room. Two independent experiments are presented in Figure 7.11. The three biological replicates of salt treated lines are presented separately to illustrate the large variation observed. No difference in *LTI/Cor78* expression can be observed between the parental lines Col-0 and C24, which is in contrast to the previous findings in section 7.5.1.3. The variation in *LTI/Cor78* expression is especially large in salt treated C24 seedlings (Figure 7.11 B). To obtain information wether the variation seen with semi-qPCR analysis is due to weaknesses in the method, qPCR was performed on selected lines of the Col×C24 population. A large difference between biological replicates can be observed (Figure 7.12). When results of semi-qPCR (Figure 7.11 B) are compared with the same samples from qPCR analysis (Figure 7.12), it suggests that there is no consistency between results.

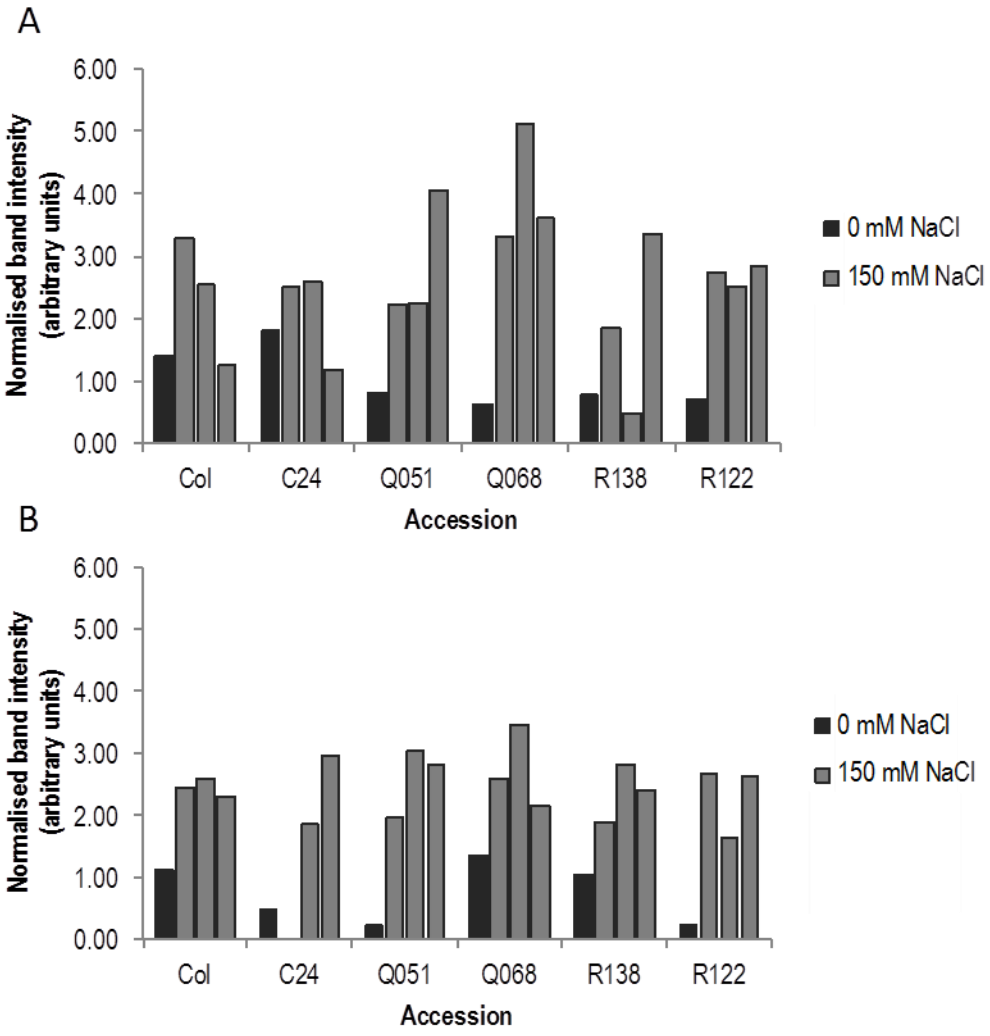

Figure 7.11: *LTI/Cor78* transcript abundance using semi-qPCR, in plate grown Col-0, C24 plants and four lines of the Col × C24 RIL population subjected to 24 h of 150mM NaCl.

LTI/Cor78 transcript abundance determined from Col-0, C24 and four lines of the Col-0 × C24 RIL population after control treatment (dark grey) or 150 mM NaCl (light grey), using semi-qPCR. Three biological replicates for salt treated plants are displayed individually for two independent experiments (A and B). Data presented are normalised with *Actin2* transcript abundance.

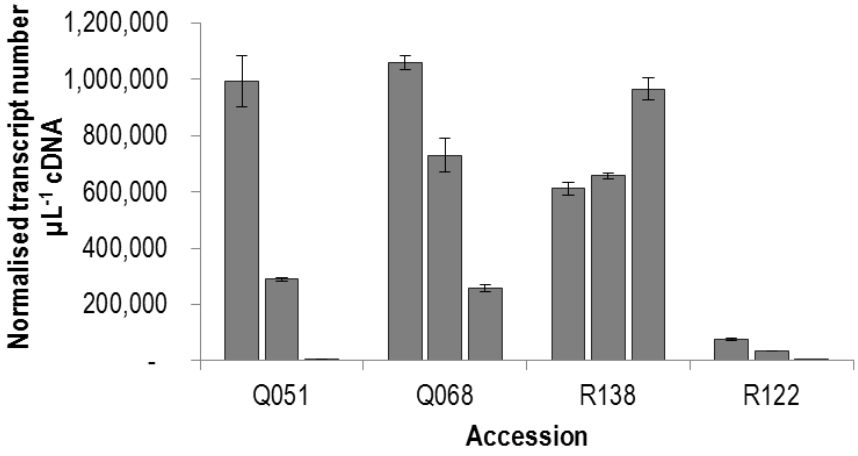

Figure 7.12: *LTI/Cor78* transcript abundance determined using qPCR from four lines of the Col × C24 RIL population after treatment with 150 mM NaCl.

LTI/Cor78 transcript abundance of three biological replicates for salt treated plants is displayed individually. Data presented are normalised with *Actin2* transcript abundance.

The subset of the mapping consisting of 30 lines was analysed using semi-qPCR and qPCR. The qPCR results are presented in Figure 7.13. The three biological replicates for salt treated samples are displayed separately to illustrate the variation. The *LTI/Cor78* transcript number for control samples was consistently low; however, the variation within the same lines in salt treated samples is substantial (Figure 7.13).

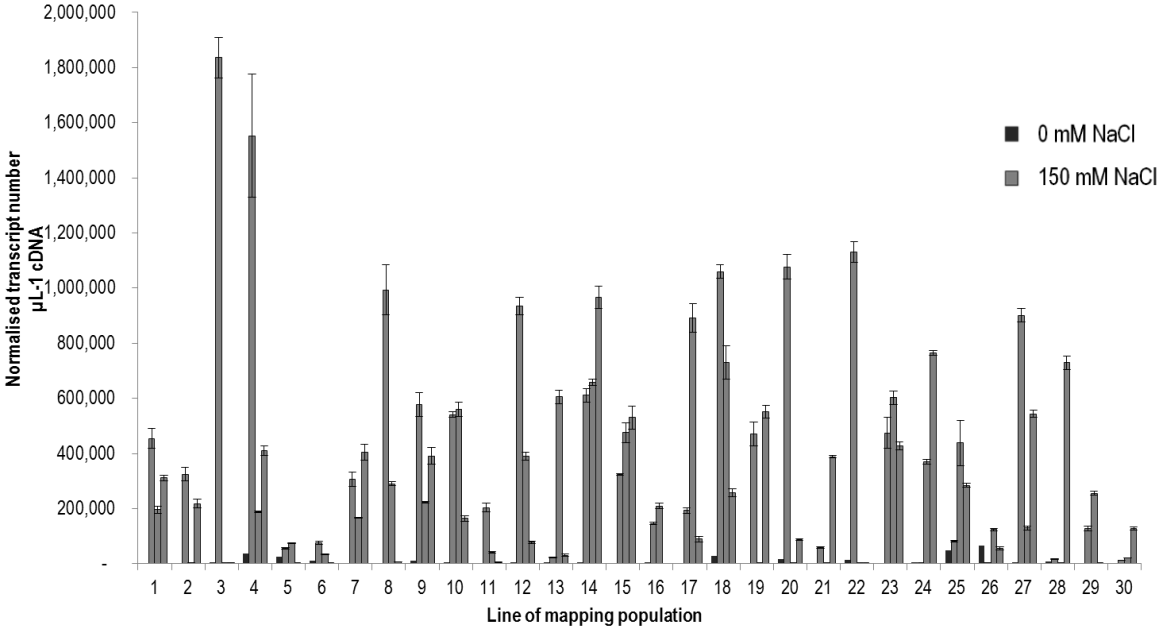

Figure 7.13: Transcript levels of *LTI/Cor78* as determined by qPCR on cDNA derived from 30 lines of the Col × C24 mapping population grown on MS-plates.

LTI/Cor78 transcript abundance in 30 lines of the Col × C24 mapping population subject to control treatment (dark gray bars) and NaCl treatment, three replicates (light gray bars) of. Error bars represent standard error derived from technical replicates of the qPCR experiment, not from biological repeats, these are displayed individually.

7.5.1.5 Testing candidate gene expression in salt stressed plants grown in hydroponics

Although *LTI/Cor78* transcript abundance in salt treated Col-0 and C24 plants on MS-agar plates had been considered suitable to set up a screening assay, the previous section clearly indicates there is great variability in *LTI/Cor78* transcript abundance between biological replicates,. Another approach using hydroponically grown Col-0 and C24 plants was tested. The main advantage of this system is that plants are grown under transpiring conditions and the application of salt is very even with minimal disturbance to the system. While not as high throughput as plate grown plants, hydroponic plants are exposed to fresh air and a constant air movement, which should make them less prone to a touch response, unlike plants grown on agar plates. 5 wk old hydroponically grown Col-0 and C24 plants were exposed to 100 mM NaCl (section 2.2.4, and 4.5.1). Root and shoot samples were collected at 5 time points (0, 30 min, 12 h, 24 h and 2 d) and subject to qPCR analysis (section 7.4.5). Again, the genes *AtAVP1*, *AtSOS1*, *AtHKT1;1* and *LTI/Cor78* were analysed. The analyses show that transcript levels of all four genes are altered upon NaCl treatment in Col-0 and

C24. For *AVP* transcript abundance, values in the root and shoot are quite variable for the control treatment, however when salt treated, a clear increase of transcript levels can be seen in the shoot for C24 and Col-0, while transcript levels in the root initially increase within 12 h to 24 h after treatment and decline after 2 d (Figure 7.14 A). For *AtSOS1*, transcripts levels under control conditions seem variable in C24 shoots, but stable over time in the Col-0 shoot and the C24 and Col-0 root tissue (Figure 7.14 B). After salt stress, *AtSOS1* transcript levels appear to be generally higher compared to the control treatment, more so in Col-0 than C24 (Figure 7.14 B). *AtHKT1;1* transcript levels are variable in C24 and Col-0 shoots under control conditions (Figure 7.14 C). *AtHKT1;1* transcript levels do not change in C24 shoots, and in Col-0 are first increased, then decline. As expected, no *AtHKT1;1* transcripts were observed at all in C24 roots, while transcript levels increase in Col-0 roots with salt treatment (Figure 7.14 C). *LTI/Cor78* transcript levels are consistently low under control conditions in both ecotypes. For Col-0, a clear increase in *LTI/Cor78* transcript levels can be observed in the shoots and the roots after NaCl treatment (Figure 7.14 D). In contrast, C24 transcript levels remain low in the C24 shoot and are only substantially increased in the root 12 hours after NaCl treatment (Figure 7.14 D).

Overall, it is difficult to determine a trend for changes in transcript abundance from the displayed data. It appears that for Col-0, transcript levels of most of these genes are substantially altered within 12 h after salt treatment. For C24, changes in transcript levels can be observed, however the changes are not consistent. Consequently, the time points were grouped and a statistical analysis performed only examining the effect of NaCl treatment on expressions levels in the root and the shoot of both ecotypes (Figure 7.15). The boxplots display the transcript abundance of the indicated genes. The second and third quartiles of the data are displayed by the box, while the line inside the box represents the median. Outliers are displayed as a cross or circle. The letters (a, b or ab) above the boxes indicate the significance at the 0.05 level determined using the Student-Newman-Keuls test. The statistical analysis shows that no significant difference can be found in C24 between the control and NaCl treatment for any of the genes or tissues analysed (Figure 7.15). In contrast, a number of significant differences comparing the control and NaCl treatment are identified for Col-0 (ANOVA, $p = 0.05$). For six out of the eight comparisons, a significant increase in transcript abundance was found between Col-0 control and NaCl treatment, for *AtAVP1* in the root, *AtSOS1* in the shoot, *AtSOS1* in the root, *AtHKT1;1* in the root, *LTI/Cor78* in the shoot and *LTI/Cor78* in the root (Figure 7.15). Contrastingly, for C24 no significant differences were found comparing the control and NaCl treatment (Figure 7.15).

While there were promising genes that could be used to measure salt responsiveness the lack of robustness of the assay and the variation was a concern. A secondary concern with this approach is the assumption that there is a difference between Col-0 and C24 which would be seen by gene expression. Therefore, there is a danger in selecting a gene to perform the analysis which is biased towards a response in Col-0 and not C24, compromising the neutrality of the experiment. For example the selecting of *LTI/Cor78* and *SOS1* for use in a plate based system for screening for salt responsiveness (because these genes show a response in Col-0 and not C24 after salt application) and not selecting *AtHKT1;1* (which showed a response in both ecotypes). Therefore, other methods were investigated to look for potential differences between Col-0 and C24 and their response to salt.

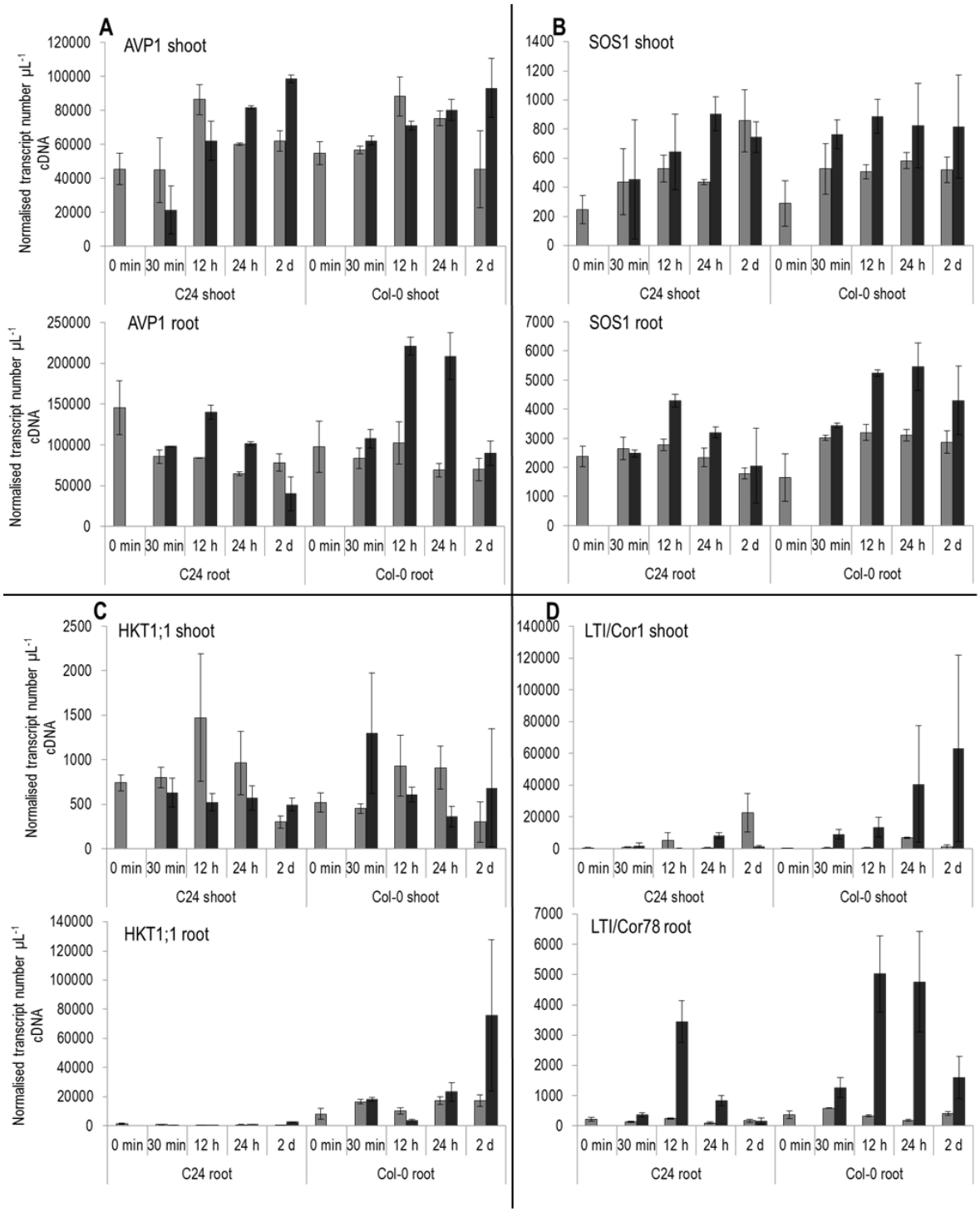

Figure 7.14: Transcript analysis of hydroponically grown Col-0 and C24 plants subjected to ± 100 mM NaCl using qPCR.

Hydroponically grown Col-0 and C24 plants, 5 wk old, were subject to control treatment (in light grey bars) or 100 mM NaCl treatment (in dark grey bars). Root and shoot samples were collected at 5 time points (0, 30 min, 12 h, 24 h and 2 d) and were subject to RNA extraction, followed by cDNA synthesis and qPCR. Transcript abundance of (A) *AtAVP1*, (B) *AtSOS1*, (C) *AtHKT1;1* and (D) *LTI/Cor78* were determined in the shoot and root tissue for both ecotypes. Data are normalised with

Actin2 transcript abundance, and error bars represent the standard error with n=3 biological replicates.

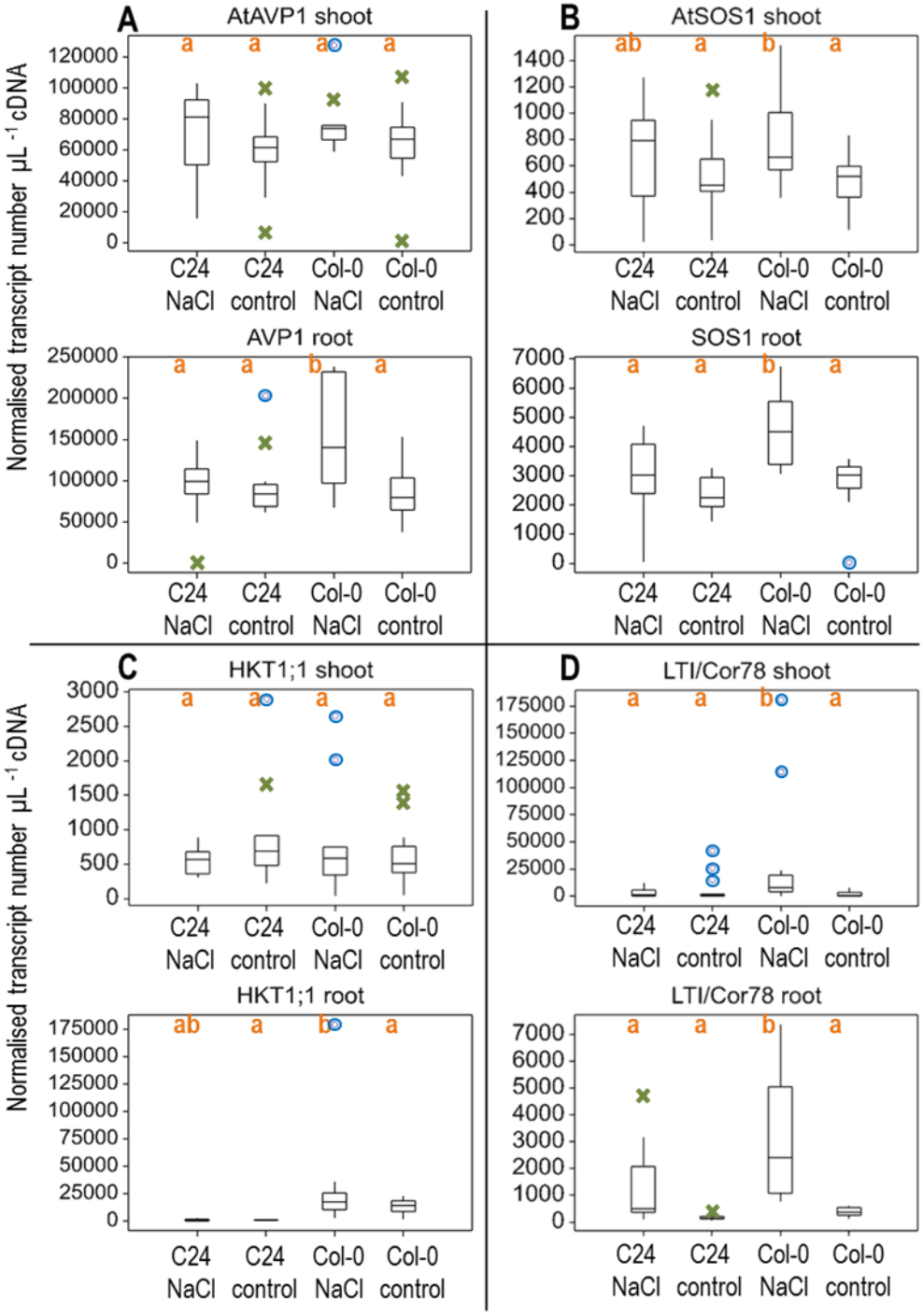

Figure 7.15: Boxplot analysis of transcript data that derived from hydroponically grown Col-0 and C24 plants subjected to ± 100 mM NaCl

Boxplots of qPCR data for ecotype (Col-0 and C24) and salt treatment (NaCl and control) sample-times were grouped. Outliers are marked with a green cross and far outliers with blue circle. Significance at the 0.05 level between groups is indicated by orange letters above the plots and was determined using ANOVA statistical analyses with Genstat and the Student-Newman-Keuls test.

7.5.2 Testing for differences in the germination rate of Col-0 and C24

In the previous section, expression levels of salt responsive genes were tested to obtain a robust and simple assay to screen a Col × C24 mapping population (section 7.5.1). Unfortunately this was not possible. A different approach to evaluate the salt responsiveness was tested by assessing the germination rate of Col-0 and C24 on NaCl. A previous study had identified a variation in germination rate between 96 Arabidopsis ecotypes when germinated on media containing high concentrations of NaCl (DeRose-Wilson and Gaut 2011); this could provide a robust and simple screening assay. In this study, germination of Col-0 and C24 was evaluated 7 d after sowing. A seed was considered germinated when it was at or beyond Arabidopsis growth stage 0.7 - hypocotyl and cotyledon emergence (Boyes *et al.* 2001). Col-0 germinated 1-2 d earlier than C24 under the tested conditions. The number of plants germinating on ½ strength MS with NaCl were compared to the number of plants germinating on ½ strength MS without addition of NaCl and presented as a percentage. For both ecotypes, the relative germination rate decreases on media with increasing amount of NaCl, however there are no substantially differences between Col-0 and C24 (Figure 7.16).

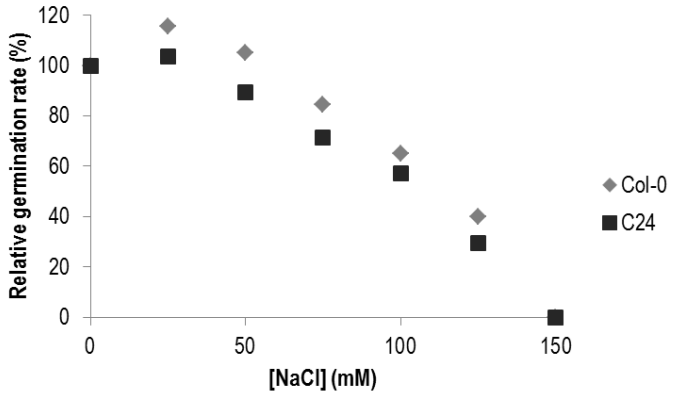

Figure 7.16: Germination rate (%) after 7 days of Col-0 and C24 seedlings on MS-plates supplemented with the indicated amount of NaCl, as compared to 0 mM NaCl control.

7.5.3 Root growth towards media containing NaCl

The germination rate of Col-0 and C24 on NaCl containing media is not substantially different between the two ecotypes; hence it is not a suitable trait as a proxy for salt responsiveness (section 7.5.2). To investigate whether root growth towards NaCl is different for Col-0 and C24, a simple plate assay was tested. The hypothesis being that the roots which sense s an area containing NaCl will deflect in order to avoid this area (Galvan-Ampudia and Testerink 2011). In this case if

Col-0 is salt responsive and C24 is salt numb, the roots of Col-0 would deflect, while roots of C24 continue to grow into the salt.

A method to evaluate how roots avoid salinity was previously described by Galvan-Ampudia and Testerink (2011); a version of this assay was used here for Col-0 and C24. Seedlings were placed about 1 cm from the top of the plate and incubated vertically to encourage root growth on the surface of the media across the plate. Germination of C24 is 1 to 2 d delayed and root growth is slower as compared to Col-0, hence the ecotypes were placed on separate plates. The area containing NaCl was not placed perpendicular to the root axis, but diagonally to allow the roots to change growth direction while still following gravity. The bottom part of the plate was replaced with media containing 0, 50, 100 or 150 mM NaCl, however no consistent deflections in root growth could be observed throughout the incubation period (Figure 7.17). The top panel in Figure 7.17 displays the seedlings at day of treatment, 4 d after germination (DAG), and the panel underneath represents the seedlings after 12 d incubation for Col and 14 d incubation for C24. The white dashed line indicated the boundary between the normal ½ strength MS media and the media supplemented with the indicated amount of NaCl. Root growth was monitored every day, but no avoidance of the area containing NaCl could be observed (Figure 7.17). A moderate reduction in lateral roots could be observed for Col-0 where the roots got in contact with increasing amount of NaCl. For C24, lateral roots were not pronounced in the elongation zone in control or NaCl conditions.

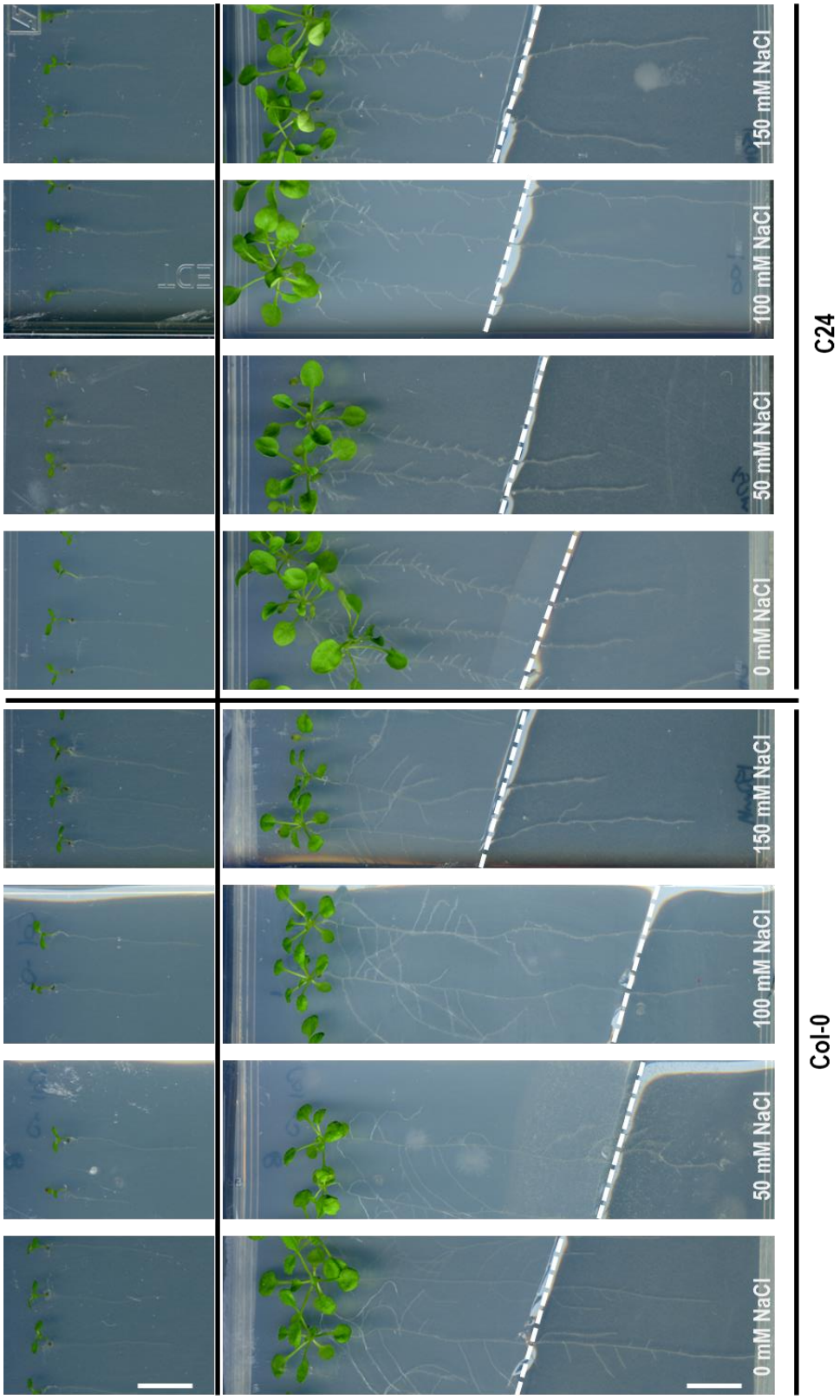

Figure 7.17: Root growth of Col-0 and C24 towards MS media containing NaCl.

Col-0 and C24 seeds were grown on MS-plates. Plates were placed vertically and 4 d after germination (top panel), the media in bottom half of the plate was replaced with solid ½ strength MS containing either 0 mM, 50 mM, 100 mM or 150 mM NaCl. White dashed line marks the interface where agar was replaced. Images in the bottom panel were taken 14 d after germination. Scale bar = 10 mm.

7.6 Discussion

7.6.1 Are changes in transcript levels of salt responsive genes a useful tool to investigate the salt responsiveness of Col-0 and C24?

7.6.1.1 Identification of candidate genes

Several candidate genes were identified that are differentially expressed in response to salt treatment (Table 7.3). The programme Genevestigator contains 8600 samples with over 100 tissue types and 2100 experimental conditions for Arabidopsis (as of May 2013), making it a useful tool to gather additional information on gene expression of a particular gene. For example, gene expression of *LTI/Cor78* is strongly up-regulated in the shoot by multiple stresses such as cold, salt, drought and ABA (Yamaguchi-Shinozaki and Shinozaki 1994). Generally, gene expression data obtained from microarrays correlate well with qPCR expression data, but this is not always the case (Dallas *et al.* 2005), hence a variety of candidate genes were selected for testing in the systems described here. Genevestigator illustrates microarray data only, therefore care needs to be taken when translating these results to a technique such as qPCR or semi-qPCR.

7.6.1.2 Changes in transcript levels of salt responsive genes are not suitable for a screening assay with soil grown plants

Establishing a screening assay in soil has a number of advantages. It is suitable for high-throughput phenotyping, while allowing non-sterile conditions and minimal handling. It also permits quick application of the stress solutions and sample collection. However, watering plants with 50 mM, 100 mM or 150 mM NaCl for 24 h did not result in a substantial induction of salt responsive genes in Col-0 or C24 (Figure 7.5, Figure 7.6 and Figure 7.7.). Changes in gene expression may not have been detected, because the plants may not have been exposed to elevated salt levels. Various factors influence if soil grown plants experience salt stress, such as soil conductivity, soil composition and water availability to the plant (Rengasamy 2006). The uptake of NaCl-solution from the tray is dependent on soil conductivity; the stress solution may not have been taken up equally across the tray and consequently the plants were not exposed to increased and equal concentrations of salt. The effect of NaCl could also be reduced due to Na^+ attaching to soil particles and not moving freely through the soil solution to interact with the plant root. Furthermore, if enough residual water was available to the plant, the applied salt solution might not have been effective - the salt was diluted to a level that does not affect the plant. To ensure plants are salt stressed, the NaCl-solution

should be applied based on the water holding capacity of the soil. However, this requires watering to weight for every pot, which is not desirable for a screening assay on a mapping population as it is labour intensive and time consuming, therefore not suitable for high throughput. Additionally, it would have been possible to lengthen the exposure to salt, but this might inhibit detection of the early response, as ionic stress occurs when NaCl accumulates in the plant within 2 d (section 4.6.1). Two QTL studies using soil grown plants were exposing the plants to 5 wk of NaCl stress to obtain a salinity tolerance phenotype that is based on the accumulation of Na^+ in the shoot (Galpaz and Reymond 2010, Roy *et al.* 2013). Alternatively, extremely high concentrations of salt (300 mM NaCl) could have been applied, but this is unrealistic and likely to induce osmotic shock responses.

7.6.1.3 Substantial changes in *LTI/Cor78* expression in response to salt stress are observed in Col-0, but not in C24 when plants are grown on MS plates

Soil grown plants did not display salt induced changes in gene expression after 24 h of salt treatment and are therefore not suitable for a screening assay. However, plants grown on plates containing ½ MS media showed promising results. Northern Blot analysis had previously shown that in Col-0 seedlings grown on MS-plates, *AtSOS1* and *LTI/Cor78* are up regulated under salt (Shi *et al.* 2000) and other QTL studies have also used MS-plates to measure salt tolerance related phenotypes such as fresh and dry weights, root length and germination rate (DeRose-Wilson and Gaut 2011, Galpaz and Reymond 2010, Quesada *et al.* 2002, Ren *et al.* 2010).

Although *AtAVP1* transcript abundance did not change upon salt treatment in both ecotypes, *AtHKT1;1* and *AtSOS1* transcript abundance changed in Col-0 by factors 3 and 2, respectively, and in C24 only by factors 2 and 1.5, respectively. Interestingly, substantial changes in *LTI/Cor78* expression were observed in the shoot of Col-0, but are not as pronounced in C24 (Figure 7.9). The transcript abundance under control conditions was very close to the background signal, making it a suitable candidate gene to assess salt responsiveness. Also semi-qPCR analysis of the same samples suggests that the overall trend is comparable to qPCR analysis (compare Figure 7.9 D with Figure 7.10). Transcript levels of *LTI/Cor78* in Col-0 salt stressed shoot samples were twice as high as in the corresponding C24 samples (Figure 7.10). Determining *LTI/Cor78* transcript levels using semi-qPCR, appeared to be a promising screening methodology for a mapping population. Also desirable is that the growth of Arabidopsis on MS plates is reasonably high-throughput and semi-qPCR analysis is an affordable technique.

7.6.1.4 Limitations of the MS-agar plate screening method

Further independent experiments were performed to ensure the screening assay is robust and substantial differences in *LTI/Cor78* expression between Col-0 and C24 are consistent. The same experimental setup on MS-plates was used and a few randomly selected lines of a Col-0 × C24 mapping population were included to get a preliminary indication for their *LTI/Cor78* transcript abundance. *LTI/Cor78* transcript abundance was analysed with semi-qPCR in a further two independent experiments (Figure 7.11). In the first repeat, no difference between the accessions Col-0 and C24 was detected (Figure 7.11 A), while in the second repeat, the variation of *LTI/Cor78* transcript abundance was so high in C24, that no trend could be recognised. The variation between biological replicates in the four selected lines of the mapping population was also substantial. To verify that the same trend can be observed with qPCR, the same cDNA samples derived from the four lines of the mapping population after salt treatment, depicted in Figure 7.11 B, were analysed (Figure 7.12). The qPCR results did not resemble semi-qPCR results suggesting major issues with the assay (comparing Figure 7.11 B with Figure 7.12).

The observed variation in *LTI/Cor78* gene expression may have occurred due to a number of factors. The variation between biological replicates may have been caused by (1) inconsistencies in salt application, (2) the timing of sampling procedure, (3) limitations in the detection method or (4) other environmental factors.

(1) Inconsistencies in salt application could have occurred when seedlings were transferred onto MS plates containing 100 mM NaCl. Although care was taken that roots are in full contact with the media, some parts of roots may have lifted off the agar, potentially not inducing salt stress and therefore not resulting in consistently increased *LTI/Cor78* expression.

(2) The timing of taking samples has an impact on gene expression levels. In C24, for example, a substantial increase in *LTI/Cor78* expression was observed after 12 h, but not after 24 h of salt stress (Figure 7.14). Rapid changes in *LTI/Cor78* expression have been previously observed during salt stress (Liu *et al.* 1998) and if these rapid changes of expression occur within the sampling timespan, they could cause the observed variation in transcript levels.

(3) The method to detect changes in *LTI/Cor78* expression was semi-qPCR. The use of a method like semi-qPCR in a screening assay requires that a substantial difference in gene expression is present, otherwise the differences will not be detected and results will not be reliable. The great variation between qPCR and semi-qPCR results led to doubts if semi-qPCR is a suitable method to obtain reliable, quantitative data for QTL analysis. Throughout the entire semi-qPCR process a

number of factors influence the accuracy of the assay itself. For instance, it is critical to use equal amounts of good quality RNA for cDNA synthesis to reduce variation that occurs in fidelity of the reverse transcriptase enzyme during the cDNA synthesis process and to reduce variation in *Actin2* transcripts between samples, because they are used for normalisation (Stahlberg *et al.* 2004). Also the gel loading procedure needs to be kept precise due to its susceptibility to errors during pipetting. Another source of variation in the assay originates from the gel imaging procedure. Uneven distribution of UV light for visualisation or variation in image capture leads to alterations in pixel counts by the imaging processing software. The variation that could occur due to pipetting errors during cDNA synthesis and PCR setup can be minimised by effective use of master mixes and automated pipetting, and also the background on the agarose gel can be reduced by using appropriate loading dyes such as Orange G in 15 % (w/v) of ficoll. Previous studies investigating eQTL have utilised large sets of microarray data (Keurentjes *et al.* 2007, West *et al.* 2007); QTL studies utilising semi-qPCR alone to obtain expression data from an Arabidopsis mapping population have not been described previously. Problems with semi-qPCR could be avoided by using another method of detecting transcript abundance, such as Northern Blot analysis, which had been previously used to determine *SOS1* and *LTI/Cor78* expression during salt stress over a range of time points (Shi *et al.* 2000). However, Northern Blot analysis would not be suitable for a high throughput screen required for QTL mapping.

(4) During both experiments that are depicted in Figure 7.11, issues were experienced with growth conditions - the growth rooms were overheating to temperatures greater than 28 °C, exposing the plants to additional stress. *LTI/Cor78* is not only responsive to salt stress but also to other stresses such as cold, drought and ABA (Yamaguchi-Shinozaki and Shinozaki 1994). Although Yamaguchi-Shinozaki and Shinozaki (1994) reported that heat stress alone does not influence *LTI/Cor78* expression, the combination of salt and heat stress may have influenced *LTI/Cor78* expression levels. The temperature rise would not have been equal throughout the growth room, potentially resulting in the great variation between biological replicates. However, in the subset of 30 lines of the Col×C24 mapping population (Figure 7.13), the *LTI/Cor78* transcript number for control samples was consistently low, suggesting that heat stress alone is not responsible for the increase in *LTI/Cor78* transcript abundance. A potential influence due to heat stress was avoided in subsequent experiments by changing to a growth room in another facility.

7.6.1.5 Salt stress in hydroponically grown Col-0 and C24 plants indicate that Col-0 is salt responsive, but a salt response in C24 is not significant

Hydroponically grown Col-0 and C24 plants were salt stressed with 100 mM NaCl and root and shoot tissue was analysed at 5 time points (0, 30 min, 12 h, 24 h and 2 d) for gene expression using qPCR. Analysed genes were *AtAVP1*, *AtSOS1*, *AtHKT1;1* and *LTI/Cor78*. The pairwise comparison of control and NaCl treated samples for each gene, tissue and time point separately (Figure 7.14) was inconclusive, with both ecotypes showing some response to NaCl treatment. However, the grouped analysis, when only analysing the effect of NaCl or control treatment on the ecotype, it stands out that for most genes and in both the root and the shoot, a significant difference can be identified between control and NaCl treatment in Col-0, while in C24 no significance was observed at all (Figure 7.15). It appears plausible to select the candidate gene *LTI/Cor78* at the time point 24 h after NaCl treatment for a screening assay. At this time point a clear difference in expression was observed for Col-0, but not for C24. Unfortunately, due to time limitations during my PhD candidature, semi-qPCR was not performed on these samples and the subset of the mapping population was not tested using the hydroponics system. Nevertheless, this hydroponics system could provide a suitable screening methodology for the Col×C24 mapping population and does not suffer from the same concerns about a touch response as the plate-based assay. The hydroponics system has previously been used successfully for QTL analysis regarding salinity tolerance (Alam *et al.* 2011, Ellis *et al.* 2002, Genc *et al.* 2010, Hamwieh and Xu 2008, Nguyen *et al.* 2013, Rivandi *et al.* 2011).

7.6.2 Germination on MS plates containing NaCl is not different between Col-0 and C24

A recently published study had successfully used germination and seedling growth as phenotypic traits to map genomic regions conferring salinity tolerance using the QTL approach and association mapping (DeRose-Wilson and Gaut 2011). QTL analysis was performed on the two RIL populations Col × Ler and Cvi × Ler, and association mapping using 96 accessions for which over 240,000 SNPs are available, including the two accessions Col-0 and C24 (DeRose-Wilson and Gaut 2011). Several QTL were obtained and expression analysis using the Affymetrix ATH1 microarray was used to narrow the number of candidate genes (DeRose-Wilson and Gaut 2011). While a reduction in germination rate on NaCl can be an indicator for salt tolerance, there is no evidence that germination is linked to a salt signalling pathway. Hence, a difference in germination rate was not an expected

phenotype, but could have provided a robust and easy screening method. Col-0 and C24 were both referred to as having a low germination rate at 150 mM NaCl (DeRose-Wilson and Gaut 2011), which was confirmed in this study. No substantial differences in germination rate on different NaCl concentrations were observed (Figure 7.16); it is therefore not a suitable screening method for this QTL analysis.

7.6.3 Root growth towards salt is not different in Col-0 and C24

When a plant experiences salt stress, the roots tissue is the first to be affected by salt exposure. An assay has been introduced by Galvan-Ampudia and Testerink (2011), in which roots deflect from their normal vertical growth in order to avoid an area containing NaCl. However, in the assay performed here, no change in root growth in response to NaCl was observed for Col-0 or C24 (Figure 7.17). The growth medium was not supplemented with sucrose as it may influence root growth and enhances the formation of lateral roots (Xu *et al.* 2013a). The use of Bacto-agar as a gelling agent and vertical incubation of the plates allowed the roots to grow on the surface, which may have reduced the contact surface of the roots with the agar and therefore NaCl. A larger effect on root growth may be visible if the roots would be allowed to grow through the agar and not on top. This may be achieved by using other gelling agents such as Phytagel™ (Sigma-Aldrich, Castle Hill, Australia), which has a reduced viscosity, and incubate the plates on an angle, as opposed to vertical. It may have been necessary to increase the NaCl concentration to levels of 200 mM NaCl or more to obtain a detectable effect. Due to insufficient preliminary results and time restrictions this assay was not further investigated.

7.6.4 Is C24 an ecotype that is non-responsive to salinity as opposed to Col-0, which is responsive?

Differences in transcript levels of salt responsive genes were clearly detected between Col-0 and C24. However, under the different growth conditions tested, C24 does display some change in transcript levels to a certain extend and in some cases physically behaves in the same manner as Col-0 e.g. similar response in germination and root growth. This is particularly clear from hydroponically grown plants where changes in the expression of some genes were observed. It still remains to be further investigated whether the difference in transcript levels can be linked back to alterations in the signalling pathway between Col-0 and C24. Transcriptional analyses are inconclusive.

Different scenarios provide plausible explanations for the differences observed on a transcriptional level. Scenario 1: both Col-0 and C24 are responsive to salt, but the timing of altering gene expression is different. Hence, changes in gene expression appear different between Col-0 and C24, because analysed sampling points were limited. Scenario 2: C24 responds to either only the osmotic or only the ionic component of NaCl stress. Therefore, a transcriptional response is detectable, but it is either reduced or the pattern of expression is different as compared to Col-0. To further investigate scenario 1, a time series with smaller sampling intervals could be performed. Here, 30 min, 12 h, 24 h and 2 d after salt treatment were evaluated and a trend was visible that C24 initially increased expression of salt responsive genes, but levels then declined, whereas Col-0 continued to have increased expression levels for most of the genes. The analysis of samples in smaller intervals and over a longer total stress duration may provide more information about the timely resolution of the salt response. The time difference in transcriptional salt stress response could then be linked to alterations in the signalling pathway or transcriptional regulators. To further investigate scenario 2, experiments should be performed with a stress that only induces osmotic stress, such as using mannitol or sorbitol. Then changes in expression could be compared between the osmotic and NaCl stress.

The initial hypothesis was that C24 is less responsive to salt because it has an altered salt signalling pathway. It has to be reconsidered if assessing the transcriptional response is a valid tool to investigate the salt responsiveness in C24. The signalling pathway described in the introduction, section 1.5, indicates that after the plant perceives salt stress, the signal is transduced by means of a second messenger (Ca^{2+}) to effectors, which include transcription factors and other regulatory elements that mediate the transcriptional change of salt responsive genes. In this chapter, this change in transcription was measured, which is far downstream in the signalling cascade. The previous chapter identified differences in the calcium signature between Col-0 and C24. These alterations in $[Ca^{2+}]_{cyt}$ are indicative of processes that involve the early stages of the salt signalling pathway. The biphasic calcium signature in Col-0 compared to the monophasic calcium signature in C24 in response to NaCl indicates a difference between the ecotypes. However, it remains inconclusive if the altered Ca^{2+} signature has indeed an effect on transcriptional regulation and if assessing the changes in the transcriptional response is therefore a suitable measure for this difference in response.

7.7 Conclusions

The salt responsiveness of Col-0 and C24 was evaluated using three approaches: by assessing the changes in gene expression of salt responsive genes, by analysing the germination rate on NaCl and by evaluating the root growth towards salt. The latter two approaches showed that the germination rate of both Col-0 and C24 decreases at the same rate on increasing concentrations of NaCl and the root growth on different NaCl containing media appeared only minor affected by increasing concentrations of NaCl for both ecotypes. However the analysis of changes in gene expression of salt responsive genes revealed that Col-0 and C24 plants grown on MS media and in hydroponics display a different response to NaCl stress. In particular one of the salt responsive genes, *LTI/Cor78*, displayed substantially increased transcript levels under NaCl stress in Col-0, but not in C24. An attempt was made to use this difference in *LTI/Cor78* expression on MS-plates as a screening methodology on a Col-0/C24 mapping population to perform QTL analysis. However, results were inconclusive as variation between biological replicates was high. The screening should be repeated in a hydroponics setup, as it showed salt stress induced significant differences for gene expression in Col-0, but not in C24.

Chapter 8 **General discussion**

8.1 Review of thesis aims and hypotheses

Soil salinity is a major abiotic stress affecting plant performance worldwide, including Australia. The osmotic and ionic stresses that soil salinity imposes on plants result in reduced growth, decreased photosynthesis and ultimately lead to premature leaf senescence and yield losses. A number of approaches have been taken to sustain crop growth on saline soils, such as improved farming practices and the development of improved crop varieties. One approach to increase a plant's salinity tolerance is to reduce the amount of Na^+ the plant accumulates in the shoot, particularly the photosynthetic active parts, to decrease the detrimental effects of Na^+ on metabolism. These improved crop varieties may be developed by conventional breeding using natural variation or by genetic modification. A thorough understanding of the processes and genes involved in plant salinity tolerance will help to inform both approaches. Two important steps in a plant's response to soil salinity are the detection of the salt stress and also the control of key regulators of ion transport. However, while these processes are subject of abundant research, substantial questions remain unanswered. The *HKT* family of genes encode ion transporters and have been shown to play a role in plant salinity tolerance in a number of species. However, questions still remain about their regulation, particularly the transcriptional and post-transcriptional regulation. Furthermore, while it is known that plants respond to salinity stress, by upregulating genes and performing post-translational modifications of key proteins etc., and that plants respond differently to the osmotic stress and Na^+ specific components of salt stress, there are still questions as to how a plant tissue/cell detects Na^+ before it builds up in the cytosol. Therefore, one aim of this thesis was to investigate the control and regulation of *AtHKT1;1* in two Arabidopsis ecotypes with different *AtHKT1;1* expression patterns. The second aim of this work was to develop a high throughput assay in Arabidopsis for measuring the early plant response to salt – an assay that would be suitable for a forward genetics study to identify novel components of the salt signalling pathway.

8.2 AtHKT1;1 has Na^+- and potentially K^+- transport activities and regulation of *AtHKT1;1* expression is complex

8.2.1 Na^+ and K^+ transport activities of AtHKT1;1

AtHKT1;1 is the only gene belonging to the *HKT* transporter family in Arabidopsis (Uozumi *et al.* 2000). It has been shown that the encoded protein AtHKT1;1 is localised in the root stele and is likely to be involved in the retrieval of Na^+ from the xylem vessel, thereby preventing Na^+ from

translocating to the shoot tissue (Davenport *et al.* 2007, Møller and Tester 2007, Rus *et al.* 2006, Sunarpi *et al.* 2005). So far, studies in the Xenopus oocyte and yeast expression system for AtHKT1;1 from the ecotype L*er* only showed Na^+ transport activity (Uozumi *et al.* 2000). Here, the *AtHKT1;1* coding sequences of the two Arabidopsis ecotypes Col-0 and C24 were used for heterologous expression in Xenopus oocytes and yeast (chapter 3). Na^+ transport activity was detected in both systems for both genes (Figure 3.6). Interestingly, it appeared that oocytes expressing either the Col-0 or C24 *AtHKT1;1* also displayed currents in the presence of K^+ (Figure 3.6), with results from *AtHKT1;1* expression in yeast suggesting the C24 AtHKT1;1 transporter may also mediate K^+ transport.

8.2.2 Expression patterns of *AtHKT1;1* are ecotype specific

In Col-0, *AtHKT1;1* expression can be detected in the root and the shoot tissue. In C24, however, *AtHKT1;1* expression cannot be detected in the root, while it is present in the shoot (Jha *et al.* 2010, Sundstrom 2011). Consequently, a variety of *promoter::GFP* transgenic lines were analysed for the spatial patterns of *GFP* expression, to test if the lack of expression is controlled by the promoter region (chapter 4). This study identified *GFP* expression in all transgenic lines in the stelar tissue (Figure 4.8 to Figure 4.11). This result suggests that firstly, the Col-0 and C24 2.7 kb promoter sequences mediate stelar specific expression in both the Col-0 and C24 backgrounds and secondly, that the lack of *AtHKT1;1* expression in C24 is not attributable to elements contained within the 2.7 kb promoter, in particular not by the 150 bp region just upstream of the *AtHKT1;1* start codon, as hypothesised by Sundstrom (2011). Instead it is hypothesised that elements in the genomic *AtHKT1;1* sequence are involved in regulating *AtHKT1;1* expression, particularly those in the second intron of the gene, where the C24 *AtHKT1;1* has a 1.6 kb insertion that is not present in the Col-0 *AtHKT1;1*. This study identified the 1.6 kb insertion to be highly similar to a SIMPLEHAT2 transposon (Figure 5.11), which is often methylated in Col-0 and the target of small RNAs. In a similar way, the corresponding insertion in the C24 *AtHKT1;1* intron may result in methylation and/or being the target of small RNA-mediated transcript degradation. Constructs were designed to test if the genomic DNA, in particular the second intron, regulates gene expression using *promoter::gDNA* and *promoter::intron::GFP/GUS* transgenic lines. Unfortunately, due to difficulties in cloning the genomic DNA of C24, transgenic lines were not completed during this candidature. The C24 genomic DNA was eventually synthesised by a commercial provider, which should facilitate future cloning attempts.

8.2.3 C24 as a model for alternative salinity tolerance mechanism?

It has been described above that the ecotype C24 accumulates more Na^+ in the shoot, and that this increase is probably caused by the lack of *AtHKT1;1* expression in the root. Interestingly, despite accumulating more Na^+ in the shoot, C24 is slightly more salt tolerant than Col-0. This would suggest that C24 has other mechanisms that mediate salt tolerance. One other mechanism could be an increased tissue tolerance, where the Na^+ is compartmentalised, for instance into the vacuole. This suggestion is supported by the observation that compatible solutes such as proline are more abundant in C24 compared to Col-0 (Korn *et al.* 2008), which could potentially enable the increased Na^+ content in the vacuole. The compartmentalisation of Na^+ into the vacuole may enable the plant to retain a large K^+ to Na^+ ratio in the shoot cytosol, therefore maintaining photosynthetic activity.

The question remains if C24 gains an evolutionary advantage from lacking *AtHKT1;1* expression in the root, while retaining *AtHKT1;1* expression in the shoot. This study provided evidence that K^+ transport may occur through the C24 AtHKT1;1. If it is thermodynamically possible, would the C24 AtHKT1;1 mediate K^+ transport from the shoot xylem sap into the shoot tissue to maintain higher K^+ to Na^+ ratio than Col-0? Further research could include measurements of the Na^+ and K^+ content in the shoot cytosol and vacuoles of C24 and C24 *hkt* knock-out mutants under control, salt stress and potentially K^+ limiting conditions. If a larger K^+ to Na^+ ratio is present in the shoot cytosol of C24 plants as opposed to C24 *hkt* knock-out plants, this might explain why C24 retained *AtHKT1;1* expression in the shoot.

Another example of ecotypes that lack *AtHKT1;1* expression in the root are Ts-1 and Tsu-1. Both ecotypes have an increased shoot Na^+ content but also are more salt tolerant than Col-0 (Rus *et al.* 2006). It has been suggested that Na^+ exclusion may not be the only salt tolerance mechanism in Arabidopsis (Jha *et al.* 2010, Møller and Tester 2007). Accordingly, C24, Tsu-1 and Ts-1 may possess great tissue tolerance or other tolerance mechanisms. A broad study on 349 Arabidopsis ecotypes using GWAS only identified *AtHKT1;1* as the sole loci underlying shoot Na^+ accumulation (Baxter *et al.* 2010). It is possible that other alleles that confer both salinity tolerance and high shoot Na^+ content are rare alleles (different mechanisms used by different ecotypes) and therefore were not identified using GWAS. To further dissect the tolerance mechanism in C24, Tsu-1 and TS-1, it may be possible to perform a QTL analysis on a Col-0 × C24 (or Col-0 × Tsu-1 or Col-0 × Ts-1) mapping population, where the shoot Na^+ content and the salinity tolerance index are combined. It is interesting that low *AtHKT1;1* expressing, high shoot Na^+ accumulating Arabidopsis ecotypes are found in regions of saline soils – such as coastal regions or areas which were inland seas (Baxter et

al., 2010). High expressing *AtHKT1;1*, low Na^+ accumulating ecotypes were not found in those coastal regions. This suggests there has been evolutionary pressure on Arabidopsis to not exclude shoot Na^+ in saline environments, which is of interest given the poor salinity tolerance of Arabidopsis (Møller and Tester 2007, Munns and Tester 2008). What remains to be explored is whether the high Na^+ accumulating Arabidopsis survive in these higher saline soils by other tolerance mechanisms, such as tissue tolerance of Na^+, or whether they avoid the high concentrations of salt in the soil by only growing when salt levels are low – for example during the wet winter months. A detailed study is required, to test whether the regulation of genes, like *AtHKT1;1*, is responsible for these ecotypes to grow in high saline areas or if it is a simple avoidance mechanism that helps the plant survive.

From studies utilising a broad range of plant species, it has been demonstrated that a number of genes are involved in mediating salinity tolerance, such as genes that encode for transport proteins enabling the translocation of ions, or genes that encode regulatory proteins. These genes are differentially expressed when a plant is exposed to salt stress in order to coordinate the response. For a plant to respond effectively to salt stress, it needs to be able to sense the salt, transmit the signal of salt stress and then activate effective responses.

8.3 NaCl induced responses in Col-0 and C24

When a plant is exposed to salt stress, salt tolerance mechanisms are activated, which include the activation of transport proteins and the alteration of gene expression to allow the plant to maintain relatively low Na^+ levels in the cytosol, thereby maintaining cellular functions. It is thought that alterations in cytosolic calcium concentrations ($[Ca^{2+}]_{cyt}$) mediate part of the signal transduction and are an early component of the signalling pathway. However, while some key components of the signalling pathways are already known (Batistič and Kudla 2012) the proteins responsible for the initial detection of Na^+ are yet to be elucidated. Here, it was shown that the two ecotypes Col-0 and C24 appear to respond differently to salt stress (chapter 6): NaCl-induced $[Ca^{2+}]_{cyt}$ alterations were found to be biphasic in Col-0, while the alterations in C24 appear monophasic (Figure 6.5). Monophasic Ca^{2+} signatures were also induced by osmotic stress in form of sorbitol or cold treatment in both Col-0 and C24 (Figure 6.5). It was proposed that the biphasic signature, which is induced by NaCl in Col-0, represents a NaCl-ion-specific response, while the monophasic response may be a general stress response. Thus, while C24 can detect other stresses, it apparently does not detect either the Na^+ or Cl^- ions. This differing Ca^{2+} signature is proposed to have implications in the salt signalling pathway and it is therefore hypothesised that by comparing the salt response of Col-0

and C24, it would enable the identification of components of the salt signalling pathway. A QTL mapping approach was proposed to test for the differences in responsiveness in Col-0 and C24. Unfortunately an *Aequorin* containing mapping population of Col-0 and C24 would be required for a forward genetics approach to identify the salt sensor using this assay, as it is based on measuring the bioluminescence in response to NaCl stimuli. However, now that differences in salt detection between Col-0 and C24 have been demonstrated, a different phenotyping approach was developed that allows QTL analysis of a previously generated and genotyped Col-0 × C24 mapping population (Törjék *et al.* 2008). Therefore, numerous approaches to assay the differences in responsiveness in Col-0 and C24 were tested (chapter 7). This study showed that changes in gene expression are more pronounced in Col-0, than in C24. A setup, in which hydroponically grown plants were exposed to salt stress, appeared suitable for screening of a mapping population. This study has provided a screening tool for a QTL mapping approach; however, the mapping population is yet to be assessed. While this QTL screening methodology based on NaCl induced transcriptional changes may lead to the identification of components in the early signalling pathway, it is not an ideal methodology. Monophasic alterations in $[Ca^{2+}]_{cyt}$ in C24 were evoked by NaCl, sorbitol and cold, indicating that the ecotype does respond to stress, but the response does not vary with changing stresses. In Col-0 on the other hand, biphasic alterations in $[Ca^{2+}]_{cyt}$ were induced by NaCl and monophasic alterations when sorbitol or cold stress were imposed. It was hypothesised that C24 does not respond to the ionic component of NaCl and therefore lacks a biphasic response. However, it has to be considered that a transcriptional response was indeed observed in C24, despite it being not as pronounced as in Col-0. It may therefore also be plausible that NaCl stress is perceived by C24, but differently compared to Col-0. It is possible, that Col-0 perceives NaCl immediately, causing alterations in $[Ca^{2+}]_{cyt}$, which transmit the NaCl stress signal and ultimately, inducing transcriptional changes. In C24 on the other hand, NaCl stress may be perceived later, once it has entered the cell, therefore only monophasic alterations in $[Ca^{2+}]_{cyt}$ are induced, which in turn also lead to transcriptional changes, but these changes may have a different timely occurrence or changes may be milder compared to Col-0.

In conclusion, a clear difference in NaCl response was seen between Col-0 and C24 when assessing NaCl induced $[Ca^{2+}]_{cyt}$ alterations. This difference in response was not as clear when transcriptional changes were assessed. The reasons for this discrepancy remain speculative, however, using a forward genetic approach as proposed here may assist to decipher the genetic cause for the difference in NaCl response between Col-0 and C24.

8.4 Future investigations - understanding the HKT transporter family

While *AtHKT1;1* is an intensively researched gene, there are still gaps in our understanding of its (1) function in the shoot, (2) regulation and (3) role in salinity tolerance in Arabidopsis and (4) role of the *HKT* family in salinity tolerance in other plant species.

(1) The function of AtHKT1;1 in Arabidopsis roots is likely to be the retrieval of Na^+ from the xylem, thereby preventing the translocation of Na^+ to the shoot (Hauser and Horie 2010, Horie *et al.* 2009, Waters *et al.* 2013). However, the role of AtHKT1;1 in the shoot is still unclear. It had been proposed that AtHKT1;1 may be involved in recirculation of Na^+ in the phloem sap (Berthomieu *et al.* 2003), however, subsequent experiments with radioactive tracers did not link AtHKT1;1 to shoot to root transport of Na^+ (Davenport *et al.* 2007). Future research may utilise the ecotype C24 to investigate the role of AtHKT1;1 in the shoot. Since C24 lacks expression of *AtHKT1;1* in the root, it may be possible to elucidate the function in the shoot by generating C24 lines that lack *AtHKT1;1* expression in the shoot, for instance by T-DNA insertion, RNA-interference or CRISPR/Cas, and then comparing the resulting phenotype to that of the C24 wild type. For instance, if AtHKT1;1 from C24 is involved in the retrieval of K^+ to maintain a higher K^+/Na^+ ratio in the shoot, it would be expected that the K^+ content in the shoot would be decreased in the C24 *hkt* knock out lines compared to the wild type. On the other hand, if AtHKT1;1 is involved in the recirculation of Na^+ from the shoot to the root, the C24 *hkt* knock out lines would have an even further increased Na^+ content in the shoot compared to the wild type while the phloem sap would have a decreased Na^+ content.

(2) This study investigated the regulation of *AtHKT1;1* expression, and demonstrated that while the promoter directed stelar-specific expression, other signals within the second intron appear to be important and may be responsible for the lack of *AtHKT1;1* expression in C24 roots. This study demonstrates that the regulation of gene expression is complex and involves more than just the promoter sequence. As shown in chapter 5, epigenetic regulation through transposons, methylation and small RNAs appears to influence spatial and temporal expression patterns. It is important to be aware of this complex network of regulation when analysing the potential function and role of a gene, but also when utilising genes for genetic engineering.

The further examination of the regulation of *AtHKT1;1* expression may also lead to the discovery of regulatory elements present in the DNA, which can be used as engineering tools to customise expression of other genes of interest. Several features of *AtHKT1;1* expression may be useful for the engineering of transgenic plants with specific expression patterns. For instance, *AtHKT1;1* expression in Col-0 is very low and has been found to be located predominantly in the root stele,

which may be beneficial for the expression of other genes encoding transporters or proteins that generally have a low expression such as transcription factors. It may also for example benefit other transporters such as the PEZ1. *Pez1* encodes for a transport protein that is localised in the stele and is involved in the transport of protocatechuic acid, which in turn leads to mobilisation of iron, which is important for plant nutrition (Ishimaru *et al.* 2011). While knock out lines of *pez1* show an iron deficiency phenotype, the over expression of *Pez1* leads to iron toxicity (Ishimaru *et al.* 2011). The stele specific- and low level- expression mediated by the *AtHKT1;1* promoter may be beneficial to drive *Pez1* expression to obtain sufficient mobilisation of nutritional iron for optimal growth of the plant. Current research focuses on the identification and use of promoters to drive tissue and temporal specific expression for applied research, for instance for the development of improved crop varieties (Lightfoot *et al.* 2013). Particularly, this is the case because constitutive expression of genes has been shown to be of disadvantage for several but not all salinity tolerance traits (Jacobs *et al.* 2007, Møller *et al.* 2009, Møller and Tester 2007, Plett and Møller 2010). Further details and examples of pyramiding different genes and traits are discussed below.

HKT1;1 may not only be regulated on the gene expression level, but also on the protein level *via* posttranslational modifications. While posttranslational modifications of AtHKT1;1 have not been directly described in the literature, evidence suggest some regulation/activation occurs in the presence of Na^+ (Xue *et al.* 2011). Future studies may endeavour to use affinity chromatography to find binding proteins and analyse the phosphorylation status. Expression of *AtHKT1;1* fused to a tag *in planta* could allow affinity chromatography and subsequent purification of the AtHKT1;1 protein fusion. The plants, from which the recombinant AtHKT1;1 protein is purified, would be subjected to different stresses to obtain a higher fraction of activated protein. The produced AtHKT1;1 protein could then be used in a pull down experiment using a plant extract to identify protein/protein interactions. This approach has been used in plants primarily to confirm protein/protein interactions (Kepinski 2009, Ueki *et al.* 2011). However, examples from the mammalian system include the identification of novel binding partners of the Huntingtin Yeast Two-Hybrid Protein K (HYPK)- a protein that is involved in Huntington's disease (Choudhury *et al.* 2012) or the identification of novel protein/protein interactions for the Amyloid precursor protein intracellular domain (AICD)- a protein involved in Alzheimer's disease (Chakrabarti and Mukhopadhyay 2012). In case of AtHKT1;1, once the protein is produced and purified, it could be subjected to mass spectrometry to identify the phosphorylation and/or the glycosylation status of the protein. This would allow gaining further insights into the HKT regulation and may inform the generation of salinity tolerant plants.

Furthermore, it has been described that reactive oxygen species (ROS) are involved in homeostasis of Na^+ in the shoot and it was speculated that ROS may mediate activation of *AtHKT1;1* (Jiang *et al.* 2012). ROS are involved in the signalling pathway of abiotic stresses such as salt stress (Pitzschke *et al.* 2006). Since ROS are possibly involved in salt signalling and potentially indirectly affect *AtHKT1;1*, it is difficult to directly test for the involvement of ROS in AtHKT1;1 activation on the protein level *in planta*. It would be possible to expose *AtHKT1;1* expressing protoplasts, which are described by Xue *et al*. (2011), to ROS and evaluate if Na^+ transport properties are altered using electrophysiological techniques. To determine if *AtHKT1;1* expression is induced by ROS, *AtHKT1;1* expression could be assessed in ROS deficient mutants described by (Jiang *et al.* 2012).

(3) While it has been demonstrated that AtHKT1;1 plays a role in salinity tolerance in Arabidopsis, the mechanisms by which it confers salinity tolerance have not been shown directly. Constitutive expression of *AtHKT1;1* in Arabidopsis plants led to a severe decrease in salinity tolerance, possibly due to the enhanced uptake of Na^+ in the root via AtHKT1;1 caused by mis-expression of *AtHKT1;1* outside of the stelar cells (Møller *et al*., 2009). In contrast, the cell specific expression of *AtHKT1;1* in the stele, using an enhancer trap system, increased the salinity tolerance compared to corresponding wild type plants (Møller *et al.* 2009). The enhancer trap system mediates strong and stele specific expression of *AtHKT1;1*. The increased salinity tolerance in these plants may be due to storage of the retrieved Na^+ in cortical cells, which have a large vacuole for storage of Na^+ (Møller *et al.* 2009).

(4) Arabidopsis contains only one *HKT* gene, in contrast to other plant species. Wheat and rice contain 11 and 7 HKT family members, respectively (Garciadeblás *et al.* 2003, Huang *et al.* 2008). While a number of HKT proteins have been characterised using heterologous expression systems, more work is yet to be done to bring together transport characteristics, expression patterns and regulation of these different *HKT*s to decipher the physiological role and importance of HKT transporters in salinity tolerance and to determine whether they play a role in K^+ nutrition. It has been hypothesised that the variety of HKT transporters with slightly different transport characteristics and with different spatial and temporal expression patterns may enable the plant to direct complex ion movements in order to maintain growth under stress conditions (Ben Amar *et al.* 2013). For example in rice, the interplay between expression pattern and transport efficiency of OsHKT1;4 and OsHKT1;5 in the two varieties Nipponbare and Pokalli influences the level of salt tolerance (Cotsaftis *et al.* 2012). Further research investigating the *in planta* role could be performed on an HKT-wide spectrum as indicated by (Horie *et al.* 2007). Analysis of HKT expression patterns could include tissue and cell type specific *in situ* PCR (Munns *et al.* 2012) under stress conditions such as salt

stress and K^+ starvation. By comparing the structural features using molecular modelling, the transport activity may be deciphered (Cotsaftis *et al.* 2012), and could be further examined using heterologous or *in vitro* expression systems (Shadiac *et al.* 2013). The field of characterising plant transport proteins is rapidly developing and new technologies are available, such as the *in vitro* production of proteins and their analysis using nanodiscs in artificial membranes to determine transport characteristics (Shadiac *et al.* 2013). The advantage of *in vitro* systems is that endogenous transport systems in the Xenopus oocyte or yeast expression system do not influence the transport properties. The *in planta* characterisation of some HKTs has proven difficult, since no phenotype is observable in some single knock-out lines (Horie *et al.* 2011, Yao *et al.* 2010). This may be due to functional redundancy of some HKTs or possibly, because under the tested conditions, they are not physiologically relevant. The combined knock-out using T-DNA insertion or knock down using RNA interference may reduce the effect of redundancy in HKTs function and reveal part of their physiological relevance. Some HKTs may not be directly involved in salt tolerance, but potentially play a role in Na^+/K^+ nutrition under saline and/or K^+ starving conditions (Horie *et al.* 2007). This hypothesis was formed, since the gene expression of some *HKTs*, particularly members of class 2, is upregulated under K^+ starving conditions and it appears that nutritional Na^+ is taken up into K^+ starved roots (Horie *et al.* 2007). The sensing of stress, in particularly salt stress, and specific changes of gene expression in response to detection of salt stress is valuable evidences to determine the pathway a gene is involved in.

What still remains to be examined is why do monocots have two different sub-families of *HKTs*, as defined by the amino acid sequence, while dicots only have one sub-family. The classification is also generally linked to the proteins ability to transporter either Na^+ or Na^+ and K^+. What was the evolutionary pressure that resulted in monocots maintaining two sub-families of *HKTs* while dicots only have one – predominately the Na^+ transporting HKTs? In addition, why do some family 1 *HKTs* in dicots have the ability to transport K^+ (Ali *et al*. 2012), is this a re-evolution of the protein's ability to transport K^+ as a nutrient?

8.5 Future investigations – Understanding the response of plants to salinity stress

This work was investigating the early stages of salt detection. The components and regulation of a proposed salt signalling pathway are vastly unknown, yet it appears that a number of salt responsive genes are regulated by this proposed pathway, enabling the plant to manage salt stress and

complete its life cycle. For instance, when a plant is exposed to salt stress, the stress signal is perceived by the plant and a signalling cascade is activated. This signalling cascade may result in activation of transporters, such as AtHKT1;1, which allows the plant to limit the amount of Na^+ taken up into the shoot, or mechanisms important in the plant's response to the shoot ion-independent aspect of salt stress. As introduced above, this activation of AtHKT1;1 may be on a transcriptional level by increasing gene expression or on a posttranslational level, for example by phosphorylation. AtHKT1;1 activation has not been directly linked to the Ca^{2+}-mediated salt signalling pathway, that has been described in this work, although it has been suggested in several articles (for example, (Zhu 2002)). However, one can imagine that the increase in cytosolic calcium, which activates calcium binding proteins, such as kinases, may phosphorylate AtHKT1;1 for activation or activate transcription factors that induce *AtHKT1;1* expression. Experiments to decipher the AtHKT1;1 activation could be similar to what has been described above; the production of recombinant AtHKT1;1 *in planta,* fused to a tag, could allow for affinity chromatography, which in turn could allow to pull down binding partners. These binding partners may facilitate phosphorylation or other modifications, which may be determined using mass spectrometry.

One major objective of future investigations may be to decipher how salt is sensed. It is unclear if a 'salt sensor-protein' exists, but the identification of how salt is sensed may enable the manipulation of how, when or how much a plant will respond to salt stress – a process important in improving yield of crop plants grown in saline environments. Also, the identification of other components of the salinity tolerance pathway may offer the opportunity to manipulate a whole cascade of salt responsive genes. For example the protein kinase CIPK16, a signalling component that is not directly involved in Na^+ transport or building up an electrochemical gradient to energise Na^+ transport, has been found to improve a plants salinity tolerance when overexpressed in Arabidopsis, barley (Roy *et al.* 2013), rice and wheat (Roy *et al.*, unpublished). CIPK16 may be involved in a signalling cascade or in activating transporters that mediate salt tolerance, therefore potentially affecting a range of salt tolerance mechanisms.

The identification of components of the early signalling pathway, potentially the sensor, will not only increase our general understanding of plant biology, but this knowledge may be transferred to other stress signalling pathways. When a plant responds to an environmental stress, physiological responses occur in an attempt for the plant to survive and/or complete its life cycle. C24 may be missing a component of the early salt signalling pathway, leading to the reduced responsiveness of C24 to NaCl (see chapter 6). It is yet to be investigated if this reduced responsiveness is directly correlated to the increased salinity tolerance of C24. C24 does not appear to have a reduced growth

or shows other severe stress symptoms, despite not responding to salt as much as Col-0 does. The question remains if the reduced responsiveness may actually be beneficial – if a crop plant is made "numb" to salt, would it be able to produce more yield? The most important feature for a farmer is a plant's ability to produce a crop, not necessarily how salt tolerant it is. If the salt sensor could be identified and knocked out in a crop plant such as wheat, it would be interesting to investigate whether this can improve yield in the field. One could also imagine that if a plant is grown solely for biomass production (fuel or food), it may be beneficial to use a plant that is non-responsive to reduced nitrogen in the soil, for instance. The plant is under care of humans (farmers), and therefore is taken care of when nutrient levels are too low. A plant that is non-responsive to low nitrogen levels would not reduce its biomass production in an attempt to survive or complete its life cycle. The plant would not invest into reproductive growth or decrease growth, thereby potentially producing more biomass while possibly reducing fertiliser requirements.

8.6 Future investigations –Improving crop plants

While Na^+ exclusion is one of the main focuses to improve salinity tolerance, it is likely that a combination of osmotic tolerance, tissue tolerance and Na^+ exclusion will yield a maximum of plant salinity tolerance (Rajendran *et al.* 2009). The manipulation of single genes has been shown to improve the salt tolerance of plants, however, it is likely that a combination of genes is necessary to yield substantial improvements. This not only includes salinity tolerance, but also traits such as drought tolerance and disease resistance. This approach of introducing multiple genes or genetic loci is also known as gene pyramiding.

In cereals, a number of HKT transporters have been identified that have been linked to improving salinity tolerance (James *et al.* 2011, James *et al.* 2012, Lindsay *et al.* 2004, Munns *et al.* 2012, Ren *et al.* 2005). One example are the wheat loci *Nax1* and *Nax2*, with the underlying genes *TmHKT1;4* and *TmHKT1;5,* that have been introduced into durum and bread wheat varieties by conventional breeding to improve crop salinity tolerance in areas of high salinity by excluding Na^+ from the photosynthetic active parts of the shoot (Byrt *et al.* 2007, James *et al.* 2011, Munns *et al.* 2012). However, plants did not perform better under low or moderate salinity, presumably because they were suffering more from the osmotic effects of salt stress. Osmotic stress is not well understood, although it already affects the plant in the presence of moderate salt levels in the soil (Roy and Tester 2012). Loci conferring osmotic tolerance are currently being identified (Tilbrook *et al*., unpublished). Breeding lines, such as those of durum and bread wheat, which contain the HKT gene

from *Triticum monococcum,* may be used for gene pyramiding. The lines containing HKT show improved yield under high salt, and loci may be introduced that confer osmotic tolerance, to increase performance under a range of salt stress conditions. Further improvements to plant yield may be possible by not only introducing loci conferring ionic and osmotic tolerance, but also by introducing tissue tolerance traits. For instance, vacuolar Na^+/K^+-H^+ antiporters (family of NHX transporters) have been linked to improving tissue tolerance (Apse *et al.* 1999, Bassil *et al.* 2012). Other desirable traits concerning abiotic or biotic stresses such as drought tolerance, rust resistance or frost tolerance may be used in this gene pyramiding approach to obtain the desirable traits and improved plant varieties.

Proof-of-concept experiments for gene pyramiding have been performed for example in tobacco. The concurrent and constitutive expression of genes encoding for a vacuolar pyrophosphatse from wheat (*TVP1*) and a wheat Na^+/K^+-H^+ antiporter (*TNHXS1*) increase the salinity tolerance of transgenic tobacco more than the single-gene transformants, as measured by plant height, plant weight and root length (Gouiaa *et al.* 2012). It may be possible to improve the salinity tolerance of a plant even further by using cell type specific expression.

Based on previous research, there is a general understanding of which tissues of the plants may be able to tolerate more Na^+ than other parts. For instance the photosynthetic active parts of the plants should have a low Na^+ content (high K^+ to Na^+ ratio) and are particularly sensitive to salt stress, while it appears that root cortex cells, for instance, are less affected by high Na^+, because Na^+ is stored in large vacuoles. Computational approaches, where ion fluxes are modelled within the plant, may be used to inform which transporter should be expressed in which cell type for optimal ion distribution. The modelling of the complex ion movements within a plant is attracting much attention from bioinformatics research (Foster and Miklavcic 2013). Modelling, together with biological approaches may help to engineer solute transport within the plant to ultimately improve the performance of a crop plant. The biological approach to engineer solute transport within a plant may be possible by modifying the selectivity of existing transporters.

With the increased understanding on how selectivity and activity of transporters is determined, directed manipulation of these characteristics may help to design ion fluxes within plants. For instance, the salt tolerant Arabidopsis relative *Thellungiella salsuginea* contains an *HKT* allele that is highly similar to the *AtHKT1;1* allele. Interestingly, TsHKT1;2 has 79.2 % amino acid sequence identity to AtHKT1;1 but has been found to have predominantly K^+ transport properties (Ali *et al.* 2012). With the understanding of the structure and functional relationship of transporters, it may be

possible that alteration of a few amino acids lead to altered ion selectivity (Waters *et al.* 2013), allowing the directed manipulation of solute distribution in the plant to benefit growth and ultimately yield. Once the important residues have been identified, transporter genes could be subject to site-directed mutagenesis, leading to an altered protein structure. These transporters could then be first analysed in heterologous or *in vitro* expression systems for selectivity and affinity of transport and then used for *in planta* studies. The directed manipulation of ion transport properties *in planta* may offer another tool to customise plant traits. The advantage of manipulating existing transporter's ion selectivity is that the regulatory mechanisms such as phosphorylation, protein/protein interactions and expression patters are potentially not affected by the manipulations. This would facilitate a targeted approach that may be more likely to yield success than other approaches, where promoter fragments and regulatory elements are artificially combined in an attempt to generate specific expression.

Conventional breeding is currently the preferred method in generating crops with improved traits that are intended for human consumption. Breeding is accepted by the public and release of the improved lines is not restricted by legislation to the extent that genetic engineered plants are. However, genetic engineering allows the introduction of new traits from different species and therefore extends the repertoire of genes available for improvement. For instance loci conferring insect or herbicide resistance are possible (Sharma *et al.* 2004), such as the Bt-cotton (Perlak *et al.* 2001), or engineering of crops with elevated nutritional value, such as golden rice (Mayer *et al.* 2008). There are crucial factors for genetic engineering to be accepted by the public for human usage. It is expected to have a precise understanding of the introduced genes, the gene products and the product's distribution within the plant. It is therefore vital to better understand the gene's regulation, identify promoters and other regulatory elements to precisely define the temporal and spatial expression patterns of transgenes used (Møller and Tester 2007, Tester and Langridge 2010).

Research into plant salinity tolerance and the future generation of more salt tolerance varieties is of major importance for the production of food for the increasing global population. It is important to maintain yield and plant growth on the continually increasing area of salt affected farmland. Ideally, it may be possible to grow salinity-tolerant crops on soil that would not be productive otherwise, for example by utilising irrigation agriculture with partially desalinised water. In arid areas, rainwater and access to fresh water is often limited, however salt water from the ocean may be partially desalinised and used for irrigation agriculture.

8.7 Concluding remarks

In this study, the detection of NaCl by plants and the subsequent regulation of salinity tolerance were investigated. It was shown that the regulation of *AtHKT1;1* is complex, and is not solely determined by the corresponding promoter region. Bioinformatics analysis of the second intron of *AtHKT1;1* in C24 demonstrated the presence of a SIMPLEHAT2 transposon-like sequence of 1.6 kb in size. This SIMPLEHAT2 transposon-like sequence may cause the lack of *AtHKT1;1* expression in C24 roots by yet unknown mechanisms. Tissue specific targeting of small RNAs may cause methylation of the transposon region and therefore lead to inactivation of *AtHKT1;1* transcription or *AtHKT1;1* transcript may be degraded by small RNAs that target the transcript. This lack of *AtHKT1;1* expression has been linked to an increased accumulation of Na^+ in the shoot. The results presented here suggest that in addition to Na^+ transport, AtHKT1;1 may also potentially play a role in K^+ transport, although this function is yet to be definitively confirmed. It was shown that NaCl induced alterations in cytosolic free calcium are different between C24 and Col-0, with C24 appearing to lack part of the signature, leading to the hypothesis that C24 has a reduced responsiveness to NaCl. This was further confirmed by analysing changes in the expression levels of salt responsive genes. An approach was presented for subsequent QTL analyses to identify the locus that is conferring the reduced responsiveness in C24, potentially allowing the identification of novel components in the salt signalling pathway.

Supplementary

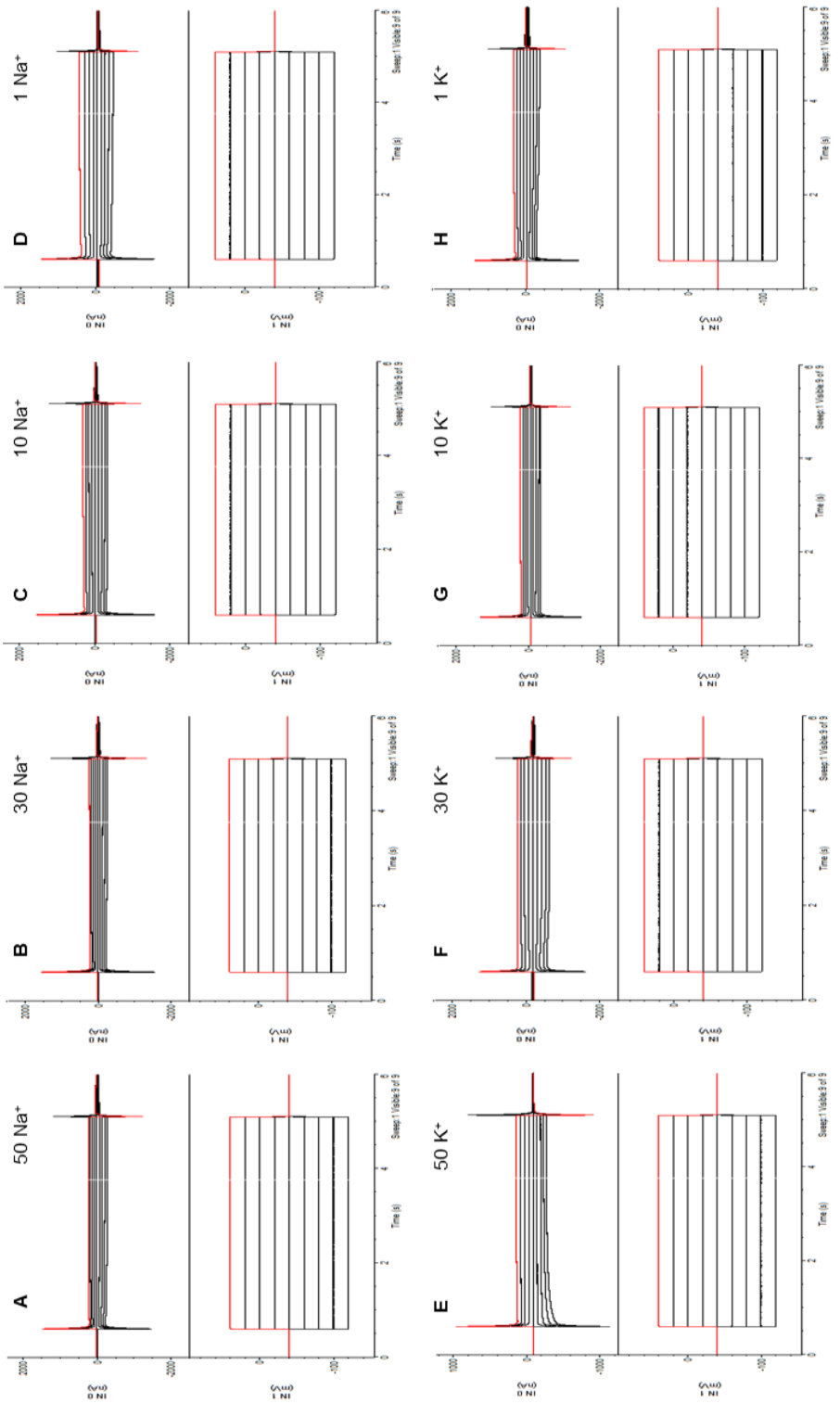

Supplementary Figure.8.1: Representative traces of water injected oocytes.

Each panel (A to H) contains representative traces of currents of water injected oocytes (in the top half of the panel) in response to the applied voltage protocol (indicated in the bottom half of each panel) in bathing solutions containing varying amounts of Na^+ and K^+. Amount of is indicated by 50, 30, 10 and 1 Na^+ or K^+ and refers to 50 mM, 30 mM, 10 mM and 1 mM Na^+ and K^+ respectively.

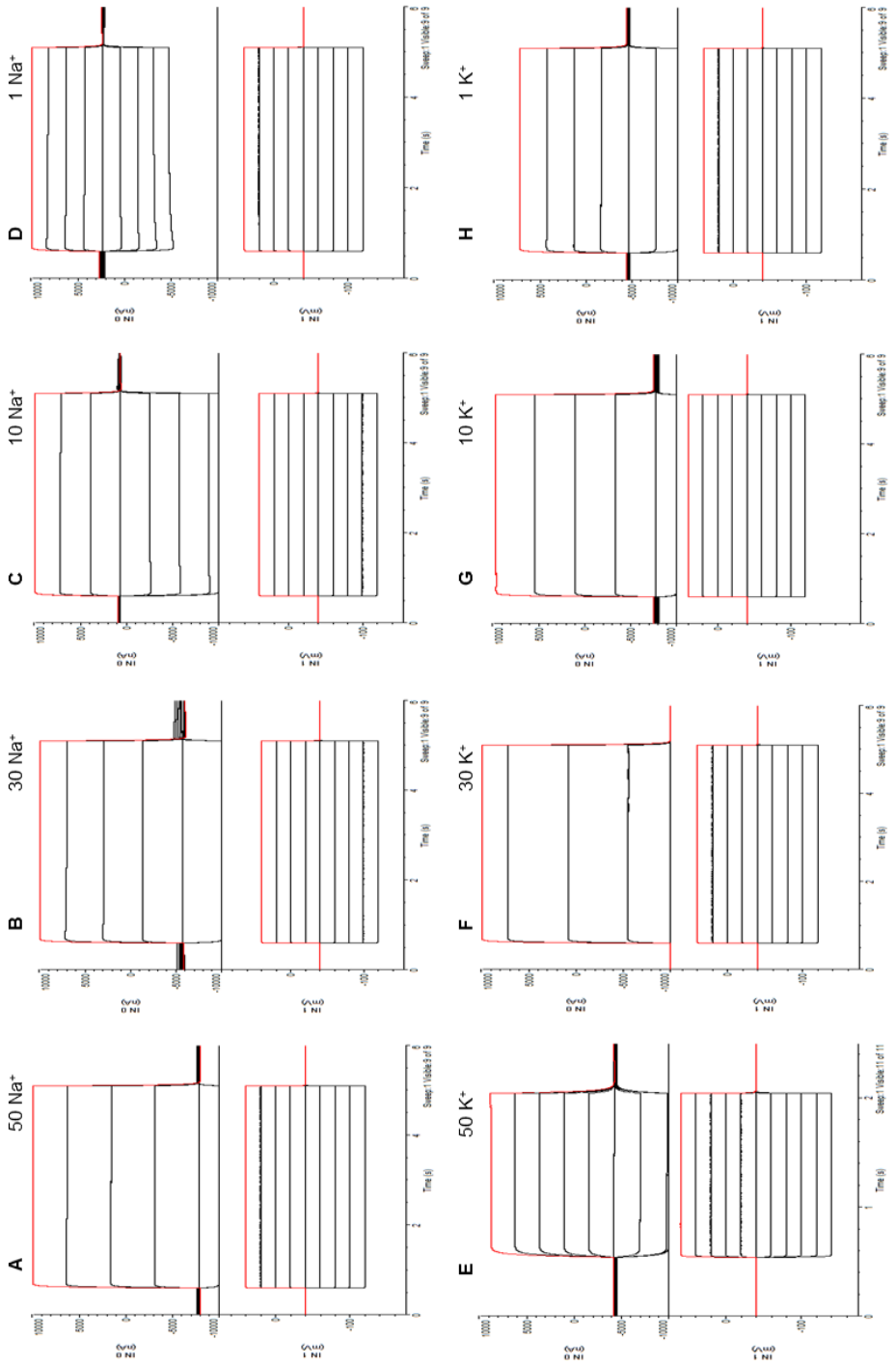

Supplementary Figure 8.2: Representative traces of *AtHKT1;1-Col* injected oocytes.

Each panel (A to H) contains representative traces of currents from *AtHKT1;1-Col* injected oocytes (in the top half of the panel) in response to the applied voltage protocol (indicated in the bottom half of each panel) in bathing solutions containing varying amounts of Na^+ and K^+. Amount of is indicated by 50, 30, 10 and 1 Na^+ or K^+ and refers to 50 mM, 30 mM, 10 mM and 1 mM Na^+ and K^+ respectively.

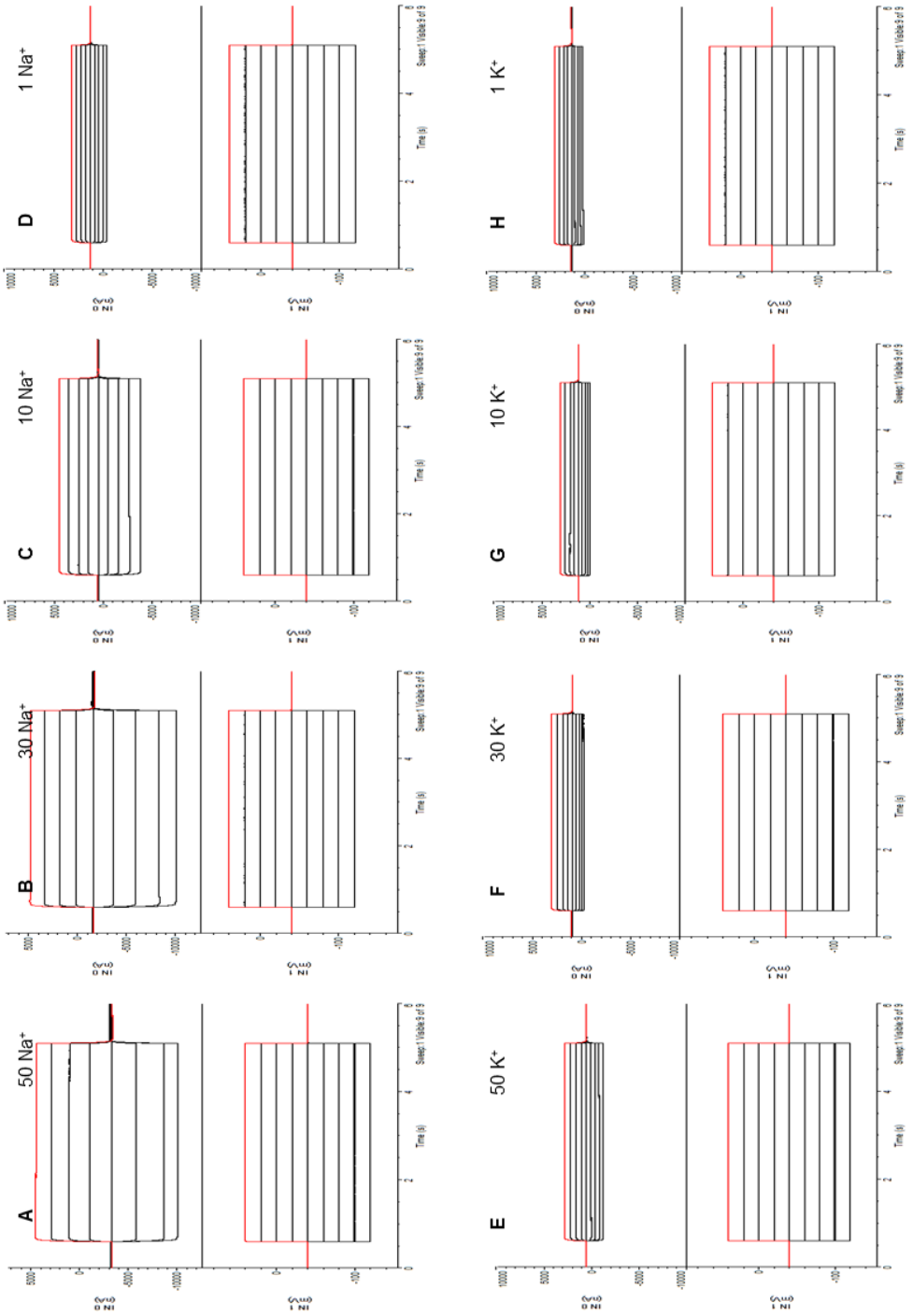

Supplementary Figure 8.3: Representative traces of *AtHKT1;1-C24* injected oocytes.

Each panel (A to H) contains representative traces of currents of *AtHKT1;1-C24* injected oocytes (in the top half of the panel) in response to the applied voltage protocol (indicated in the bottom half of each panel) in bathing solutions containing varying amounts of Na^+ and K^+. Amount of is indicated by 50, 30, 10 and 1 Na^+ or K^+ and refers to 50 mM, 30 mM, 10 mM and 1 mM Na^+ and K^+ respectively.

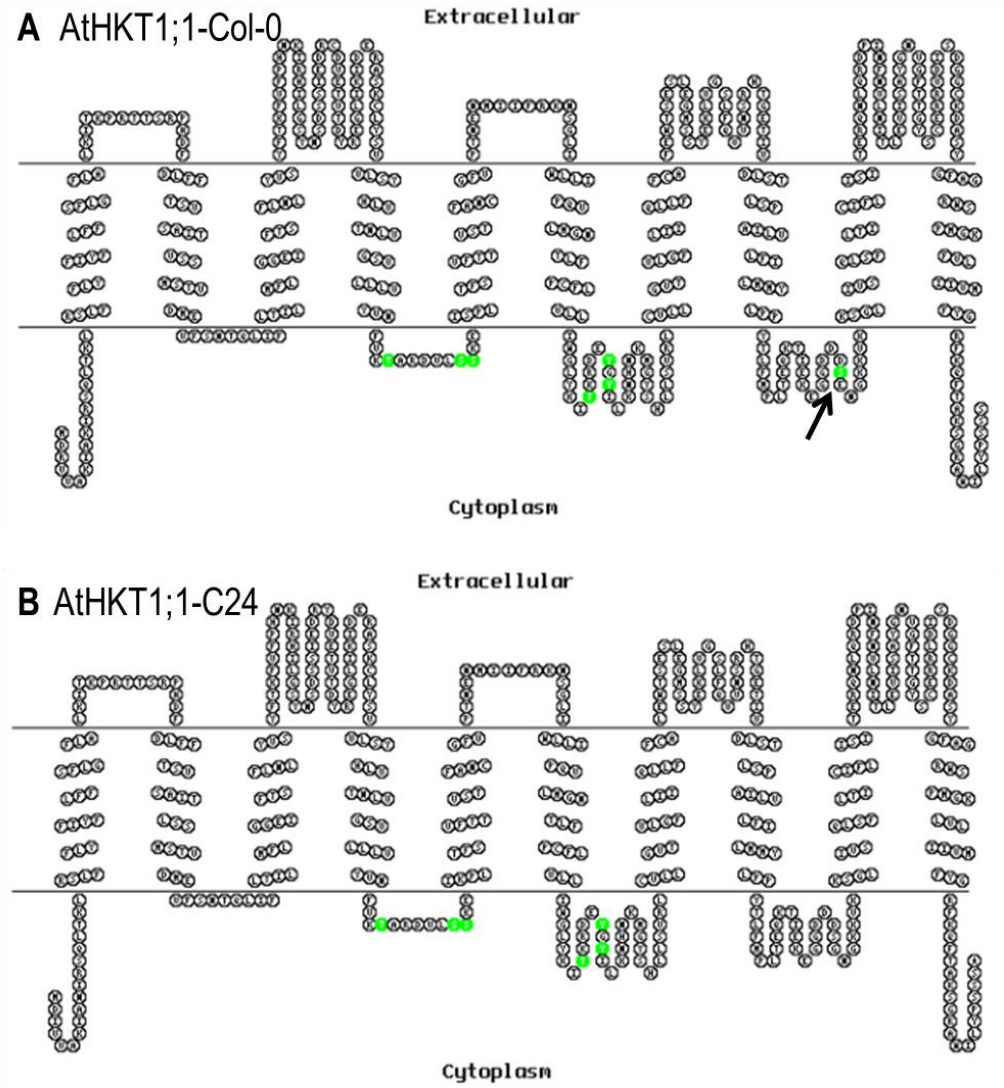

Supplementary Figure 8.4: A topology model of (A) AtHKT1;1 Col-0 and (B) AtHKT1;1-C24.

The topology was predicted by TopPred v2 and phosphorylation sites using NetPhos v2 (Blom *et al.* 1999). Predicted phosphorylation sites in the cytosolic loops are marked in green colour. The black arrow indicates the predicted phosphorylated site S384 in AtHKT1;1-Col-0, which is absent in AtHKT1;1-C24. The topology map was drawn with TOPO (http://www.sacs.ucsf.edu/cgi-bin/open-topo2.py).

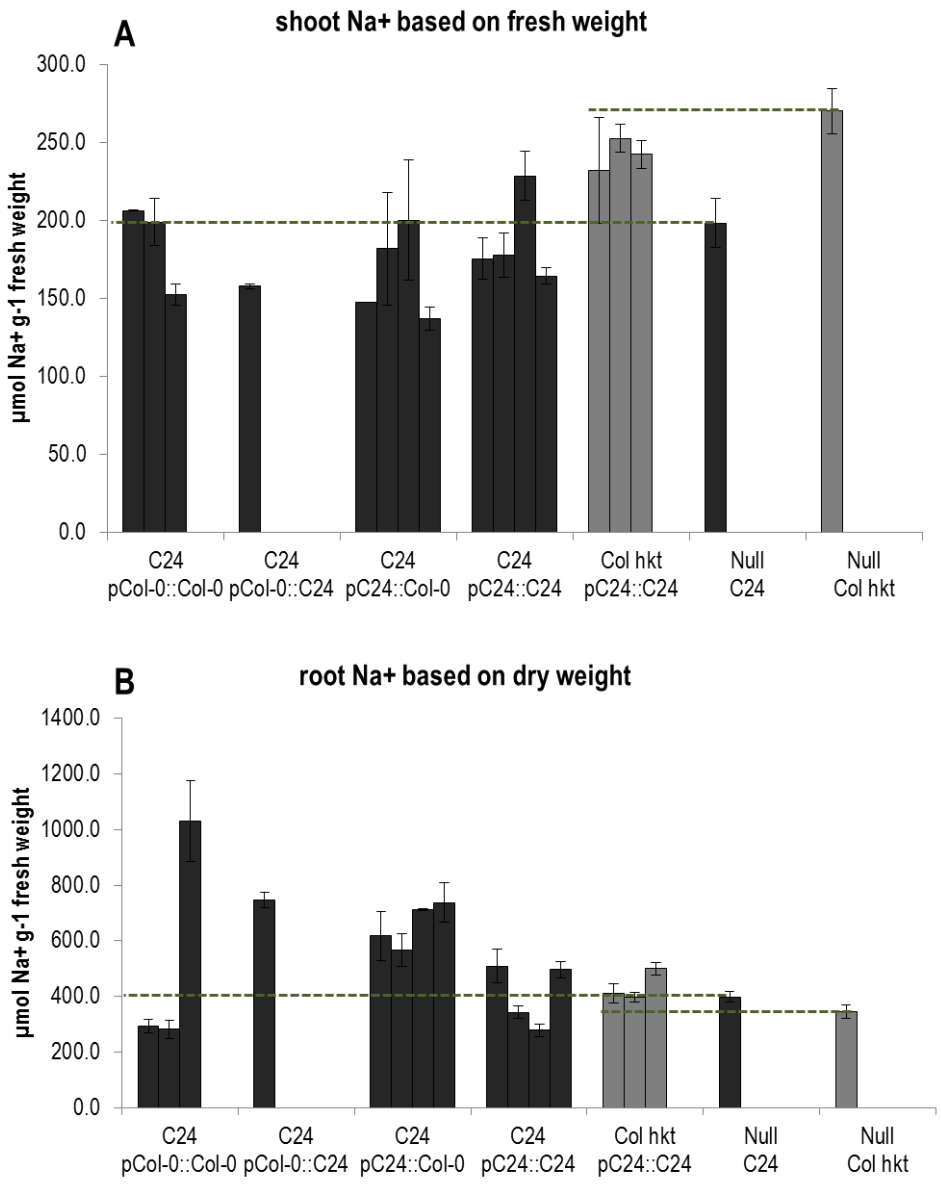

Supplementary Figure 8.5: Na^+ content of (A) shoot and (B) root of NaCl treated transgenic lines containing promoter::cDNA constructs.

Independent transgenic lines displayed separately. Figure is in addition to Figure 4.13. Transgenic lines in the C24 background are presented in dark grey bars and transgenic lines in the Col-0 *gl1 hkt1*-4 background are presented in light grey bars. Green dashed line indicates the mean of the Null background ecotype. Values are mean±SEM (n=3-5).

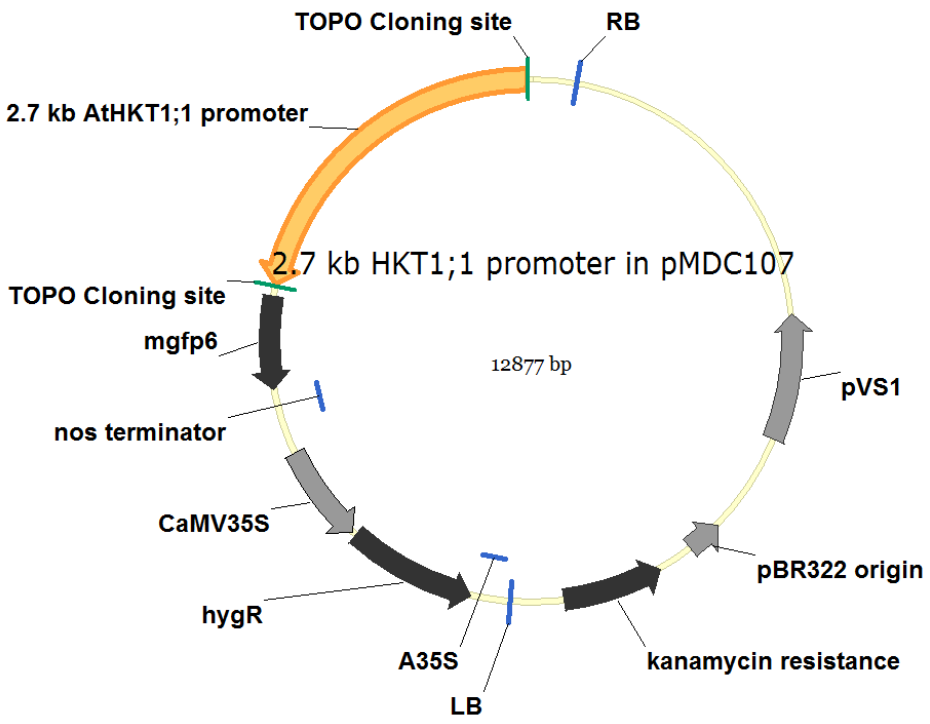

Supplementary Figure 8.6: Vector map of an expression vector containing the 2.7 kb *AtHKT1;1* promoter upstream of the *GFP* coding sequence to investigate *AtHKT1;1* promoter activity *in planta*.

The T-DNA cassette inserted into the plant genome commences at the right border (RB), and contains the 2.7 kb *AtHKT1;1* promoter, *GFP* gene (mgfp6), bacterial nopaline synthase terminator (nos terminator), Cauliflower Mosaic Virus 35S promoter (CaMV35S), hygromycin resistance gene (hygR), Cauliflower Mosaic Virus 35S 3′ UTR polyA signal (A35S) and left border sequence (LB).

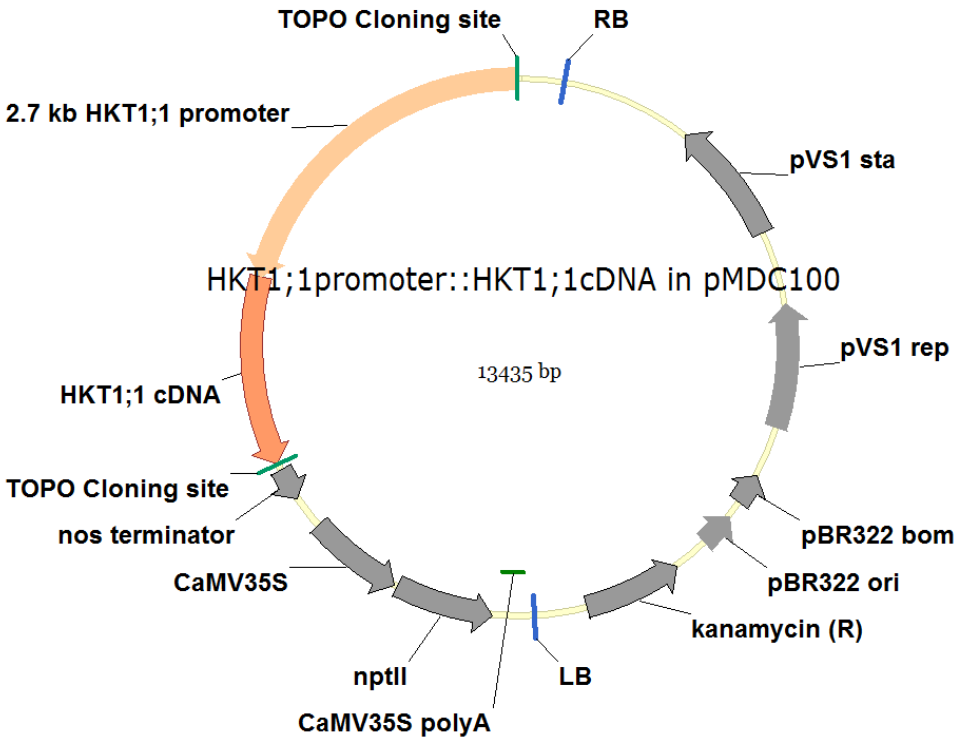

Supplementary Figure 8.7**: Vector map of an expression vector containing the 2.7 kb AtHKT1;1 promoter upstream of the AtHKT1;1 cDNA sequence to investigate AtHKT1;1 transgene activity in planta.**

The T-DNA cassette inserted into the plant genome commences at the right border (RB), and contains the 2.7 kb *AtHKT1;1* promoter, *AtHKT1;1* cDNA, bacterial nopaline synthase terminator (nos terminator), Cauliflower Mosaic Virus 35S promoter (CaMV35S), neomycin phosphotransferase resistance gene mediating kanamycin resistance (*NptII*), Cauliflower Mosaic Virus 35S 3′ UTR polyA signal (A35S) and left border sequence (LB).

Supplementary Table 8.1: Detailed legend description for Methylome tracks (adopted from http://signal.salk.edu/NOTE_methylome.html)

Legend item	Description
mCIP col/met1 BU	signal: posterior probability of HMM by TileMap (significantly higher signal in wild type when the wild type methylated DNA is used as probe data compared to methylated DNA in met1 mutant.); sample: enriched DNA by methyl cytosine antibody; tissue: whole plant tissue (aerial part); plant: wild type and met1 mutant (columbia background)
mCIP met1/col BU	signal: posterior probability of HMM by TileMap (significantly higher signal in met1 mutant when the mutant methylated DNA is used as probe data compared to wild type methylated DNA.); sample: enriched DNA by methyl cytosine antibody; tissue: whole plant tissue (aerial part); plant: met1 mutant and wild type
mCIP col/ddc BU	signal: posterior probability of HMM by TileMap (significantly higher signal in wild type when the wild type methylated DNA is used as probe data compared to methylated DNA in ddc mutant); sample: enriched DNA by methyl cytosine antibody; tissue: whole plant tissue (aerial part); plant: wild type and ddc triple mutant (columbia background)
mCIP ddc/col BU	signal: posterior probability of HMM by TileMap (significantly higher signal in ddc mutant when the mutant methylated DNA is used as probe data compared to wild type methylated DNA.); sample: enriched DNA by methyl cytosine antibody; tissue: whole plant tissue (aerial part); plant: ddc triple mutant and wild type
mCIP col BU/UB	signal: posterior probability of HMM by TileMap (up in enriched DNA by methyl cytosine antibody); sample: enriched DNA by methyl cytosine antibody and un-bounded DNA fraction by the antibody; tissue: whole plant tissue (aerial part); plant: wild type (columbia)
mCIP met1 BU/UB	signal: posterior probability of HMM by TileMap (up in enriched DNA by methyl cytosine antibody); sample: enriched DNA by methyl cytosine antibody and un-bounded DNA fraction by the antibody; tissue: whole plant tissue (aerial part); plant: met1 mutant (columbia background)
mCIP ddc BU/UB	signal: posterior probability of HMM by TileMap (up in enriched DNA by methyl cytosine antibody); sample: enriched DNA by methyl cytosine antibody and un-bounded DNA fraction by the antibody; tissue: whole plant tissue (aerial part); plant: ddc triple mutant (columbia background)
HMBD col BU/UB	signal: posterior probability of HMM by TileMap (up in enriched DNA by methylcytosine-binding domain of the human MeCP2 protein (MBD)); sample: enriched DNA by MBD and un-bounded DNA fraction by MBD; tissue: whole plant tissue (aerial part); plant: wild type (columbia)


Exon 1
AtHKT1_1-C24 ATGGACATAGTGGTGGCAAAAATAGCAAACATTCGTTCGCAGCTTACTAAATTACGTTCT 60
AtHKT1_1-Col-0 ATGGACAGAGTGGTGGCAAAAATAGCAAAAATCCGTTCGCAGCTTACTAAATTACGTTCA 60
AtHKT1_1-C24 CTATTCTTCCTTTACTTCATCTACTTCTTGTTCTTCTCCTTTTTAGGGTTTTTGGCACTC 120
AtHKT1_1-Col-0 CTATTCTTCCTTTACTTCATCTACTTCTTGTTCTTCTCCTTTTTAGGGTTTTTGGCACTC 120
AtHKT1_1-C24 AAGATCACAAAGCCAAGAACCACTTCACGTCCTCATGACTTTGACCTTTTCTTCACTTCT 180
AtHKT1_1-Col-0 AAGATCACAAAGCCAAGAACCACTTCACGTCCTCATGACTTTGACCTTTTCTTCACTTCT 180
AtHKT1_1-C24 GTCTCTGCCATAACCCTCTCTTCCATGTCTACCGTCGACATGGAAGTCTTCTCCAACACC 240
AtHKT1_1-Col-0 GTCTCTGCCATCACCGTCTCTTCCATGTCTACCGTCGACATGGAAGTCTTCTCCAACACC 240
AtHKT1_1-C24 CAACTTATCTTCCTCACTATCCTCATGTTCCTTGGTGGCGAAATCTTCACCTCCTTTCTC 300
AtHKT1_1-Col-0 CAACTTATCTTCCTCACTATCCTCATGTTCCTCGGTGGCGAAATCTTCACCTCCTTTCTC 300
AtHKT1_1-C24 AACCTCTATGTCTCCTATTTCACCAAGTTCGTCTTCCCTCATAACAAGATTAGACATATT 360
AtHKT1_1-Col-0 AACCTCTACGTCTCCTATTTCACCAAGTTCGTCTTCCCTCATAACAAGATTAGACATATT 360
AtHKT1_1-C24 TTGGGATCTTATAATTCGGACAGTTCCATCGAGGATCGCTATGACGTTGAGACTGTTACT 420
AtHKT1_1-Col-0 TTGGGATCTTATAATTCGGACAGTTCCATCGAGGATCGCTGTGACGTTGAGACTGTTACT 420
AtHKT1_1-C24 GATTATCGCGAGGGTCTTATCAAGATCGATGAAAGGGCATCTAAGTGCTTGTACTCGGTG 480
AtHKT1_1-Col-0 GATTATCGCGAGGGTCTTATCAAGATCGATGAAAGGGCATCTAAGTGCTTGTACTCGGTG 480
AtHKT1_1-C24 GTTCTTAGTTACCATCTTGTTACTAACCTAGTTGGCTCTGTGTTGCTTCTTGTGTACGTA 540
AtHKT1_1-Col-0 GTTCTTAGTTACCATCTTGTTACTAACCTAGTTGGCTCTGTGTTGCTTCTTGTGTACGTA 540
AtHKT1_1-C24 AATTTTGTTAAAACGGCGAGAGATGTTCTTAGTTCCAAAGAAATCAAACCTCTCACTTTC 600
AtHKT1_1-Col-0 AATTTTGTTAAAACGGCGAGAGATGTTCTTAGTTCCAAAGAAATCTCACCTCTCACTTTC 600
AtHKT1_1-C24 TCCGTCTTCACAACAGTTTCCACGTTTGCAAACTGCGGATTTGTCCCTACGAATGAGAAT 660
AtHKT1_1-Col-0 TCCGTCTTCACAACTGTTTCCACGTTTGCAAACTGCGGATTTGTCCCCACGAATGAGAAC 660
AtHKT1_1-C24 ATGATCATCTTTCGCAAGAACTCTGGTCTCATCTGGCTCCTAATCCCTCAAGTACTGATG 720
AtHKT1_1-Col-0 ATGATCATCTTTCGCAAGAACTCTGGTCTCATCTGGCTCCTAATCCCTCAAGTACTGATG 720
AtHKT1_1-C24 GGAAACACTTTGTTCCCTTGCTTCTTGGTTTTGCTCATATGGGGACTTTATAAGATCACA 780
AtHKT1_1-Col-0 GGAAACACTTTGTTCCCTTGCTTCTTGGTTTTGCTCATATGGGGACTTTATAAGATCACA 780
AtHKT1_1-C24 AAGCGTGACGAGTATGGTTACATTCTCAAGAACCACAATAAGATGGGATACTCTCATCTA 840
AtHKT1_1-Col-0 AAGCGTGACGAGTATGGTTACATTCTCAAGAACCACAATAAGATGGGATACTCTCATCTA 840
AtHKT1_1-C24 CTCTCGGTTCGTCTATGTGTTCTTCTTGGAGTGACGGTGCTAGGGTTTCTGATAATACAG 900
AtHKT1_1-Col-0 CTCTCGGTTCGTCTATGTGTTCTTCTTGGAGTGACGGTGCTAGGGTTTCTGATAATACAG 900

```
AtHKT1_1-C24        CTTCTTTTCTTCTGCGCCCTTGAATGGACCTCTGAGTCTCTAGAAGGAATGAGTTCGTAC 960
AtHKT1_1-Col-0      CTTCTTTTCTTCTGCGCCTTTGAATGGACCTCTGAGTCTCTAGAAGGAATGAGTTCGTAC 960
                    ****************** ****************************************

AtHKT1_1-C24        GAGAAGTTGGTTGGATCGTTGTTTCAAGTGGTGAATTCGCGACACACCGGAGAAACTATA 1020
AtHKT1_1-Col-0      GAGAAGTTGGTTGGATCGTTGTTTCAAGTGGTGAATTCGCGACACACCGGAGAAACTATA 1020
                    ************************************************************

                                                          Exon 1
AtHKT1_1-C24        GTAGACCTCTCTACACTTTCCCCAGCTATCTTGGTACTCTTTATTCTTATGATGTAAGTT 1080
AtHKT1_1-Col-0      GTAGACCTCTCTACACTTTCCCCAGCTATCTTGGTACTCTTTATTCTTATGATGTAAGTT 1080
                    ************************************************************

AtHKT1_1-C24        TCTTTCAATCCTCTCCTCATATATCGAATCATTTGCATGAACTCAAAATATTTAGATCGA 1140
AtHKT1_1-Col-0      TCTTTCAATCCTCTCCTCATATATCGAATCATTTGCATGAACTCGAAATATTTAGATCGA 1140
                    ******************************************** ***************

AtHKT1_1-C24        AAGGTGCACTTATTTCGACATAATTTTCACATATGAGGTGATATGCATGCACACATAGGT 1200
AtHKT1_1-Col-0      AAGGTGCACTTATTTCGACATAATTTTCACATATGAGGTGATATGCATGCACACATAGGT 1200
                    ************************************************************

AtHKT1_1-C24        GCAGTTTTACGAATACATTAAACTAAAACAATTGAGATATAGTGAAATTAAATGGTTGAC 1260
AtHKT1_1-Col-0      GCAGTTTTACGAATACATTAAACTAAAACAATTGAGATATAGTGAAATTAAATGGTTGAC 1260
                    ************************************************************

AtHKT1_1-C24        TTTTCACTACAGAAACAATAAAAAGTCACCGCATGAATTAAAGTTGGTTGACATTTCACA 1320
AtHKT1_1-Col-0      ATTTCACTACAGAAACAATAAAAAGTCACCGCATGAATTAAAGTTGGTTGACATTTCACA 1320
                     ************************************************************

AtHKT1_1-C24        ACAGAAACACCAAACATATTATTATCTCACGTAATGTAGTTTGGAAAATTATCAAATCAT 1380
AtHKT1_1-Col-0      ACAGAAACACCAAACATATTATTATCTCACGTAATGTAGTTTGGAAAATTATCAAATCAT 1380
                    ************************************************************

AtHKT1_1-C24        TTACCTAAATTTTTTTTTTTATGAAGCAAACATTTTCCTAACTATTATTGTTTATTCCATA 1440
AtHKT1_1-Col-0      TTACCTAATTTTTTTTTTTATGAAGCAAACATTTTCCTAACTATTATTGTTTATTCCATA 1440
                    ******** ****************************************************

AtHKT1_1-C24        CCAAAAAAAAAAAAACGTTTATGATTTATTTAATGATTTTTTTAATTACTACGTAAAGGCC 1500
AtHKT1_1-Col-0      CCAAAAAAAAAAA-CGTTTATGATTTATTTAAGGATTTTTTTAATTACTACGTAAAGGCC 1499
                    ************* ****************** ****************************

AtHKT1_1-C24        AATCATGCATGAGTGGGGTGGTAGAACCATAGATTTGCATTAGTTTTAGTGCTATTCTTT 1560
AtHKT1_1-Col-0      AATCATGCATGAGTGGGGTGGTAGAACCATAGATTTGCATTAGTTTTAGTGCTATTCTTT 1559
                    ************************************************************

AtHKT1_1-C24        TGGCTGAATCCACCAATTAATCAGCTTAGCAATTGAAAGCATATTTTATTAACCAAAATT 1620
AtHKT1_1-Col-0      TGGCTGAATCCACCAATTAATCAGCTTAGCAATTGAAAGCATATTTTATTAACCAAAATT 1619
                    ************************************************************

AtHKT1_1-C24        AATTTTAACATATCTAACGTGGTCCATTTGGTTAAAGTATTCACTCCCATGGATTGAGGA 1680
AtHKT1_1-Col-0      AATTTTAACATATCTAACGTGGTCCATTTGGTTAAAGTATTCACTCCCATGGATTGAGGA 1679
                    ************************************************************

AtHKT1_1-C24        AGTAAGATTTAAGTTATAACCATGCTTGGCAATTATACATTTAATGAATAGTTTGAATAC 1740
AtHKT1_1-Col-0      AGTAAGATTTAAGTTATAACCATGCTTGGCAATTATACATTTAATGAATAGTTTGAATAC 1739
                    ************************************************************

AtHKT1_1-C24        CAAGCTAATATATAATTTTTGGAGATTAATTAGTATTTATTTCGGTAAATCATTCTTGTA 1800
AtHKT1_1-Col-0      CAAGCTAATTTATAATTTTTGGAGATTAATTAGTATTTATTTCGGTAAATCATTCTTGTA 1799
                    ********* ****************************************************
```


AtHKT1_1-C24 ACAAAAAAA-TACTAATAATATAAAAAATTGAGATTGTGAAGTTTATTTTTTCACCACAA 1859
AtHKT1_1-Col-0 ACAAAAAAAATACTAATAATATAAAAAATTGAGATTGTGAAGTTTATTTTTTCACCACAA 1859
AtHKT1_1-C24 ACACAAATTTCATAGAATTTTTCAAGGTTTCCACAAATTAGTTTACGCTCTTAAAATAAC 1919
AtHKT1_1-Col-0 ACACAAATTTCATAGAATTTTTCAAGGTTTCCACAAATTAGTTTACGCTCTTAAAATAAC 1919
AtHKT1_1-C24 AAACAAAACCAAAATTAGTATGCTTGTCAAACTTTCCACAAAAACATTAACGCCGGAAAA 1979
AtHKT1_1-Col-0 AAACAAAACAAAAAGTAGTATGCTTGTCAAACTTTCCACAAAAACATTAACGCCGGAAAA 1979
AtHKT1_1-C24 CTTAAAACAAATAGTCATAATACATCTTTATTAAATAAATAAAAAGAAGGCATAATACAT 2039
AtHKT1_1-Col-0 CTTAAAACAAATAGTCATAATACATCTTTATTAAATAAATAAAAAGAAGGCATAATACAT 2039
AtHKT1_1-C24 ATATAAGTTGATAAAACTCTCCATCACTTAAGAGTAATTTTTTGATGTTTTCACTTAGAA 2099
AtHKT1_1-Col-0 ATATAAGTTGATAAAACTCTCCATCACTTAAGAGTAATTTTTTGATGTTTTCACTTAGAA 2099
AtHKT1_1-C24 GAATTTATATATATCTATATTAACCATTAATTAAGGAACCTACAAGAGAATGTGGTAGCT 2159
AtHKT1_1-Col-0 GAATTTATATATATCTATATTAACCATTAATTAAGGAACCTACAAGAGAATGTGGTAGCT 2159
AtHKT1_1-C24 AGACAAGATTTGATAGAGTGAATCAGAATATATGTCCATGGTTTTAGATTCAGTAAAAAA 2219
AtHKT1_1-Col-0 AGACAAGATTTGATAGAGTGAATCAGAATATATGTCCATGGTTTTAGATTCAGTAAAAAA 2219
AtHKT1_1-C24 AAAATGTCCCTTCAATGTAGTGGAGACTGGAGAATGTCCCTTCATCATATTCACAAAGCA 2279
AtHKT1_1-Col-0 AAAATGTCCCTTCAATGTAGTGGAGACTGGAGAATGTCCCTTCATCATATTCACAAAGCA 2279
AtHKT1_1-C24 TTATTCTCTGTTTTTCCATAAAAACTTCTTTGGACTAATTAATAAGTAAAATATAATTGC 2339
AtHKT1_1-Col-0 TTATTCTCTGTTTTTCCATAAAAACTTCTTTGGACTAATTAAAAAGTAAAATATAATTGC 2339
Exon 2
AtHKT1_1-C24 GTTTCCAAGGTATCTTCCTCCATACACTTTATTTATGCCGTTGACGGAACAAAAGACGAT 2399
AtHKT1_1-Col-0 GTTTCCAAGGTATCTTCCTCCATACACTTTATTTATGCCGTTGACGGAACAAAAGACGAT 2399
AtHKT1_1-C24 AGAGAAAGAAGGAGGAGATGATGATTCCGGAAATGGAAAGAAAGTTAAAAAGAGTGGACT 2459
AtHKT1_1-Col-0 AGAGAAAGAAGGAGGAGATGATGATTCCGAAAATGGAAAGAAAGTTAAAAAGAGTGGACT 2459
AtHKT1_1-C24 CATCGTGTCACAACTTTCCTTTTTGACGATATGTATCTTTCTCATTTCAATCACCGAAAG 2519
AtHKT1_1-Col-0 CATCGTGTCACAACTTTCCTTTTTGACGATATGTATCTTTCTCATTTCAATCACCGAAAG 2519
AtHKT1_1-C24 GCAAAATCTACAACGTGATCCGATAAATTTCAACGTCCTTAACATCACTCTCGAAGTTAT 2579
AtHKT1_1-Col-0 GCAAAATCTACAACGTGATCCGATAAATTTCAACGTCCTTAACATCACTCTCGAAGTTAT 2579
Exon 2
AtHKT1_1-C24 CAGGTATGTTTCTATATCTCAAGATCCTTTAACCAAAACCAAAAAAAAAAATTGTTTCAG 2639
AtHKT1_1-Col-0 CAGGTATGTTTCTATATCTCAAGATTCTTTAACCAAAACCAAATAAAAAAATTGTTTCAG 2639
AtHKT1_1-C24 CAATATCTCTAGCT--ATATTACATATTCTGCATCCATGATAACTAAAAAGTTCAAAATC 2697
AtHKT1_1-Col-0 CAATATATAAATCTCTATATTACATATCATGCATCCATAATAACTAAAAATTTCAAAATA 2699

```
AtHKT1_1-C24        TTTTCAAAAATATATACGACATCTAGGTGATACATTATCATACAATTTGACAACCCAAGT 2757
AtHKT1_1-Col-0      TTTTCAAACA-AAATACGTCATCTAGGTGATACATTATTCTACAATTTGACAACCCAAGT 2758
                    ******** * * ***** ********************  ********************

AtHKT1_1-C24        ATTCGTAATTCACCTAACAAAATAAGAGGACGTGAATAGAATCGTATAAGAAACATATAT 2817
AtHKT1_1-Col-0      ATTCGTAATTCACCTAACAAAAAAAGAGGACGTGAATAAAATCGTATAAGAAACATATAT 2818
                    ********************** *************** ********************

AtHKT1_1-C24        ACAGTAAAACCTTTATAAATTAATAATGTTGGGACTGCAAAATTTTATTAATTTAGAAAA 2877
AtHKT1_1-Col-0      ACAGTAAAATCTCTATAAATTAATAATGTTGGGACTGCAAAATTTTATTAATTTAGAGAG 2878
                    ********* ** ********************************************* *

AtHKT1_1-C24        GTTTTTTATTGATCGATAAATTAATAAATTAATAGAGAAATCTTCCTAATTTAATAACTT 2937
AtHKT1_1-Col-0      ATTTTTTACTTATCGATAAATTAATAAATTAATAGAGAGATCTTCATAATTTAATAACTT 2938
                     ******* * *************************** ****** **************

AtHKT1_1-C24        TGAAAAAATTTCTCATTATAAAAAATATCTTTCTAAAATCAATTACAAGTAAAAAATAAT 2997
AtHKT1_1-Col-0      TGAAAAAATTTCTCATTATAGAAAATATCTTTCTAAAATCAATTACAAGTAAAAAATAAT 2998
                    ******************** ****************************************

AtHKT1_1-C24        ATCATGTCTAGAAAACAACACCAATATGTTTTGATACAGTAAAATATTAGAACTAAATTT 3057
AtHKT1_1-Col-0      ATCATGTATAGAAAACAACACCAATATGTTTTGATATAGTAAAATATTAGAACTAAATTT 3058
                    ******* ***************************** ************************

AtHKT1_1-C24        CAAATAAGAATAAATACAAATTTAAGCAAAAAAATATTAGAAATATATTTTTAAGAAATT 3117
AtHKT1_1-Col-0      CAAATAAGAATATATACAAATTTAAGCAAAAAAATATCAGAAATATATTTTTAAGAAATT 3118
                    ************ ************************ ************************

AtHKT1_1-C24        TCTTACATATAATGTGTATATATATAGTTGATATATTTGTGCAATTATTAATTTATGATA 3177
AtHKT1_1-Col-0      TCTTACATATAATGT--ATATATATAGTTGATATATTTGTGCAATTATTAATTTCTGATA 3176
                    ***************  ************************************ *****

AtHKT1_1-C24        TTGATGGACCATATATTTACATAGGACTTTCAAAAAAATTATTATCTAATTAATTTATCG 3237
AtHKT1_1-Col-0      TTGATGGACCATATATTTACATAGGACTTTCAAAAAAATTATTATCTAATTAATTTATCG 3236
                    ************************************************************

AtHKT1_1-C24        ATTTATGTCATTTTTTACACTAGTCCCAACTCGGGACCGGAAGAATTTATTAATTTATAG 3297
AtHKT1_1-Col-0      ATTTATGTCATTTTTTATACTACTCCCAACTCGGGACCGGAAGAATTTATTAATTTATAG 3296
                    ****************** **** ****************************************

AtHKT1_1-C24        AGGTTATTAATTTATCGAGTATAAATTTATAAAATAAAAAGAAACATATATATATATATA 3357
AtHKT1_1-Col-0      AGGTTATTAATTTATCGAGTATAAATTTATAAAATAAAAAGAAACATATATATATATATA 3356
                    ************************************************************

AtHKT1_1-C24        TAAATATATAGATATAGGGTTGTCAAAATGGGTCAAAATTCATGTGTCAACTCAACTCAA 3417
AtHKT1_1-Col-0      ---ATATATATATATA---------------------------------------------- 3369
                       ******* *****

AtHKT1_1-C24        TTCAACCCATGAACCCTAATGAGTTGAAAATTTTGACTCAAATGAGTTAATGAGTCAAAT 3477
AtHKT1_1-Col-0      ------------------------------------------------------------

AtHKT1_1-C24        GAGTAGATGAGTCAATTAGTTTGATGAGTAAAATGAGTTGGGTTGTAATGGTTAATGGTT 3537
AtHKT1_1-Col-0      ------------------------------------------------------------

AtHKT1_1-C24        TCAATGGTTTACCCAATTAACCCATCAAGTTTTGTAAAATTCAATTAAAATACTAAAATC 3597
AtHKT1_1-Col-0      --------------------------------TATATAATTCA----------------- 3380
                                                    * ** ******
```

```
AtHKT1_1-C24        TCTAAACCAATGTCAATTTAAGTTTAACCAACACATCTAAACCAATTTAATAAAATTAAT 3657
AtHKT1_1-Col-0      ------------------------------------------------------------

AtHKT1_1-C24        ATTTTTCCAAATTTCTTAAATGTACAAGCGATGAAATTGAGAAAAAGTAAACTCGTAATA 3717
AtHKT1_1-Col-0      ------------------------------------------------------------

AtHKT1_1-C24        TTTCCACCAAAAAACATAAACCCGTGATTTTCCCGCCAAAAACGTAAACCCGTGATTTTC 3777
AtHKT1_1-Col-0      ------------------------------------------------------------

AtHKT1_1-C24        CTGCCAAAAACGAAAATCCGTAATTTTCCCGGCAAATACGTAAATCCGTGATTTTCCCGC 3837
AtHKT1_1-Col-0      ------------------------------------------------------------

AtHKT1_1-C24        CAAAAACGTAAACCCGAGATTTTCCCGCCAAAAACGTAAATCCATAAATTTCCCGCCAAA 3897
AtHKT1_1-Col-0      ------------------------------------------------------------

AtHKT1_1-C24        AACTTAAACCCGTAATTTTCCCGCCAAAAATGTAAACCCGTGATTTTCCCGCCAAAAACG 3957
AtHKT1_1-Col-0      ------------------------------------------------------------

AtHKT1_1-C24        TAAATCCGTGATTTTCCCGCCAAAAACGTAAACCCGAGATTTTCCCGCCAAAAANATAAA 4017
AtHKT1_1-Col-0      ------------------------------------------------------------

AtHKT1_1-C24        CCCGTAATTTTCCCGCCAAAAATGTAAACCCGAGATTTTCCCGCCAAAAACGTAAATCCA 4077
AtHKT1_1-Col-0      ------------------------------------------------------------

AtHKT1_1-C24        TAATTTTCCCGCCAAAAACGTAAACCCCTGATTTTCCCGCCAAAAACGTAAACCCCTGAT 4137
AtHKT1_1-Col-0      ------------------------------------------------------------

AtHKT1_1-C24        TTTCCCGCCAAAAACGTAAACCCCTGATTTTCCCGCCAAAAACTTAAACCCGTAATTTTT 4197
AtHKT1_1-Col-0      ------------------------------------------------------------

AtHKT1_1-C24        CCGCCAAAAACGTAAATCCGTAATTTTTGCGCCAAAAATGTAAGCCTATAATTTTCCGCT 4257
AtHKT1_1-Col-0      ------------------------------------------------------------

AtHKT1_1-C24        AAAAATGTAAACCCGTGATTTTCCCGCCAAAAACGTAAATCCGTGATTTTCCCGCCAAAA 4317
AtHKT1_1-Col-0      ------------------------------------------------------------

AtHKT1_1-C24        ACGTAAACCCGAGATTTTCCCGCCAAAAAGATAAACCCGTAATTTTCCCGCCAAAAATGT 4377
AtHKT1_1-Col-0      ------------------------------------------------------------

AtHKT1_1-C24        AAACCCGAGATTTTCCCGCCAAAAACGTAAATCCATAATTTTCCCGCCAAAAACGTAAAC 4437
AtHKT1_1-Col-0      ------------------------------------------------------------

AtHKT1_1-C24        CCCTGATTTTCCCGCCAAAAACGTAAACCCCTGATTTTCCCGCCAAAAACGTAAACCCCT 4497
AtHKT1_1-Col-0      ------------------------------------------------------------
```

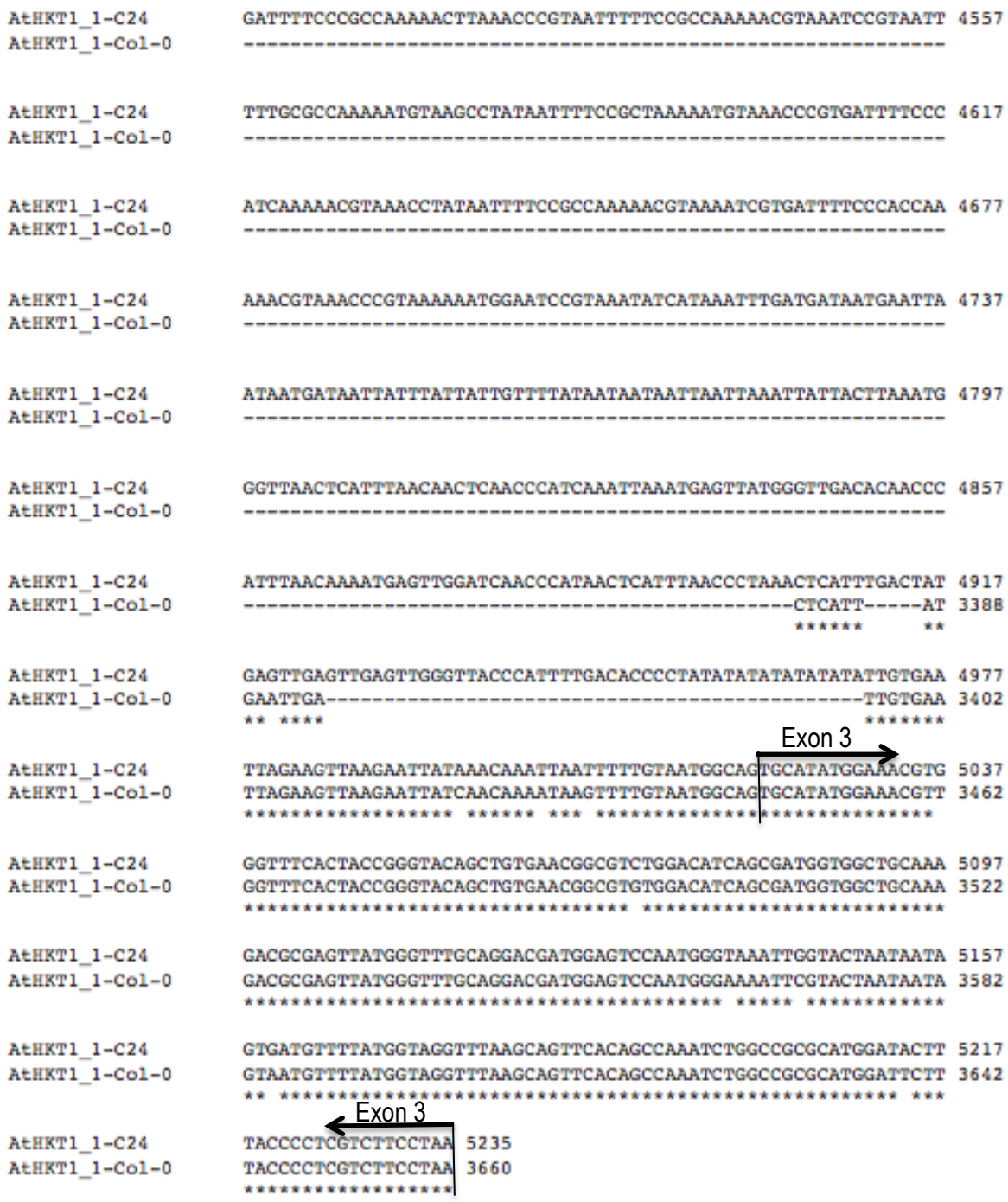

Supplementary Figure 8.8: Alignment of genomic DNA of AtHKT1;1-Col-0 and AtHKT1;1-C24.

Sequence alignment performed using Clustal W v2.1. Start and end of the each *AtHKT1;1* exon are marked with black arrows. The first codon, ATG, is the start codon of *AtHKT1;1* and the last codon, TAA, is the stop codon.

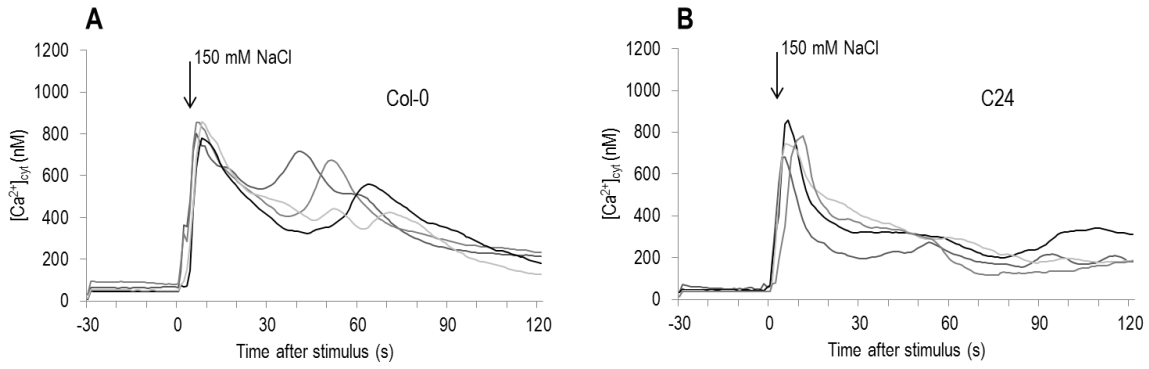

Supplementary Figure 8.9: Luminometric measurements of 13 d to 15 d old whole Arabidopsis seedlings, constitutively expressing *Aequorin,* in hyperpolarising base solution.

Alterations of $[Ca^{2+}]_{cyt}$ induced by 150 mM NaCl, in ecotype (a) Col-0 and in (b) C24. Each panel contains data from four representative individual seedlings. Stimulus was applied at time point 0.

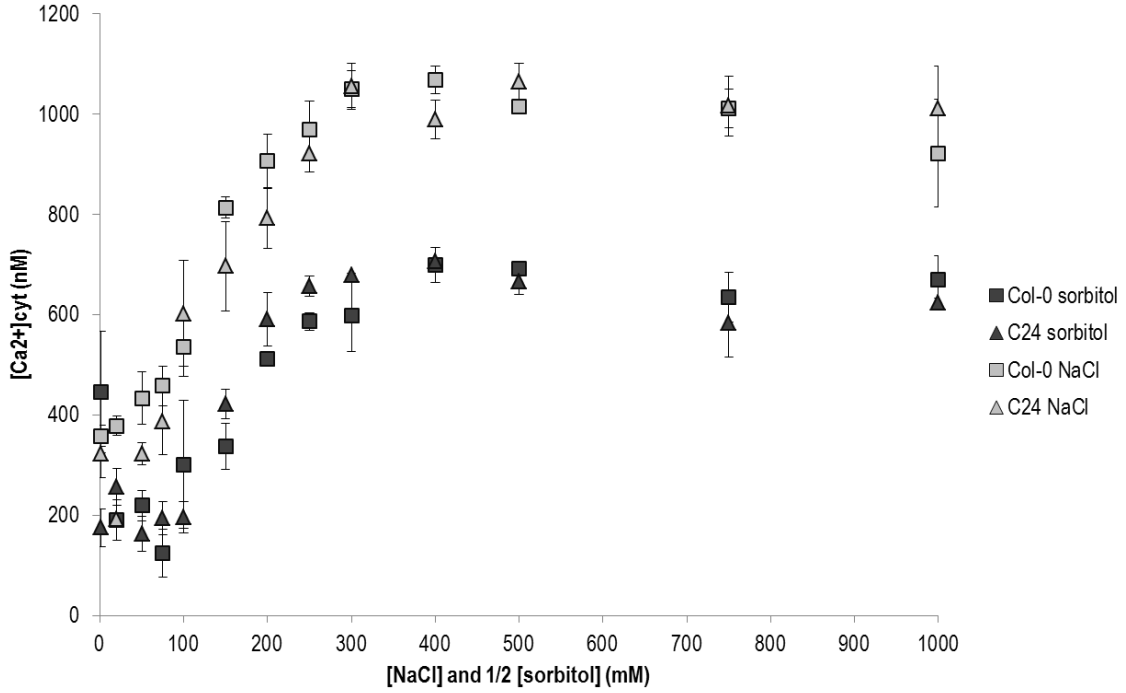

Supplementary Figure 8.10: Amplitude of the first $[Ca^{2+}]_{cyt}$ peak from luminometric measurements of Col-0 and C24 in response to [NaCl] and [sorbitol] treatment.

The 13 d to 15 d old Col-0 and C24 seedlings constitutively expressing *Apoaequorin* were treated with a range of NaCl and corresponding similar osmotic strength of sorbitol concentrations. Each point represents the average peak height of the first $[Ca^{2+}]_{cyt}$ peak of three replicates, error bars indicate the standard error of the mean (S.E.M.).

This is the end of the thesis! If you can honestly say you read this book cover-to-cover, please contact me, I want to get to know you! You deserve acknowledgement and Schoko-bons!

References

Alam, R., Rahman, M.S., Seraj, Z.I., Thomson, M.J., Ismail, A.M., Tumimbang-Raiz, E. and Gregorio, G.B. (2011) Investigation of seedling-stage salinity tolerance QTLs using backcross lines derived from *Oryza sativa* L. Pokkali. *Plant Breeding*, **130**, 430-437.

Ali, Z., Park, H.C., Ali, A., Oh, D.H., Aman, R., Kropornicka, A., Hong, H., Choi, W., Chung, W.S., Kim, W.Y., Bressan, R.A., Bohnert, H.J., Lee, S.Y. and Yun, D.J. (2012) TsHKT1;2, a HKT1 homolog from the extremophile Arabidopsis relative *Thellungiella salsuginea*, shows K^+ specificity in the presence of NaCl. *Plant Physiology*, **158**, 1463-1474.

Allen, E., Xie, Z., Gustafson, A.M. and Carrington, J.C. (2005) microRNA-directed phasing during trans-acting siRNA biogenesis in plants. *Cell*, **121**, 207-221.

Allen, G.J., Chu, S.P., Harrington, C.L., Schumacher, K., Hoffman, T., Tang, Y.Y., Grill, E. and Schroeder, J.I. (2001) A defined range of guard cell calcium oscillation parameters encodes stomatal movements. *Nature*, **411**, 1053-1057.

Altschul, S.F., Madden, T.L., Schäffer, A.A., Zhang, J.H., Zhang, Z., Miller, W. and Lipman, D.J. (1997) Gapped BLAST and PSI-BLAST: a new generation of protein database search programs. *Nucleic Acids Research*, **25**, 3389-3402.

Ammar, M.H.M., Pandit, A., Singh, R.K., Sameena, S., Chauhan, M.S., Singh, A.K., Sharma, P.C., Gaikwad, K., Sharma, T.R., Mohapatra, T. and Singh, N.K. (2009) Mapping of QTLs controlling Na^+, K^+ and Cl^- ion concentrations in salt tolerant indica rice variety CSR27. *Journal of Plant Biochemistry and Biotechnology*, **18**, 139-150.

Anderson, J.M., Charbonneau, H., Jones, H.P., McCann, R.O. and Cormier, M.J. (1980) Characterization of the plant nicotinamide adenine-dinucleotide kinase activator protein and its identification as calmodulin. *Biochemistry*, **19**, 3113-3120.

Apse, M.P., Aharon, G.S., Snedden, W.A. and Blumwald, E. (1999) Salt tolerance conferred by overexpression of a vacuolar Na^+/H^+ antiport in Arabidopsis. *Science*, **285**, 1256-1258.

Apse, M.P. and Blumwald, E. (2007) Na^+ transport in plants. *FEBS Letters*, **581**, 2247-2254.

Apse, M.P., Sottosanto, J.B. and Blumwald, E. (2003) Vacuolar cation/H^+ exchange, ion homeostasis, and leaf development are altered in a T-DNA insertional mutant of AtNHX1, the Arabidopsis vacuolar Na^+/H^+ antiporter. *The Plant Journal*, **36**, 229-239.

Ardie, S.W., Xie, L., Takahashi, R., Liu, S. and Takano, T. (2009) Cloning of a high-affinity K^+ transporter gene *PutHKT2;1* from *Puccinellia tenuiflora* and its functional comparison with OsHKT2;1 from rice in yeast and Arabidopsis. *Journal of Experimental Botany*, **60**, 3491-3502.

Arraouadi, S., Badri, M., Abdelly, C., Huguet, T. and Aouani, M.E. (2012) QTL mapping of physiological traits associated with salt tolerance in *Medicago truncatula* recombinant inbred lines. *Genomics*, **99**, 118-125.

Arraouadi, S., Chardon, F., Huguet, T., Aouani, M.E. and Badri, M. (2011) QTLs mapping of morphological traits related to salt tolerance in *Medicago truncatula*. *Acta Physiologiae Plantarum*, **33**, 917-926.

Asins, M.J., Bolarín, M.C., Pérez-Alfocea, F., Estañ, M.T., Martínez-Andújar, C., Albacete, A., Villalta, I., Bernet, G.P., Dodd, I.C. and Carbonell, E.A. (2010)

Genetic analysis of physiological components of salt tolerance conferred by *Solanum* rootstocks. What is the rootstock doing for the scion? *Theoretical and Applied Genetics*, **121**, 105-115.

Axtell, M.J. (2013) Classification and comparison of small RNAs from plants. *Annual Review of Plant Biology*, **64**, 137-159.

Baek, D., Jiang, J.F., Chung, J.S., Wang, B.S., Chen, J.P., Xin, Z.G. and Shi, H.Z. (2011) Regulated *AtHKT1* gene expression by a distal enhancer element and DNA methylation in the promoter plays an important role in salt tolerance. *Plant and Cell Physiology*, **52**, 149-161.

Bañuelos, M.A., Sychrová, H., Bleykasten-Grosshans, C., Souciet, J.L. and Potier, S. (1998) The Nha1 antiporter of *Saccharomyces cerevisiae* mediates sodium and potassium efflux. *Microbiology*, **144 (Pt 10)**, 2749-2758.

Bassil, E., Coku, A. and Blumwald, E. (2012) Cellular ion homeostasis: emerging roles of intracellular NHX Na+/H+ antiporters in plant growth and development. *Journal of Experimental Botany*, **63**, 5727-5740.

Bassil, E., Tajima, H., Liang, Y.-C., Ohto, M.-a., Ushijima, K., Nakano, R., Esumi, T., Coku, A., Belmonte, M. and Blumwald, E. (2011) The Arabidopsis Na^+/H^+ Antiporters NHX1 and NHX2 control vacuolar pH and K^+ homeostasis to regulate growth, flower development and reproduction. *The Plant Cell*, **23**, 3482-3497.

Batistič, O. and Kudla, J. (2012) Analysis of calcium signaling pathways in plants. *Biochimica et Biophysica Acta*, **1820**, 1283-1293.

Baxter, I., Brazelton, J.N., Yu, D.N., Huang, Y.S., Lahner, B., Yakubova, E., Li, Y., Bergelson, J., Borevitz, J.O., Nordborg, M., Vitek, O. and Salt, D.E. (2010) A coastal cline in sodium accumulation in *Arabidopsis thaliana* is driven by natural variation of the sodium transporter AtHKT1;1. *PLoS Genetics*, **6**.

Ben Amar, S., Brini, F., Sentenac, H., Masmoudi, K. and Véry, A.-A. (2013) Functional characterization in Xenopus oocytes of Na^+ transport systems from durum wheat reveals diversity among two HKT1;4 transporters. *Journal of Experimental Botany*, doi: 10.1093/jxb/ert1361.

Bernstein, L., Brown, J.W. and Hayward, H.E. (1956) The influence of rootstock on growth and salt accumulation in stone-fruit trees and almonds. *Proceedings of the American Society for Horticulture and Science*, **68**, 86-95.

Berthomieu, P., Conejero, G., Nublat, A., Brackenbury, W.J., Lambert, C., Savio, C., Uozumi, N., Oiki, S., Yamada, K., Cellier, F., Gosti, F., Simonneau, T., Essah, P.A., Tester, M., Very, A.A., Sentenac, H. and Casse, F. (2003) Functional analysis of *AtHKT1* in Arabidopsis shows that Na^+ recirculation by the phloem is crucial for salt tolerance. *EMBO Journal*, **22**, 2004-2014.

Birnboim, H.C. and Doly, J. (1979) A rapid alkaline extraction procedure for screening recombinant plasmid DNA. *Nucleic Acids Research*, **7**, 1513-1523.

Blom, N., Gammeltoft, S. and Brunak, S. (1999) Sequence and structure-based prediction of eukaryotic protein phosphorylation sites. *Journal of molecular biology*, **294**, 1351-1362.

Bonilla, P., Dvorak, J., Mackill, D., Deal, K. and Gregorio, G. (2002) RFLP and SSLP mapping of salinity tolerance genes in chromosome 1 of rice (*Oryza sativa* L.) using recombinant inbred lines. *Philippine Agricultural Scientist*, **85**, 68-76.

Borsani, O., Zhu, J., Verslues, P.E., Sunkar, R. and Zhu, J.K. (2005) Endogenous siRNAs derived from a pair of natural cis-antisense transcripts regulate salt tolerance in Arabidopsis. *Cell*, **123**, 1279-1291.

Boyes, D.C., Zayed, A.M., Ascenzi, R., McCaskill, A.J., Hoffman, N.E., Davis, K.R. and Gorlach, J. (2001) Growth stage-based phenotypic analysis of Arabidopsis: a model for high throughput functional genomics in plants. *The Plant Cell*, **13**, 1499-1510.

Brem, R.B. and Kruglyak, L. (2005) The landscape of genetic complexity across 5,700 gene expression traits in yeast. *Proceedings of the National Academy of Sciences of the United States of America*, **102**, 1572-1577.

Brem, R.B., Yvert, G., Clinton, R. and Kruglyak, L. (2002) Genetic dissection of transcriptional regulation in budding yeast. *Science*, **296**, 752-755.

Buescher, E., Achberger, T., Amusan, I., Giannini, A., Ochsenfeld, C., Rus, A., Lahner, B., Hoekenga, O., Yakubova, E., Harper, J.F., Guerinot, M.L., Zhang, M., Salt, D.E. and Baxter, I.R. (2010) Natural genetic variation in selected populations of *Arabidopsis thaliana* is associated with ionomic differences. *Plos One*, **5**, e11081.

Buisine, N., Quesneville, H. and Colot, V. (2008) Improved detection and annotation of transposable elements in sequenced genomes using multiple reference sequence sets. *Genomics*, **91**, 467-475.

Burton, R.A., Jobling, S.A., Harvey, A.J., Shirley, N.J., Mather, D.E., Bacic, A. and Fincher, G.B. (2008) The genetics and transcriptional profiles of the cellulose synthase-like *HvCslF* gene family in barley. *Plant Physiology*, **146**, 1821-1833.

Byrt, C. (2008) Genes for sodium exclusion in wheat. PhD thesis at University of Adelaide, School for Agriculture, Food and Wine.

Byrt, C.S., Platten, J.D., Spielmeyer, W., James, R.A., Lagudah, E.S., Dennis, E.S., Tester, M. and Munns, R. (2007) HKT1;5-like cation transporters linked to Na^+ exclusion loci in wheat, *Nax2* and *Kna1*. *Plant Physiology*, **143**, 1918-1928.

Cakirlar, H. and Bowling, D.J.F. (1981) The effect of salinity on the membrane-potential of sunflower roots. *Journal of Experimental Botany*, **32**, 479-485.

Callis, J., Fromm, M. and Walbot, V. (1987) Introns increase gene expression in cultured maize cells. *Genes and development*, **1**, 1183-1200.

Campbell, M.A., Haas, B.J., Hamilton, J.P., Mount, S.M. and Buell, C.R. (2006) Comprehensive analysis of alternative splicing in rice and comparative analyses with Arabidopsis. *BMC Genomics*, **7**, 327.

Cao, J., Schneeberger, K., Ossowski, S., Günther, T., Bender, S., Fitz, J., Koenig, D., Lanz, C., Stegle, O., Lippert, C., Wang, X., Ott, F., Müller, J., Alonso-Blanco, C., Borgwardt, K., Schmid, K.J. and Weigel, D. (2011) Whole-genome sequencing of multiple *Arabidopsis thaliana* populations. *Nature Genetics*, **43**, 956-963.

Cessna, S.G., Chandra, S. and Low, P.S. (1998) Hypo-osmotic shock of tobacco cells stimulates Ca^{2+} fluxes deriving first from external and then internal Ca^{2+} stores. *The Journal of Biological Chemistry*, **273**, 27286-27291.

Chakrabarti, A. and Mukhopadhyay, D. (2012) Novel adaptors of amyloid precursor protein intracellular domain and their functional implications. *Genomics Proteomics Bioinformatics*, **10**, 208-216.

Chapman, E.J. and Carrington, J.C. (2007) Specialization and evolution of endogenous small RNA pathways. *Nature Reviews Genetics*, **8**, 884-896.

Charbonneau, H., Walsh, K.A., McCann, R.O., Prendergast, F.G., Cormier, M.J. and Vanaman, T.C. (1985) Amino acid sequence of the calcium-dependent photoprotein aequorin. *Biochemistry*, **24**, 6762-6771.

Cheng, L.R., Wang, Y., Meng, L.J., Hu, X., Cui, Y.R., Sun, Y., Zhu, L.H., Ali, J., Xu, J.L. and Li, Z.K. (2012) Identification of salt-tolerant QTLs with strong genetic background effect using two sets of reciprocal introgression lines in rice. *Genome*, **55**, 45-55.

Chiba, Y. and Green, P.J. (2009) mRNA degradation machinery in plants. *Journal of Plant Biology*, **52**, 114-124.

Chomczynski, P. (1993) A reagent for the single-step simultaneous isolation of RNA, DNA and proteins from cell and tissue samples. *Biotechniques*, **15**, 532.

Choudhury, K.R., Raychaudhuri, S. and Bhattacharyya, N.P. (2012) Identification of HYPK-interacting proteins reveals involvement of HYPK in regulating cell growth, cell cycle, unfolded protein response and cell death. *Plos One*, **7**, e51415.

Clark, R.M., Schweikert, G., Toomajian, C., Ossowski, S., Zeller, G., Shinn, P., Warthmann, N., Hu, T.T., Fu, G., Hinds, D.A., Chen, H.M., Frazer, K.A., Huson, D.H., Schölkopf, B., Nordborg, M., Rätsch, G., Ecker, J.R. and Weigel, D. (2007) Common sequence polymorphisms shaping genetic diversity in *Arabidopsis thaliana*. *Science*, **317**, 338-342.

Clough, S.J. and Bent, A.F. (1998) Floral dip: a simplified method for Agrobacterium-mediated transformation of *Arabidopsis thaliana*. *The Plant Journal*, **16**, 735-743.

Collard, B.C.Y., Jahufer, M.Z.Z., Brouwer, J.B. and Pang, E.C.K. (2005) An introduction to markers, quantitative trait loci (QTL) mapping and marker-assisted selection for crop improvement: The basic concepts. *Euphytica*, **142**, 169-196.

Conn, S.J., Hocking, B., Dayod, M., Xu, B., Athman, A., Henderson, S., Aukett, L., Conn, V., Shearer, M.K., Fuentes, S., Tyerman, S.D. and Gilliham, M. (2013) Protocol: optimising hydroponic growth systems for nutritional and physiological analysis of *Arabidopsis thaliana* and other plants. *Plant Methods*, **9**, 4.

Corratgé-Faillie, C., Jabnoune, M., Zimmermann, S., Véry, A.A., Fizames, C. and Sentenac, H. (2010) Potassium and sodium transport in non-animal cells: the Trk/Ktr/HKT transporter family. *Cellular and Molecular Life Sciences*, **67**, 2511-2532.

Cotsaftis, O., Plett, D., Shirley, N., Tester, M. and Hrmova, M. (2012) A two-staged model of Na^+ exclusion in rice explained by 3D modeling of HKT transporters and alternative splicing. *Plos One*, **7**, e39865-e39865.

Curie, C., Axelos, M., Bardet, C., Atanassova, R., Chaubet, N. and Lescure, B. (1993) Modular organization and development activity of an *Arabidopsis thaliana EF-1* alpha gene promoter. *Molecular Genetics and Genomics*, **238**, 428-436.

Curtis, M.D. and Grossniklaus, U. (2003) A gateway cloning vector set for high-throughput functional analysis of genes *in planta*. *Plant Physiology*, **133**, 462-469.

Dallas, P., Gottardo, N., Firth, M., Beesley, A., Hoffmann, K., Terry, P., Freitas, J., Boag, J., Cummings, A. and Kees, U. (2005) Gene expression levels assessed by oligonucleotide microarray analysis and quantitative real-time RT-PCR - how well do they correlate? *BMC Genomics*, **6**, 59.

Davenport, R.J., Muñoz-Mayor, A., Jha, D., Essah, P.A., Rus, A. and Tester, M. (2007) The Na^+ transporter AtHKT1;1 controls retrieval of Na^+ from the xylem in Arabidopsis. *Plant Cell and Environment*, **30**, 497-507.

de León, J.L.D., Escoppinichi, R., Geraldo, N., Castellanos, T., Mujeeb-Kazi, A. and Röder, M.S. (2011) Quantitative trait loci associated with salinity tolerance in field grown bread wheat. *Euphytica*, **181**, 371-383.

DeFalco, T.A., Bender, K.W. and Snedden, W.A. (2010) Breaking the code: Ca^{2+} sensors in plant signalling. *Biochemical Journal*, **425**, 27-40.

DeRose-Wilson, L. and Gaut, B.S. (2011) Mapping salinity tolerance during *Arabidopsis thaliana* germination and seedling growth. *Plos One*, **6**.

DeWald, D.B., Torabinejad, J., Jones, C.A., Shope, J.C., Cangelosi, A.R., Thompson, J.E., Prestwich, G.D. and Hama, H. (2001) Rapid accumulation of phosphatidylinositol 4,5-bisphosphate and inositol 1,4,5-trisphosphate correlates with calcium mobilization in salt-stressed Arabidopsis. *Plant Physiology*, **126**, 759-769.

Dodd, A.N., Jakobsen, M.K., Baker, A.J., Telzerow, A., Hou, S.W., Laplaze, L., Barrot, L., Poethig, R.S., Haseloff, J. and Webb, A.A. (2006) Time of day modulates low-temperature Ca^{2+} signals in Arabidopsis. *The Plant Journal*, **48**, 962-973.

Dodd, A.N., Kudla, J. and Sanders, D. (2010) The language of calcium signaling. In *Annual Review of Plant Biology, Vol 61*. Palo Alto: Annual Reviews, pp. 593-620.

Doerge, R.W. (2002) Mapping and analysis of quantitative trait loci in experimental populations. *Nature Reviews Genetics*, **3**, 43-52.

Dreyer, I., Horeau, C., Lemaillet, G., Zimmermann, S., Bush, D.R., Rodríguez-Navarro, A., Schachtman, D.P., Spalding, E.P., Sentenac, H. and Gaber, R.F. (1999) Identification and characterization of plant transporters using heterologous expression systems. *Journal of Experimental Botany*, **50**, 1073-1087.

Durell, S.R., Hao, Y., Nakamura, T., Bakker, E.P. and Guy, H.R. (1999) Evolutionary relationship between K^+ channels and symporters. *Biophysical Journal*, **77**, 775-788.

Ehlig, C.F. (1960) Effects of salinity on four varieties of a table grapes grown in sand culture. *Proceedings of the American Society for Horticulture and Science*, **76**, 323-331.

Ellis, R.P., Forster, B.P., Gordon, D.C., Handley, L.L., Keith, R.P., Lawrence, P., Meyer, R., Powell, W., Robinson, D., Scrimgeour, C.M., Young, G. and Thomas, W.T.B. (2002) Phenotype/genotype associations for yield and salt tolerance in a barley mapping population segregating for two dwarfing genes. *Journal of Experimental Botany*, **53**, 1163-1176.

Ellis, R.P., Forster, B.P., Waugh, R., Bonar, N., Handley, L.L., Robinson, D., Gordon, D.C. and Powell, W. (1997) Mapping physiological traits in barley. *New Phytologist*, **137**, 149-157.

FAO (2002) The salt of the earth: hazardous for food production. (http://www.fao.org/worldfoodsummit/english/newsroom/focus/focus1.htm). 12/11/2013.

FAO (2008) FAO land and plant nutrition management service. (http://www.fao.org/ag/agl/agll/spush). 2010/04/27.

Forster, B.P. (2001) Mutation genetics of salt tolerance in barley: An assessment of Golden Promise and other semi-dwarf mutants. *Euphytica*, **120**, 317-328.

Foster, K.J. and Miklavcic, S.J. (2013) Mathematical modelling of the uptake and transport of salt in plant roots. *Journal of Theoretical Biology*, **336**, 132-143.

Frary, A., Nesbitt, T.C., Grandillo, S., Knaap, E., Cong, B., Liu, J., Meller, J., Elber, R., Alpert, K.B. and Tanksley, S.D. (2000) *fw2.2*: a quantitative trait locus key to the evolution of tomato fruit size. *Science*, **289**, 85-88.

Galpaz, N. and Reymond, M. (2010) Natural variation in *Arabidopsis thaliana* revealed a genetic network controlling germination under salt stress. *Plos One*, **5**, e15198.

Galvan-Ampudia, C.S. and Testerink, C. (2011) Salt stress signals shape the plant root. *Current Opinion in Plant Biology*, **14**, 296-302.

Gan, X., Stegle, O., Behr, J., Steffen, J.G., Drewe, P., Hildebrand, K.L., Lyngsoe, R., Schultheiss, S.J., Osborne, E.J., Sreedharan, V.T., Kahles, A., Bohnert, R., Jean, G., Derwent, P., Kersey, P., Belfield, E.J., Harberd, N.P., Kemen, E., Toomajian, C., Kover, P.X., Clark, R.M., Ratsch, G. and Mott, R. (2011) Multiple reference genomes and transcriptomes for *Arabidopsis thaliana*. *Nature*, **477**, 419-423.

Garciadeblás, B., Senn, M.E., Bañuelos, M.A. and Rodríguez-Navarro, A. (2003) Sodium transport and HKT transporters: the rice model. *The Plant Journal*, **34**, 788-801.

Garthwaite, A.J., von Bothmer, R. and Colmer, T.D. (2005) Salt tolerance in wild Hordeum species is associated with restricted entry of Na^+ and Cl^- into the shoots. *Journal of Experimental Botany*, **56**, 2365-2378.

Gaxiola, R.A., Li, J., Undurraga, S., Dang, L.M., Allen, G.J., Alper, S.L. and Fink, G.R. (2001) Drought- and salt-tolerant plants result from overexpression of the *AVP1* H^+-pump. *Proceedings of the National Academy of Sciences of the United States of America*, **98**, 11444-11449.

Gaxiola, R.A., Rao, R., Sherman, A., Grisafi, P., Alper, S.L. and Fink, G.R. (1999) The *Arabidopsis thaliana* proton transporters, AtNhx1 and Avp1, can function in cation detoxification in yeast. *Proceedings of the National Academy of Sciences of the United States of America*, **96**, 1480-1485.

Geiger, D., Scherzer, S., Mumm, P., Stange, A., Marten, I., Bauer, H., Ache, P., Matschi, S., Liese, A., Al-Rasheid, K.A.S., Romeis, T. and Hedrich, R. (2009) Activity of guard cell anion channel SLAC1 is controlled by drought-stress signaling kinase-phosphatase pair. *Proceedings of the National Academy of Sciences of the United States of America*, **106**, 21425-21430.

Genc, Y., Oldach, K., Gogel, B., Wallwork, H., McDonald, G.K. and Smith, A.B. (2013) Quantitative trait loci for agronomic and physiological traits for a bread wheat population grown in environments with a range of salinity levels. *Molecular Breeding*, **32**, 39-59.

Genc, Y., Oldach, K., Verbyla, A.P., Lott, G., Hassan, M., Tester, M., Wallwork, H. and McDonald, G.K. (2010) Sodium exclusion QTL associated with improved seedling growth in bread wheat under salinity stress. *Theoretical and Applied Genetics*, **121**, 877-894.

Ghomi, K., Rabiei, B., Sabouri, H. and Sabouri, A. (2013) Mapping QTLs for traits related to salinity tolerance at seedling stage of rice (*Oryza sativa* L.): An agrigenomics study of an iranian rice population. *Omics-a Journal of Integrative Biology*, **17**, 242-251.

Gibson, G. and Weir, B. (2005) The quantitative genetics of transcription. *Trends in Genetics*, **21**, 616-623.

Gietz, R.D. and Woods, R.A. (2002) Transformation of yeast by lithium acetate/single-stranded carrier DNA/polyethylene glycol method. *Methods in Enzymology*, **350**, 87-96.

Gifford, J.L., Walsh, M.P. and Vogel, H.J. (2007) Structures and metal-ion-binding properties of the Ca^{2+}-binding helix-loop-helix EF-hand motifs. *Biochemical Journal*, **405**, 199-221.

Gilliham, M. (2007) Membrane structure and the study of solute transport across plant membranes. In *Plant Solute Transport*: Blackwell Publishing Ltd, pp. 47-74.

Goldin, A.L. (2006) Expression of ion channels in Xenopus oocytes. In *Expression and Analysis of Recombinant Ion Channels*: Wiley-VCH Verlag GmbH & Co. KGaA, pp. 1-25.

Gong, J.M., Zheng, X.W., Du, B.X., Qian, Q., Chen, S.Y., Zhu, L.H. and He, P. (2001) Comparative study of QTLs for agronomic traits of rice (*Oriza sativa* L.) between salt stress and nonstress environment. *Science in China Series C-Life Sciences*, **44**, 73-82.

Gorham, J. (1990) Salt tolerance in the triticeae-K^+/Na^+ discrimination in synthetic hexaploid wheats. *Journal of Experimental Botany*, **41**, 623-627.

Gouiaa, S., Khoudi, H., Leidi, E.O., Pardo, J.M. and Masmoudi, K. (2012) Expression of wheat Na^+/H^+ antiporter *TNHXS1* and H^+- pyrophosphatase *TVP1* genes in tobacco from a bicistronic transcriptional unit improves salt tolerance. *Plant Molecular Biology*, **79**, 137-155.

Greenway, H. and Munns, R. (1983) Interactions between growth, uptake of Cl^- and Na^+, and water relations of plants in saline environments. 2. Highly vacuolated cells *Plant Cell and Environment*, **6**, 575-589.

Gregory, B.D., O'Malley, R.C., Lister, R., Urich, M.A., Tonti-Filippini, J., Chen, H., Millar, A.H. and Ecker, J.R. (2008) A link between RNA metabolism and silencing affecting Arabidopsis development. *Developmental Cell*, **14**, 854-866.

Guillemaut, P. and Maréchal-Drouard, L. (1992) Isolation of plant DNA: A fast, inexpensive, and reliable method. *Plant Molecular Biology Reporter*, **10**, 60-65.

Gupta, R., Jung, E.a. and S., B. (2004) Prediction of N-glycosylation sites in human proteins. *in preparation, http://www.cbs.dtu.dk/services/NetNGlyc*.

Gustafson, A.M., Allen, E., Givan, S., Smith, D., Carrington, J.C. and Kasschau, K.D. (2005) ASRP: the Arabidopsis Small RNA Project Database. *Nucleic Acids Research*, **33**, D637-D640.

Ha, B.K., Vuong, T.D., Velusamy, V., Nguyen, H.T., Shannon, J.G. and Lee, J.D. (2013) Genetic mapping of quantitative trait loci conditioning salt tolerance in wild soybean (*Glycine soja*) PI 483463. *Euphytica*, **193**, 79-88.

Halfter, U., Ishitani, M. and Zhu, J.K. (2000) The Arabidopsis SOS2 protein kinase physically interacts with and is activated by the calcium-binding protein SOS3. *Proceedings of the National Academy of Sciences of the United States of America*, **97**, 3735-3740.

Hamwieh, A., Tuyen, D.D., Cong, H., Benitez, E.R., Takahashi, R. and Xu, D.H. (2011) Identification and validation of a major QTL for salt tolerance in soybean. *Euphytica*, **179**, 451-459.

Hamwieh, A. and Xu, D.H. (2008) Conserved salt tolerance quantitative trait locus (QTL) in wild and cultivated soybeans. *Breeding Science*, **58**, 355-359.

Hanahan, D. (1985) Techniques for transformation of E.coli. *DNA-Cloning*, **1**

Haq, T.U., Gorham, J., Akhtar, J., Akhtar, N. and Steele, K.A. (2010) Dynamic quantitative trait loci for salt stress components on chromosome 1 of rice. *Functional Plant Biology*, **37**, 634-645.

Haro, R., Bañuelos, M.A., Senn, M.A.E., Barrero-Gil, J. and Rodríguez-Navarro, A. (2005) HKT1 mediates sodium uniport in roots. Pitfalls in the expression of *HKT1* in yeast. *Plant Physiology*, **139**, 1495-1506.

Hauser, F. and Horie, T. (2010) A conserved primary salt tolerance mechanism mediated by HKT transporters: a mechanism for sodium exclusion and maintenance of high K^+/Na^+ ratio in leaves during salinity stress. *Plant Cell and Environment*, **33**, 552-565.

Herr, A.J., Jensen, M.B., Dalmay, T. and Baulcombe, D.C. (2005) RNA Polymerase IV Directs Silencing of Endogenous DNA. *Science*, **308**, 118-120.

Hetherington, A. and Trewavas, A. (1982) Calcium-dependent protein-kinase in pea shoot membranes. *FEBS Letters*, **145**, 67-71.

Hetherington, A.M. and Brownlee, C. (2004) The generation of Ca^{2+} signals in plants. *Annual Review of Plant Biology*, **55**, 401-427.

Hirotsu, N., Murakami, N., Kashiwagi, T., Ujiie, K. and Ishimaru, K. (2010) Protocol: a simple gel-free method for SNP genotyping using allele-specific primers in rice and other plant species. *Plant Methods*, **6**, 12-12.

Ho, C.H., Lin, S.H., Hu, H.C. and Tsay, Y.F. (2009) CHL1 functions as a nitrate sensor in plants. *Cell*, **138**, 1184-1194.

Horie, T., Brodsky, D.E., Costa, A., Kaneko, T., Lo Schiavo, F., Katsuhara, M. and Schroeder, J.I. (2011) K^+ transport by the OsHKT2;4 transporter from rice with atypical Na^+ transport properties and competition in permeation of K^+ over Mg^{2+} and Ca^{2+} ions. *Plant Physiology*, **156**, 1493-1507.

Horie, T., Costa, A., Kim, T.H., Han, M.J., Horie, R., Leung, H.-Y., Miyao, A., Hirochika, H., An, G. and Schroeder, J.I. (2007) Rice OsHKT2;1 transporter mediates large Na^+ influx component into K^+-starved roots for growth. *EMBO Journal*, **26**, 3003-3014.

Horie, T., Hauser, F. and Schroeder, J.I. (2009) HKT transporter-mediated salinity resistance mechanisms in Arabidopsis and monocot crop plants. *Trends in Plant Science*, **14**, 660-668.

Horie, T., Horie, R., Chan, W.Y., Leung, H.Y. and Schroeder, J.I. (2006) Calcium regulation of sodium hypersensitivities of *sos3* and *athkt1* mutants. *Plant Cell Physiology*, **47**, 622-633.

Horie, T. and Schroeder, J.I. (2004) Sodium transporters in plants. Diverse genes and physiological functions. *Plant Physiology*, **136**, 2457-2462.

Horie, T., Yoshida, K., Nakayama, H., Yamada, K., Oiki, S. and Shinmyo, A. (2001) Two types of HKT transporters with different properties of Na^+ and K^+ transport in *Oryza sativa*. *The Plant Journal*, **27**, 129-138.

Huang, S., Spielmeyer, W., Lagudah, E.S., James, R.A., Platten, J.D., Dennis, E.S. and Munns, R. (2006) A sodium transporter (HKT7) is a candidate for *Nax1*, a gene for salt tolerance in durum wheat. *Plant Physiology*, **142**, 1718-1727.

Huang, S., Spielmeyer, W., Lagudah, E.S. and Munns, R. (2008) Comparative mapping of HKT genes in wheat, barley, and rice, key determinants of Na^+ transport, and salt tolerance. *Journal of Experimental Botany*, **59**, 927-937.

Huxley, J.S. (1942) *Evolution. The modern synthesis.* London: George Allen & Unwin, Ltd.

Ikura, M. and Ames, J.B. (2006) Genetic polymorphism and protein conformational plasticity in the calmodulin superfamily: two ways to promote multifunctionality. *Proceedings of the National Academy of Sciences of the United States of America*, **103**, 1159-1164.

Ishimaru, Y., Kakei, Y., Shimo, H., Bashir, K., Sato, Y., Sato, Y., Uozumi, N., Nakanishi, H. and Nishizawa, N.K. (2011) A Rice Phenolic Efflux Transporter Is Essential for Solubilizing Precipitated Apoplasmic Iron in the Plant Stele. *Journal of Biological Chemistry*, **286**, 24649-24655.

Isshiki, M., Yamamoto, Y., Satoh, H. and Shimamoto, K. (2001) Nonsense-mediated decay of mutant *waxy* mRNA in rice. *Plant Physiology*, **125**, 1388-1395.

Jacobs, A., Lunde, C., Bacic, A., Tester, M. and Roessner, U. (2007) The impact of constitutive heterologous expression of a moss Na+ transporter on the metabolomes of rice and barley. *Metabolomics*, **3**, 307-317.

James, R.A., Blake, C., Byrt, C.S. and Munns, R. (2011) Major genes for Na^+ exclusion, *Nax1* and *Nax*2 (wheat *HKT1;4* and *HKT1;5)*, decrease Na^+ accumulation in bread wheat leaves under saline and waterlogged conditions. *Journal of Experimental Botany*, **62**, 2939-2947.

James, R.A., Blake, C., Zwart, A.B., Hare, R.A., Rathjen, A.J. and Munns, R. (2012) Impact of ancestral wheat sodium exclusion genes *Nax1* and *Nax2* on grain yield of durum wheat on saline soils. *Functional Plant Biology*, **39**, 609-618.

James, R.A., Davenport, R.J. and Munns, R. (2006) Physiological characterization of two genes for Na^+ exclusion in durum wheat, *Nax1* and *Nax2*. *Plant Physiology*, **142**, 1537-1547.

Jansen, R.C. and Nap, J.P. (2001) Genetical genomics: the added value from segregation. *Trends in Genetics*, **17**, 388-391.

Jefferson, R.A., Kavanagh, T.A. and Bevan, M.W. (1987) GUS fusions: beta-glucuronidase as a sensitive and versatile gene fusion marker in higher plants. *EMBO Journal*, **6**, 3901-3907.

Jeong, Y.M., Mun, J.H., Lee, I., Woo, J.C., Hong, C.B. and Kim, S.G. (2006) Distinct roles of the first introns on the expression of Arabidopsis *profilin* gene family members. *Plant Physiology*, **140**, 196-209.

Jha, D., Shirley, N., Tester, M. and Roy, S.J. (2010) Variation in salinity tolerance and shoot sodium accumulation in Arabidopsis ecotypes linked to differences in the natural expression levels of transporters involved in sodium transport. *Plant Cell and Environment*, **33**, 793-804.

Jiang, C.F., Belfield, E.J., Mithani, A., Visscher, A., Ragoussis, J., Mott, R., Smith, J.A.C. and Harberd, N.P. (2012) ROS-mediated vascular homeostatic control of root-to-shoot soil Na delivery in Arabidopsis. *EMBO Journal*, **31**, 4359-4370.

Johansson, I., Wulfetange, K., Porée, F., Michard, E., Gajdanowicz, P., Lacombe, B., Sentenac, H., Thibaud, J.B., Mueller-Roeber, B., Blatt, M.R. and Dreyer, I. (2006) External K^+ modulates the activity of the Arabidopsis potassium channel SKOR via an unusual mechanism. *The Plant Journal*, **46**, 269-281.

Johnston, M. (1987) A model fungal gene regulatory mechanism: the *GAL* genes of *Saccharomyces cerevisiae*. *Microbiological reviews*, **51**, 458-476.

Jones, H.G. and Jones, M.B. eds (1989) Introduction: some terminology and common mechanisms Cambridge: Cambridge university Press, 1-10.

Joshi, C.P. (1987) An inspection of the domain between putative TATA box and translation start site in 79 plant genes. *Nucleic Acids Research*, **15**, 6643-6653.

Juenger, T., Purugganan, M. and Mackay, T.F. (2000) Quantitative trait loci for floral morphology in *Arabidopsis thaliana*. *Genetics*, **156**, 1379-1392.

Jurka, J., Kapitonov, V.V., Pavlicek, A., Klonowski, P., Kohany, O. and Walichiewicz, J. (2005) Repbase update, a database of eukaryotic repetitive elements. *Cytogenetic and Genome Research*, **110**, 462-467.

Kanno, T., Huettel, B., Mette, M.F., Aufsatz, W., Jaligot, E., Daxinger, L., Kreil, D.P., Matzke, M. and Matzke, A.J.M. (2005) Atypical RNA polymerase subunits required for RNA-directed DNA methylation. *Nature Genetics*, **37**, 761-765.

Kato, Y., Hazama, A., Yamagami, M. and Uozumi, N. (2003) Addition of a peptide tag at the C-terminus of AtHKT1 inhibits its Na^+ transport. *Bioscience Biotechnology and Biochemistry*, **67**, 2291-2293.

Kato, Y., Sakaguchi, M., Mori, Y., Saito, K., Nakamura, T., Bakker, E.P., Sato, Y., Goshima, S. and Uozumi, N. (2001) Evidence in support of a four transmembrane-pore-transmembrane topology model for the *Arabidopsis thaliana* Na^+/K^+ translocating AtHKT1 protein, a member of the superfamily of K^+ transporters. *Proceedings of the National Academy of Sciences of the United States of America*, **98**, 6488-6493.

Katori, T., Ikeda, A., Iuchi, S., Kobayashi, M., Shinozaki, K., Maehashi, K., Sakata, Y., Tanaka, S. and Taji, T. (2010) Dissecting the genetic control of natural variation in salt tolerance of *Arabidopsis thaliana* accessions. *Journal of Experimental Botany*, **61**, 1125-1138.

Kawasaki, H., Nakayama, S. and Kretsinger, R.H. (1998) Classification and evolution of EF-hand proteins. *Biometals*, **11**, 277-295.

Kearsey, M.J. (1998) The principles of QTL analysis (a minimal mathematics approach). *Journal of Experimental Botany*, **49**, 1619-1623.

Kendall, J.M. and Badminton, M.N. (1998) *Aequorea victoria* bioluminescence moves into an exciting new era. *Trends in Biotechnology*, **16**, 216-224.

Kepinski, S. (2009) Pull-Down Assays for Plant Hormone Research. In *Methods in molecular biology* (Cutler, S. and Bonetta, D. eds): Humana Press Inc, 999 Riverview Dr, Ste 208, Totowa, Nj 07512-1165 USA, pp. 61-80.

Kere, G.M., Guo, Q., Shen, J., Xu, J. and Chen, J. (2013) Heritability and gene effects for salinity tolerance in cucumber (*Cucumis sativus* L.) estimated by generation mean analysis. *Scientia Horticulturae*, **159**, 122-127.

Kervestin, S. and Jacobson, A. (2012) NMD: a multifaceted response to premature translational termination. *Nature Reviews Molecular Cell Biology*, **13**, 700-712.

Keurentjes, J.J., Fu, J., Terpstra, I.R., Garcia, J.M., van den Ackerveken, G., Snoek, L.B., Peeters, A.J., Vreugdenhil, D., Koornneef, M. and Jansen, R.C. (2007) Regulatory network construction in Arabidopsis by using genome-wide gene expression quantitative trait loci. *Proceedings of the National Academy of Sciences of the United States of America*, **104**, 1708-1713.

Kiegle, E., Moore, C.A., Haseloff, J., Tester, M.A. and Knight, M.R. (2000) Cell-type-specific calcium responses to drought, salt and cold in the Arabidopsis root. *The Plant Journal*, **23**, 267-278.

Kilian, J., Whitehead, D., Horak, J., Wanke, D., Weinl, S., Batistic, O., D'Angelo, C., Bornberg-Bauer, E., Kudla, J. and Harter, K. (2007) The AtGenExpress global stress expression data set: protocols, evaluation and model data analysis of UV-B light, drought and cold stress responses. *The Plant Journal*, **50**, 347-363.

Kim, D.Y., Jin, J.Y., Alejandro, S., Martinoia, E. and Lee, Y. (2010) Overexpression of *AtABCG36* improves drought and salt stress resistance in Arabidopsis. *Physiologia Plantarum*, **139**, 170-180.

Knight, H. (2000) Calcium signaling during abiotic stress in plants. *International Review of Cytology*, **195**, 269-324.

Knight, H., Trewavas, A.J. and Knight, M.R. (1996) Cold calcium signaling in Arabidopsis involves two cellular pools and a change in calcium signature after acclimation. *The Plant Cell*, **8**, 489-503.

Knight, H., Trewavas, A.J. and Knight, M.R. (1997) Calcium signalling in *Arabidopsis thaliana* responding to drought and salinity. *The Plant Journal*, **12**, 1067-1078.

Knight, M.R., Campbell, A.K., Smith, S.M. and Trewavas, A.J. (1991) Transgenic plant Aequorin reports the effects of touch and cold-shock and elicitors on cytoplamic calcium. *Nature*, **352**, 524-526.

Ko, C.H., Brendel, V., Taylor, R.D. and Walbot, V. (1998) U-richness is a defining feature of plant introns and may function as an intron recognition signal in maize. *Plant Molecular Biology*, **36**, 573-583.

Kochian, L.V. and Lucas, W.J. (1989) Potassium transport in roots. In *Advances in Botanical Research* (Callow, J.A. ed: Academic Press, pp. 93-178.

Konieczny, A. and Ausubel, F.M. (1993) A procedure for mapping Arabidopsis mutations using co-dominant ecotype-specific PCR-based markers. *The Plant Journal*, **4**, 403-410.

Koohafkan, P. and Stewart, B.A. (2008) *Water and cereals in drylands.* Rome: FAO.

Korn, M., Peterek, S., Mock, H.P., Heyer, A.G. and Hincha, D.K. (2008) Heterosis in the freezing tolerance, and sugar and flavonoid contents of crosses between Arabidopsis thaliana accessions of widely varying freezing tolerance. *Plant, Cell & Environment*, **31**, 813-827.

Korte, A. and Farlow, A. (2013) The advantages and limitations of trait analysis with GWAS: a review. *Plant Methods*, **9**, 29.

Kotchoni, S. and Gachomo, E. (2009) A rapid and hazardous reagent free protocol for genomic DNA extraction suitable for genetic studies in plants. *Molecular Biology Reports*, **36**, 1633-1636.

Koyama, M.L., Levesley, A., Koebner, R.M.D., Flowers, T.J. and Yeo, A.R. (2001) Quantitative trait loci for component physiological traits determining salt tolerance in rice. *Plant Physiology*, **125**, 406-422.

Kreps, J.A., Wu, Y., Chang, H.S., Zhu, T., Wang, X. and Harper, J.F. (2002) Transcriptome changes for Arabidopsis in response to salt, osmotic, and cold stress. *Plant Physiology*, **130**, 2129-2141.

Kudla, J., Batistič, O. and Hashimoto, K. (2010) Calcium signals: the lead currency of plant information processing. *The Plant Cell*, **22**, 541-563.

Kudla, J., Xu, Q., Harter, K., Gruissem, W. and Luan, S. (1999) Genes for calcineurin B-like proteins in Arabidopsis are differentially regulated by stress signals. *Proceedings of the National Academy of Sciences of the United States of America*, **96**, 4718-4723.

Kusnetsov, V., Landsberger, M., Meurer, J. and Oelmüller, R. (1999) The assembly of the CAAT-box binding complex at a photosynthesis gene promoter is regulated by light, cytokinin, and the stage of the plastids. *Journal of Biological Chemistry*, **274**, 36009-36014.

Kwon, S.J., Choi, E.Y., Choi, Y.J., Ahn, J.H. and Park, O.K. (2006) Proteomics studies of post-translational modifications in plants. *Journal of Experimental Botany*, **57**, 1547-1551.

Lan, W.-Z., Wang, W., Wang, S.-M., Li, L.-G., Buchanan, B.B., Lin, H.-X., Gao, J.-P. and Luan, S. (2010) A rice high-affinity potassium transporter (HKT) conceals a calcium-permeable cation channel. *Proceedings of the National Academy of Sciences of the United States of America*, **107**, 7089-7094.

Law, J.A. and Jacobsen, S.E. (2010) Establishing, maintaining and modifying DNA methylation patterns in plants and animals. *Nature Reviews Genetics*, **11**, 204-220.

Lee, S.Y., Ahn, J.H., Cha, Y.S., Yun, D.W., Lee, M.C., Ko, J.C., Lee, K.S. and Eun, M.Y. (2007) Mapping QTLs related to salinity tolerance of rice at the young seedling stage. *Plant Breeding*, **126**, 43-46.

Lefebvre, V., Kiani, S.P. and Durand-Tardif, M. (2009) A focus on natural variation for abiotic constraints response in the model species *Arabidopsis thaliana*. *International Journal of Molecular Sciences*, **10**, 3547-3582.

Li, C.C. (1955) *Population Genetics.* University of Chicago Press, Chicago, Illinois.

Li, C.F., Pontes, O., El-Shami, M., Henderson, I.R., Bernatavichute, Y.V., Chan, S.W.L., Lagrange, T., Pikaard, C.S. and Jacobsen, S.E. (2006) An ARGONAUTE4-containing nuclear processing center colocalized with cajal bodies in *Arabidopsis thaliana*. *Cell*, **126**, 93-106.

Li, S., Liu, L., Zhuang, X., Yu, Y., Liu, X., Cui, X., Ji, L., Pan, Z., Cao, X., Mo, B., Zhang, F., Raikhel, N., Jiang, L. and Chen, X. (2013) MicroRNAs inhibit the translation of target mRNAs on the endoplasmic reticulum in Arabidopsis. *Cell*, **153**, 562-574.

Liew, M., Pryor, R., Palais, R., Meadows, C., Erali, M., Lyon, E. and Wittwer, C. (2004) Genotyping of single-nucleotide polymorphisms by high-resolution melting of small amplicons. *Clinical Chemistry*, **50**, 1156-1164.

Lightfoot, D.J., Orford, S.J. and Timmis, J.N. (2013) Identification and characterisation of cotton boll wall-specific gene promoters for future transgenic cotton varieties. *Plant Molecular Biology Reporter*, **31**, 174-184.

Liman, E.R., Tytgat, J. and Hess, P. (1992) Subunit stoichiometry of a mammalian K^+ channel determined by construction of multimeric cDNAs. *Neuron*, **9**, 861-871.

Lin, H.X., Zhu, M.Z., Yano, M., Gao, J.P., Liang, Z.W., Su, W.A., Hu, X.H., Ren, Z.H. and Chao, D.Y. (2004) QTLs for Na^+ and K^+ uptake of the shoots and roots controlling rice salt tolerance. *Theoretical and Applied Genetics*, **108**, 253-260.

Lindsay, M.P., Lagudah, E.S., Hare, R.A. and Munns, R. (2004) A locus for sodium exclusion (*Nax1*), a trait for salt tolerance, mapped in durum wheat. *Functional Plant Biology*, **31**, 1105-1114.

Lisec, J., Steinfath, M., Meyer, R.C., Selbig, J., Melchinger, A.E., Willmitzer, L. and Altmann, T. (2009) Identification of heterotic metabolite QTL in *Arabidopsis thaliana* RIL and IL populations. *The Plant Journal*, **59**, 777-788.

Lister, R., O'Malley, R.C., Tonti-Filippini, J., Gregory, B.D., Berry, C.C., Millar, A.H. and Ecker, J.R. (2008) Highly integrated single-base resolution maps of the epigenome in Arabidopsis. *Cell*, **133**, 523-536.

Litt, M. and Luty, J.A. (1989) A hypervariable microsatellite revealed by *in vitro* amplification of a dinucleotide repeat within the cardiac-muscle actin gene. *American Journal of Human Genetics*, **44**, 397-401.

Liu, B.-H. (1997) *Statistical genomics: linkage, mapping, and QTL analysis.* CRC Press, New York.

Liu, B. (1998) *Statistical genomics: linkage, mapping and QTL analysis.* CRC Press.

Liu, J., He, Y., Amasino, R. and Chen, X. (2004) siRNAs targeting an intronic transposon in the regulation of natural flowering behavior in Arabidopsis. *Genes and development*, **18**, 2873-2878.

Liu, J. and Zhu, J.K. (1997a) An Arabidopsis mutant that requires increased calcium for potassium nutrition and salt tolerance. *Proceedings of the National Academy of Sciences of the United States of America*, **94**, 14960-14964.

Liu, J. and Zhu, J.K. (1997b) Proline accumulation and salt-stress-induced gene expression in a salt-hypersensitive mutant of Arabidopsis. *Plant Physiology*, **114**, 591-596.

Liu, J. and Zhu, J.K. (1998) A calcium sensor homolog required for plant salt tolerance. *Science*, **280**, 1943-1945.

Liu, J.P., Ishitani, M., Halfter, U., Kim, C.S. and Zhu, J.K. (2000) The *Arabidopsis thaliana SOS2* gene encodes a protein kinase that is required for salt tolerance. *Proceedings of the National Academy of Sciences of the United States of America*, **97**, 3730-3734.

Liu, K.H. and Tsay, Y.F. (2003) Switching between the two action modes of the dual-affinity nitrate transporter CHL1 by phosphorylation. *EMBO Journal*, **22**, 1005-1013.

Liu, Q., Kasuga, M., Sakuma, Y., Abe, H., Miura, S., Yamaguchi-Shinozaki, K. and Shinozaki, K. (1998) Two transcription factors, DREB1 and DREB2, with an EREBP/AP2 DNA binding domain separate two cellular signal transduction pathways in drought- and low-temperature-responsive gene expression, respectively, in Arabidopsis. *The Plant Cell*, **10**, 1391-1406.

Liu, W.H., Fairbairn, D.J., Reid, R.J. and Schachtman, D.P. (2001) Characterization of two HKT1 homologues from *Eucalyptus camaldulensis* that display intrinsic osmosensing capability. *Plant Physiology*, **127**, 283-294.

Loke, J.C., Stahlberg, E.A., Strenski, D.G., Haas, B.J., Wood, P.C. and Li, Q.Q. (2005) Compilation of mRNA polyadenylation signals in Arabidopsis revealed a new signal element and potential secondary structures. *Plant Physiology*, **138**, 1457-1468.

Long, S.B., Campbell, E.B. and MacKinnon, R. (2005) Crystal structure of a mammalian voltage-dependent *Shaker* family K^+ channel. *Science*, **309**, 897-903.

Lowry, D.B., Hall, M.C., Salt, D.E. and Willis, J.H. (2009) Genetic and physiological basis of adaptive salt tolerance divergence between coastal and inland *Mimulus guttatus*. *New Phytologist*, **183**, 776-788.

Lu, C., Tej, S.S., Luo, S.J., Haudenschild, C.D., Meyers, B.C. and Green, P.J. (2005) Elucidation of the small RNA component of the transcriptome. *Science*, **309**, 1567-1569.

Ma, L.Q., Zhou, E.F., Huo, N.X., Zhou, R.H., Wang, G.Y. and Jia, J.Z. (2007) Genetic analysis of salt tolerance in a recombinant inbred population of wheat (*Triticum aestivum* L.). *Euphytica*, **153**, 109-117.

Ma, W. and Berkowitz, G.A. (2007) The grateful dead: calcium and cell death in plant innate immunity. *Cellular Microbiology*, **9**, 2571-2585.

Maathuis, F.J.M. and Amtmann, A. (1999) K^+ nutrition and Na^+ toxicity: The basis of cellular K^+/Na^+ ratios. *Annals of Botany*, **84**, 123-133.

Maathuis, F.J.M. and Sanders, D. (1993) Energization of potassium uptake in *Arabidopsis thaliana*. *Planta*, **191**, 302-307.

Maathuis, F.J.M. and Sanders, D. (1996) Mechanisms of potassium absorption by higher plant roots. *Physiologia Plantarum*, **96**, 158-168.

Mahajan, S., Pandey, G.K. and Tuteja, N. (2008) Calcium- and salt-stress signaling in plants: shedding light on SOS pathway. *Archives of Biochemistry and Biophysics*, **471**, 146-158.

Mahajan, S. and Tuteja, N. (2005) Cold, salinity and drought stresses: an overview. *Archives of Biochemistry and Biophysics*, **444**, 139-158.

Manly, K.F., Cudmore, R.H., Jr. and Meer, J.M. (2001) Map Manager QTX, cross-platform software for genetic mapping. *Mammalian Genome*, **12**, 930-932.

Manly, K.F. and Olson, J.M. (1999) Overview of QTL mapping software and introduction to map manager QT. *Mammalian Genome*, **10**, 327-334.

Mano, Y. and Takeda, K. (1997) Mapping quantitative trait loci for salt tolerance at germination and the seedling stage in barley (*Hordeum vulgare* L.). *Euphytica*, **94**, 263-272.

Mantis, J. and Tague, B.W. (2000) Comparing the utility of beta-glucuronidase and green fluorescent protein for detection of weak promoter activity in *Arabidopsis thaliana*. *Plant Molecular Biology Reporter*, **18**, 319-330.

Marschner, H. (1995) *Mineral nutrition of higher plants.* London.

Martin, T.F. (1998) Phosphoinositide lipids as signaling molecules: common themes for signal transduction, cytoskeletal regulation, and membrane trafficking. *Annual Review of Cell and Developmental Biology*, **14**, 231-264.

Mäser, P., Eckelman, B., Vaidyanathan, R., Horie, T., Fairbairn, D.J., Kubo, M., Yamagami, M., Yamaguchi, K., Nishimura, M., Uozumi, N., Robertson, W., Sussman, M.R. and Schroeder, J.I. (2002) Altered shoot/root Na^+ distribution and bifurcating salt sensitivity in Arabidopsis by genetic disruption of the Na^+ transporter AtHKT1. *FEBS Letters*, **531**, 157-161.

Mason, M.G., Jha, D., Salt, D.E., Tester, M., Hill, K., Kieber, J.J. and Schaller, G.E. (2010) Type-B response regulators ARR1 and ARR12 regulate expression of *AtHKT1;1* and accumulation of sodium in Arabidopsis shoots. *The Plant Journal*, **64**, 753-763.

Matzke, M., Kanno, T., Daxinger, L., Huettel, B. and Matzke, A.J. (2009) RNA-mediated chromatin-based silencing in plants. *Current Opinion of Cell Biology*, **21**, 367-376.

Mayer, J.E., Pfeiffer, W.H. and Beyer, P. (2008) Biofortified crops to alleviate micronutrient malnutrition. *Current Opinion in Plant Biology*, **11**, 166-170.

McAinsh, M.R. and Pittman, J.K. (2009) Shaping the calcium signature. *The New Phytologist*, **181**, 275-294.

Methfessel, C., Witzemann, V., Takahashi, T., Mishina, M., Numa, S. and Sakmann, B. (1986) Patch clamp measurements on *Xenopus laevis* oocytes: currents through endogenous channels and implanted acetylcholine receptor and sodium channels. *Pflügers Archiv*, **407**, 577-588.

Mian, A., Oomen, R., Isayenkov, S., Sentenac, H., Maathuis, F.J.M. and Véry, A.A. (2011) Over-expression of an Na^+- and K^+-permeable HKT transporter in barley improves salt tolerance. *The Plant Journal*, **68**, 468-479.

Michaels, S.D., He, Y., Scortecci, K.C. and Amasino, R.M. (2003) Attenuation of FLOWERING LOCUS C activity as a mechanism for the evolution of summer-annual flowering behavior in Arabidopsis. *Proceedings of the National Academy of Sciences of the United States of America*, **100**, 10102-10107.

Møller, I.S., Gilliham, M., Jha, D., Mayo, G.M., Roy, S.J., Coates, J.C., Haseloff, J. and Tester, M. (2009) Shoot Na^+ exclusion and increased salinity tolerance engineered by cell type-specific alteration of Na^+ transport in Arabidopsis. *The Plant Cell*, **21**, 2163-2178.

Møller, I.S. and Tester, M. (2007) Salinity tolerance of Arabidopsis: a good model for cereals? *Trends in Plant Science*, **12**, 534-540.

Molnar, A., Melnyk, C.W., Bassett, A., Hardcastle, T.J., Dunn, R. and Baulcombe, D.C. (2010) Small silencing RNAs in plants are mobile and direct epigenetic modification in recipient cells. *Science*, **328**, 872-875.

Montero, M., Brini, M., Marsault, R., Alvarez, J., Sitia, R., Pozzan, T. and Rizzuto, R. (1995) Monitoring dynamic changes in free Ca^{2+} concentration in the endoplasmic-reticulum of intact-cells. *EMBO Journal*, **14**, 5467-5475.

Morello, L. and Breviario, D. (2008) Plant spliceosomal introns: not only cut and paste. *Current Genomics*, **9**, 227-238.

Morello, L., Gianí, S., Troina, F. and Breviario, D. (2011) Testing the IMEter on rice introns and other aspects of intron-mediated enhancement of gene expression. *Journal of Experimental Botany*, **62**, 533-544.

Morita, S., Tsukamoto, S., Sakamoto, A., Makino, H., Nakauji, E., Kaminaka, H., Masumura, T., Ogihara, Y., Satoh, S. and Tanaka, K. (2012) Differences in intron-mediated enhancement of gene expression by the first intron of cytosolic superoxide dismutase gene from rice in monocot and dicot plants. *Plant Biotechnology*, **29**, 115-119.

Morley, M., Molony, C.M., Weber, T.M., Devlin, J.L., Ewens, K.G., Spielman, R.S. and Cheung, V.G. (2004) Genetic analysis of genome-wide variation in human gene expression. *Nature*, **430**, 743-747.

Muir, S.R. and Sanders, D. (1997) Inositol 1,4,5-trisphosphate-sensitive Ca^{2+} release across nonvacuolar membranes in cauliflower. *Plant Physiology*, **114**, 1511-1521.

Mullis, K.B. and Faloona, F.A. (1987) Specific synthesis of DNA in vitro via a polymerase-catalyzed chain reaction. *Methods in Enzymology*, **155**, 335-350.

Munnik, T. and Testerink, C. (2009) Plant phospholipid signaling: "in a nutshell". *Journal of Lipid Research*, **50 Suppl**, S260-265.

Munns, R. and James, R.A. (2003) Screening methods for salinity tolerance: a case study with tetraploid wheat. *Plant and Soil*, **253**, 201-218.

Munns, R., James, R.A., Xu, B., Athman, A., Conn, S.J., Jordans, C., Byrt, C.S., Hare, R.A., Tyerman, S.D., Tester, M., Plett, D. and Gilliham, M. (2012) Wheat grain yield on saline soils is improved by an ancestral Na^+ transporter gene. *Nature Biotechnology*, **30**, 360-U173.

Munns, R. and Passioura, J.B. (1984) Effext of prolonged exposure to NaCl on the osmotic-pressure of leaf xylem sap from intact, transpiring barley plants. *Australian Journal of Plant Physiology*, **11**, 497-507.

Munns, R., Rebetzke, G.J., Husain, S., James, R.A. and Hare, R.A. (2003) Genetic control of sodium exclusion in durum wheat. *Australian Journal of Agricultural Research*, **54**, 627-635.

Munns, R. and Tester, M. (2008) Mechanisms of salinity tolerance. *Annual Review of Plant Biology*, **59**, 651-681.

Murguía, J.R., Bellés, J.M. and Serrano, R. (1995) A salt-sensitive 3'(2'),5'-bisphosphate nucleotidase involved in sulfate activation. *Science*, **267**, 232-234.

Nakano, M., Nobuta, K., Vemaraju, K., Tej, S.S., Skogen, J.W. and Meyers, B.C. (2006) Plant MPSS databases: signature-based transcriptional resources for analyses of mRNA and small RNA. *Nucleic Acids Research*, **34**, D731-D735.

Neff, M.M., Neff, J.D., Chory, J. and Pepper, A.E. (1998) dCAPS, a simple technique for the genetic analysis of single nucleotide polymorphisms: experimental applications in *Arabidopsis thaliana* genetics. *The Plant Journal*, **14**, 387-392.

Negrão, S., Cecilia Almadanim, M., Pires, I.S., Abreu, I.A., Maroco, J., Courtois, B., Gregorio, G.B., McNally, K.L. and Margarida Oliveira, M. (2013) New allelic variants found in key rice salt-tolerance genes: an association study. *Plant Biotechnology Journal*, **11**, 87-100.

Nekrutenko, A. and Li, W.H. (2001) Transposable elements are found in a large number of human protein-coding genes. *Trends in Genetics*, **17**, 619-621.

Ng, C.K.Y., McAinsh, M.R., Gray, J.E., Hunt, L., Leckie, C.P., Mills, L. and Hetherington, A.M. (2001) Calcium-based signalling systems in guard cells. *New Phytologist*, **151**, 109-120.

Nguyen, V.L., Ribot, S.A., Dolstra, O., Niks, R.E., Visser, R.G.F. and van der Linden, C.G. (2013) Identification of quantitative trait loci for ion homeostasis and salt tolerance in barley (*Hordeum vulgare* L.). *Molecular Breeding*, **31**, 137-152.

Norris, S., Meyer, S. and Callis, J. (1993) The intron of *Arabidopsis thaliana POLYUBIQUITIN* genes is conserved in location and is a quantitative determinant of chimeric gene expression. *Plant Molecular Biology*, **21**, 895-906.

Nyikó, T., Kerényi, F., Szabadkai, L., Benkovics, A.H., Major, P., Sonkoly, B., Mérai, Z., Barta, E., Niemiec, E., Kufel, J. and Silhavy, D. (2013) Plant nonsense-mediated mRNA decay is controlled by different autoregulatory circuits and can be induced by an EJC-like complex. *Nucleic Acids Research*, **41**, 6715-6728.

Okamoto, M., Vidmar, J.J. and Glass, A.D.M. (2003) Regulation of *NRT1* and *NRT2* gene families of *Arabidopsis thaliana*: Responses to nitrate provision. *Plant and Cell Physiology*, **44**, 304-317.

Oldroyd, G.E., Harrison, M.J. and Paszkowski, U. (2009) Reprogramming plant cells for endosymbiosis. *Science*, **324**, 753-754.

Onodera, Y., Haag, J.R., Ream, T., Nunes, P.C., Pontes, O. and Pikaard, C.S. (2005) Plant nuclear RNA polymerase IV mediates siRNA and DNA methylation-dependent heterochromatin formation. *Cell*, **120**, 613-622.

Oomen, R.J.F.J., Benito, B., Sentenac, H., Rodríguez-Navarro, A., Talón, M., Véry, A.-A. and Domingo, C. (2012) HKT2;2/1, a K^+-permeable transporter identified in a salt-tolerant rice cultivar through surveys of natural genetic polymorphism. *The Plant Journal*, **71**, 750-762.

Pan, Z., Zhao, Y., Zheng, Y., Liu, J., Jiang, X. and Guo, Y. (2012) A high-throughput method for screening Arabidopsis mutants with disordered abiotic stress-induced calcium signal. *Journal of Genetics and Genomics*, **39**, 225-235.

Pardo, J.M., Cubero, B., Leidi, E.O. and Quintero, F.J. (2006) Alkali cation exchangers: roles in cellular homeostasis and stress tolerance. *Journal of Experimental Botany*, **57**, 1181-1199.

Parra, G., Bradnam, K., Rose, A.B. and Korf, I. (2011) Comparative and functional analysis of intron-mediated enhancement signals reveals conserved features among plants. *Nucleic Acids Research*, **39**, 5328-5337.

Pauly, N., Knight, M.R., Thuleau, P., Graziana, A., Muto, S., Ranjeva, R. and Mazars, C. (2001) The nucleus together with the cytosol generates patterns of specific cellular calcium signatures in tobacco suspension culture cells. *Cell Calcium*, **30**, 413-421.

Pearlman, S.M., Serber, Z. and Ferrell, J.E., Jr. (2011) A mechanism for the evolution of phosphorylation sites. *Cell*, **147**, 934-946.

Perlak, F.J., Oppenhuizen, M., Gustafson, K., Voth, R., Sivasupramaniam, S., Heering, D., Carey, B., Ihrig, R.A. and Roberts, J.K. (2001) Development and commercial use of Bollgard cotton in the USA--early promises versus today's reality. *The Plant Journal*, **27**, 489-501.

Pitzschke, A., Forzani, C. and Hirt, H. (2006) Reactive oxygen species signaling in plants. *Antioxid Redox Signal*, **8**, 1757-1764.

Platten, J.D., Cotsaftis, O., Berthomieu, P., Bohnert, H., Davenport, R.J., Fairbairn, D.J., Horie, T., Leigh, R.A., Lin, H.X., Luan, S., Mäser, P., Pantoja, O., Rodríguez-Navarro, A., Schachtman, D.P., Schroeder, J.I., Sentenac, H., Uozumi, N., Véry, A.A., Zhu, J.K., Dennis, E.S. and Tester, M. (2006) Nomenclature for HKT transporters, key determinants of plant salinity tolerance. *Trends in Plant Science*, **11**, 372-374.

Plett, D., Safwat, G., Gilliham, M., Møller, I.S., Roy, S., Shirley, N., Jacobs, A., Johnson, A. and Tester, M. (2010) Improved salinity tolerance of rice through cell type-specific expression of *AtHKT1;1*. *Plos One*, **5**.

Plett, D.C. and Møller, I.S. (2010) Na^+ transport in glycophytic plants: what we know and would like to know. *Plant Cell and Environment*, **33**, 612-626.

Plieth, C. (2010) Signal percolation through plants and the shape of the calcium signature. *Plant Signaling & Behavior*, **5**, 379-385.

Potokina, E., Druka, A., Luo, Z., Wise, R., Waugh, R. and Kearsey, M. (2008) Gene expression quantitative trait locus analysis of 16 000 barley genes reveals a complex pattern of genome-wide transcriptional regulation. *The Plant Journal*, **53**, 90-101.

Poustini, K. and Siosemardeh, A. (2004) Ion distribution in wheat cultivars in response to salinity stress. *Field Crops Research*, **85**, 125-133.

Prasad, S.R., Bagali, P.G., Hittalmani, S. and Shashidhar, H.E. (2000) Molecular mapping of quantitative trait loci associated with seedling tolerance to salt stress in rice (*Oryza sativa* L.). *Current Science*, **78**, 162-164.

Qi, Y., He, X., Wang, X.J., Kohany, O., Jurka, J. and Hannon, G.J. (2006) Distinct catalytic and non-catalytic roles of ARGONAUTE4 in RNA-directed DNA methylation. *Nature*, **443**, 1008-1012.

Quarrie, S.A., Steed, A., Calestani, C., Semikhodskii, A., Lebreton, C., Chinoy, C., Steele, N., Pljevljakusić, D., Waterman, E., Weyen, J., Schondelmaier, J., Habash, D.Z., Farmer, P., Saker, L., Clarkson, D.T., Abugalieva, A., Yessimbekova, M., Turuspekov, Y., Abugalieva, S., Tuberosa, R., Sanguineti, M.C., Hollington, P.A., Aragués, R., Royo, A. and Dodig, D. (2005) A high-density genetic map of hexaploid wheat (*Triticum aestivum* L.) from the cross Chinese Spring X SQ1 and its use to compare QTLs for grain yield across a range of environments. *Theoretical and Applied Genetics*, **110**, 865-880.

Quesada, V., García-Martínez, S., Piqueras, P., Ponce, M.R. and Micol, J.L. (2002) Genetic architecture of NaCl tolerance in Arabidopsis. *Plant Physiology*, **130**, 951-963.

Quintero, F.J., Ohta, M., Shi, H., Zhu, J.K. and Pardo, J.M. (2002) Reconstitution in yeast of the Arabidopsis SOS signaling pathway for Na^+ homeostasis. *Proceedings of the National Academy of Sciences of the United States of America*, **99**, 9061-9066.

Rajendran, K., Tester, M. and Roy, S.J. (2009) Quantifying the three main components of salinity tolerance in cereals. *Plant Cell and Environment*, **32**, 237-249.

Ranf, S., Wunnenberg, P., Lee, J., Becker, D., Dunkel, M., Hedrich, R., Scheel, D. and Dietrich, P. (2008) Loss of the vacuolar cation channel, AtTPC1, does not impair Ca2+ signals induced by abiotic and biotic stresses. *The Plant Journal*, **53**, 287-299.

Ren, Z., Zheng, Z., Chinnusamy, V., Zhu, J., Cui, X., Iida, K. and Zhu, J.K. (2010) *RAS1*, a quantitative trait locus for salt tolerance and ABA sensitivity in Arabidopsis. *Proceedings of the National Academy of Sciences of the United States of America*, **107**, 5669-5674.

Ren, Z.H., Gao, J.P., Li, L.G., Cai, X.L., Huang, W., Chao, D.Y., Zhu, M.Z., Wang, Z.Y., Luan, S. and Lin, H.X. (2005) A rice quantitative trait locus for salt tolerance encodes a sodium transporter. *Nature Genetics*, **37**, 1141-1146.

Rengasamy, P. (2006) World salinization with emphasis on Australia. *Journal of Experimental Botany*, **57**, 1017-1023.

Rivandi, J., Miyazaki, J., Hrmova, M., Pallotta, M., Tester, M. and Collins, N.C. (2011) A *SOS3* homologue maps to *HvNax4*, a barley locus controlling an environmentally sensitive Na^+ exclusion trait. *Journal of Experimental Botany*, **62**, 1201-1216.

Rogers, K. and Chen, X. (2013) Biogenesis, turnover, and mode of action of plant microRNAs. *The Plant Cell*, **25**, 2383-2399.

Rose, A.B. (2008) Intron-mediated regulation of gene expression. *Current Topics in Microbiology and Immunology*, **326**, 277-290.

Rose, A.B., Elfersi, T., Parra, G. and Korf, I. (2008) Promoter-proximal introns in *Arabidopsis thaliana* are enriched in dispersed signals that elevate gene expression. *The Plant Cell Online*, **20**, 543-551.

Roy, S.J., Gilliham, M., Berger, B., Essah, P.A., Cheffings, C., Miller, A.J., Davenport, R.J., Liu, L.H., Skynner, M.J., Davies, J.M., Richardson, P., Leigh, R.A. and Tester, M. (2008) Investigating glutamate receptor-like gene co-expression in *Arabidopsis thaliana*. *Plant, Cell & Environment*, **31**, 861-871.

Roy, S.J., Huang, W., Wang, X.J., Evrard, A., Schmöckel, S.M., Zafar, Z.U. and Tester, M. (2013) A novel protein kinase involved in Na^+ exclusion revealed from positional cloning. *Plant, Cell & Environment*, **36**, 553-568.

Roy, S.J. and Tester, M. (2012) Approaches for increasing salinity tolerance of crops. In *Encyclopaedia of Sustainable Science and Technology*. New York, USA: Springer.

Roy, S.J., Tester, M., Gaxiola, R.A. and Flowers, T.J. (2012) Plants of saline environments. In *McGraw-Hill Encyclopaedia of Science and Technology*. New York, USA: McGraw-Hill.

Rozen, S. and Skaletsky, H.J. (2000) *Primer3 on the WWW for general users and for biologist programmers.* Totowa, NJ: Humana Press.

Rubio, F., Gassmann, W. and Schroeder, J.I. (1995) Sodium-driven potassium uptake by the plant potassium transporter HKT1 and mutations conferring salt tolerance. *Science*, **270**, 1660-1663.

Rubio, F., Schwarz, M., Gassmann, W. and Schroeder, J.I. (1999) Genetic selection of mutations in the high affinity K^+ transporter HKT1 that define functions of a loop site for reduced Na^+ permeability and increased Na^+ tolerance. *Journal of Biological Chemistry*, **274**, 6839-6847.

Rus, A., Baxter, I., Muthukumar, B., Gustin, J., Lahner, B., Yakubova, E. and Salt, D.E. (2006) Natural variants of AtHKT1 enhance Na^+ accumulation in two wild populations of Arabidopsis. *PLoS Genetics*, **2**, e210.

Rus, A., Lee, B.H., Muñoz-Mayor, A., Sharkhuu, A., Miura, K., Zhu, J.K., Bressan, R.A. and Hasegawa, P.M. (2004) *AtHKT1* facilitates Na^+ homeostasis and K^+ nutrition *in planta*. *Plant Physiology*, **136**, 2500-2511.

Rus, A., Yokoi, S., Sharkhuu, A., Reddy, M., Lee, B.-h., Matsumoto, T.K., Koiwa, H., Zhu, J.-K., Bressan, R.A. and Hasegawa, P.M. (2001) AtHKT1 is a salt tolerance determinant that controls Na^+ entry into plant roots. *Proceedings of the National Academy of Sciences of the United States of America*, **98**, 14150-14155.

Sassi, A., Mieulet, D., Khan, I., Moreau, B., Gaillard, I., Sentenac, H. and Véry, A.-A. (2012) The rice monovalent cation transporter OsHKT2;4: revisited ionic selectivity. *Plant Physiology*, **160**, 498-510.

Sax, K. (1923) The association of size differences with seed-coat pattern and pigmentation in *Phaseolus vulgaris*. *Genetics*, **8**, 552-560.

Saze, H. and Kakutani, T. (2007) Heritable epigenetic mutation of a transposon-flanked Arabidopsis gene due to lack of the chromatin-remodeling factor DDM1. *EMBO Journal*, **26**, 3641-3652.

Schachtman, D.P. and Munns, R. (1992) Sodium accumulation in leaves of triticum species that differ in salt tolerance. *Australian Journal of Plant Physiology*, **19**, 331-340.

Schachtman, D.P. and Schroeder, J.I. (1994) Structure and transport mechanism of a high-affinity potassium uptake transporter from higher plants. *Nature*, **370**, 655-658.

Schadt, E.E., Monks, S.A., Drake, T.A., Lusis, A.J., Che, N., Colinayo, V., Ruff, T.G., Milligan, S.B., Lamb, J.R., Cavet, G., Linsley, P.S., Mao, M., Stoughton, R.B.

and Friend, S.H. (2003) Genetics of gene expression surveyed in maize, mouse and man. *Nature*, **422**, 297-302.

Seemann, J.R. and Critchley, C. (1985) Effects of salt stress on the growth, ion content, stomatal behaviour and photosynthetic capacity of a salt-sensitive species, *Phaseolus vulgaris L. Planta*, **164**, 151-162.

Semagn, K., Babu, R., Hearne, S. and Olsen, M. (2013) Single nucleotide polymorphism genotyping using Kompetitive Allele Specific PCR (KASP): overview of the technology and its application in crop improvement. *Molecular Breeding*, 1-14.

Sennesal, F.-X. Versailles mapping populations. (http://dbsgap.versailles.inra.fr/vnat/). 2010/09/23.

Serrano, R. and Rodríguez-Navarro, A. (2001) Ion homeostasis during salt stress in plants. *Current Opinion in Cell Biology*, **13**, 399-404.

Shabala, S., Shabala, L. and Van Volkenburgh, E. (2003) Effect of calcium on root development and root ion fluxes in salinised barley seedlings. *Functional Plant Biology*, **30**, 507-514.

Shadiac, N., Nagarajan, Y., Waters, S. and Hrmova, M. (2013) Close allies in membrane protein research: Cell-free synthesis and nanotechnology. *Molecular Membrane Biology*, **30**, 229-245.

Shah, S.H., Gorham, J., Forster, B.P. and Jones, R.G.W. (1987) Salt tolerance in the triticeae- the contribution of the D-genome to cation selectivity in hexaploid wheat. *Journal of Experimental Botany*, **38**, 254-269.

Shao, Q., Zhao, C., Han, N. and Wang, B.-S. (2008) Cloning and expression pattern of *SsHKT1* encoding a putative cation transporter from halophyte *Suaeda salsa*. *DNA Sequence*, **19**, 106-114.

Sharma, H.C., Sharma, K.K. and Crouch, J.H. (2004) Genetic transformation of crops for insect resistance: Potential and limitations. *Critical Reviews in Plant Sciences*, **23**, 47-72.

Shavrukov, Y., Gupta, N.K., Miyazaki, J., Baho, M.N., Chalmers, K.J., Tester, M., Langridge, P. and Collins, N.C. (2010) *HvNax3-a* locus controlling shoot sodium exclusion derived from wild barley (*Hordeum vulgare ssp. spontaneum*). *Functional & Integrative Genomics*, **10**, 277-291.

Shearer, M.K. (2013) Characterisation of AtPQL1, AtPQL2 and AtPQL3 as candidate voltage insensitive Non-Selective Cation Channels (vi-NSCCs). PhD thesis at The University of Adelaide, School for Agriculture, Food and Wine.

Shi, H., Ishitani, M., Kim, C. and Zhu, J.K. (2000) The *Arabidopsis thaliana* salt tolerance gene *SOS1* encodes a putative Na^+/H^+ antiporter. *Proceedings of the National Academy of Sciences of the United States of America*, **97**, 6896-6901.

Shkolnik-Inbar, D., Adler, G. and Bar-Zvi, D. (2013) ABI4 downregulates expression of the sodium transporter *HKT1;1* in Arabidopsis roots and affects salt tolerance. *The Plant Journal*, **73**, 993-1005.

Slotkin, R.K., Vaughn, M., Borges, F., Tanurdžic, M., Becker, J.D., Feijó, J.A. and Martienssen, R.A. (2009) Epigenetic reprogramming and small RNA silencing of transposable elements in pollen. *Cell*, **136**, 461-472.

Sobczak, K., Bangel-Ruland, N., Leier, G. and Weber, W.-M. (2010) Endogenous transport systems in the *Xenopus laevis* oocyte plasma membrane. *Methods*, **51**, 183-189.

Somerville, C. and Koornneef, M. (2002) Timeline - A fortunate choice: the history of Arabidopsis as a model plant. *Nature Reviews Genetics*, **3**, 883-889.

Stahlberg, A., Hakansson, J., Xian, X., Semb, H. and Kubista, M. (2004) Properties of the reverse transcription reaction in mRNA quantification. *Clinical Chemistry*, **50**, 509-515.

Su, H., Balderas, E., Vera-Estrella, R., Golldack, D., Quigley, F., Zhao, C., Pantoja, O. and Bohnert, H.J. (2003) Expression of the cation transporter *McHKT1* in a halophyte. *Plant Molecular Biology*, **52**, 967-980.

Sunarpi, Horie, T., Motoda, J., Kubo, M., Yang, H., Yoda, K., Horie, R., Chan, W.Y., Leung, H.Y., Hattori, K., Konomi, M., Osumi, M., Yamagami, M., Schroeder, J.I. and Uozumi, N. (2005) Enhanced salt tolerance mediated by AtHKT1 transporter-induced Na^+ unloading from xylem vessels to xylem parenchyma cells. *The Plant Journal*, **44**, 928-938.

Sundstrom, J.F. (2011) Role and control of *HKT* in *Oryza sativa* & *Arabidopsis thaliana*. PhD thesis at University of Adelaide, School for Agriculture, Food and Wine.

Takahashi, R., Liu, S. and Takano, T. (2007) Cloning and functional comparison of a high-affinity K^+ transporter gene *PhaHKT1* of salt-tolerant and salt-sensitive reed plants. *Journal of Experimental Botany*, **58**, 4387-4395.

Takahashi, S., Katagiri, T., Hirayama, T., Yamaguchi-Shinozaki, K. and Shinozaki, K. (2001) Hyperosmotic stress induces a rapid and transient increase in inositol 1,4,5-trisphosphate independent of abscisic acid in Arabidopsis cell culture. *Plant and Cell Physiology*, **42**, 214-222.

Takahashi, S., Seki, M., Ishida, J., Satou, M., Sakurai, T., Narusaka, M., Kamiya, A., Nakajima, M., Enju, A., Akiyama, K., Yamaguchi-Shinozaki, K. and Shinozaki, K. (2004) Monitoring the expression profiles of genes induced by hyperosmotic, high salinity, and oxidative stress and abscisic acid treatment in Arabidopsis cell culture using a full-length cDNA microarray. *Plant Molecular Biology*, **56**, 29-55.

Tanksley, S. (1983) Molecular markers in plant breeding. *Plant Molecular Biology Reporter*, **1**, 3-8.

Tester, M. (1997) Techniques for studying ion channels: An introduction. *Journal of Experimental Botany*, **48**, 353-359.

Tester, M. and Davenport, R. (2003) Na^+ tolerance and Na^+ transport in higher plants. *Annals of Botany*, **91**, 503-527.

Tester, M. and Langridge, P. (2010) Breeding technologies to increase crop production in a changing world. *Science*, **327**, 818-822.

The Arabidopsis Genome Initiative (2000) Analysis of the genome sequence of the flowering plant *Arabidopsis thaliana*. *Nature*, **408**, 796-815.

The Arabidopsis Information Resource (TAIR) (www.arabidopsis.org). 2010/09/23.

Thoday, J.M. (1961) Location of polygenes. *Nature*, **191**, 368-370.

Thomson, M.J., de Ocampo, M., Egdane, J., Rahman, M.A., Sajise, A.G., Adorada, D.L., Tumimbang-Raiz, E., Blumwald, E., Seraj, Z.I., Singh, R.K., Gregorio, G.B. and Ismail, A.M. (2010) Characterizing the *Saltol* Quantitative Trait Locus for salinity tolerance in rice. *Rice*, **3**, 148-160.

Tian, B., Pan, Z. and Lee, J.Y. (2007) Widespread mRNA polyadenylation events in introns indicate dynamic interplay between polyadenylation and splicing. *Genome Research*, **17**, 156-165.

Tian, L., Tan, L.B., Liu, F.X., Cai, H.W. and Sun, C.Q. (2011) Identification of quantitative trait loci associated with salt tolerance at seedling stage from *Oryza rufipogon*. *Journal of Genetics and Genomics*, **38**, 593-601.

Törjék, O., Berger, D., Meyer, R.C., Mussig, C., Schmid, K.J., Rosleff Sorensen, T., Weisshaar, B., Mitchell-Olds, T. and Altmann, T. (2003) Establishment of a high-efficiency SNP-based framework marker set for Arabidopsis. *The Plant Journal*, **36**, 122-140.

Törjék, O., Meyer, R.C., Zehnsdorf, M., Teltow, M., Strompen, G., Witucka-Wall, H., Blacha, A. and Altmann, T. (2008) Construction and analysis of 2 reciprocal Arabidopsis introgression line populations. *Journal of Heredity*, **99**, 396-406.

Törjék, O., Witucka-Wall, H., Meyer, R.C., von Korff, M., Kusterer, B., Rautengarten, C. and Altmann, T. (2006) Segregation distortion in Arabidopsis C24/Col-0 and Col-0/C24 recombinant inbred line populations is due to reduced fertility caused by epistatic interaction of two loci. *Theoretical and Applied Genetics*, **113**, 1551-1561.

Tozlu, I., Guy, C.L. and Moore, G.A. (1999a) QTL analysis of morphological traits in an intergeneric BC1 progeny of Citrus and Poncirus under saline and non-saline environments. *Genome*, **42**, 1020-1029.

Tozlu, I., Guy, C.L. and Moore, G.A. (1999b) QTL analysis of Na^+ and Cl^- accumulation related traits in an intergeneric BC1 progeny of Citrus and Poncirus under saline and nonsaline environments. *Genome*, **42**, 692-705.

Tozlu, I., Guy, C.L. and Moore, G.A. (2002) QTL analysis of salt stress related traits in Citrus and related genus Poncirus. In *Proceedings of the International Symposium on Techniques to Control Salination for Horticultural Productivity* (Aksoy, U., Anac, D., Anac, S., Beltrao, J., BenAsher, J., Cuartero, J., Flowers, T.J. and Hepaksoy, S. eds), pp. 237-246.

Tracy, F.E., Gilliham, M., Dodd, A.N., Webb, A.A.R. and Tester, M. (2008) NaCl-induced changes in cytosolic free Ca^{2+} in *Arabidopsis thaliana* are heterogeneous and modified by external ionic composition. *Plant Cell and Environment*, **31**, 1063-1073.

Tsugane, K., Kobayashi, K., Niwa, Y., Ohba, Y., Wada, K. and Kobayashi, H. (1999) A recessive Arabidopsis mutant that grows photoautotrophically under salt stress shows enhanced active oxygen detoxification. *The Plant Cell*, **11**, 1195-1206.

Tuyen, D.D., Lal, S.K. and Xu, D.H. (2010) Identification of a major QTL allele from wild soybean (*Glycine soja* Sieb. & Zucc.) for increasing alkaline salt tolerance in soybean. *Theoretical and Applied Genetics*, **121**, 229-236.

Tuyen, D.D., Zhang, H.M. and Xu, D.H. (2013) Validation and high-resolution mapping of a major quantitative trait locus for alkaline salt tolerance in soybean using residual heterozygous line. *Molecular Breeding*, **31**, 79-86.

Ueki, S., Lacroix, B. and Citovsky, V. (2011) Protein membrane overlay assay: a protocol to test interaction between soluble and insoluble proteins in vitro. *Journal of visualized experiments : JoVE*.

Uozumi, N., Kim, E.J., Rubio, F., Yamaguchi, T., Muto, S., Tsuboi, A., Bakker, E.P., Nakamura, T. and Schroeder, J.I. (2000) The Arabidopsis *HKT1* gene homolog mediates inward Na^+ currents in *Xenopus laevis* oocytes and Na^+ uptake in *Saccharomyces cerevisiae*. *Plant Physiology*, **122**, 1249-1259.

Vadez, V., Krishnamurthy, L., Thudi, M., Anuradha, C., Colmer, T.D., Turner, N.C., Siddique, K.H.M., Gaur, P.M. and Varshney, R.K. (2012) Assessment of ICCV 2

x JG 62 chickpea progenies shows sensitivity of reproduction to salt stress and reveals QTL for seed yield and yield components. *Molecular Breeding*, **30**, 9-21.

van Ooijen, J.W. (1999) LOD significance thresholds for QTL analysis in experimental populations of diploid species. *Heredity*, **83**, 613-624.

Vasil, V., Clancy, M., Ferl, R.J., Vasil, I.K. and Hannah, L.C. (1989) Increased gene expression by the first intron of maize *shrunken-1* locus in grass species. *Plant Physiology*, **91**, 1575-1579.

Villalta, I., Reina-Sánchez, A., Bolarín, M.C., Cuartero, J., Belver, A., Venema, K., Carbonell, E.A. and Asins, M.J. (2008) Genetic analysis of Na^+ and K^+ concentrations in leaf and stem as physiological components of salt tolerance in Tomato. *Theoretical and Applied Genetics*, **116**, 869-880.

Wakeel, A., Farooq, M., Qadir, M. and Schubert, S. (2011) Potassium substitution by sodium in plants. *Critical Reviews in Plant Sciences*, **30**, 401-413.

Wang, B.B. and Brendel, V. (2006) Genomewide comparative analysis of alternative splicing in plants. *Proceedings of the National Academy of Sciences of the United States of America*, **103**, 7175-7180.

Wang, R., Okamoto, M., Xing, X. and Crawford, N.M. (2003) Microarray analysis of the nitrate response in Arabidopsis roots and shoots reveals over 1,000 rapidly responding genes and new linkages to glucose, trehalose-6-phosphate, iron, and sulfate metabolism. *Plant Physiolology*, **132**, 556-567.

Wang, S., Basten, C.J. and Zeng., Z.-B. (2010) Windows QTL Cartographer 2.5. Department of Statistics, N.C.S.U., Raleigh, NC. (http://statgen.ncsu.edu/qtlcart/WQTLCart.htm).

Wang, T.B., Gassmann, W., Rubio, F., Schroeder, J.I. and Glass, A.D.M. (1998) Rapid up-regulation of *HKT1*, a high-affinity potassium transporter gene, in roots of barley and wheat following withdrawal of potassium. *Plant Physiology*, **118**, 651-659.

Wang, Y., Zang, J.P., Sun, Y., Ali, J., Xu, J.L. and Li, Z.K. (2012a) Identification of genetic overlaps for salt and drought tolerance using simple sequence repeat markers on an advanced backcross population in rice. *Crop Science*, **52**, 1583-1592.

Wang, Z.F., Chen, Z.W., Cheng, J.P., Lai, Y.Y., Wang, J.F., Bao, Y.M., Huang, J. and Zhang, H.S. (2012b) QTL analysis of Na^+ and K^+ concentrations in roots and shoots under different levels of NaCl stress in rice (*Oryza sativa* L.). *Plos One*, **7**.

Waters, S., Gilliham, M. and Hrmova, M. (2013) Plant High-affinity Potassium (HKT) transporters involved in salinity tolerance: structural insights to probe differences in ion selectivity. *International Journal of Molecular Sciences*, **14**, 7660-7680.

Weber, W.-M. (1999) Ion currents of *Xenopus laevis* oocytes: state of the art. *Biochimica et Biophysica Acta (BBA) - Biomembranes*, **1421**, 213-233.

Wei, W.X., Bilsborrow, P.E., Hooley, P., Fincham, D.A., Lombi, E. and Forster, B.P. (2003) Salinity induced differences in growth, ion distribution and partitioning in barley between the cultivar Maythorpe and its derived mutant Golden Promise. *Plant and Soil*, **250**, 183-191.

Weigel, D. and Glazebrook, J. (2006) Transformation of Agrobacterium using the freeze-thaw method. *Cold Spring Harbor Protocols*, **2006**, pdb.prot4666.

West, M.A., Kim, K., Kliebenstein, D.J., van Leeuwen, H., Michelmore, R.W., Doerge, R.W. and St Clair, D.A. (2007) Global eQTL mapping reveals the complex genetic architecture of transcript-level variation in Arabidopsis. *Genetics*, **175**, 1441-1450.

Whalley, H.J. and Knight, M.R. (2013) Calcium signatures are decoded by plants to give specific gene responses. *New Phytologist*, **197**, 690-693.

White, P.J. (2000) Calcium channels in higher plants. *Biochimica Et Biophysica Acta-Biomembranes*, **1465**, 171-189.

Wu, L., Zhou, H., Zhang, Q., Zhang, J., Ni, F., Liu, C. and Qi, Y. (2010) DNA methylation mediated by a microRNA pathway. *Molecular Cell*, **38**, 465-475.

Wu, S.J., Ding, L. and Zhu, J.K. (1996) *SOS1*, a genetic locus essential for salt tolerance and potassium acquisition. *The Plant Cell*, **8**, 617-627.

Xia, Y., Yu, K., Navarre, D., Seebold, K., Kachroo, A. and Kachroo, P. (2010) The *glabra1* mutation affects cuticle formation and plant responses to microbes. *Plant Physiology*, **154**, 833-846.

Xiao, J., Li, J., Yuan, L. and Tanksley, S.D. (1995) Dominance is the major genetic basis of heterosis in rice as revealed by QTL analysis using molecular markers. *Genetics*, **140**, 745-754.

Xie, Z., Johansen, L.K., Gustafson, A.M., Kasschau, K.D., Lellis, A.D., Zilberman, D., Jacobsen, S.E. and Carrington, J.C. (2004) Genetic and functional diversification of small RNA pathways in plants. *PLoS Biology*, **2**, e104.

Xu, J., Tian, Y.S., Peng, R.H., Xiong, A.S., Zhu, B., Jin, X.F., Gao, F., Fu, X.Y., Hou, X.L. and Yao, Q.H. (2010) *AtCPK6*, a functionally redundant and positive regulator involved in salt/drought stress tolerance in Arabidopsis. *Planta*, **232**, 1007-1007.

Xu, R.G., Wang, J.M., Li, C.D., Johnson, P., Lu, C. and Zhou, M.X. (2012a) A single locus is responsible for salinity tolerance in a Chinese landrace barley (*Hordeum vulgare* L.). *Plos One*, **7**.

Xu, W., Ding, G., Yokawa, K., Baluska, F., Li, Q.-F., Liu, Y., Shi, W., Liang, J. and Zhang, J. (2013a) An improved agar-plate method for studying root growth and response of *Arabidopsis thaliana*. *Scientific Reports*, **3**.

Xu, Y., Li, S., Li, L., Zhang, X., Xu, H. and An, D. (2013b) Mapping QTLs for salt tolerance with additive, epistatic and QTL × treatment interaction effects at seedling stage in wheat. *Plant Breeding*, **132**, 276-283.

Xu, Y.F., An, D.G., Liu, D.C., Zhang, A.M., Xu, H.X. and Li, B. (2012b) Mapping QTLs with epistatic effects and QTL x treatment interactions for salt tolerance at seedling stage of wheat. *Euphytica*, **186**, 233-245.

Xue, D.W., Huang, Y.Z., Zhang, X.Q., Wei, K., Westcott, S., Li, C.D., Chen, M.C., Zhang, G.P. and Lance, R. (2009) Identification of QTLs associated with salinity tolerance at late growth stage in barley. *Euphytica*, **169**, 187-196.

Xue, S., Yao, X., Luo, W., Jha, D., Tester, M., Horie, T. and Schroeder, J.I. (2011) AtHKT1;1 mediates nernstian sodium channel transport properties in Arabidopsis root stelar cells. *Plos One*, **6**, e24725-e24725.

Yamaguchi-Shinozaki, K. and Shinozaki, K. (1994) A novel cis-acting element in an Arabidopsis gene is involved in responsiveness to drought, low-temperature, or high-salt stress. *The Plant Cell*, **6**, 251-264.

Yano, M. (2001) Genetic and molecular dissection of naturally occurring variation. *Current Opinion in Plant Biology*, **4**, 130-135.

Yao, X., Horie, T., Xue, S., Leung, H.-Y., Katsuhara, M., Brodsky, D.E., Wu, Y. and Schroeder, J.I. (2010) Differential sodium and potassium transport selectivities of the rice OsHKT2;1 and OsHKT2;2 transporters in plant cells. *Plant Physiology*, **152**, 341-355.

Yeo, A.R. (1992) Variation and inheritance of sodium-transport in rice. *Plant and Soil*, **146**, 109-116.

Zhai, J., Liu, J., Liu, B., Li, P., Meyers, B.C., Chen, X. and Cao, X. (2008) Small RNA-directed epigenetic natural variation in *Arabidopsis thaliana*. *PLoS Genetics*, **4**, e1000056.

Zhang, G.Y., Guo, Y., Chen, S.L. and Chen, S.Y. (1995) Rflp tagging of a salt tlerance gene in rice. *Plant Science*, **110**, 227-234.

Zhang, S.H., Lawton, M.A., Hunter, T. and Lamb, C.J. (1994) ATPK1, a novel ribosomal protein kinase gene from Arabidopsis. I. Isolation, characterization, and expression. *Journal of Biological Chemistry*, **269**, 17586-17592.

Zhang, X., Yazaki, J., Sundaresan, A., Cokus, S., Chan, S.W., Chen, H., Henderson, I.R., Shinn, P., Pellegrini, M., Jacobsen, S.E. and Ecker, J.R. (2006a) Genome-wide high-resolution mapping and functional analysis of DNA methylation in Arabidopsis. *Cell*, **126**, 1189-1201.

Zhang, X.R., Henriques, R., Lin, S.S., Niu, Q.W. and Chua, N.H. (2006b) Agrobacterium-mediated transformation of *Arabidopsis thaliana* using the floral dip method. *Nature Protocols*, **1**, 641-646.

Zheng, X., Zhu, J., Kapoor, A. and Zhu, J.K. (2007) Role of Arabidopsis AGO6 in siRNA accumulation, DNA methylation and transcriptional gene silencing. *EMBO Journal*, **26**, 1691-1701.

Zhou, G.F., Johnson, P., Ryan, P.R., Delhaize, E. and Zhou, M.X. (2012) Quantitative trait loci for salinity tolerance in barley (*Hordeum vulgare* L.). *Molecular Breeding*, **29**, 427-436.

Zhu, G.Y., Kinet, J.M. and Lutts, S. (2001) Characterization of rice (*Oryza sativa L*.) F-3 populations selected for salt resistance. I. Physiological behaviour during vegetative growth. *Euphytica*, **121**, 251-263.

Zhu, J.-K., Liu, J. and Xiong, L. (1998) Genetic analysis of salt tolerance in Arabidopsis: evidence for a critical role of potassium nutrition. *The Plant Cell*, **10**, 1181-1191.

Zhu, J.H., Lee, B.H., Dellinger, M., Cui, X.P., Zhang, C.Q., Wu, S., Nothnagel, E.A. and Zhu, J.K. (2010) A cellulose synthase-like protein is required for osmotic stress tolerance in Arabidopsis. *The Plant Journal*, **63**, 128-140.

Zhu, J.K. (2000) Genetic analysis of plant salt tolerance using Arabidopsis. *Plant Physiology*, **124**, 941-948.

Zhu, J.K. (2002) Salt and drought stress signal transduction in plants. *Annual Review of Plant Biology*, **53**, 247-273.

Zhu, J.K. (2003) Regulation of ion homeostasis under salt stress. *Current Opinion in Plant Biology*, **6**, 441-445.

Zhu, X., Feng, Y., Liang, G., Liu, N. and Zhu, J.-K. (2013) Aequorin-based luminescence imaging reveals stimulus- and tissue-specific Ca^{2+} dynamics in Arabidopsis plants. *Molecular Plant*, **6**, 444-455.

Zilberman, D., Cao, X. and Jacobsen, S.E. (2003) ARGONAUTE4 control of locus-specific siRNA accumulation and DNA and histone methylation. *Science*, **299**, 716-719.

Zimmermann, P., Hirsch-Hoffmann, M., Hennig, L. and Gruissem, W. (2004) GENEVESTIGATOR. Arabidopsis microarray database and analysis toolbox. *Plant Physiology*, **136**, 2621-2632.